Synthesis and Solid-State Reactions of Substituted Cyclopentadienyl Complexes of Rhenium, Tungsten and Molybdenum

Lin Cheng

A thesis submitted to the Faculty of Science, University of the Witwatersrand, Johannesburg, in fulfillment of the requirements for the degree of Doctor of Philosophy.

Abstract

About one hundred diagonal and lateral isomers of mono- or di-substituted cyclopentadienyl four-legged piano stool transition metal complexes (η^5-$C_5H_3R_1R_2$)ML_4 (R_1 = R_2 = H, Alkyl; M = Re, W, Mo; L = CO, isonitrile, phosphite, phosphine, Br⁻ I⁻) were synthesized and fully characterized by elemental analysis, IR and NMR spectroscopy.

All complexes studied were found to undergo solid-state *diag-lat* isomerization reactions under either thermal or silica gel mediated photochemical conditions. This indicates that solid-state isomerization reactions are a common reaction type for cyclopentadienyl four-legged piano stool transition metal complexes (M = Re, W, Mo). It was found that the direction of the solid-state isomerization reaction always proceeded from the low melting point isomer to the high melting point isomer.

A review of the literature was performed to place the solid-state reactions in perspective. This revealed that this was the first systematic solid-state study of isomerization reactions of organometallic complexes at a metal center.

The solid-state photochemical *diag-lat* isomerization reactions of (η^3-C_3H_4R)$Re(CO)(L)X_2$ (R = H, alkyl; L = CO, $P(OR)_3$; X = Br, I) on the surface of

silica gel were studied. A mechanism to rationalize the role of the silica surface hydroxyl groups is described.

The thermal solid-state isomerization processes of $(\eta^5\text{-}C_5H_4R)Re(CO)(L)Br_2$ (R = Me, tBu, $SiMe_3$; L = CO, $NCC_6H_3Me_2$, $P(OMe)_3$, $P(OPh)_3$) were studied by Differential Scanning Calorimetry (DSC), thermomicroscopy and X-ray powder diffraction techniques. The results indicated that the solid-state isomerization reactions proceeded exothermically and *via* a nuclear formation and growth mechanism.

The crystal and molecular structures of the diagonal and lateral isomers of $(\eta^5\text{-}C_5H_4Me)Re(CO)_2Br_2$, $(\eta^5\text{-}C_5H_4Me)Re(CO)[P(OPh)_3]Br_2$ and $(\eta^5\text{-}C_5H_4tBu)Re(CO)_2Br_2$ were determined by X-ray single crystal diffraction techniques. Inter- and intra-molecular interactions in these molecules in the crystalline environment were analyzed and used to rationalize the solid-state isomerization results.

Declaration

I declare that this thesis was carried out exclusively by myself under the supervision of Professor Neil J. Coville. It is being submitted for the degree of Doctor of Philosophy at the University of the Witwatersrand, Johannesburg, It has not been submitted for any degree or examination at any other University.

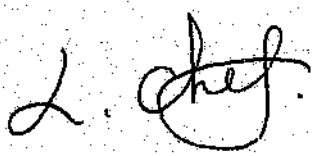

Lin Cheng

October 1997

To My Parents and My Wife.

Acknowledgments

I would like to express my sincere gratitude to the following people for all their assistance and advice, without which this thesis would not have been possible.

- My supervisor, Professor Neil J. Coville, for his many hours of patient wisdom which made this work possible. Also for his never ending advice, assistance, enthusiasm and encouragement which have made working for him a pleasure and an unforgettable experience in my life.
- Professor Jan C.A. Boeyens, Dr Demetrious C. Levendis, Ms. Leane Cook, Mr. Manuel Fernandes and Mr. Keith McIntosh for measuring X-ray single-crystal structures and many helpful discussion.
- Sigi Heiss and Dr Laurence Carlton for the recording of NMR spectra.
- Jiksha Morar and Bongani Ngoma deserve special thanks for preparing a range of tungsten complexes as part of final year projects.
- Neil Grimmer, for his enthusiastic help with computer software, Internet, laboratory facilities and with proof reading this thesis.
- All of my colleagues in the lab: Miranda Momabolo, Bhekie Mamba, Joseph Mofokeng and Tshepo Malefetse. Thanks for an enjoyable research atmosphere.

- Barry Fairbrother, Basil Chassoulas and Steve van der Schyff for their technical support.
- Rowena Birrel and Lyn Daniell for their efficient administrative work.
- Lastly, I would like to thank my family for their invaluable support and encouragement during this work.

List of Abbreviations

Cp	Cyclopentadienyl
diag	Diagonal
DSC	Differential Scanning Calorimetry
Et	Ethyl
FT	Fourier Transform
h	Hour(s)
^{i}Pr	*iso*-propyl
IR	Infra-red
L	Ligand
lat	Lateral
M	Metal
Me	Methyl
m.p.	Melting point
NMR	Nuclear magnetic resonance
NOE	Nuclear overhauser effect
PR_3	Phosphine
$P(OR)_3$	Phosphite
ppm	Parts per million
R	An organic group
RNC	Isonitrile
R^2	Percentage of variance explained by model

$SiMe_3$	Trimethylsilyl
tBu	*tert*-butyl
TLC	Thin layer chromatography
TMS	Tetramethylsilane
X	Halogen
XRD	X-ray diffraction

Table of Contents

List of Tables

List of Figures

CHAPTER 1

INTRODUCTION

The solution chemistry of organometallic compounds has been studied for more than one hundred years. The rapid development of organometallic chemistry was stimulated by the discovery of ferrocene in 1950's, and again most of the significant developments since this date have related to organometallic chemistry in the solution state. Interestingly the study of organometallic chemistry in the gas phase has been made possible since the late 1980's by the development of new mass spectrometers. However, the development of solid-state organometallic chemistry has hardly been exploited during the past 40 or so years.

In this thesis the diagonal and lateral isomers of substituted cyclopentadienyl four-legged piano stool transition metal complexes $(\eta^5\text{-}C_5H_4R)ML_4$ (M = Re, W, Mo), a class of cyclopentadienyl organometallic compounds, which have been little studied, were chosen for the investigation of solid state reactivity. This arose from a serendipitous discovery which will be mentioned in the thesis. These complexes have permitted the investigation of solid-state isomerization and halogen-exchange reactions under both thermal and photochemical conditions.

As this is one of the first times that the solid-state reactions of organometallic

compounds have been systematically studied, a literature survey was undertaken on this topic. In particular the literature was evaluated with respect to the solid state reactions of organometallic (and where appropriate non-organometallic) compounds as the topic pertains to: (a) solid-state reactions in general, (b) catalytic isomerization reactions, and (c) silica gel catalyzed reactions (Chapter 2).

To place the specific reactions described in the thesis in context, the chemistry of cyclopentadienyl four-legged piano stool rhenium complexes is also reviewed in Chapter 2.

The thermal solid-state isomerization reactions of the rhenium complexes (η^5-C_5H_4R)$Re(CO)_2Br_2$ with different ring-substituents R (R = H, Et, C_6H_{11}, ^iPr, tBu, $SiMe_3$) were first examined. The results of this study and the comparison with solution reactions are presented in Chapter 3.

It was found that (η^5-C_5H_4R)$Re(CO)_2Br_2$ (R = Me, ^iPr) underwent a reversible phase-dependent isomerization reaction. However, the solid-state isomerization was not observed for the other ring-substituted complexes (R = H, Et, tBu, $SiMe_3$). A number of monocarbonyl substituted rhenium complexes *diag*- and *lat*-(η^5-C_5H_4R)$Re(CO)(L)X_2$ (R = Me, tBu, $SiMe_3$; L = isonitrile, phosphite, phosphine; X = Br, I) were then synthesized and their thermal solid-state isomerization and halogen-exchange reactions were investigated (Chapter 6).

The solid-state isomerization reactions of the cyclopentadienyl four-legged piano stool rhenium complexes were studied in depth by DSC and thermomicroscopy. This information provided data such that mechanistic features of the reaction could be proposed. The results are presented in Chapter 7.

In order to understand the solid-state isomerization reaction at the molecular level, the X-ray single-crystal structures of *diag*- and *lat*-(η^5-C_5H_4Me)$Re(CO)_2Br_2$ and (η^5-C_5H_4Me)$Re(CO)[P(OPh)_3]Br_2$, which underwent solid-state isomerization reactions, and *diag*- and *lat*-(η^5-C_5H_4tBu)$Re(CO)_2Br_2$, which did not isomerize thermally in the solid state, were determined. The results of this study are presented in Chapters 4 and 8.

Silica gel has shown to be an effective catalyst in many organic reactions. The solid-state silica gel-mediated photochemical isomerization and halogen-exchange reactions of (η^5-C_5H_4R)$Re(CO)(L)X_2$ were investigated. The results and a proposed mechanism for the reaction are presented in Chapter 5.

An analysis of the steric and electronic effects associated with the new rhenium complexes was studied using NMR spectroscopy. The analysis was based on a similar analysis carried out on related cyclopentadienyl iron complexes (η^5-C_5H_4R)$Fe(CO)(L)I$ (R= alkyl group; L = isonitrile, phosphine, phosphite). The attempt to correlate the steric sizes of the substituted ring C_5H_4R and the ligands L of the *diag*- and *lat*-(η^5-C_5H_4R)$Re(CO)(L)Br_2$ isomers with the NMR parameters

is presented in Chapter 9.

Chapter 11 describes a facile synthesis and solid-state thermal and photochemical isomerization reactions of the disubstituted cyclopentadienyl rhenium complexes *diag*- and *lat*-(η^5-$C_5H_3R_1R_2$)$Re(CO)_2Br_2$ (R_1 = Me, tBu, $SiMe_3$; R_2 = $SiMe_3$).

Finally, to explore the generality of the above solid-state reactions, an investigation of the solid-state isomerization reactions of the tungsten and molybdenum complexes, *diag*- and *lat*-(η^5-C_5H_4R)$M(CO)_2(L)I$ (R = Me, tBu; L = phosphite, phosphine) was undertaken. The results of this study are presented in Chapter 10.

Figures and schemes are integrated within the text. Tables are collected at the end of each Experimental Section for easy reference, followed by a detailed listing of the references to each chapter. Supplementary crystallographic data are saved on a diskette, attached to the back cover of this thesis.

CHAPTER 2

LITERATURE SURVEY

2.1. Synthesis, Characterization and Reactions of Cyclopentadienyl Four-Legged Piano Stool Rhenium Complexes

2.1.1. Cyclopentadienyl Dicarbonyldihalogen Rhenium Complexes

Cyclopentadienyltricarbonyl rhenium, $(\eta^5\text{-}C_5H_5)Re(CO)_3$, the starting material for preparing cyclopentadienyl four-legged piano stool rhenium complexes, was first unintentionally prepared by Wilkinson *et al.* in 1958 when they attempted to synthesize $(\eta^5\text{-}C_5H_5)(\eta^2\text{-}C_5H_6)Re(CO)_2$, by refluxing dicyclopentadiene with rhenium carbonyl $Re_2(CO)_{10}$.[1] Eleven years later, Nesmeyanov *et al* investigated the chemical properties of $(\eta^5\text{-}C_5H_5)Re(CO)_3$. They found that bromination of $(\eta^5\text{-}C_5H_5)Re(CO)_3$ in trifluoroacetic acid or methylene chloride in the presence of $AlCl_3$ led to the replacement of one molecule of CO by two bromine atoms. This reaction gave red crystals of $(\eta^5\text{-}C_5H_5)Re(CO)_2Br_2$ (Scheme 2.1), the first cyclopentadienyl four-legged piano stool rhenium complex.[2]

In 1973, the same authors extended their work to the bromination of the monosubstituted analogues, $(\eta^5\text{-}C_5H_4R)Re(CO)_3$ (R = Me, I, CH_3COO) and

reactions of $(\eta^5\text{-}C_5H_5)Re(CO)_3$ with the Grignard reagents CH_3MgI and C_6H_5MgBr. A small number of cyclopentadienyl four-legged half sandwich rhenium complexes have been prepared since these early discoveries (Table 2.1).[3]

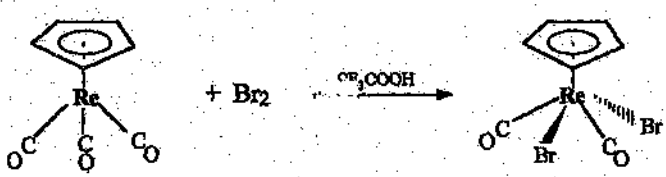

Scheme 2.1

Although not initially recognized by Nesmayanov, piano stool complexes of the type $(\eta^5\text{-}C_5H_5)MA_2B_2$ and $(\eta^5\text{-}C_5H_5)MA_2BC$ exist as two nonequivalent stereoisomers that are commonly referred to as *cis* and *trans*, or more precisely, *lateral* and *diagonal* isomers (Figure 2.1).

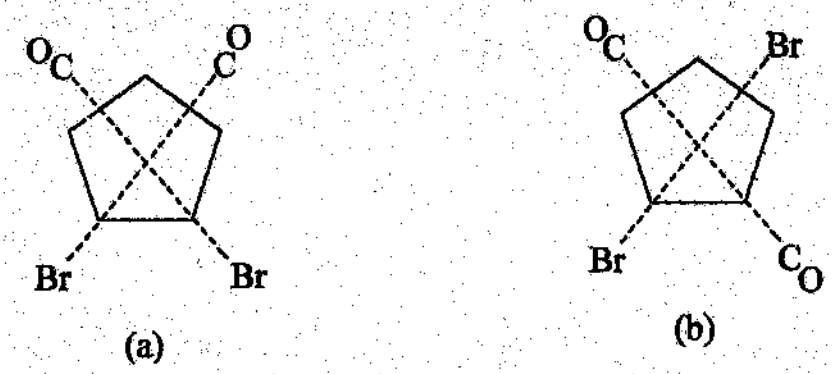

Figure 2.1. (a) Lateral and (b) diagonal isomers of $(\eta^5\text{-}C_5H_5)Re(CO)_2Br_2$.

In 1975, a simple and reproducible chromatographic technique for the separation of *lat*-$(\eta^5\text{-}C_5H_5)Re(CO)_2Br_2$ (Figure 2.1a) and *diag*-$(\eta^5\text{-}C_5H_5)Re(CO)_2Br_2$ (Figure

2,1b) was reported by King *et al.*[4] This separation procedure made possible the study of the *diag-lat* isomerization reactions of cyclopentadienyl four-legged piano stool rhenium complexes. For example the authors found that the lateral isomer of $(\eta^5\text{-}C_5H_5)Re(CO)_2Br_2$ was readily converted to the corresponding diagonal isomer upon mild heating in dichloromethane and chloroform, and that the substituted derivatives *diag*-$(\eta^5\text{-}C_5H_5)Re(CO)[P(OR)_3]Br_2$ (R = CH_3, C_2H_5, C_6H_5) isomerize to the corresponding lateral isomers in boiling toluene.

King *et al* identified the diagonal and lateral isomer structures of $(\eta^5\text{-}C_5H_5)Re(CO)_2Br_2$ by measurements of the relative intensities of two infrared ν(CO) bands.[5] In these measurements, the angles between the two M-C-O bonds in $(\eta^5\text{-}C_5H_5)Re(CO)_2Br_2$ isomers were determined by the relationship $\tan^2\theta = I_a / I_s$ where 2θ is the angle between the two M-C-O bonds, I_a is the area under the asymmetric ν(CO) band, and I_s is the area under the symmetric ν(CO) band with the ratio I_a / I_s being extrapolated to infinite dilution. Thus, for the diagonal and lateral isomers of $(\eta^5\text{-}C_5H_5)Re(CO)_2Br_2$ the angles 2θ were found to be 120° and 78°, respectively. However, this method cannot be used to identify the isomers of $(\eta^5\text{-}C_5H_5)Re(CO)[P(OR)_3]Br_2$.[4] Other techniques such as NMR spectroscopy are then needed.

It was not until 1985 that the dichloride and the pentamethylcyclopentadienyl analogues $(\eta^5\text{-}C_5Me_5)Re(CO)_2X_2$ (X = Cl, Br, I) were synthesized by Sutton *et al* from the reaction of the dinitrogen complex $(\eta^5\text{-}C_5Me_5)Re(CO)_2(N_2)$ with HX.[6]

The *lat*-to-*diag* solution isomerization of the dihalide complexes was observed under both thermal and photochemical conditions and the diagonal and lateral structures of the piano stool complexes were confirmed by X-ray structure determinations on *diag*-(η^5-C_5Me_5)$Re(CO)_2Br_2$ and *lat*-(η^5-C_5Me_5)$Re(CO)_2I_2$.[6] These were the first crystal structures reported on these types of isomers (Table 2.2). An improved synthetic method to produce (η^5-C_5Me_5)$Re(CO)_2X_2$ (X = Cl, Br, I) has subsequently been reported by Diaz *et al.*[7]

The mechanism of the photochemical *diag-lat* isomerism of (η^5-C_5Me_5)$Re(CO)_2X_2$ (X = Me, Cl, Br, I) in solution has been studied at low temperature by Hill and co-workers using FTIR spectroscopy. It was found that photolysis of *diag*- or *lat*-(η^5-C_5Me_5)$Re(CO)_2X_2$ at 13 K in methylcyclohexane or (1,2-epoxyethyl)benzene resulted in the removal of a carbonyl ligand and production of a three-legged unsaturated photoproduct, (η^5-C_5Me_5)$Re(CO)X_2$. This intermediate recombines with the photoproduced CO at 100 K to yield only *diag*-(η^5-C_5Me_5)$Re(CO)_2X_2$.[8] A similar mechanism was proposed for the photochemical isomerism of (η^5-C_5Me_5)$Re(CO)_2Br_2$ on a Si(III) surface by the same authors.[9]

2.1.2. Cyclopentadienyl Dialkyldicarbonyl Rhenium Complexes

The first synthesis of a cyclopentadienyldialkyldicarbonyl rhenium complex, (η^5-C_5H_5)$Re(CO)_2(Me)_2$, was reported by Nesmeyanov *et al* in 1973 from the direct reaction of (η^5-C_5H_5)$Re(CO)_2Br_2$ with CH_3MgI.[3,10] The diagonal and lateral

stereoisomers of this complex were not noticed at the time. Later Richmond *et al* reported that they were unable to repeat Nesmeyanov's findings. Reactions of $(\eta^5\text{-}C_5Me_5)Re(CO)_2Br_2$ with different Grignard and organolithium reagents did not result in the incorporation of the organo-ligand. Instead, only the formation of the monoanion $[(\eta^5\text{-}C_5H_5)Re(CO)_2Br]^-$ was observed.[11]

An indirect preparation for the synthesis of $(\eta^5\text{-}C_5H_5)Re(CO)_2X_2$ was developed by Hoyano and Graham *et al* starting from $(\eta^5\text{-}C_5H_5)Re(CO)_2H_2$ (Scheme 2.2).[12] This method was modified by Yang and Bergman *et al*,[13] who also prepared a related new metal-alkylated complex $(\eta^5\text{-}C_5H_5)Re(CO)_2(CH_3)(COCH_3)$ (Scheme 2.3) several years later.[14]

$$(\eta^5\text{-}C_5H_5)Re(CO)_3 \xrightarrow[h\nu]{Et_2SiH_2} (\eta^5\text{-}C_5H_5)Re(CO)_2(SiEt_2H)H$$

$$(\eta^5\text{-}C_5H_5)Re(CO)_2(SiEt_2H)H \xrightarrow[CHCl_3]{\text{Silicic acid}} (\eta^5\text{-}C_5H_5)Re(CO)_2H_2$$

$$(\eta^5\text{-}C_5H_5)Re(CO)_2H_2 \xrightarrow[\text{Ethanol}]{KOH} [(\eta^5\text{-}C_5H_5)Re(CO)_2]^{2-}$$

$$[(\eta^5\text{-}C_5H_5)Re(CO)_2]^{2-} \xrightarrow[THF]{MeI} (\eta^5\text{-}C_5H_5)Re(CO)_2Me_2$$

Scheme 2.2

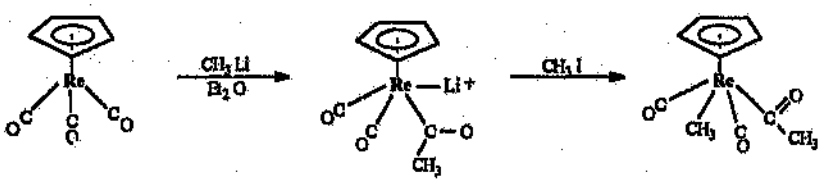

Scheme 2.3

The first synthesis of *lat*-(η^5-C_5Me_5)Re(CO)$_2$Me$_2$ and *diag*-(η^5-C_5Me_5)Re(CO)$_2$Et$_2$ were recently reported by Klahn *et al.* These compounds were obtained from the alkylation of the dichloride (η^5-C_5Me_5)Re(CO)$_2$Cl$_2$ using the corresponding organocopper reagent RCu (R = Me, Et).[15] The aryl-iodo and aryl-methyl derivatives *diag*-(η^5-C_5Me_5)Re(CO)$_2$(Ar)X (X = I, Me) were also prepared by using the corresponding organocopper reagent and methyl lithium.[16]

To date a total of seven alkyl complexes, (η^5-C_5H_5)Re(CO)$_2$(Br)(Me),[17] *diag*-(η^5-C_5H_5)Re(CO)$_2$(H)(CH_2Ph),[18] (η^5-C_5Me_5)Re(CH_3)$_4$,[19] *diag*-(η^5-C_5H_5)Re(CO)$_2$(Me)(COMe), *diag*-(η^5-C_5Me_5)Re(CO)$_2$Et$_2$, *diag*-(η^5-C_5Me_5)Re(CO)$_2$(Ph)I and *diag*-(η^5-C_5H_5)Re(CO)$_2$(η^1-PhCO)Br,[20] have been studied by X-ray crystallography (Table 2.2). No lateral isomer crystal structures have been reported to date.

2.1.3. Other Cyclopentadienyl Four-Legged Rhenium Complexes

The complexes *diag*- and *lat*-(η^5-C_5H_5)Re(CO)(L)Br$_2$ (L = CNC(CH_3)$_3$, P(OMe)$_3$, P(OEt)$_3$, P(OPh)$_3$) have been synthesized by the direct reactions of *diag*-(η^5-C_5H_5)Re(CO)$_2$Br$_2$ with ligand L in boiling benzene or toluene.[4ii] (η^5-C_5Me_5)Re(CO)(PMe_3)X$_2$ (X = Cl, Br, I) and *lat*-(η^5-C_5Me_5)Re(CO)(L)I$_2$ (L = P(OMe)$_3$, P(OPh)$_3$, PMe_3, PMe_2Ph) have also been prepared, but by indirect oxidation of (η^5-C_5Me_5)Re(CO)(PMe_3)N$_2$ with X$_2$ [21] or by Me_3NO induced decarbonylation of cationic [(η^5-C_5Me_5)Re(CO)$_2$(L)I]$^+$.[22]

Table 2.1. Cyclopentadienyl four-legged piano stool rhenium complexes[a]

No	Complex	year	ref.
1.	$(\eta^5\text{-}C_5H_5)Re(CO)_2Br_2$	1969	2
2.	$(\eta^5\text{-}C_5H_4R)Re(CO)_2Br_2$ (R = Me, I, CH_3COO)	1973	3
3.	$(\eta^5\text{-}C_5H_5)Re(CO)_2MeX$ (X = Me, Br)	1973,1983	3,13,17
4.	$(\eta^5\text{-}C_5H_5)Re(CO)_2I(HgCl)$	1973	3
5.	$(\eta^5\text{-}C_5H_5)Re(CO)_2Br(HgBr)$	1973	3
6.	$(\eta^5\text{-}C_5H_5)Re(CO)_2(X)H$ (X = Br, I)	1973	3
7.	$(\eta^5\text{-}C_5H_5)Re(CO)_2(I)(R)$ (R = CH_3, $COCH_3$, COC_6H_5)	1975	10
8.	diag- and lat-$(\eta^5\text{-}C_5H_5)Re(CO)_2Br_2$	1975	4
9.	diag- and lat-$(\eta^5\text{-}C_5H_5)Re(CO)(L)Br_2$ (L = CNtBu, $P(OMe)_3$, $P(OEt)_3$, $P(OPh)_3$)	1975	4
10.	lat-$(\eta^5\text{-}C_5H_5)Re(CO)_2(H)(CH_2Ph)$	1978	18
11.	diag-$(\eta^5\text{-}C_5H_5)Re(CO)_2XH$ (X = $SiPh_3$, $GeCl_3$, $GeBr_3$, $SnCl_3$) diag-$(\eta^5\text{-}C_5H_5)Re(CO)_2(L)_2$ (L = $GeCl_3$, $SnPh_3$) lat-$(\eta^5\text{-}C_5H_5)Re(CO)_2(L)H$ (L = $SiPh_3$, $Si(CH_2Ph)_3$, SiPhH)	1980	24
12.	$(\eta^5\text{-}C_5H_5)Re(CO)_2(SnCl_3)H$ $(\eta^5\text{-}C_5H_5)Re(CO)_2(SnMe_3)$	1981	12
13.	$(\eta^5\text{-}C_5H_5)Re(CO)_2(H)_2$	1981,1995	12,26
14.	$(\eta^5\text{-}C_5Me_5)Re(CO)_2(H)_2$	1982	33
15.	$(\eta^5\text{-}C_5H_5)Re(CO)_2(CH_3)H$	1983	13
16.	diag- and lat-$(\eta^5\text{-}C_5Me_5)Re(CO)_2X_2$ (X = Cl, Br, I)	1986	6,7
17.	$(\eta^5\text{-}C_5Me_5)Re(CH_3)_4$	1987	19
18.	$(\eta^5\text{-}C_5Me_5)Re[PPh(CH_3)_2]_2(H)_2$	1989	31
19.	$(\eta^5\text{-}C_5H_5)Re(CO)_2(CH_3)(COCH_3)$	1989	14
20.	diag- and lat-$(\eta^5\text{-}C_5Me_5)Re(CO)(PMe_3)X_2$ (X = Cl, Br, I)	1989	21
21.	diag-$(\eta^5\text{-}C_5Me_5)Re(CO)_2I(COOR)$ (R = Me, Et, ^{i}Pr)	1989	29
22.	lat-$[(\eta^5\text{-}C_5Me_5)Re(CO)_2(L)I]^+$ (L = $P(OMe)_3$, $P(OPh)_3$, PMe_3, PMe_2Ph)	1991	22,27
23.	diag-$(\eta^5\text{-}C_5Me_5)Re(CO)_2[PO(OCH_3)_2]I$	1991	30
24.	lat-$(\eta^5\text{-}C_5Me_5)Re(CO)(L)I_2$ (L = $P(OMe)_3$, $P(OPh)_3$, PMe_3, PMe_2Ph)	1994	22
25.	diag-$(\eta^5\text{-}C_5Me_5)ReX(CO)_2\{PO(OR)_2\}$ (X = Cl, Br, I; R = Me, Et)	1994	28
26.	diag-$(\eta^5\text{-}C_5Me_5)Re(CO)_2Et_2$	1996	15

	lat-(η^5-C_5Me_5)Re(CO)$_2$Me$_2$		
27.	diag-(η^5-C_5Me_5)Re(CO)$_2$(Ar)X (Ar = Ph, $PhCH_2$; X = I, Me)	1996	16
28.	diag- and lat-(η^5-C_5Me_5)Re(CO)$_2$(η^1-PhCO)X (X = Br, I)	1996	20
29.	diag- and lat-[(η^5-C_5Me_5)ReH(N_2)(PMe_3)$_2$]$^+$	1996	25
30	diag- and lat-(η^5-C_5Me_5)Re(CO)$_2$XY (X = D, Me; Y = D, Me, Cl)	1997	23
31	[(η^5: η^1-$C_5H_4CH_2CH_2N(CH_3)_2$)Re(CO)$_2$Br]$^+$ Br$^-$	1997	32

[a] Only complexes 1-23 had been prepared prior to the commencement of the work reported in this thesis.

Table 2.2. Cyclopentadienyl four-legged piano stool rhenium complexes which structures have been determined by X-ray diffraction

No	Complex	year	ref.
1.	diag-(η^5-C_5H_5)Re(CO)$_2$(Br)(Me)	1972	17
2.	lat-(η^5-C_5H_5)Re(CO)$_2$(H)(CH_2Ph)	1978	18
3.	diag-(η^5-C_5Me_5)Re(CO)$_2$Br$_2$	1985	6
4.	lat-(η^5-C_5Me_5)Re(CO)$_2$I$_2$	1985	6
5.	(η^5-C_5Me_5)Re(CH_3)$_4$	1987	19
6.	dia$_2$-(η^5-C_5Me_5)Re[PPh(CH_3)$_2$](H)$_2$	1989	31
7.	diag-(η^5-C_5H_5)Re(CO)$_2$(Me)(COMe)	1989	14
8.	diag-(η^5-C_5Me_5)Re(CO)$_2$[PO(OCH_3)$_2$]I	1991	30
9.	diag-(η^5-C_5H_5)Re(CO)$_2$($SnPh_3$)$_2$	1995	26
10.	diag-(η^5-C_5Me_5)Re(CO)$_2$Et$_2$	1996	15
11.	diag-(η^5-C_5Me_5)Re(CO)$_2$(Ph)I	1996	16
12.	diag-(η^5-C_5H_5)Re(CO)$_2$(η^1-PhCO)I	1996	20
13.	diag-(η^5-C_5Me_5)Re(CO)$_2$(H)$_2$	1997	23

The synthesis and photochemical isomerization reactions of *diag-* and *lat*-(η^5-C_5Me_5)$Re(CO)_2(H)_2$ have been recently reported.[23] The preparation method was similar to that used for preparing (η^5-C_5H_5)$Re(CO)_2(H)_2$ i.e. *via* Zn/HOAc reduction of dicarbonyl dihalo compounds.[13]

The preparation of (η^5-C_5H_5)$Re(CO)_2XH$ (X = $SiPh_3$, GeX_3, $SnCl_3$),[24] (η^5-C_5Me_5)$Re(H)(N_2)(PMe_3)_2^+$,[25] *diag*-(η^5-C_5H_5)$Re(CO)_2(SnPh_3)_2$,[26] [(η^5-C_5Me_5)$ReX(CO)_2${$P(OR)_3$}]$^+$,[27] *diag*-(η^5-C_5Me_5)$ReX(CO)_2${$PO(OR)_2$},[28] *diag*-(η^5-C_5Me_5)$Re(CO)_2(I)(COOR)$,[29] *diag*-(η^5-C_5Me_5)$Re(CO)_2[PO(OCH_3)_2]I$,[30] *diag*-(η^5-C_5Me_5)$Re[PPh(CH_3)_2](H)_2$[31] and [(η^5: η^1-$C_5H_4CH_2CH_2N(CH_3)_2$)$Re(CO)_2Br]^+$ Br^-[32] have also been reported (Table 2.1).

2.1.4. Summary

Not including the work reported in this thesis, only seventy compounds and thirteen crystal structures have been reported for cyclopentadienyl four-legged piano stool rhenium complexes to date. The solution isomerization reactions and mechanisms of these complexes have been extensively studied, but no solid-state isomerization has been reported. Little detail of the synthesis and chemical reactivities of diagonal and lateral monosubstituted cyclopentadienyl rhenium complexes have been reported.

2.2. Solid-State Reactions

2.2.1 Solid-State Isomerization Reactions of Organometallic Complexes

Studies on solid-state isomerization reactions of organometallic complexes have been little discussed. The only exception has related to the systematic study of cobaloxime complexes in which isomerization of the ligand attached to the metal was noted. Since the first discovery of the X-ray induced racemisation of the chiral cyanoethyl (cn) group in a cobaloxime complex in 1977 by Ohashi *et al* (Figure 2.2),[34] related complexes have been thoroughly studied. It has also been found that chiral groups bonded to the cobalt atom can also racemize under visible light.[35-37] The above complexes entail isomerization of the ligand and do not entail isomerization at the metal atom.

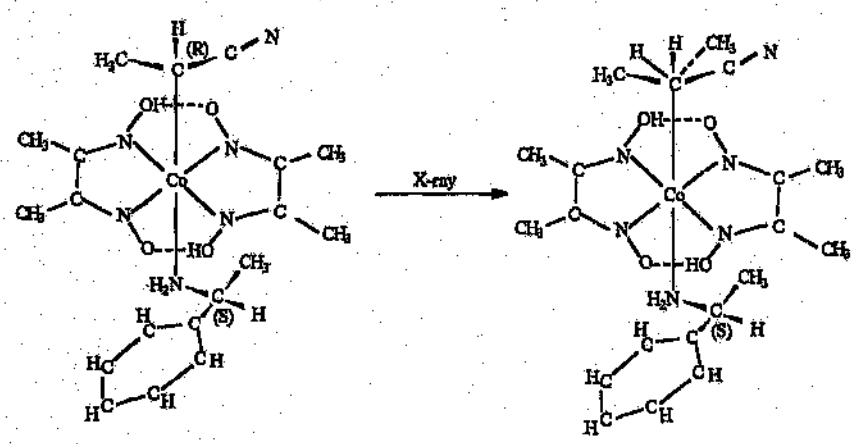

Figure 2.2. Racemization of the cn group in a crystal of a cobalt complex

2.2.2. Solid-State Isomerization Reactions of Coordination Compounds

Solid-state isomerization reactions of coordination complexes were first recognized by Werner in the early 1900's.[38] Since then numerous studies have been reported on these types of reactions but it is only since the 1960's that significant advances in the explanation of the phenomena have been achieved. This has been brought about by the availability of modern physical techniques, particularly thermogravimetric analysis (TGA) and differential thermal calorimetry (DSC). LeMay reviewed the area of solid state coordination compounds ten years ago.[39]

Solid-state *cis-trans* isomerization reactions of four-coordinate square planar platinum complexes PtL_2X_2 (L = neutral donor ligand, X = halide), were reported by Orchin *et al* in 1970.[40] They inadvertently found that pure *trans*-$Pt(CO)(NH_2R)Cl_2$ (e.g. R = CHMePh) directly rearranges to the *cis* isomer under thermal conditions. The isomerization processes were studied by DTA/TGA methods. Since that time, the solid-state isomerization reactions of platinum complexes have been thoroughly investigated by varying the halide (X) and ligand (L), e.g. by use of phosphines,[41-44] amines,[45-51] sulfoxides,[46,52,53] oximes,[54] thiophanes.[55-57]

The six-coordinate transition metal complexes $[MX_2(a\text{-}a)_2]X$, where M = Co(III), Cr(III); a-a = diamine; X = halide, e.g. *trans*-$[CoCl_2(Pn)_2](H_5O_2)Cl_2$ [58,59] and *trans*-$[CoBr_2(Pn)_2](H_5O_2)Br_2$ (Pn = propylenediamine),[60] were reported in 1968 to

undergo a solid-state isomerization reaction. However, the presence of the H_2O in these complexes resulted in the isomerization and melting processes being inseparable in many instances. A so-called "aquation-anation" isomerization mechanism was proposed to explain the findings.[59,60] Later it was observed that *trans*-$[CrBr_2(Pn)_2]Br \cdot H_2O$ was found to isomerize in the anhydrous state, and this led to alternative mechanistic proposals.[61-63]

Ruthenium six-coordinate complexes have also been found to undergo similar solid-phase rearrangements.[64,65] The *cis-trans* solid-state isomerization of ML_2X_2 (L = mono or bidentate donor ligand) can proceed either *via* an intramolecular bond rupture process [50,66,67] or *via* an intramolecular twist mechanism.[68]

Topochemical studies have shown that most solid-state reactions which involve coordination compounds proceed *via* a nuclear formation and growth mechanism. The topography and kinetics of these solid-state isomerization processes are determined by the crystal structures of the initial material and the reaction product, and by the contact conditions at the interface.[69-71]

Generally, the reactants and products obtained from the solid-state isomerization reactions are determined from IR and NMR spectroscopic studies, while the isomerization energy change is measured in DSC or DTA experiments. Thermomicrography has been used for topochemical, topography and kinetics studies. X-ray powder and single crystal diffraction techniques are very useful tools

for mechanistic studies of solid-state isomerization reactions of coordination compounds. In recent years, atomic force microscopy (AFM) has been shown to be a powerful technique for investigating solid-state reactions of organic crystals.[72]

Another type of solid-state isomerization reaction that has been studied is the nitrito-nitro linkage isomerization of some Co(III)-amine complexes, e.g. $[Co(NH_3)_5ONO]XY \longleftrightarrow [Co(NH_3)_5NO_2]XY$ (XY = Cl_2, Br_2, I_2, $(NO_3)_2$, $Cl(NO_3)$). Transition metals other than cobalt have also been studied and much effort has been made to clarify the mechanism of this solid-state isomerization reaction.

As early as the end of last century, both nitro (NO_2, nitrogen coordination) and nitrito (ONO, oxygen coordination) cobalt isomers were synthesized by Jorgensen. He found that ONO isomers could be synthesized in solution reactions as well as by irradiating the corresponding s[illegible]s in the solid state (Scheme 2.3).[73] A solid-state reversible isomerization reaction was achieved by employing thermal and photochemical reaction conditions.

$$[Co(NH_3)_5ONO]X_2 \underset{h\nu}{\overset{\Delta\ Sol^{n}}{\rightleftharpoons}} [Co(NH_3)_5NO_2]X_2 \quad \text{(Solid-State)}$$

Scheme 2.3

Structural studies, initiated by Grenthe and Nordin in 1978, were used to probe the mechanism of the above isomerization reaction. The isomerization reaction was

shown to be intramolecular, with no exchange of the ligands between different complex cations.[74] They also found that the powder diffraction patterns of $[Co(NH_3)ONO]Cl_2$, obtained either after precipitation of the complex from aqueous solutions, or after photochemical synthesis, differed. This indicated that the solid-state nitro-nitrito isomerization reaction produced two polymorphs of the nitrito-chloride complex.

An attempt to use single crystal techniques to study the structure of photochemically synthesized $[Co(NH_3)ONO]Cl_2$ was not successful, because the crystals fragmented as a result of mechanical stress generated during the photochemical reaction.[75] The structure of the photochemically synthesized $[Co(NH_3)ONO]Cl_2$ was finally solved, by using a tedious and complex X-ray powder diffraction technique.[76]

The kinetics of the above solid-state linkage isomerization, the effect of the crystalline surroundings (different anions, XY) and the application of hydrostatic pressure on the intramolecular linkage isomerization of Co(III)-amine complexes have also been reported.[77-81]

2.2.3. Surface-mediated Organometallic Synthesis

Although surface organometallic chemistry is a relatively new field of study, it has attracted some interest in the last decade. The basic concept in the field, is to use the interaction between organometallic compounds and inorganic oxides (silica,

alumina, magnesia and zeolites) to activate some chemical bonds in an organometallic complex. In the presence of other reactants such as CO, new organometallic compounds or catalyst precursors could be formed on the surface of inorganic oxides by thermal or irradiation procedures.

By using this methodology, $[Ir(CO)_3Cl]_n$, $[Rh(CO)_2Cl]_2$, $[Ru(CO)_3Cl_2]_2$, $[Os(CO)_3Cl_2]_2$, and the related clusters $[Ir_4(CO)_{12}]$, $[Rh_4(CO)_{12}]$ and $[Rh_6(CO)_{16}]$ have been synthesized in high yields from the corresponding metal trichloride supported on the silica surface by reductive carbonylation at atmospheric pressure.[82] Addition of an alkali carbonate to silica favors removal of chloro ligands and allows for the synthesis of neutral and even anionic metal carbonyl clusters. Therefore, $[M_3(CO)_{12}]$, $[H_4M_4(CO)_{12}]$ (M = Ru, Os) and various anionic ruthenium and osmium carbonyl clusters have been synthesized selectively and in high yields by reductive carbonylation at atmospheric pressure of $MCl_3 \cdot H_2O$ or $[M(CO)_3Cl_2]_2$ supported on silica in the presence of alkali carbonates.[83,84] A number of other transition metal carbonyl complexes and clusters have been synthesized by the same strategy.[85-92] Mechanisms for the surface reaction processes have been proposed.[93,94] Recently, these structurally well-defined transition metal complexes or clusters have been used as catalysts or catalyst precursors for organic reactions such as catalytic toluene hydrogenation and ethylene hydroformylation.[95-98]

2.2.4. Solid-Gas Organometallic Reactions

One of the earliest reported reactions between an 'organometallic' complex and a gas molecule, in the solid state, is the report of a series of Vaska type complexes with gaseous alkyl halides.[99] During the intensive investigation of organometallic heterogeneous reactions, other organometallic solid-gas reactions have been observed and finally systematic studies have started to appear in recent years.[100] Solid-gas reactions between transition metal complexes such as $Rh(PPh_3)_3Cl$,[101] 'tripodal polyphosphine' Ni [102] and Ir complexes,[103] and small molecules, such as CO, ethylene, have been shown to occur within the constraining environment of the reactant crystal lattice. This environment controls both the kinetic behavior and the nature of the products.[104] Because the gaseous molecules penetrate the crystals of the solid reactant, the solid-gas reaction kinetics and products depend on the physical and chemical nature of both the organometallic compound and the gaseous molecules. It has been found that the diffusion of small organic molecules into the crystals of a solid reactant is favored when the latter contains an extensive hydrophobic region provided by the carbon backbones of the ligands.[105-107]

Very few non solid-gas organometallic solid-state reactions have been mentioned in the literature.[108,109]

2.2.5. Theoretical Approaches to the Study of Organometallic Solid-State Chemistry.

Modern X-ray diffraction techniques allows one to precisely and accurately determine the molecular structures in organometallic crystals. However, the chemical and physical properties of solid organometallic compounds not only depend on the individual molecular components and structures, but also, and more importantly, depend on other factors such as intermolecular interaction, reaction cavity, steric compression and reaction-induced stress. Clearly, we cannot predict and explain the *crystal or solid properties* by only considering the *molecular structures*. Therefore, much effort has been put into finding the relationship between isolated molecules and a collection of molecules. One approach is via statistical methods such as the examination of structures stored in the Cambridge Structure Database (CSD).[110] Another is *via* theoretical calculations such as extended-Hückel calculations and packing potential energy calculations. Many interesting results have been obtained by these procedures and reviews in this field have been published (Braga and Grepioni).[111,112]

The developments in solid-state organic chemistry have been significant,[113-118] and since the areas of organometallic and organic chemistry have much in common much of the information should be transferable between the fields. However the differences between the fields should also result in unique features being associated with solid-state organometallic chemistry.[112]

2.2.6. Summary

The solid-state isomerization reactions of four or six coordinate transition metal complexes of the type ML_2X_2 (L = mono, or, bidentate donor ligand) have been studied for nearly one hundred years. In recent years organometallic solid-gas reactions mediated or not mediated by inorganic oxides have been investigated. However, very few non solid-gas solid-state reactions of organometallic compounds have been reported to date.

2.3. Catalytic Isomerization

2.3.1. Introduction

Since the discovery of isomers of coordination compounds, many catalytic isomerization reactions have been observed and studied. These include square-planar *cis-trans,* octahedral *cis-trans*, linkage and *fac-mer* isomerization reactions. Most involve metals such as platinum, chromium, palladium, cobalt, ruthenium, molybd num, copper and nickel. Two mechanisms, consecutive displacement and intramolecular rearrangement of five-coordinate intermediates, have been proposed for the catalyzed isomerization of square-planar complexes.

In nearly all cases the complexes studied did not have a metal-carbon bond in the complex and are hence strictly speaking not organometallic complexes.

Two generalizations can be made : (1) many of the isomerization reactions proceed in the presence of neutral or ionic free ligands as catalysts,[119] (2) isomerization

reactions which can be catalyzed offer a mild, high yielding , sometimes unique, route to isomer synthesis.

2.3.2. Catalyzed Isomerization Reactions

The catalysts used for the isomerization reactions of organometallic/coordination complexes can be placed into three categories: ligands, metal ions and acid-base.

(1) ligands

Free ligands often catalyze the isomerization reactions. These ligands comprise part of the complex under study and numerous reactions have been catalyzed using this procedure. Below some typical examples are discussed.

Stoufer *et al* found that only *cis*-$[PtX_2(PPh_3)_2]$ (X = Cl, Br) and not the *trans* isomer was isolated from a reaction mixture. This was shown to arise from the presence of a trace of free triphenylphosphine in the reaction mixture which catalyzed the *trans* to *cis* isomerization of $[PtX_2(PPh_3)_2]$. It was possible to isolate the *trans* isomer by "tying up" the free ligand.[120] Similar catalytic effects using other tertiary phosphines have been reported by other authors and the mechanism has been investigated for these isomerization reactions.[121]

In addition to tertiary phosphine ligands, Erickson *et al* reported that both Cl^- and Me_2SO catalyzed the isomerization of complexes of the type [Pt(N-O)(Me_2SO)Cl] where N-O is the anion of an α-amino acid.[122] Later, the kinetics and mechanism of

this reaction were studied by Cattalini *et al.*[123] Water was also found to increase the *trans-cis* isomerization rate of bis(oxalato) diaquochromate complexes, in which a so-called "reversed micelle catalysis" was reported.[124]

(2) metal ions

The common metal ions that have been used as isomerization catalysts are ions of mercury, lanthanum, cobalt and magnesium.

Sutin *et al* reported that the linkage isomerization of $[Co(NH_3)_5SCN]^{2+}$ to the more stable nitrogen-bonded isomer $[Co(NH_3)_5NCS]^{2+}$ was catalyzed by mercury (II).[125] Cross *et al* found that treatment of solutions of *cis*-$[Pt(C{\equiv}CPh)_2(PMePh_2)_2]$ with a catalytic amount of $HgCl_2$, steadily converted the *cis* isomer into the *trans* isomer. The process was faster in THF than in $CHCl_3$ or toluene.[126]

Huchital *et al* systematically investigated the catalytic conversion of *trans*-bis(oxalato)diaquochromate (III) and *trans*-bis(malonato) diaquochromate (III) to the *cis* isomer in the presence of lanthanide ions. They suggested that the reaction mechanism was related to the formation of monocarboxylate complex intermediates.[127] This reaction was also catalyzed by $CoSO_4$ [128] and $MgSO_4$.[129] A similar ring-opening mechanism was confirmed.

(3) acid-base

Krause *et al* reported that the hydroxide ion catalyzed the conversion of *trans*-γ-

$[Ru(AZPy)_2Cl_2]$ to the *cis*-β and *cis*-α isomers.[130] Hydroxide ion was also found to catalyze the linkage isomerization of *cis*- and *trans*-$[Co(en)_2(ONO)_2]^+$. The volumes of activation indicated an intramolecular isomerization process.[131]

Other acid catalyzed isomerization reactions include the linkage isomerization of $[Cr(en)_2(CN)_2]^+$,[132] *fac-mer* isomerization of $[W(CO)_3(dppm\text{-}pp)L]$ (dppm = $Ph_2PCH_2PPh_2$, L = PEt_3 or PEt_2Ph),[133] and *cis-trans* isomerization of $[Cr(oxalato)_2(H_2O)_2]^-$.[134]

Some isomerization reactions have been found to be both acid and base catalyzed.[135]

2.3.3. Mechanism of the Catalyzed Isomerization Reaction

For the trialkyl phosphine catalyzed isomerization of square-planar complexes $[MX_2L_2]$, two mechanisms have been proposed. Basolo and Pearson postulated a consecutive displacement mechanism (Scheme 2.6).[136]

Haake and co-workers, by contrast, postulated a pseudorotation mechanism involving "a distorted penta-coordinate state in which L' occupies a unique position. This distorted state must be able to undergo fluxional change which interconverts the positions of L and X and, therefore enables isomerization" to occur (Scheme 2.7).[137]

It seems that both mechanisms are applicable, and depend on the complexes, ligands, and solvents used in the appropriate study.

The mechanism of metal-ion catalyzed isomerization reactions have also been explored.

Metal ions were thought to attack coordinated ligands, alter the rate of ligand replacement, participate in the removal of unidentate ligands, and promote isomerization (Scheme 2.8).[126]

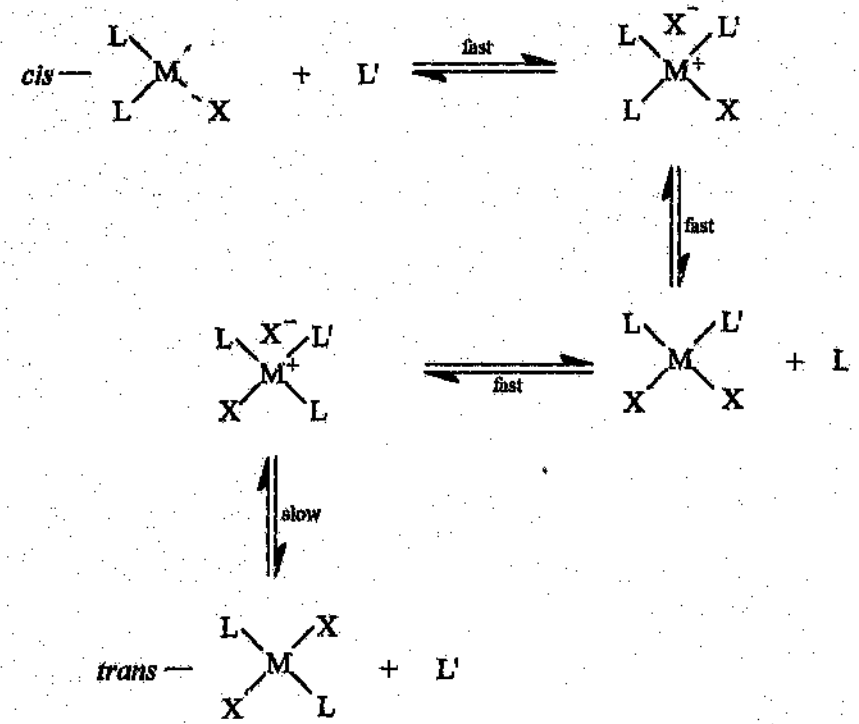

Scheme 2.6. The consecutive displacement mechanism

Lanthanium, cobalt and magnesium ions are proposed to be involved in a similar mechanism to that shown in Scheme 2.8.

2.3.4. Summary

Metal ions, acids-bases and ligands, especially trialkyl phosphines, catalyze isomerization reactions of metal containing complexes and have been thoroughly investigated in the solution phase. The kinetics and mechanisms of these isomerization reactions have also been reported. Most studies concentrated on *cis-trans* isomerization of square-planar complexes.

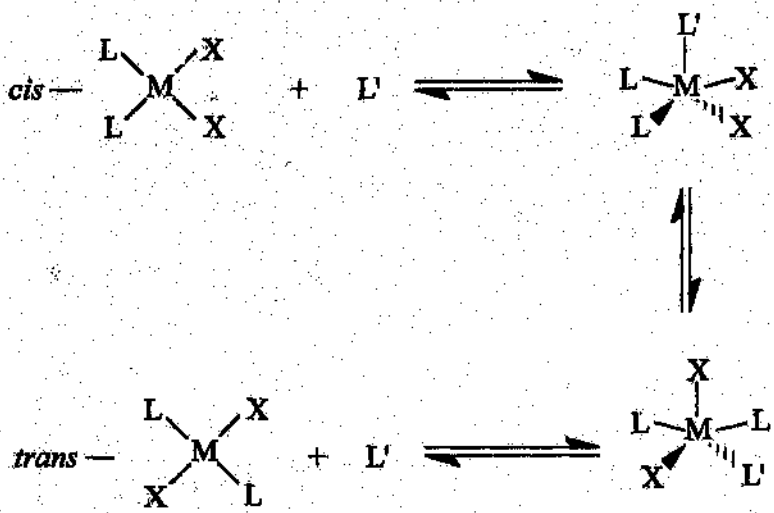

Scheme 2.7. The pseudorotation mechanism

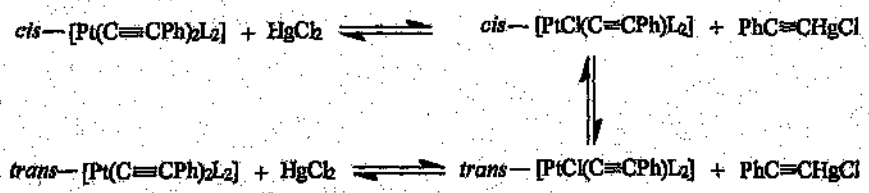

Scheme 2.8. The mechanism for mercury ion catalyzed *cis-trans* isomerization

2.4. Silica Gel Catalyzed Reactions

2.4.1. Introduction

It appears that little in the field of organometallic chemistry has been described in the literature in this area of chemistry. To indicate the potential of the area some examples from the organic chemistry literature will thus be described. The reason for this relates to some work described in this thesis (see Chapter 5).

Silica gel as a catalyst has attracted much interest owing to its simplicity, efficiency, selectivity, cheapness and commercial availability. Many kinds of (mainly) organic reactions are catalyzed by silica gel under mild conditions in high yield and usually in excellent purity. Some photochemical reactions and solid state reactions on silica gel surfaces have been reported and differences arising from the different reaction media (solution or solid state) have been noted. Two reviews [138,139] and one thesis report [140] in this field have already appeared in the literature.

2.4.2. Catalytic organic reactions

(1) Isomerization

It was found that aldoximes isomerized into the corresponding amids in high yields when refluxed in xylene in the presence of activated silica gel (Scheme 2.9).[141]

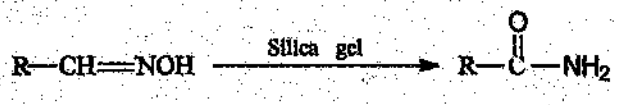

Scheme 2.9

Some catalytic isomerization reactions even occurred at room temperature. For example, contact of *cis*-aldehyde (**1**) with a silica gel column in chloroform at room temperature produced the *trans*-isomer quantitatively.[141]

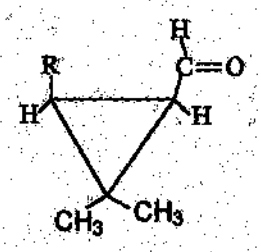

(1)

Ellis *et al* reported that irradiation at 514.5 nm wavelength of a cyclohexane slurry of silica gel containing *all-trans*-retinal yielded a mixture of four isomers. It was suggested that the silanol groups of silica gel serve as the primary binding sites. Retention of the isomers by silica gel was noted and this resulted in incomplete recovery of the products.[143]

(2) Oxidation

Photooxidation of 1,4-diphenyl-1,3-butadiene and 1,3-cyclohexdiene, and some aryl-substituted ethylenes, such as tetraphenylethylene, 1,1-diphenylethylene, *trans*-stilbene, on silica gel has been reported.[144,145] It was also observed that, in the presence of silica gel, methane and cyclopentenones reacted directly with oxygen to form formaldehyde and hydroxyl derivatives.[146,147]

(3) Bromination

The reaction of alkoxybenzenes with N-bromosuccinimide catalyzed by silica gel in carbon tetrachloride at room temperature produced monobromination products in high yields and good selectivity.[148] A similarly excellent yield and selectivity was observed for the reaction of estradiol, estrone, ethynylestradiol or 2,4-dibromoestradiol with bromine in the presence of silica gel at room temperature.[149] Silica gel also catalyzed the chlorination of aromatic compounds.[150-153]

(4) Cycloaddition

It was found that silica gel promoted effective Diels-Alder addition of 3-methoxycarbonyl-2-pyrone with butyl vinyl ether and with benzyl vinyl ether at room temperature to form only the *endo* bicyclic diastereomer, shown in Scheme 2.10.[154]

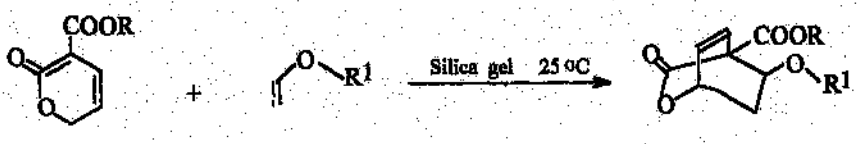

Scheme 2.10

(5) Hydrohalogenation

Appropriately treated silica gel has been found to mediate the addition of HCl, HBr and HI to alkenes, such as cycloheptene, 1-octene, and 3,3-dimethyl-1-butene (Scheme 2.11). The authors proposed a mechanism for this surface-mediated addition/elimination reaction.[155,156]

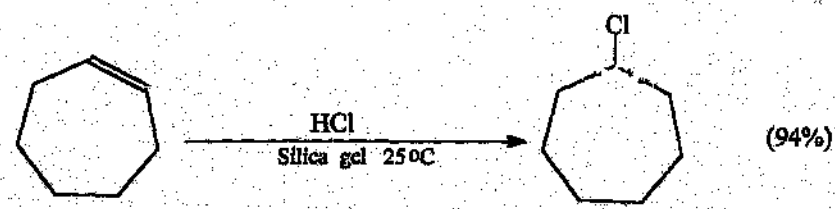

Scheme 2.11

(6) Knoevenagel condensation

Knoevenagel condensation of peptidyl cyanomethyl ketones with aromatic aldehydes and ketones was catalyzed by silica gel and the transformation was brought about without significant epimerization (Scheme 2.12).[157]

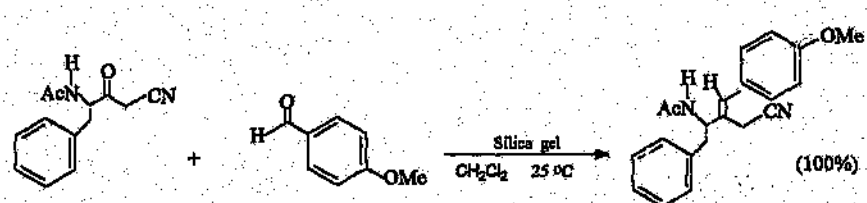

Scheme 2.12

In addition, silica gel has also been found to catalyze cyclization,[158] cyclodehydration,[159] alcohol methylation,[160] dehydrohalogenation,[161] esterification,[162] enantioselective hydantoinase mimics,[163] photolysis,[164] and the

water gas shift reactions.[165]

It is thus clear that the area of silica mediated organic chemistry is well established.

2.4.3. Catalyzed Reactions in Dry Media

Except for a few reactions initiated by heat and pulverization, most reactions on dry silica gel surface have been induced by irradiation. Results have shown that high yields of relatively pure products can be obtained by this process.

(1) Photosubstitution

Irradiation of solid Λ-*cis*-$[CoCl_2(en)_2]^+$ complex and potassium carbonate or hydroxamates ligand RCONHOK adsorbed on a silica gel thin layer formed only one reaction product in high yield (Scheme 2.13). It was suggested that the nucleophilic character of the silica gel OH groups very probably plays an important role in the reaction.[166]

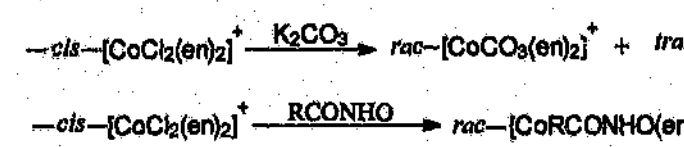

Scheme 2.13

(2) Oxidative cleavage

It was observed that substituted phenylethylenes adsorbed on chromatographic grade silica gel were oxidatively cleaved to ketones or aldehydes under illumination in the presence of oxygen . Photoreactions of some electron-rich olefins led mainly to dimerization, not oxidation.[167]

(3) Photo-Fries rearrangement

Comparing the same reaction in solution, the amide Photo-Fries rearrangement on dry silica gel had a higher quantum yield and a greater selectivity towards the *ortho* product (Scheme 2.14).[168]

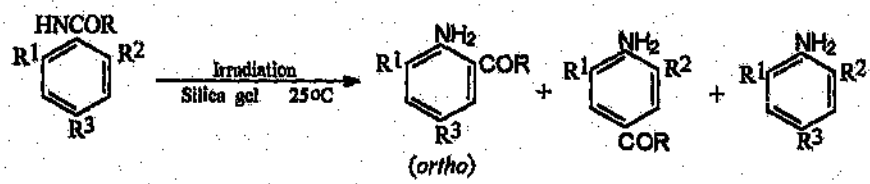

Scheme 2.14

(4) Isomerization

On irradiation on a dry silica gel surface, 2-(dialkylamino)ethyl-3-benzylacrylates underwent selective E-Z isomerization. Competing processes, such as remote-hydrogen abstraction via a charge-transfer state, on photoisomerization in solution were completely suppressed on the solid surface. Thermal isomerization of the Z to the E isomer also occurred on the silica gel surface.[169]

(5) Photolysis

The photolysis of α-methoxy acetophenones in solution, generally in methanol,

which was thought to have a similar polarity to that of silica gel, and on a silica gel surface have been reported. A major deviation in the reaction pathway was found owing to two functions of silica gel on the reacting species: conformational control and restricted movement.[170,171]

(6) Cyclization

Silica gel mediated a novel cyclization of 1,1,1,2,2-pentafluoroalkan-3,4-dione-4-diakyl hydrazones to afford 5-trifluoromethyl-4-pyridazinones in high yield (Scheme 2.15). This was a thermal reaction, obtained by heating the starting material adsorbed on silica gel at 70-90 °C.[172]

(7) Reaction of iodosobenzene with unsaturated hydrocarbons

The silica gel was first treated with hydrogen halide HX, then mixed with iodosobenzene and unsaturated hydrocarbons, such as *trans*-stilbene. Pulverization of the solid mixture of the starting materials gave halogenated or oxidized products in good yields (Scheme 2.16).[173]

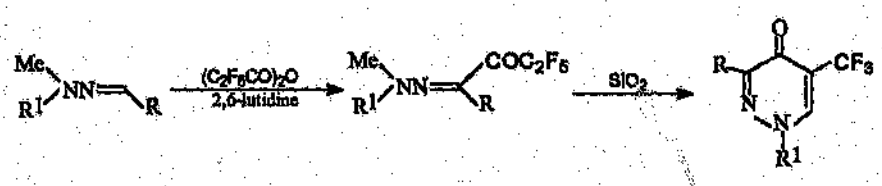

Scheme 2.15

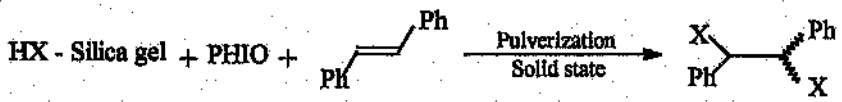

Scheme 2.16

2.4.4. Catalytic Mechanism on Silica Gel

The precise and detailed catalytic mechanism to explain the use of silica gel in the above reaction has not as yet been reported. However, it is clear that the silica gel surface is composed of siloxane and silanol functional groups. The silanol groups, which may be isolated, vicinal or germinal, are not uniformly distributed (Figure 2.3).

These groups constitute the principal sites for the adsorption of organic and inorganic molecules on the silica gel surface. Electrostatic interactions, dispersion forces, and hydrogen bonding (8-40 KJ/mol) are assumed to be the forces responsible for the adsorption. What is clear is that the -OH groups on the silica gel surface play an important role in the catalytic reactions and the type and amount of OH groups should be related to the activity.

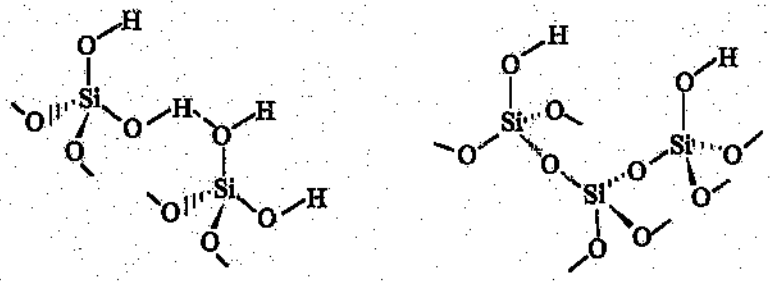

Figure 2.3 Surface siloxane and silanol functional groups of silica gel.

2.4.5. Summary

Silica gel has been successfully used as a catalyst for many organic reactions, either in solution or in the solid state. Practical, simple, inexpensive and environmentally benign are the attractive characteristics associated with the material. However, silica gel catalysts have not been used in organometallic syntheses and reactions. Indeed, only one preliminary result of a solid state photosubstitution reaction of a coordinate complex adsorbed on silica gel has been reported.[166]

2.5. Conclusion

Synthetic solid-state organometallic chemistry has been little developed to date. The many reports of solid-state reactions of coordination complexes and organic compounds indicate that synthetic and reactivity studies should be possible.

2.6. References

1. Green, M. L. H.; Wilkinson, G. *J. Chem. Soc.* **1958**, 4314.
2. Nesmeyanov, A. N.; Kolobova, N. E.; Makarov, Yu. V.; Anisimov, K. N. *Izv. Akad. Nauk SSSR, Ser. Khim.* **1969**, 1826.
3. Nesmeyanov, A. N.; Kolobova, N. E.; Makarov, Yu. V.; Anisimov, K. N. *Zh. Obstch. Khim.* **1974**, *44*, 2222.
4. (a) King, R. B.; Reimann, R. H.; Darensbourg, D. J. *J. Organomet. Chem.* **1975**, *93*, C23. (b) King, R. B.; Reimann, R. H. *Inorg. Chem.* **1975**, *15*, 179.
5. (a) Brown, T. L.; Darensbourg, D. J. *Inorg. Chem.* **1967**, *6*, 971. (b) Beck, W.; Melnikoff, A.; Stahl, R. *Angew. Chem.* **1965**, *77*, 719. (c) Manning, A. R. *J. Chem. Soc. A* **1967**, 1984.
6. Einstein, F. W. B.; Klahn-Oliva, A. H.; Sutton, D.; Tyers, K. G. *Organometallic,* **1986**, *5*, 53.
7. Diaz, G.; Klahn, A. H.; Manzur, C. *Polyhedron* **1988**, *7*, 2743.
8. Hill, R. H.; Palmer, B. J. *Organometallics* **1989**, *8*, 1651.
9. Palmer, B. J.; Becalska, A.; Hader, R.; Hill, R. H. *Polyhedron* **1991**, *10*, 877.
10. Nesmeyanov, A. N.; Kolobova, N. E.; Makarov, Yu. V.; Kazimirchuk, E. I.; Anisimov, K. N. *Izves. Akad. Nauk SSSR, Ser. Khim.* **1976**, *1*, 159.
11. Nunn, C. M.; Cowley, A. H.; Lee, S. W.; Richmond, M. G. *Inorg. Chem.* **1990**, *29*, 2105.

12. Hoyano, J. K.; Graham, W. A. G. *Organometallics* **1982**, *1*, 783.

13. Yang, G. K.; Bergman, R. G. *J. Am. Chem. Soc.* **1983**, *105*, 6500.

14. Goldberg, K. I.; Bergman, R. G. *J. Am. Chem. Soc.* **1989**, *111*, 1285.

15. Klahn, A. H.; Manzur, C.; Toro, A.; Moore, M. *J. Organomet. Chem.* **1996**, *516*, 51.

16. Klahn, A. H.; Toro, A.; Arenas, M.; Manriquez, V.; Whittle, O. *J. Organomet. Chem.* **1997**, *532*, 39

17. Aleksandrov, G. G.; Struchkov, Yu. T.; Makarov, Yu. V. *Zhurnal Strukturnoi Khimii* **1973**, *14*, 98.

18. Fischer, E. O.; Frank, A. *Chem. Ber.* **1978**, *111*, 3740.

19. Floel, M.; Herdtweck, E.; Wagner, W.; Kulpe, J.; Harter, P.; Herrmann, W. A. *Angew. Chem., Int. Ed. Engl.* **1987**, *26*, 787.

20. Filippou, A. C.; Lungwitz, B.; Kociok-Kohn, G.; Hinz, I. *J. Organomet. Chem.* **1996**, *524*, 133.

21. Klahn-Oliva, A. H.; Singer, R. D.; Aramini, M.; Sutton, D. *Inorg. Chem.* **1989**, *28*, 4217.

22. Arenas, M.; Silva, S.; Toro, A.; Klahn, A. H. *Bol. Soc. Chil. Quim.* **1994**, *39*, 285.

23. Ball, P. G.; Campen, A. K.; Graham, W. A. G.; Hamley, P. A.; Kazarian, S. G.; Ollino, M. A.; Poliakoff, M.; Rest, A. J.; Sturgeoff, L.; Whitewell, L. *Inorg. Chim. Acta* **1997**, *259*, 137.

24. Dong, D. F.; Hoyano, J. K.; Graham, W. A. G. *Can. J. Chem.* **1980**, *59*, 1455.

25. Cusanelli, A.; Sutton, D.; *Organometallics* **1996**, *15*, 3717.

26. Lee, S. W.; Yang, K.; Martin, J. A.; Bott, S. G.; Richmond, M. G. *Inorg. Chim. Acta* **1995**, *232*, 57.

27. Klahn, A. H.; Leiva, C.; Mossert, K.; Zhang, X. *Polyhedron* **1991**. *10*, 1873.

28. Leiva, C.; Mossert, K.; Klahn, A. H.; Sutton, D. *J. Organomet. Chem.* **1994**, *469*, 69.

29. Klahn, A. H.; Manzur, C. *Polyhedron* **1990**, *9*, 1131.

30. Einstein, F. W. B.; Rickard, C. E. F.; Klahn, H.; Leiva, C. *Acta Crystallogr., Sect. C* **1991**, *47*, 862

31. Herrmann, W. A.; Theiler, H. G.; Herdtweck, E.; Kiprof, P. *J. Organomet. Chem.* **1989**, *367*, 291.

32. Wang, T. F.; Hwu, C. C.; Tsai, C, W.; Lin, K. J. *Organometallics* **1997**, *16*, 3089.

33. Hoyano, J. K.; Graham, W. A. G. *J. Am. Chem. Soc.* **1982**, *104*, 3722.

34. Ohashi, Y.; Sasada, Y. *Nature* **1977**, *267*, 142.

35. Ohashi, Y.; Yanagi, K.; Kurihara, T.; Sasada, Y.; Ohgo, Y. *J. Am. Chem. Soc.* **1981**, *103*, 5805.

36. Ohashi, Y. *Acc. Chem. Res.* **1988**, *21*, 268.

37. Sekine, A.; Tatsuki, H.; Ohashi, Y. *J. Organomet. Chem.* **1997**, *536-537*, 389.

38. Werner, A.; Frohlich, A. *Chem. Ber.* **1907**, *40*, 2228.

39. LeMay, H.E. Jr. In Comprehensive Coordination Chemistry; G. Wilkinson, G.; Gillard, R. D.; McLeverty, J. A. Eds.; Pergamon Press, New York, 1987, Vol.1, P463.

40. Ellis, R.; Weil, T. A.; Orchin, M. *J. Am. Chem. Soc.* **1970**, 1078.

41. Kukushkin, Yu. N.; Sedova, G. N.; Demchenko, L. N. *Koord. Khim.* **1980**, *6*, 967.

42. Kukushkin, Yu. N.; Budanova, V. F.; Sedova, G. N.; Pogareva, V. G. *Zh. Neorg. Khim.* **1977**, *22*, 1305.

43. Kukushkin, Yu. N.; Budanova, V. F.; Sedova, G. N. *Zh. Neorg. Khim.* **1976**, *21*, 1405.

44. Allen, E. A.; Del Graudio, J.; Wilkinson, W. *Thermochim. Acta* **1975**, *11*, 197.

45. Kukushkin, Yu. N.; Fedotova, G. P.; Yustratova, V. F.; Postnikova, E. S. *Zh. Neorg. Khim.* **1979**, *24*, 730.

46. Kukushkin, Yu. N.; Budanova, V. F.; Sedova, G. N. *Zh. Neorg. Khim.* **1977**, *22*, 551.

47. Kukushkin, Yu. N.; Stefanova, O. V. *Zh. Neorg. Khim.* **1977**, *22*, 851.

48. Astakhova, N. A.; Bondarenko, V. S.; Gabuda, S. P.; Malchikov, G. D.; Shestakova, N. A. *Zh. Strukt. Khim.* **1978**, *3*, 427.

49. Kukushkin, Yu. N.; Budanova, V. F.; Sedova, G. N.; Pogareva, V. G.; Fadeev, Yu. V.; Soboleva, M. S. *Zh. Neorg. Khim.* **1976**, *21*, 1265.

50. Macdonald, F. M.; Sadler, P. J. *Polyhedron* **1991**, *10*, 1443.

51. Koner, S.; Ghosh, A.; Chaudhuri, N. R.; Mukherjee, M.; Muukherjee, A. K. *Polyhedron* **1993**, *12*, 2551.

52. Kukushkin, Yu. N.; Lobantsova, V. F. *Zh. Neorg. Khim.* **1977**, *22*, 1999.

53. Kukushkin, Yu. N.; Grigorov, E. I.; Khokhryakov, K. [illegible] nikov I. G., Postnikova, E. S. *Koord. Khim.* **1984**, *10*, 543.

54. Kukushkin, Yu. N.; Strelin, S. G.; Byankina, L. S.; Bakhireva, S. I. *Zh. Neorg. Khim.* **1977**, *22*, 1720.

55. Andronov, E. A.; Kukushkin, Yu. N.; Lukicheva, T. M.; Konovalov, L. V.; Bakhireva, S. I.; Postnikova, E. S. *Zh. Neorg. Khim.* **1976**, *21*, 2443.

56. Kukushkin, Yu. N.; Sedova, G. N.; Andronov, E. A.; Lukicheva, T. M. *Zh. Neorg. Khim.* **1978**, *23*, 3154.

57. Kukushkin, Yu. N.; Pankova, Yu. E.; Afanasev, E. A. *Zh. Neorg. Khim.* **1989**, *34*, 1342.

58. LeMay, H. E. Jr., *Inorg. Chem.* **1968**, *7*, 2631.

59. Tsuchiya, R.; Natsume, Y.; Uehara, A.; Kyuno, E. *Bull. Chem. Soc. Jpn.* **1970**, *43*, 1383.

60. Tsuchiya, R.; Natsume, Y.; Uehara, A.; Kyuno, E. *Thermochim. Acta* **1975**, *12*, 147.

61. Tsuchiya, R.; Ohki, T.; Uehara, A.; Kyuno, E. *Thermochim. Acta* **1975**, *12*, 413.

62. Yoshikuni, T.; Tsuchiya, R.; Uehara, A.; Kyuno, E. *Bull. Chem. Soc. Jpn.* **1978**, *51*, 113.

63. Sato, C.; Hatakeyama, S. *Bull. Chem. Soc. Jpn.* **1972**, *45*, 646.

64. Krassowski, D. W.; Reimer, K.; LeMay, H. E. Jr.; Nelson, J. H. *Inorg. Chem.* **1988**, *27*, 4307.

65. Kaizaki, K.; Ooyama, Y.; Okamoto, M.; Yamamoto, Y. *Inorg. Chim. Acta* **1994**, *217*, 181.

66. Orrell, K. G.; *Mech. Inorg. Organomet. React.* **1994**, *8*, 321-61, 469-74.

67. Tsuchiya, R.; Uehara, A.; Yoshikuni, T. *Inorg. Chem.* **1982**, *21*, 590.

68. Ashurova, N. Kh.; Tsivadze, A. Yu.; Yakubov, K. G.; Basitova, S. M. *Koord. Khim.* **1993**, *19*, 606.

69. Cohen, M. D. *Angew. Chem. Int. Ed. Engl.* **1975**, *14*, 386.

70. Shakhtshneider, T. P.; Tvanov, E. Yu.; Boldyrev, V. V. *Thermochim. Acta* **1985**, *92*, 469.

71. Shakhtshneider, T.; Ivanov, E.; Boldyrev, V. *J. Therm. Anal.* **1988**, *33*, 525.

72. Kaupp, G. In "Comprehensive Supramolecular Chemistry", Pergamon Press, 1996, Vol.8, P381-421.

73. Jorgensen, S. *Z. Anorg. Chem.* **1893**, *5*, 168.

74. Grenthe, I.; Nordin, E. *Inorg. Chem.* **1979**, *18*, 1869.

75. Kubota, M.; Ohba, S. *Acta Cryst.* **1992**, *B48*, 627.

76. Masciocchi, N.; Kolyshev, A.; Dulepov, V.; Boldyreva, E.; Sironi, A. *Inorg. Chem.* **1994**, *33*, 2579.

77. Dulepov, V. E.; Boldyreva, E. V. *Sibir. Khim. Zh.* **1992**, *5*, 109.

78. Johnson, D. A.; Pashman, K. A. *Inorg. Nucl. Chem. Lett.* **1994**, *53*, 289.

79. Dulepov, V. E.; Boldyreva, E. V. *React. Kinet. Catal. Lett.* **1994**, *53*, 289.

80. Boldyreva, E. V. *Mol. Cryst. Liq. Cryst.* **1994**, *242*, 17.

81. Boldyreva, E.; Kivikoski, J.; Howard, J. A. K. *Acta Cryst.* **1997**, *B53*, 394-404, 405-414.

82. Roberto, D.; Psaro, R.; Ugo, R. *Organometallics* **1993**, *12*, 2292.

83. Roberto, D.; Cariati, E.; Ugo, R.; Psaro, R. *Inorg. Chem.* **1996**, *35*, 2311.

84. Roberto, D.; Cariati, E.; Psaro, R.; Ugo, R. *Organometallics* **1994**, *13*, 734.

85. Roberto, D.; Psaro, R.; Ugo, R. *J. Mol. Catal.* **1994**, *86*, 109.

86. Porta, F.; Tollari, S.; Bianchi, C.; Recchia, S. *Inorg. Chim. Acta* **1996**, *249*, 79.

87. Taoufik, M.; Santini, C. C.; Candy, J. P.; de Mallmann, A.; Basset, J. M. *J. Am. Chem. Soc.* **1996**, *118*, 4167.

88. Roberto, D.; Cariati, E.; Pizzotti, M.; Psaro, R. *J. Mol. Catal. A* **1996**, *111*, 97.

89. Roberto, D.; Cariati, E.; Psaro, R.; Ugo, R. *J. Organomet. Chem.* **1995**, *488*, 109.

90. Roberto, D.; Cariati, E.; Psaro, R.; Ugo, R. *Organometallics* **1994**, *13*, 4227.

91. Vizi-Orosz, A.; Ugo, R.; Psaro, R.; Sironi, A.; Moret, M.; Zucchi, C.; Ghelfi,

F.; Palyi, G. *Inorg. Chem.* **1994**, *33*, 4600.

92. Purnell, S. K.; Gates, B. C. *J. Mol. Catal.* **1994**, *94*, L1.

93. Beutel, T.; Kawi, S.; Purnell, S. K.; Knozinger, H.; Gates, B. C. *J. Phys. Chem.* **1993**, *97*, 7284.

94. Platero, E. E.; Mentruit, M. P. *Inorg. Chem.* **1994**, *33*, 1506.

95. Wagner, G. W.; Hanson, B. E. *Organometallics* **1987**, *6*, 2494.

96. Zhao, A.; Gates, B. C. *J. Am. Chem. Soc.* **1996**, *118*, 2458.

97. Fusi, A.; Psaro, R.; Dossi, C.; Garlaschelli, L.; Cozzi, F. *J. Mol. Catal. A* **1996**, *107*, 255.

98. Ugo, R.; Dossi, C.; Psaro, R. *J. Mol. Catal. A* **1996**, *107*, 13.

99. Vaska, L. *J. Am. Chem. Soc.* **1966**, *88*, 5325.

100. Bianchini, C.; Graziani, M.; Kaspar, J.; Meli, A.; Vizza, F. *Organometallics* **1994**, *13*, 1165, and Refs. therein.

101. Porta, F.; Tollari, S.; Bianchini, C.; Recchia, S. *Inorg. Chim. Acta* **1996**, *249*, 79.

102. Bianchini, C.; Zanobini, F.; Aime, A.; Gobetto, R.; Psaro, R.; Sordelli, L. *Organometallics* **1993**, *12*, 4757.

103. Bianchini, C.; Farnetti, E.; Graziani, M.; Kaspar, J.; Vizza, F. *J. Am. Chem. Soc.* **1993**, *115*, 1753.

104. Thomas, J. M.; Morsi, S. E.; Desergne, J. P. *Adv. Phys. Org. Chem.* **1977**, *15*, 63.

105. Bianchini, C.; Peruzzini, M.; Zanobini, F. *Organometallics* **1991**, *10*, 3415.

106. Siedle, A. R.; Newmark, R. A. *J. Am. Chem. Soc.* **1989**, *111*, 2058.

107. Bianchini, C.; Peruzzini, M.; Vacca, A.; Zanobini, F. *Organometallics* **1991**, *10*, 3698.

108. Chihara, T.; Komori, K.; Ogawa, H.; Watatsuki, Y. *J. Organomet. Chem.* **1996**, *515*, 27.

109. Siedle, A. R.; Newmark, R. A.; Lyon, P. A.; Hunt, S. L.; Day, V. W. *Inorg. Chim. Acta* **1997**, *259*, 241.

110. *Structure Correlation* Burgi, H. B.; Dunitz, J. D.; Eds. VCH, Weinheim, 1994, Chapter 11, 431-500.

111. Braga, D.; Grepioni, F. *Acc. Chem. Res.* **1994**, *27*, 51.

112. Braga, D.; Grepioni, F. *Chem. Comm.* **1996**, 571.

113. Peachey, N. M.; Eckhardt, C. J. *J. Phys. Chem.* **1994**, *98*, 7106.

114. Toda, F. *Acc. Chem. Res.* **1995**, *28*, 480.

115. Dunitz, J. D.; Bernstein, J. *Acc. Chem. Res.* **1995**, *28*, 193.

116. Luty, T.; Eckhardt, C. J. *J. Am. Chem. Soc.* **1995**, *117*, 2441.

117. [illegible] *Angew. Chem. Int. Ed. Engl.* **1996**, *35*, 2195.

118. [illegible]orn, R. *Angew. Chem. Int. Ed. Engl.* **1996**, *35*, 2338.

119. Favez, R.; Roulet, R.; Pinkerton, A. A.; Schwarzenbach, D. *Inorg. Chem.* **1980**, *19*, 1356.

120. Lee, T. W.; Stoufer, R. C. *J. Am. Chem. Soc.* **1975**, *97*, 195.

121. (a) Cooper, D. G.; Powell, J. *J. Am. Chem. Soc.* **1973**, *95*, 1102. (b) Holt, M. S.; Nelson, J. H.; *Inorg. Chem.* **1986**, *25*, 1316. (c) Tanaka, H.; Isobe, K.; Kawaguchi, S. *Inorg. Chem. Acta* **1981**, *54*, L201. (d) Louw, W. J. *Inorg. Chem.* **1977**, *16*, 2147. (e) Redfield, D. A.; Nelson, J. H.; Henry, R.

A.; Moore, D. W.; Jonassen, H. B. *J. Am. Chem. Soc.* **1974**, *96*, 6298. (f) Redfield, D. A.; Nelson, J. H. *J Am. Chem. Soc.* **1974**, *96*, 6219.

122. Erickson, L. E.; Ferrett, T. A.; Buhse, L. F. *Inorg. Chem.* **1983**, *22*, 1461.

123. Annibale, G.; Cattalini, L.; Canovese, L.; Pitteri, B.; Tiripicchio, A.; Camellini, M. T.; Tobe, M. L. *J. Chem. Soc., Dalton Trans.* **1986**, 1101.

124. O'Connor, C. J.; Fendler, E. J.; Fendler, J. H. *J. Am. Chem. Soc.* **1974**, *96*, 370.

125. Adegite, A.; Orhanovic, M.; Sutin, N. *Inorg. Chem. Acta* **1975**, *15*, 185.

126. (a) Cross, R. J.; Davidson, M. F.; *Inorg. Chem. Acta* **1985**, *97*, L35. (b) Cross, R. J.; Davidson, M. F. *J. Chem. Soc., Dalton Trans.* **1986**, *9*, 1987.

127. Huchital, D. H.; Brittain, H. G.; Beutelman, L. K.; Yang, X. *Inorg. Chem. Acta* **1984**, *95*, 127.

128. Peng, D.; [illegible]ng, X.; Wu, L.; Luo, X.; Chen, K. *Huaxi Yike Daxue Xuebao* **1988**, *19*, 30.

129. Huchital, D.; Yang, X. *J. Coord. Chem.* **1981**, *11*, 57.

130. Bao, T.; Krause, K.; Krause, R. A. *Inorg. Chem.* **1988**, *27*, 759.

131. Rindermann, W.; Van Eldik, R. *Inorg. chem. Acta* **1983**, *68*, 35.

132. Heatherington, A.; Oon, S. M.; Vargas, R.; Kane-Maguire, N. A. P. *Inorg. Chem. Acta* **1980**, *44*, L279.

133. Vila, J. M.; Shaw, B. L. *J. Chem. Soc., Chem Commun.* **1987**, 1778.

134. Rophael, M. W.; Malati, M. A. *J. Inorg. Nucl. Chem.* **1974**, *36*, 1355.

135. (a) Vitiello, J. D.; Billo, E. J. *Inorg. Chem.* **1980**, *19*, 3477. (b) Farago, M. E.; Mason, C. F. V.; Page, B. A. *Proc. Symp. Coord.* 3rd, **1970**, *1*, 313.

136. Basolo, F.; Pearson, R. G. *Mechanisms of Inorganic Reactions* 2nd ed, Wiley, New York, N. Y., 1967, Chapter V.

137. Haake, P.; Pfeiffer, R. M. *J. Am. Chem. Soc.* **1970**, *42*, 4996.

138. Hojo, M. *Stud. Surf. Sci. Catal.* **1986**, *25*, 43.

139. Xie, R.; Li, Y. *Huaxue Shiji* **1990**, *12*, 344.

140. Zawadzki, M. E. *Diss. Abst. Int. B* **1984**, *44*, 2421.

141. Chattopadhyaya, J. B.; Rama Rao, A. V. *Tetrahedron* **1974**, *30*, 2899.

142. Sasaki, T.; Egughi, S.; Ohno, M. *Bull. Chem. Soc. Jpn.* **1980**, *53*, 1469.

143. Zawadzki, M. E.; Ellis, A. B. *J. Org. Chem.* **1983**, *48*, 3156.

144. Zhang, B.; Chen, J.; Cao, Y. *Huaxie Xuebao* **1989**, *47*, 502.

145. Wu, W.; Ming, Y.; Cao, Y. *Ganguang Kexue Yu Kuang Huaxue* **1990**, *3*, 226.

146. Dai, H.; Qiu, F. *J. Nat. Gas Chem.* **1994**, *3*, 459.

147. Okano, K.; Suemune, H.; Sakai, K. *Chem. Pharm. Bull,* **1990**, *38*, 532.

148. Konishi, H.; Ariyomi, K.; Okano, T.; Kiji, J. *Bull. Chem. Soc. Jpn.* **1989**, *62*, 591.

149. Li, Y.; Xie, R. *Huaxie Shiji* **1991**, *13*, 11.

150. Yaroslavsky, C. *Tetrahedron Lett.* **1974**, 3395.

151. Hojo, M.; Masuda, R. *Synth. Commun.* **1975**, *5*, 169.

152. Smith, K.; Butters, M.; Paget, W. E.; Nay, B. *Synthesis* **1985**, 1155.

153. Konishi, H.; Yokota, K.; Ichihashi, Y.; Okano, T; Kiji, J. *Chem. Lett.* **1980**, 1423.

154. Posner, H. G.; Carry, J.; Lee, K. J.; Bull, D. S.; Dai, H. *Tetrahydron Lett.* **1994**, 1321.

155. Kropp, J. P.; Daus, A. K.; Tuberger, W. M.; Kepler, D. K.; Wilson, P. V.; Craig, L. S.; Baillargeon, M. [illegible] *J. Am. Chem. Soc.* **1993**, *115*, 3071.

156. Kropp, J. P.; Daus, A. K.; Crawford, D. S.; [illegible] W. M.; Kepler, D. K.; Craig, L. S.; Wilson, P. V. *J. Am. Chem. Soc.* **1990**, *112*, 7433.

157. Brillon, D.; Sauvé, G. *J. Org. Chem.* **1992**, *57*, 1838.

158. Sangwan, N. K.; Varma, B. S.; Dhindsa, K. S. *Chem. Ind.* **1984**, *7*, 271.

159. Bladé-Front, A. *Tetrahedron Lett.* **1980**, *21*, 2443.

160. Ohno, K.; Nishiyama, H.; Nagase, H. *Tetrahedron Lett.* **1979**, *45*, 4405.

161. Suárez, R. A.; Mazzieri, R. M. *J. Org. Chem.* **1987**, *52*, 1145.

162. Matman, R.; Mahaffy, P.; Mellema, R. *J. Catal.* **1984**, *35*, 44.

163. Matsuishi, T.; Shimada, T.; Morihara, K. *Bull. Chem. Soc. Jpn.* **1994**, *67*, 748.

164. Ceppan, M.; Lapcik, L.; Sivova, M. *J. Photochem.* **1987**, *36*, 211.

165. Nagai, S.; Arai, H.; Hatada, M. *Nippon Kagaku Kaishi* **1984**, *10*, 1656.

166. Benda, F.; Hájek, B. *Inorg. Chim. Acta* **1979**, *36*, L401.

167. Aronovitch, C.; Mazur, Y. *J. Org. Chem.* **1985**, *50*, 149.

168. Abdel-Malik, M. M.; Mayo, P. *Can. J. Chem.* **1984**, *62*, 1275.

169. Hasegawa, T.; Yamazaki, Y.; Yoshioka, M.; *J. Phys. Org. Chem.* **1995**, *8*, 31.

170. Mayo, P.; Nakamura, A.; Tsang, P. W. K.; Wong, K. S. *J. Am. Chem. Soc.* **1982**, *104*, 6824.

171. Mayo, P.; Ramnath, N. *Can. J. Chem.* **1986**, *64*, 1293.

172. Kamitori, Y.; Hojo, M.; Masuda, R.; Ikemura, T.; Mori, Y. *Tetrahedron Lett.* **1993**, *34*, 5135.

173. Sohmiya, H.; Kimura, T.; Bauchat, P.; Fujita, M.; Ando, T. *Chem. Lett.* **1991**, 1391.

CHAPTER 3

PHASE-DEPENDENT DIAGONAL AND LATERAL ISOMERISM OF THE RHENIUM COMPLEXES $(\eta^5\text{-}C_5H_4Me)Re(CO)_2Br_2$

3.1. Introduction

In the extensive organometallic chemistry of ring-substituted cyclopentadienyl transition metal complexes there is much evidence to indicate that ring substitution can considerably influence not only the physical properties but also, and more importantly, the catalytic selectivities and activities of such complexes.[1-3] To further explore these type of complexes, we have commenced a thorough investigation of the little studied substituted cyclopentadienyl four-legged piano stool rhenium complexes of the type $(\eta^5\text{-}C_5H_4R)Re(CO)_2X_2$ (R = ring substituent, X = halogen). The unsubstituted parent complex $CpRe(CO)_2Br_2$ was first synthesized by Nesmeyanov *et al.* in 1969.[4] Complexes of the type $CpMX_2Y_2$ exist as two nonequivalent stereoisomers that are commonly referred to as *cis* and *trans*, or more precisely, *lateral* and *diagonal*, isomers. It was not until 1975 that a simple and reproducible chromatographic technique for the separation of *lat*-$CpRe(CO)_2Br_2$ (Figure 3.1a) and *diag*-$CpRe(CO)_2Br_2$ (Figure 3.1b) was reported by King *et al.*[5] The only other report on related complexes involving substituents

on the cyclopentadienyl ring $(\eta^5\text{-}C_5H_4R)Re(CO)_2Br_2$ (R = Me, I, COOMe) contained preliminary information, without comment on the separation, characterization, and stereochemistry of the diagonal and lateral isomers, of the new complexes.[7] Here we report the syntheses of a range of complexes, *diag*- and *lat*-$(\eta^5\text{-}C_5H_4R)Re(CO)_2Br_2$ (R = Me, Et, tBu, $Si(CH_3)_3$, C_6H_{11}). Of significance has been the finding of unusual solid and solution state isomerization reactions for these new complexes. Previously only mention has been made of the solution state isomerization of the lateral to diagonal isomers of $CpRe(CO)_2Br_2$ and $Cp^*Re(CO)_2Br_2$.[5,6] A tantalizing comment on the solid state isomerization of $(\eta^5\text{-}C_5H_5)Mo(CO)_2(PBu_3)I$ appeared in the literature some years ago.[8]

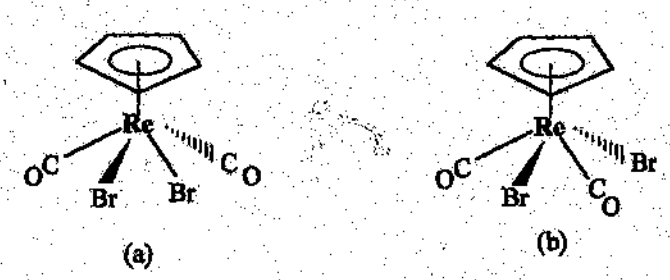

Figure 3.1. (a) Lateral and (b) diagonal isomers of $(\eta^5\text{-}C_5H_5)Re(CO)_2Br_2$.

A literature survey revealed that most isomerization reactions of organometallic compounds are unidirectional. Reversible isomerization reactions have been observed for a few organometallic complexes, and this has been achieved by changing the reaction conditions from that of a thermal reaction to a photochemical reaction [9] or by changing the reaction medium from a polar solvent

to a nonpolar solvent.[10] A unique phase-dependent isomerization reaction has been reported for *trans*-[Pt(Me_2S)(Py)Cl_2], which isomerizes into the *cis* isomer on heating in the solid state. In the presence of excess ligand (Me_2S), a reverse *cis* to *trans* solution isomerization reaction occurs.[11] As far as we are aware, no organometallic complex has been reported to undergo a completely reversible phase-dependent isomerization reaction. Here we report an example of this phenomenon, which is shown by (η^5-C_5H_4Me)Re$(CO)_2Br_2$, and also report a study of the influence of the ring substituent on the *diag-lat* isomerism of related complexes.

3.2. Experimental Section

The ligands ethylcyclopentadiene and *tert*-butylcyclopentadiene and the complex $CpRe(CO)_3$ were prepared by the literature methods.[12-14] All reactions were carried out under dry N_2 in either a Schlenk apparatus or a flask connected to a double manifold providing low vacuum or nitrogen. Solvents were dried by conventional methods, distilled under nitrogen, and used immediately. Differential scanning calorimetry was obtained on 5–15-mg samples under flowing nitrogen at a constant heating rate of 10 °C/min on a Du Pont 910 DSC instrument. Melting points were recorded on a Kofler hot-stage melting point apparatus. Infrared spectra were measured on a Perkin-Elmer 580B IR spectrometer, usually in KBr cells (solutions). NMR spectra were measured on a Bruker AC200 spectrometer operating at 200 MHz. Microanalyses were carried out at the CSIR, Pretoria, South Africa.

3.2.1. Synthesis of (η^5-C_5H_4R)$Re(CO)_3$ (R = Me, Et, tBu)

A 100-ml round-bottom flask was charged with freshly distilled monosubstituted cyclopentadiene (3–7 mL), $Re_2(CO)_{10}$ (0.32–1.00 g, 0.049–1.53 mmol), and a magnetic stirrer bar and was fitted with a reflux condenser and a N_2 inlet/oil bubbler. The reaction mixture was stirred, heated, and kept at 210 °C for 2 h. At this point, gas evolution had ceased. The flask was then allowed to cool to room temperature. IR spectroscopy and silica gel TLC showed that no $Re_2(CO)_{10}$ remained. The reaction mixture was then chromatographed on a silica gel column prepared in hexane. For R = Me and Et, elution with hexane gave first unreacted monosubstituted cyclopentadiene and then the products as a colorless crystalline solid. For R = tBu, elution with hexane gave unreacted *tert*-butylcyclopentadiene, followed by a mixture containing (η^5-C_5H_4tBu)$Re(CO)_3$ and a small amount of *tert*-butylcyclopentadiene polymer which could not easily be separated by column chromatography. This mixture was used as such in further reactions. (η^5-C_5H_4Me)$Re(CO)_3$: 96% yield, IR (cm^{-1}, CH_2Cl_2) ν_{co}: 1922, 2020. ^1H NMR(ppm, $CDCl_3$): 2.23 (s, 3H), 5.21–5.25 (m, 4H). (η^5-C_5H_4Et)$Re(CO)_3$: 75% yield, IR (cm^{-1}, CH_2Cl_2) ν_{co}: 1920, 2022. ^1H NMR(ppm, $CDCl_3$): 1.15 (t, 3H), 2.48 (q, 2H), 5.25 (m, 4H). (η^5-C_5H_4tBu)$Re(CO)_3$: ~90% yield, IR (cm^{-1}, CH_2Cl_2) ν_{co}: 1922, 2018. ^1H NMR(ppm, $CDCl_3$): 1.22 (s, 9H), 5.19 (t, 2H), 5.34 (t, 2H).

3.2.2. Synthesis of $[\eta^5\text{-}C_5H_4Si(CH_3)_3]Re(CO)_3$

To a stirred solution of $(\eta^5\text{-}C_5H_5)Re(CO)_3$ (0.60 g, 1.79 mmol) in 45 mL of THF at −65 °C was added n-C_4H_9Li (2.3 mL of 1.6 M solution, 3.68 mmol) in hexane. After stirring at −40 to −50 °C for 120 min, $(CH_3)_3SiCl$ (2.5 mL, 19.7 mmol) was added, and the reaction mixture was allowed to warm to 20 °C. Solvent was then removed under reduced pressure, and the product was purified by column chromatography (hexane eluent). $[\eta^5\text{-}C_5H_4Si(CH_3)_3]Re(CO)_3$ was obtained as white needles (0.63 g, 87% yield). IR (cm^{-1}, CH_2Cl_2) ν_{co}: 1924, 2022. ^1H NMR (ppm, $CDCl_3$): 0.24 (s, 9H), 5.39–5.43 (m, 4H).

3.2.3. Syntheses of Diagonal and Lateral $(\eta^5\text{-}C_5H_4Me)Re(CO)_2Br_2$ Complexes

A solution of Br_2 (220 mg, 1.38 mmol) in 2 mL of trifluoroacetic acid was added dropwise at 25 °C to a solution of $(\eta^5\text{-}C_5H_4Me)Re(CO)_3$ (484 mg, 1.38 mmol) in 3 mL of trifluoroacetic acid. After the reaction mixture was stirred for an additional 40 min at room temperature, the reaction was quenched by pouring it into 100 mL of water at 25 °C. The resulting brown precipitate, which contained unreacted $(\eta^5\text{-}C_5H_4Me)Re(CO)_3$ and both isomers of $(\eta^5\text{-}C_5H_4Me)Re(CO)_2Br_2$, was filtered and dried at 25 °C (0.1 mmHg). This solid was dissolved in dichloromethane and chromatographed on a 2 × 60 cm silica gel column prepared in hexane. Successive elution with hexane, hexane/dichloromethane (1:1), and dichloromethane gave unreacted $(\eta^5\text{-}C_5H_4Me)Re(CO)_3$ (261 mg, 54% recovery), *diag*-$(\eta^5\text{-}$

$C_5H_4Me)Re(CO)_2Br_2$ (142 mg, 21% conversion, 46% yield) from a red band, and *lat*-(η^5-$C_5H_4Me)Re(CO)_2Br_2$ (71 mg, 11% conversion, 23% yield) from a brown band, respectively. The complexes, diagonal and lateral (η^5-$C_5H_4Me)Re(CO)_2Br_2$, were characterized by elemental analysis and by IR and NMR spectroscopy (Table 3.1).

3.2.4. Syntheses of Diagonal and Lateral (η^5-$C_5H_4Et)Re(CO)_2Br_2$ Complexes

A solution of Br_2 (350 mg, 2.19 mmol) in 3 mL of trifluoroacetic acid was added dropwise at 25 °C to a solution of (η^5-$C_5H_4Et)Re(CO)_3$ (780 mg, 2.14 mmol) in 5 mL of trifluoroacetic acid. After the reaction mixture was stirred for an additional 1 h at room temperature, the reaction was quenched by pouring it into 100 mL of water at 25 °C. The resulting brown precipitate, which contained unreacted (η^5-$C_5H_4Et)Re(CO)_3$ and both isomers of (η^5-$C_5H_4Et)Re(CO)_2Br_2$, was filtered and dried at 25 °C (0.1 mmHg). This solid was dissolved in dichloromethane and chromatographed on a 2 × 60 cm silica gel column prepared in hexane. Successive elution with hexane, hexane/dichloromethane (1:1), and dichloromethane gave unreacted (η^5-$C_5H_4Et)Re(CO)_3$ (350 mg, 45% recovery), *diag*-(η^5-$C_5H_4Et)Re(CO)_2Br_2$ (180 mg, 17% conversion, 31% yield) from a red band, and *lat*-(η^5-$C_5H_4Et)Re(CO)_2Br_2$ (108 mg, 10% conversion, 18% yield) from a brown band, respectively. The complexes, diagonal and lateral (η^5-$C_5H_4Et)Re(CO)_2Br_2$, were characterized by elemental analysis and by IR and NMR spectroscopy (Table

3.1).

3.2.5. Syntheses of Diagonal and Lateral $(\eta^5\text{-}C_5H_4tBu)Re(CO)_2Br_2$ Complexes

A solution of Br_2 (170 mg, 1.06 mmol) in 2 mL of trifluoroacetic acid was added dropwise at 25 °C to a solution of the impure $(\eta^5\text{-}C_5H_4tBu)Re(CO)_3$ (prepared from 0.49 mmol $Re_2(CO)_{10}$) in 3 mL of trifluoroacetic acid. After the reaction mixture was stirred for an additional 40 min at room temperature, the reaction was quenched by the addition of 100 mL of water. The resulting sticky brown precipitate, which contained unreacted $(\eta^5\text{-}C_5H_4tBu)Re(CO)_3$ and both isomers of $(\eta^5\text{-}C_5H_4tBu)Re(CO)_2Br_2$, was washed with water (2 × 50 mL) and dried at 25 °C (0.1 mmHg). This precipitate was dissolved in dichloromethane and chromatographed on a 2 × 60 cm silica gel column prepared in hexane. Successive elution with hexane, hexane/dichloromethane (1:1), and dichloromethane gave unreacted impure $(\eta^5\text{-}C_5H_4tBu)Re(CO)_3$, *diag*-$(\eta^5\text{-}C_5H_4tBu)Re(CO)_2Br_2$ ([illegible] mg, 18% conversion, based on $Re_2(CO)_{10}$) from a red band, and *lat*-$(\eta^5\text{-}C_5H_4tBu)Re(CO)_2Br_2$ (97 mg, 38% conversion, based on $Re_2(CO)_{10}$) from a brown band, respectively. The complexes, diagonal and lateral $(\eta^5\text{-}C_5H_4tBu)Re(CO)_2Br_2$, were characterized by elemental analysis, and by IR and NMR spectroscopy (Table 3.1).

3.2.6. Syntheses of Diagonal and Lateral [η^5-$C_5H_4Si(CH_3)_3$]$Re(CO)_2Br_2$ Complexes

A solution of Br_2 (230 mg, 1.44 mmol) in 5 mL of $CHCl_3$ was added dropwise at 0 °C to a solution of [η^5-$C_5H_4Si(CH_3)_3$]$Re(CO)_3$ (530 mg, 1.30 mmol) in 15 mL of $CHCl_3$. After the reaction mixture was stirred for an additional 60 min at 0 °C, the reaction was stopped and the solvent was removed under reduced pressure. The resulting dark red solid was dissolved in dichloromethane and chromatographed on a silica gel column prepared in hexane. Successive elution with hexane, hexane/dichloromethane (1:1), and dichloromethane gave unreacted [η^5-$C_5H_4Si(CH_3)_3$]$Re(CO)_3$ (300 mg, 57% recovery), *diag*-[η^5-$C_5H_4Si(CH_3)_3$]$Re(CO)_2Br_2$ (55 mg, 7.8% conversion, 18% yield) from a red band, and *lat*-[η^5-$C_5H_4Si(CH_3)_3$]$Re(CO)_2Br_2$ (66 mg, 9.4% conversion, 22% yield) from a brown band, respectively. The complexes, diagonal and lateral [η^5-$C_5H_4Si(CH_3)_3$]$Re(CO)_2Br_2$, were characterized by elemental analysis and by IR and NMR spectroscopy (Table 3.1).

3.2.7. Solution Isomerization of *lat*-(η^5-C_5H_4R)$Re(CO)_2Br_2$ (R = Me, Et, tBu, $Si(CH_3)_3$)

A solution of 20–200 mg of *lat*-(η^5-C_5H_4R)$Re(CO)_2Br_2$ complex (R = Me, Et, tBu, $Si(CH_3)_3$) in 15 mL of toluene was refluxed under nitrogen for 2–5 h. Silica gel TLC showed that the reaction yield was ~95%. Removal of solvent at 25 °C (0.1 mmHg) gave a red solid shown to be the corresponding diagonal isomer by its

ν_{co} frequency in dichloromethane solution and ^{1}H NMR spectrum.

3.2.8. Solid State Isomerization of *diag*-(η^5-C_5H_4Me)$Re(CO)_2Br_2$

Solid *diag*-(η^5-C_5H_4Me)$Re(CO)_2Br_2$ (20–100 mg) was heated in a 25-mL round-bottom flask at 106–110 °C under nitrogen for 2–5 h. The color of the solid changed gradually from red to brown. No decomposition was observed after the heating process. Silica gel TLC and IR and NMR spectroscopy confirmed that the brown solid was *lat*-(η^5-C_5H_4Me)$Re(CO)_2Br_2$.

3.2.9. Molten State Isomerization of *diag*-(η^5-C_5H_4R)$Re(CO)_2Br_2$ (R = Et, tBu, $Si(CH_3)_3$)

Solid *diag*-(η^5-C_5H_4Et)$Re(CO)_2Br_2$ or *diag*-(η^5-C_5H_4tBu)$Re(CO)_2Br_2$ (5–20 mg) was sealed into a capillary tube under N_2 and heated in an oil bath at 100 °C for 5 h or at 120 °C for 10 h, respectively. At these temperatures, the complexes were in the homogeneous molten state. No decomposition was observed after heating process. Silica gel TLC and IR and NMR spectroscopy confirmed that the products showed that 65% and 30% of the lateral isomers had formed for the ethyl and *tert*-butyl substituted complexes, respectively.

Table 3.1. Spectroscopic and Analytic data for $(\eta^5\text{-}C_5H_4R)Re(CO)_2Br_2$ Complexes

compound	mp (°C)	ν_{co}[a] (cm^{-1})	^1H NMR[b] (ppm)		analysis (%)		
			Cp ring	R		C	H
diag-$(\eta^5\text{-}C_5H_4Me)Re(CO)_2Br_2$	116–118	2064, 1998	5.50 (t, 2H), 5.65 (t, 2H)	2.32 (s, 3H)	calcd	19.97	1.47
					found	19.94	1.30
diag-$(\eta^5\text{-}C_5H_4Et)Re(CO)_2Br_2$	93–95	2064, 1999	5.46 (t, 2H), 5.68 (t, 2H)	1.23 (t, 3H)	calcd	21.83	1.83
				2.63 (q, 2H)	found	21.64	1.71
diag-$(\eta^5\text{-}C_5H_4tBu)Re(CO)_2Br_2$	95–97	2062, 1998	5.21 (t, 2H), 5.76 (t, 2H)	1.40 (s, 9H)	calcd	25.25	2.50
					found	25.13	2.38
diag-$[\eta^5\text{-}C_5H_4Si(CH_3)_3]Re(CO)_2Br_2$	92–94	2062, 2000	5.23 (t, 2H), 5.94 (t, 2H)	0.38 (s, 9H)	calcd	22.27	2.43
					found	22.21	2.32
diag-$(\eta^5\text{-}C_5H_4C_6H_{11})Re(CO)_2Br_2$	122–124	2064, 1997	5.38 (t, 2H), 5.70 (t, 2H)	1.21–2.48 (m, 11H)			
lat-$(\eta^5\text{-}C_5H_4Me)Re(CO)_2Br_2$	158–160 dec	2050, 1978	5.80 (t, 2H), 5.91 (t, 2H)	2.32 (s, 3H)	calcd	19.97	1.47
					found	19.90	1.36
lat-$(\eta^5\text{-}C_5H_4Et)Re(CO)_2Br_2$	94–96	2052, 1976	5.84 (t, 2H), 5.91 (t, 2H)	1.26 (t, 3H)	calcd	21.83	1.83
				2.67 (q, 2H)	found	21.54	1.63
lat-$(\eta^5\text{-}C_5H_4tBu)Re(CO)_2Br_2$	115–117	2048, 1976	5.96 (t, 2H), 6.11 (t, 2H)	1.31 (s, 9H)	calcd	25.25	2.50
					found	25.18	2.36
lat-$[\eta^5\text{-}C_5H_4Si(CH_3)_3]Re(CO)_2Br_2$	109–111	2050, 1978	5.96 (t, 2H), 6.28 (t, 2H)	0.34 (s, 9H)	calcd	22.27	2.43
					found	22.20	2.31
lat-$(\eta^5\text{-}C_5H_4C_6H_{11})Re(CO)_2Br_2$	133–135	2052, 1078	5.87 (t, 2H), 5.89 (t, 2H)	1.21–2.60 (m, 11H)			

[a] Recorded in CH_2Cl_2. [b] Recorded in $CDCl_3$, relative to TMS. s, singlet; t, triplet; q, quintet; m, multiplet.

About 10% of *diag*-[η^5-$C_5H_4Si(CH_3)_3$]$Re(CO)_2Br_2$ complex isomerized into the lateral isomer when heated at 110 °C for 3 h in the molten state, but some decomposition occurred during the process.

3.3. Results and Discussion

3.3.1. Syntheses of (η^5-C_5H_4R)$Re(CO)_3$ (R = Me, Et, tBu, $Si(CH_3)_3$, C_6H_{11}) Complexes

Direct reaction of $Re_2(CO)_{10}$ with monosubstituted cyclopentadiene gave (η^5-C_5H_4R)$Re(CO)_3$ (R = Me, Et, tBu) in good yield (75%–96%, Scheme 3.1). This constituted a distinct improvement over the literature methods.[15,16] The (η^5-C_5H_4R)$Re(CO)_3$ complexes have good solubility in organic solvents, which makes it difficult to separate them from the reaction mixture of the monosubstituted

$$Re_2(CO)_{10} + C_5H_5R \xrightarrow{170-210\ ^oC} (\eta 5\text{-}C_5H_4R)Re(CO)_3 \quad (R = Me, Et, tBu)$$

Scheme 3.1

cyclopentadiene and its polymer [17] by traditional sublimation or recrystallization methods. We found that (η^5-C_5H_4Me)$Re(CO)_3$ and (η^5-C_5H_4Et)$Re(CO)_3$ could be easily separated by column chromatography as a colorless crystalline solid; (η^5-C_5H_4tBu)$Re(CO)_3$ could be separated from most of the corresponding *tert*-butylcyclopentadiene polymer by the same method. The product was, however, always contaminated with some *tert*-butylcyclopentadiene polymer, which had the

same solubility as that of the product and was difficult to remove by column chromatography. However, the small amount of diene polymer in the product did not have any influence on the subsequent bromination reaction.

$[\eta^5\text{-}C_5H_4Si(CH_3)_3]Re(CO)_3$ was synthesized in good yield by following the procedures used to synthesize $[\eta^5\text{-}C_9H_6Si(CH_3)_3]Re(CO)_3$.[18] Reaction of $Re_2(CO)_{10}$ with cyclohexylcyclopentadiene gave $(\eta^5\text{-}C_5H_4C_6H_{11})Re(CO)_3$ in good yield (monitored by IR spectroscopy). However, it was difficult to separate the product from the cyclohexylcyclopentadiene polymer even by repeated column chromatography.

In summary, our results show that direct reaction of $Re_2(CO)_{10}$ with monosubstituted cyclopentadiene provides a good route for the preparation of monosubstituted cyclopentadienyltricarbonylrhenium complexes and that column chromatography is an effective separation method for most of these complexes.

3.3.2. Syntheses of Diagonal and Lateral $(\eta^5\text{-}C_5H_4R)Re(CO)_2Br_2$ (R = Me, Et, tBu, $Si(CH_3)_3$, C_6H_{11}) Complexes

The reaction of $(\eta^5\text{-}C_5H_4R)Re(CO)_3$ with bromine in trifluoroacetic acid at room temperature was carried out by the procedure used for the syntheses of the unsubstituted analogue [5] (Scheme 3.2) and gave *diag*-and *lat*-$(\eta^5\text{-}C_5H_4R)Re(CO)_2Br_2$ complexes which were separated by a chromatographic

technique. Surprisingly, $[\eta^5\text{-}C_5H_4Si(CH_3)_3]Re(CO)_3$ lost the ring substituent $Si(CH_3)_3$ and formed $(\eta^5\text{-}C_5H_5)Re(CO)_3$ quantitatively when dissolved in trifluoroacetic acid. However, reaction of $[\eta^5\text{-}C_5H_4Si(CH_3)_3]Re(CO)_3$ with bromine in chloroform gave *diag*-and *lat*-$[\eta^5\text{-}C_5H_4Si(CH_3)_3]Re(CO)_2Br_2$ in good yield (Scheme 3.2). Monitoring of the bromination reaction by TLC revealed that a new yellow product assumed to be $\{[\eta^5\text{-}C_5H_4Si(CH_3)_3]Re(CO)_3Br\}Br$ [19] formed rapidly and decomposed slowly to form *diag*-$[\eta^5\text{-}C_5H_4Si(CH_3)_3]Re(CO)_2Br_2$, *lat*-$[\eta^5\text{-}C_5H_4Si(CH_3)_3]Re(CO)_2Br_2$, $[\eta^5\text{-}C_5H_4Si(CH_3)_3]Re(CO)_3$ and a red product which has as yet not been characterized.

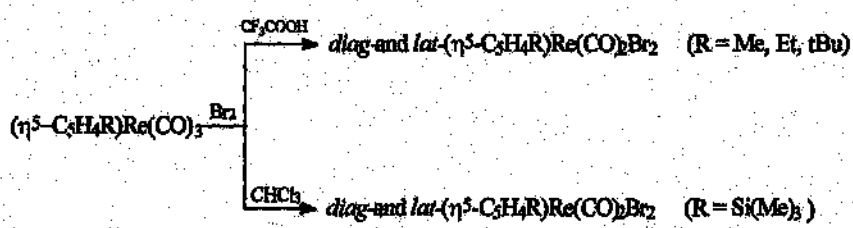

Scheme 3.2

Reaction of the mixture of $(\eta^5\text{-}C_5H_4C_6H_{11})Re(CO)_3$ and the cyclohexylcyclopentadiene polymer with bromine in trifluoroacetic acid or in THF indeed gave *diag*- and *lat*-$(\eta^5\text{-}C_5H_4C_6H_{11})Re(CO)_2Br_2$ complexes, which were separated by column chromatography, but the yield was low (~10%). The complexes were characterized by IR and ^1H NMR spectroscopy, and data are given in Table 3.1.

3.3.3. Characterization of Diagonal and Lateral (η^5-C_5H_4R)$Re(CO)_2Br_2$ (R = Me, Et, tBu, $Si(CH_3)_3$) Complexes

The new complexes were characterized by IR and NMR spectroscopy and by elemental analysis. In every instance, correct intensity ratios as well as the requisite number of adsorption bands were observed in the NMR spectrum. The identification of the diagonal and lateral isomers was based on the angles between their two carbonyl groups (Table 3.2) which were estimated from the relationship $\tan^2\theta = I_{as}/I_s$, where 2θ is the angle between the two carbonyl bonds, I_{as} is the height of the asymmetric ν_{co} band, and I_s is the height of the symmetric ν_{co} band.[20]

3.3.4. Solution Isomerization of *lat*-(η^5-C_5H_4R)$Re(CO)_2Br_2$ (R = Me, Et, tBu, $Si(CH_3)_3$)

The (η^5-C_5H_4R)$Re(CO)_2Br_2$ complexes have solution isomerization behavior similar to the unsubstituted (R = H) analogue. The *lat*-(η^5-C_5H_4R)$Re(CO)_2Br_2$ isomers were stable in solution at room temperature over a period of hours and ~5% of the reactants isomerized to the corresponding diagonal isomers over a period of days. They were readily converted into the corresponding diagonal isomers when refluxed in toluene. In refluxing toluene, an equilibrium was established and our preliminary results showed that the equilibrium constant K = [*diag*]/[*lat*] was larger than 20 and independent of the R group. The *lat*-(η^5-C_5H_4R)$Re(CO)_2Br_2$ were slightly more difficult to isomerize than the unsubstituted

Table 3.2. Bond Angle 2θ between Two CO Groups for the (η^5-C_5H_4R)$Re(CO)_2Br_2$ Complexes

complex	I_{as}/I_s	2θ
Diag-(η^5-C_5H_5)$Re(CO)_2Br_2$	2.50	115 (120)[a]
diag-(η^5-C_5H_4Me)$Re(CO)_2Br_2$	2.44	115
diag-(η^5-C_5H_4Et)$Re(CO)_2Br_2$	2.25	113
diag-(η^5-$C_5H_4C_6H_{11}$)$Re(CO)_2Br_2$	2.25	113
diag-(η^5-C_5H_4tBu)$Re(CO)_2Br_2$	2.26	113
diag-[η^5-$C_5H_4Si(CH_3)_3$]$Re(CO)_2Br_2$	2.20	112
lat-(η^5-C_5H_5)$Re(CO)_2Br_2$	0.658	78 (78)[a]
lat-(η^5-C_5H_4Me)$Re(CO)_2Br_2$	0.649	78
lat-(η^5-C_5H_4Et)$Re(CO)_2Br_2$	0.646	78
lat-(η^5-$C_5H_4C_6H_{11}$)$Re(CO)_2Br_2$	0.635	78
lat-(η^5-C_5H_4tBu)$Re(CO)_2Br_2$	0.706	80
lat-[η^5-$C_5H_4Si(CH_3)_3$]$Re(CO)_2Br_2$	0.713	80

[a] Recorded data.

analogue. For example, unsubstituted *lat*-(η^5-C_5H_5)Re(CO)$_2$Br$_2$ completely changed into the diagonal isomer in boiling chloroform after a few minutes,[5] whereas only 17% of the lateral (η^5-C_5H_4Me)Re(CO)$_2$Br$_2$ complex isomerized to the corresponding diagonal isomer after 6 h in refluxing chloroform. The *diag*-(η^5-C_5H_4R)Re(CO)$_2$Br$_2$ complexes were stable to isomerization in solution even at temperature as high as 130 °C. The polarity of the solvent did not change the lateral to diagonal solution isomerization direction. *diag*- and *lat*-(η^5-C_5H_4Me)Re(CO)$_2$Br$_2$ were heated under reflux in $CHCl_3$, benzene, toluene and C_6H_5Cl for the same period of time. In all cases, the lateral complex isomerized into the diagonal isomer, while the reverse isomerization reaction did not take place (Table 3.3).

3.3.5. Solid State Isomerization of *diag*-(η^5-C_5H_4Me)Re(CO)$_2$Br$_2$

Surprisingly, the *diag*-(η^5-C_5H_4Me)Re(CO)$_2$Br$_2$ isomerized into the corresponding lateral isomer in almost quantitative yield when it was heated in the solid state at 106–110 °C under nitrogen for 2–5 h. Thus, a completely reversible isomerization takes place at the same temperature (110 °C), the direction of the isomerization being dependent on the phase of the complex. By contrast, no isomerization occurred when solid *diag*-(η^5-C_5H_5)Re(CO)$_2$Br$_2$ was heated at temperature as high as 150 °C. A similar negative result for the isomerization of solid *diag*-Cp*Re(CO)$_2$Br$_2$ under photochemical conditions was reported by Hill *et al.*[21] A

Table 3.3. *Diag–Lat* Isomerization of $(\eta^5\text{-}C_5H_4Me)Re(CO)_2Br_2$ in Different Solvents

complex	solvent	Reaction time[a] (h)	product[b] (%) *diag*	*lat*
lat-$(\eta^5\text{-}C_5H_4Me)Re(CO)_2Br_2$	$CHCl_3$	6.0	17	83
	benzene	4.5	79	21
	toluene	1.0	>95[c]	<5
	C_6H_5Cl	2.0	>95[c]	<5
diag-$(\eta^5\text{-}C_5H_4Me)Re(CO)_2Br_2$	$CHCl_3$	6.0	100	0
	benzene	4.5	100	0
	toluene	1.0	>95[c]	<5
	C_6H_5Cl	2.0	>95[c]	<5

[a] The solution was heated under reflux. [b] Calculated from the integration of peaks in the ^1H NMR spectrum. [c] From silica gel TLC.

DSC plot of powdered *diag*-(η^5-C_5H_4Me)$Re(CO)_2Br_2$ (Figure 3.3b) shows that one exothermic peak beginning at 118 °C and one endothermic peak at 171 °C were observed. The exotherm corresponded to the *diag* to *lat* isomerization of the complex. This was verified by the color change from red to brown (the latter color corresponding to that of the lateral isomer), and by the IR and ^1H NMR spectra recorded on the cooled sample after completion of the exotherm. The IR and ^1H NMR spectra indicated complete conversion to the lateral isomer. This DSC result suggests that the solid state *diag* to *lat* isomerization of the (η^5-C_5H_4Me)$Re(CO)_2Br_2$ proceeds under thermodynamic control. The endothermic peak at 171 °C correlated with the melting point of the lateral isomer obtained after isomerization of the diagonal isomer. For comparison, the DSC curve of unsubstituted *diag*-(η^5-C_5H_5)$Re(CO)_2Br_2$ is also given in Figure 3.3; here only one endothermic peak corresponding to the melting peak of the starting material was observed.

3.3.6. Molten State Isomerization of *diag*-(η^5-C_5H_4R)$Re(CO)_2Br_2$ (R = Et, tBu, $Si(CH_3)_3$)

When *diag*-(η^5-C_5H_4R)$Re(CO)_2Br_2$ (R = Et, tBu, $Si(CH_3)_3$) was heated at a temperature below its melting point (in the solid state), no isomerization was observed. DSC curves reveal only one endothermic peak for these complexes (Figure 3.3c–e) which corresponds to the melting point of starting material. However, diagonal to lateral isomerization, a reversed direction to that of the solution isomerization, occurred for these complexes in the molten state. Further, if

solution isomerization, occurred for these complexes in the molten state. Further, if *lat*-(η^5-C_5H_4R)$Re(CO)_2Br_2$ was heated in the molten state, lateral to diagonal isomerization occurred.

The ratio of *lat* to *diag* isomers for the R = Et complex in the molten state was found to be independent of the direction of the isomerization reaction and reached an equilibrium value of 65/35 as determined by NMR spectroscopy. Raising the heating temperature or increasing reaction time did not improve the reaction yield substantially. It is to be noted that in all cases the isomerization reaction was carried out at a temperature higher than the melting points of both the diagonal and lateral isomers and that a homogenous melt was observed under a microscope. For R = $Si(CH_3)_3$, the *diag*-[η^5-$C_5H_4Si(CH_3)_3$]$Re(CO)_2Br_2$ complex decomposed slowly in the molten state. It appears that a *diag–lat* equilibrium is set up in the homogenous melt, which is dependent on the R group (R = Et, K = [*lat*]/[*diag*] = 1.85; R = tBu, K = 0.42; and R = $Si(CH_3)_3$, K = 0.11). Molten state isomerization thus provides an alternative method to the preparation of *lat*-(η^5-C_5H_4R)$Re(CO)_2Br_2$, and our data indicate that the reversible isomerization is a general phenomenon for the monosubstituted (η^5-C_5H_4R)$Re(CO)_2Br_2$ complexes. The mechanism of such bi-directional isomerization is not as yet clear. Solvation effects clearly play a role in the isomerization reaction and overcome the thermodynamic constraints for the *diag* to *lat* isomerization reaction observed in the absence of solvents. The limited solvent study data suggest that the reaction is faster in nonpolar solvents, which means that a nondissociative mechanism is

involved.

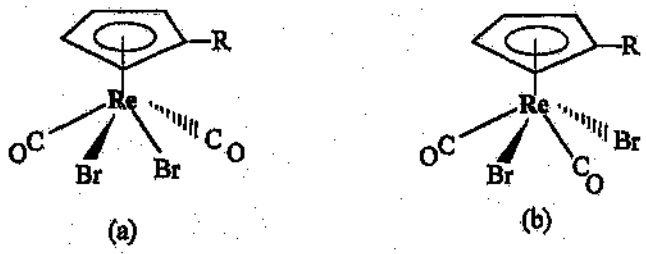

Figure 3.2 (a) Lateral and (b) diagonal isomers of $(\eta^5\text{-}C_5H_4R)Re(CO)_2Br_2$.

Solid state studies to investigate the latter isomerization are needed to establish the expected intramolecular nature of the reaction (unit cell volume changes, mode of Br-CO interconversion, etc.). Both lateral and diagonal conformations of $(\eta^5\text{-}C_5H_4R)Re(CO)_2Br_2$ must be sterically and /or electronically favored in the different phases (Figure 3.2).

3.4. Conclusion

The diagonal and lateral monosubstituted cyclopentadienyl four-legged piano stool rhenium complexes $(\eta^5\text{-}C_5H_4R)Re(CO)_2Br_2$ (R = Me, Et, tBu, $Si(CH_3)_3$, C_6H_{11}) were synthesized for the first time, and their structures were determined by elemental analysis and by IR and NMR spectroscopy. Similar to the unsubstituted analogue, the lateral $(\eta^5\text{-}C_5H_4R)Re(CO)_2Br_2$ complexes isomerized to the corresponding diagonal isomers upon refluxing in solution. Quite different from the parent complex $(\eta^5\text{-}C_5H_5)Re(CO)_2Br_2$, the reverse *diag* to *lat* isomerization was observed for the monosubstituted ring complexes $(\eta^5\text{-}C_5H_4R)Re(CO)_2Br_2$ in the solid state. Our results showed that the different ring-substituted complexes had

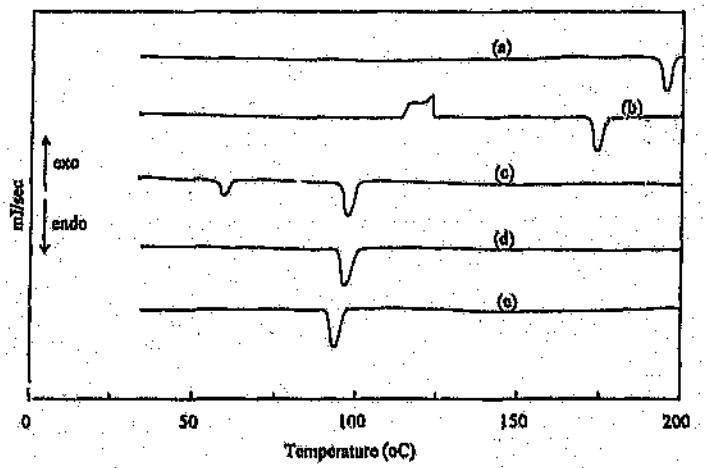

Figure 3.3. DSC curves for *diag*-(η^5-C_5H_4R)$Re(CO)_2Br_2$ complexes, (a) R = H, ΔH_f = +1.0 kJ/mol, (b) R = Me, ΔH_l = -0.44 kJ/mol, ΔH_f = +2.2 kJ/mol, (c) R = Et, ΔH_{mb} = +0.041 kJ/mol, ΔH_f = +2.2 kJ/mol, (d) R = tBu, ΔH_f = +2.1 kJ/mol and (e) R = $Si(CH_3)_3$, ΔH_f = +2.0 kJ/mol.

different *diag* to *lat* isomerization behavior. The diagonal $(\eta^5\text{-}C_5H_4Me)Re(CO)_2Br_2$ complex isomerized to the corresponding lateral isomer in almost quantitative yield when heated in the solid state and the isomerization proceeded exothermically. This is the first example of an organometallic complex that undergoes a nearly quantitative phase-dependent reversible isomerization reaction under only thermal conditions. The diagonal $(\eta^5\text{-}C_5H_4R)Re(CO)_2Br_2$ (R = Et, tBu, $Si(CH_3)_3$) complexes isomerized incompletely into the corresponding lateral isomers in the molten state, and the results revealed that the larger the ring substituent, the more difficult the *diag* to *lat* isomerization reaction. Solid state studies (single-crystal and powder X-ray diffraction) to explore the reasons for this unusual behavior will be presented in Chapter 4 and Chapter 8.

3.5. References

1. (a) Coville, N. J.; du Plooy, K. E.; Pickl, W. *Coord. Chem. rev.* **1992**, *116*, 1. (b) Janiak, K.; Schumann, H.; *Adv. Organomet. Chem.* **1991**, *33*, 291.
2. (a) Okuda, J. *Top. Curr. Chem.* **1991**, *160*, 97. (b) Halterman, L. R. *Chem. Rev.* **1992**, *92*, 965.
3. Möhring, P. C.; Coville, N. J. *J. Organomet. Chem.* **1994**, *479*, 1.
4. Nesmeyanov, A. N.; Kolobova, N. E.; Makarov, Yu. V.; Anisimov, K. M. *Izv. Akad. Nauk SSSR, Ser. Khim.* **1969**, 1826.
5. (a) King, R. B.; Reimann, R. H. *Inorg. Chem.* **1976**, *12*, 183. (b) King, R. B.; Reimann, R. H.; Darensburg, D. J. *J. Organomet. Chem.* **1975**, *93*, C23.
6. Einstein, F. W. B.; Klahn-Oliva, A. H.; Sutton, D.; Tyers, K. G. *Organometallics* **16**, *5*, 53.
7. Nesmeyanov, A. N.; Kolobova, N. E.; Makarov, Yu. N.; Anisimov, K. N. *Zh. Obshch. Khim.* **1974**, *44*, 2222.
8. Beach, L. D.; Dattilo, M.; Barnett, K. W. *J. Organomet. Chem.* **1977**, *140*, 47.
9. (a) Masciocchi, N.; Kolyshev, A.; Dulepov, V.; Boldyreva, E.; Sironi, A. *Inorg. Chem.* **1994**, *33*, 2579. (b) Grenthe, I.; Nordin, E. *Inorg. Chem.* **1979**, *18*, 1869. (c) Kawano, Y.; Tobita, H.; Ogino, H. *Organometallics* **1992**, *11*, 499.
10. Forder, J. R.; Mitchell, S. I.; Reid, G.; Simpson, H. R. *Polyhedron* **1994**, *13*, 2129.

11. Kukushkin, V. Yu.; Pan'kova, E. Yu.; Afanas'ev, E. A. *Zh. Neorg. Khim.* **1989**, *34*, 1342.

12. Cozak, D.; Gauvia, F.; Demers, J. *Can. J. Chem.* **1986**, *64*, 71.

13. Lappert, M. F.; Pickett, C. J.; Reley, P. I.; Yarrow, P. I. W. *J. Chem. Soc., Dalton Trans.* **1981**, 805.

14. Tam, W.; Lin, G. Y.; Wong, W. K.; Kiel, W. A.; Wong, V. K.; Gladysz, J. A. *J. Am. Chem. Soc.* **1982**, *104*, 141.

15. Nesmeyanov, A. N.; Anisimov, K. N.; Barlchnikov, L. I. *Izv. Akad. Nauk SSSR, Ser. Khim.* **1963**, 193.

16. Abel, E. W.; Moorhouse, S. *Angew. Chem., Int. Ed. Engl.* **1971**, *10*, 339.

17. Singh, P.; Rausch, D. M.; Bitterwolf, E. T. *J. Organomet. Chem.* **1988**, *352*, 273.

18. Lobanova, I. A.; Zdanovich, V. I.; Petrovskii, P. V.; Kolobova, N. E. *J. Organomet. Chem.* **1985**, *292*, 395.

19. Diaz, G.; Klahn, A. H.; Manzur, C. *Polyhedron* **1988**, *7*, 2743.

20. Beck, W.; Melnikoff, A. *Angew. Chem., Int. Ed. Engl.* **1965**, *4*, 692.

21. Palmer, B. J.; Becalska, A.; Hader, R.; Hill, R. H. *Polyhedron* **1991**, *10*, 877.

CHAPTER 4

INTERMOLECULAR INTERACTIONS IN CRYSTAL STRUCTURES: X-RAY SINGLE-CRYSTAL STRUCTURES OF *DIAG-* AND *LAT-* (η^5-C_5H_4Me)$Re(CO)_2Br_2$

4.1. Introduction

Chapter 3 described a unique phase-dependent isomerization reaction of (η^5-C_5H_4R)$Re(CO)_2Br_2$ (R = Me). It was observed that a reversible isomerization reaction occurred at nearly the same temperature in different phases (Scheme 4.1)

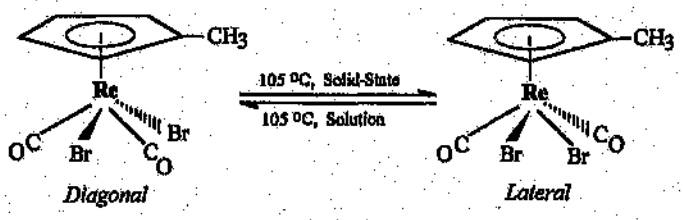

Scheme 4.1

A literature survey has shown that the solid-state isomerization reactions of coordination compounds have been studied for almost one hundred years (Chapter 2). Reactions include *cis-trans* isomerization reactions of four or six coordinate

metal complexes, nitro to nitrito linkage isomerization reactions of some Co(III)–amine complexes and isomerization reactions at a ligand. However, in no instance has a *thermal* reversible isomerization reaction been reported for any of these complexes.

It is thus obvious that the *diag-lat* isomerization reaction of $(\eta^5\text{-}C_5H_4Me)Re(CO)_2Br_2$ provides an unique example with which to explore factors that influence inter and intramolecular bonding interactions. We have thus undertaken a single-crystal, as well as a powder diffraction study of the title compounds and report here are our findings obtained from this study.

4.2. Experimental Section

The diagonal and lateral isomers of $(\eta^5\text{-}C_5H_4Me)Re(CO)_2Br_2$ complexes were synthesized as described in Chapter 3. Single crystals of the two isomers were crystallized from a mixture of dichloromethane/hexane under nitrogen at room temperature.

Crystals of both isomers were selected for single-crystal X-ray analysis by standard oscillation and Weissenberg techniques. Accurate cell constants and intensity data were measured on an Enraf-Nonius CAD4 diffractometer, using standard instrument settings at room temperature. The structures were solved by standard Patterson procedures and refined by least-squares methods based on F^2. The SHELX [1] suite of programs were used for all crystallographic computations. In the

final stages of refinement hydrogen atoms were placed in geometrically calculated positions and refined in riding mode with displacement parameters linked to those of their connected carbon atoms.

Powder diffraction data were measured on a Philips spectrometer equipped with a Cu K_α radiation source (λ = 1.5418 Å) and samples were prepared by spreading about 100 mg powder (the samples were not ground since grinding could initiate the solid-state isomerization) on a silicon crystal disc, held in place by a thin silicone grease.

4.3. Results and Discussion

The X-ray powder diffraction spectra of pure *diag*- and *lat*-(η^5-C_5H_4Me)$Re(CO)_2Br_2$, and the product of the solid-state isomerization of the diagonal isomer are given in Figure 4.1. It is clear that the powder diffraction patterns and intensities of *lat*-(η^5-C_5H_4Me)$Re(CO)_2Br_2$, obtained from (i) the diagonal isomer in the solid state and (ii) from the bromination of the corresponding tricarbonyl complex in solution, were the same. This confirms that the lateral structure is the thermal solid-state isomerization product of the diagonal isomer.

Crystal data and structure refinement data for *diag*- and *lat*-(η^1-C_5H_4Me)$Re(CO)_2Br_2$ are given in Table 4.1. Stereoscopic views of both of the

three-dimensional molecular structures are shown in Figures 4.2–4.5. Crystallographic data, fractional atomic coordinates, bond lengths and angles, structure factors are given in Appendix A.

4.3.1 Analysis of the structures

A literature review has shown that only ten single crystal structures of cyclopentadienyl four-legged piano stool rhenium complexes, mostly solution stable diagonal isomers, have been reported (Chapter 2, Table 2.2). This is the first time that the crystal structures of both diagonal and lateral isomers of the same rhenium complex have been established.

All bond lengths and angles of *diag*- and *lat*-(η^5-C_5H_4Me)$Re(CO)_2Br_2$ are comparable with literature values of similar complexes. The Re–C(CO) bond lengths are in the range 1.85–2.05 Å that have been reported for *diag*-(η^5-C_5Me_5)$Re(CO)_2Br_2$,[2] *lat*-(η^5-C_5Me_5)$Re(CO)_2I_2$,[2] *diag*-(η^5-C_5Me_5)$Re(CO)_2(H)_2$,[3] *diag*-(η^5-C_5Me_5)$Re(CO)_2Et_2$,[4] *diag*-(η^5-C_5H_5)$Re(CO)_2(\eta^1$-PhCO)Br,[5] *diag*-(η^5-C_5Me_5)$Re(CO)_2(Ph)I$,[6] *diag*-(η^5-C_5H_5)$Re(CO)_2(SnPh_3)_2$,[7] *diag*-(η^5-C_5H_5)$Re(CO)_2(CH_3)(COCH_3)$,[8] *diag*-(η^5-C_5H_5)$Re(CO)_2(Me)Br$[9] and *lat*-(η^5-C_5H_5)$Re(CO)_2(H)(CH_2Ph)$.[10] The interbond angle relating to the carbonyl groups C(1)–Re–C(2) of 104.0 ° of the diagonal isomer is similar to that observed for the *diag*-(η^5-C_5Me_5)$Re(CO)_2Br_2$ (104.3 °),[2] *diag*-(η^5-C_5Me_5)$Re(CO)_2(H)_2$ (100.1 °),[3] *diag*-(η^5-C_5Me_5)$Re(CO)_2Et_2$ (103.1 °),[4] *diag*-(η^5-C_5H_5)$Re(CO)_2(\eta^1$-PhCO)Br

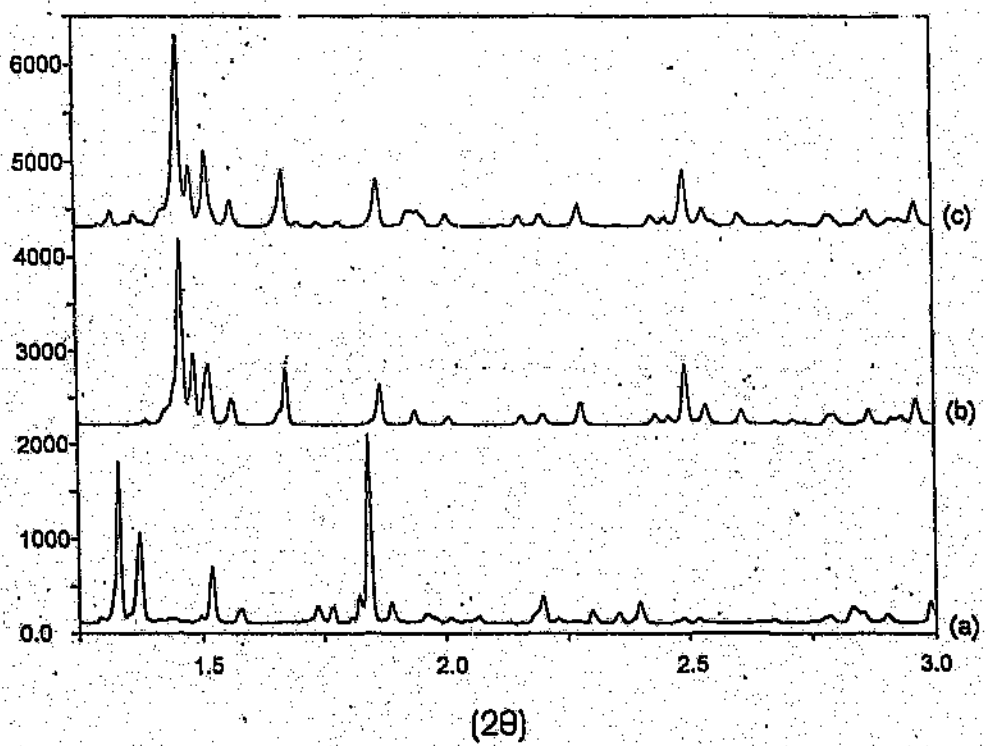

Figure 4.1. XRD powder diffraction data for (a) *dtag*- (b) *lat*- and (c) *lat*-(η^5-C_5H_4Me)$Re(CO)_2Br_2$ after thermal isomerization from the diagonal isomer.

(110.1 °),[5] *diag*-(η^5-C_5Me_5)Re(CO)$_2$(Ph)I (102.3 °),[6] *diag*-(η^5-C_5H_5)Re(CO)$_2$($SnPh_3$)$_2$ (100.4 °),[7] *diag*-(η^5-C_5H_5)Re(CO)$_2$(CH_3)($COCH_3$) (101.2 °)[8] and *diag*-(η^5-C_5H_5)Re(CO)$_2$(Me)Br (102 °)[9] and indicates the diagonal orientation of the two CO ligands. The carbonyl group interbond angle C(1)–Re–C(2) in the lateral isomer is 78.6 ° comparable with that observed for *lat*-(η^5-C_5Me_5)Re(CO)$_2$I$_2$ (78.5 °)[2] and *lat*-(η^5-C_5H_5)Re(CO)$_2$(H)(CH_2Ph) (84.2 °).[10] The Re–Br bond lengths of both isomers of 2.58 Å are almost same as those reported for *diag*-(η^5-C_5Me_5)Re(CO)$_2$Br$_2$ (2.58 Å).[2] The average Re–C(ring) bond distances of diagonal and lateral isomers are also comparable with those observed in other rhenium complexes containing the Cp group, with the average values of 2.280 Å and 2.285 Å, respectively.

The interesting asymmetry in the Re–C bond lengths to the cyclopentadienyl ring corresponding to a "tilting" of the ring reported for *lat*-(η^5-C_5Me_5)Re(CO)$_2$I$_2$ [2] was also observed for our *lat*-(η^5-C_5H_4Me)Re(CO)$_2$Br$_2$ and *lat*-(η^5-C_5H_4tBu)Re(CO)$_2$Br$_2$ (Chapter 8), i.e. the longest Re–C(ring) bonds, Re–C_3 (2.388 Å) and Re–C_7 (2.363 Å), are on the same side of the two bromide ligands while the shortest Re–C_5 (2.199 Å) is on the same side of carbonyl groups (Figure 4.5). Sutton has proposed that the CO ligands of *lat*-(η^5-C_5Me_5)Re(CO)$_2$I$_2$ withdraw π–electron density and diminish the π–contribution to the Re–C(ring) bonds *trans* to them, thereby resulting in lengthening.[2] Hoffmann has suggested that a degree of tilting of the Cp ring observable in some $CpML_4$ compounds is

Table 4.1. Crystal data and details of structure refinement for *diag*- and *lat*-(η^5-C_5H_4Me)$Re(CO)_2Br_2$

Complex	diag-(η^5-C_5H_4Me)$Re(CO)_2Br_2$	Lat-(η^5-C_5H_4Me)$Re(CO)_2Br_2$
Identification code	OM 69	OM 68
Empirical formula	$C_8H_7Br_2O_2Re$	$C_8H_7Br_2O_2Re$
Formula weight	481.16	481.16
Temperature	293(2) K	293(2) K
Wavelength	0.71069 A	0.71069 A
Crystal system	Triclinic	monoclinic
Space group	P-1	$P2_1/c$
Unit cell dimensions	a = 6.751(2)Å, α = 96.698(12)° b = 8.5366(13)Å, β = 93.15(2)° c = 9.7578(14)Å, γ= 105.96(2)°	a= 11.8196(11)Å, α=90.000(11)° b = 7.1330(9)Å, β = 98.278(8)° c= 12.9236(13)Å, γ= 90.000(12)°
Volume ($Å^3$)	534.8(2)	1078.2(2)
Z	2	4
Density (calculated)	2.988 g/cm^3	2.964 g/cm^3
Absorption coefficient	18.797 nm^{-1}	18.646 nm^{-1}
F (000)	432	864
Crystal size	0.4 × 0.2 × 0.4 mm	0.3 × 0.3 × 0.2 mm
θ range for data collection	2.11 to 34.95 °	1.74 to 34.95 °
Index ranges	-10 ≤ h ≤ 10 , -13 ≤ k ≤ 13 , -15 ≤ l ≤ 15 ,	-19 ≤ h ≤ 18 , 0 ≤ k ≤ 11 , 0 ≤ l ≤ 20 ,
Reflections collected	6936	5818
Independent reflections	3711, [R(int) = 0.0222]	4731, [R(int) = 0.0999]
Refinement method	Full-matrix less-squares on F^2	Full-matrix less-squares on F^2
Data / restrains / parameters	3711 / 0 / 108	4731 / 0 / 109
Goodness-of-fit on F^2	1.180	1.264
Final R indices [I > 2σ (I)]	R1 = 0.0295, wR2 = 0.0776	R1 = 0.0717, wR2 = 0.1551
R indices (all data)	R1 = 0.0295, wR2 = 0.0776	R1 = 0.0744, wR2 = 0.1565
Largest diff. peak and hole / e.$Å^{-3}$	1.539 and -2.000	2.381 and -2.659

accountable by interactions involving σ orbitals of the metal and Cp ligand. In essence, it appears that (in projection) the eclipsing of a M–C(Cp) bond with a M–L bond results in a slightly long M–C(Cp) bond length, whereas when a M–C(Cp) bond is staggered between the M–L bonds, it is short.[11]

However, neither postulate can account for our results and intra-steric factors may play an important role in the observed tilting. For example, the longest Re–C(ring) bond in *diag*-(η^5-C_5H_4Me)Re(CO)[P(OPh)$_3$]Br$_2$, Re–C$_6$ (2.365 Å, Figure 8.2), is *cis*, not *trans*, to the CO group. From our six single crystal structures of diagonal and lateral isomers of (η^5-C_5H_4Me)Re(CO)$_2$Br$_2$, (η^5-C_5H_4Me)Re(CO)[P(OPh)$_3$]Br$_2$ and (η^5-C_5H_4tBu)Re(CO)$_2$Br$_2$, and crystal data of *lat*-(η^5-C_5Me_5)Re(CO)$_2$I$_2$,[2] it appears that the steric repulsion between the eclipsing ligand atoms and the Cp ring atoms is the determining factor for the degree of tilting of the Cp ring. The bigger the atoms eclipsed, the longer the Re–C(ring) bond. In these complexes, the relative sizes of atoms and groups are I > Br > P > C and tBu > Me > H, therefore, the observed differences between the average value of two longest Re–C(ring) bonds and the shortest Re–C(ring) bond, which represents a degree of the tilting of the Cp ring, are 0.19 Å, 0.176 Å and 0.10 Å for *lat*-(η^5-C_5Me_5)Re(CO)$_2$I$_2$,[2] *lat*-(η^5-C_5H_4Me)Re(CO)$_2$Br$_2$ (Figure 4.5) and *lat*-(η^5-C_5H_4tBu)Re(CO)$_2$Br$_2$ (Figure 8.5), respectively. From the projection views, the eclipsing or nearly eclipsing two groups in these complexes are I and C–Me (ring), Br and C–Me (ring) and Br and C–H (ring). In other complexes the

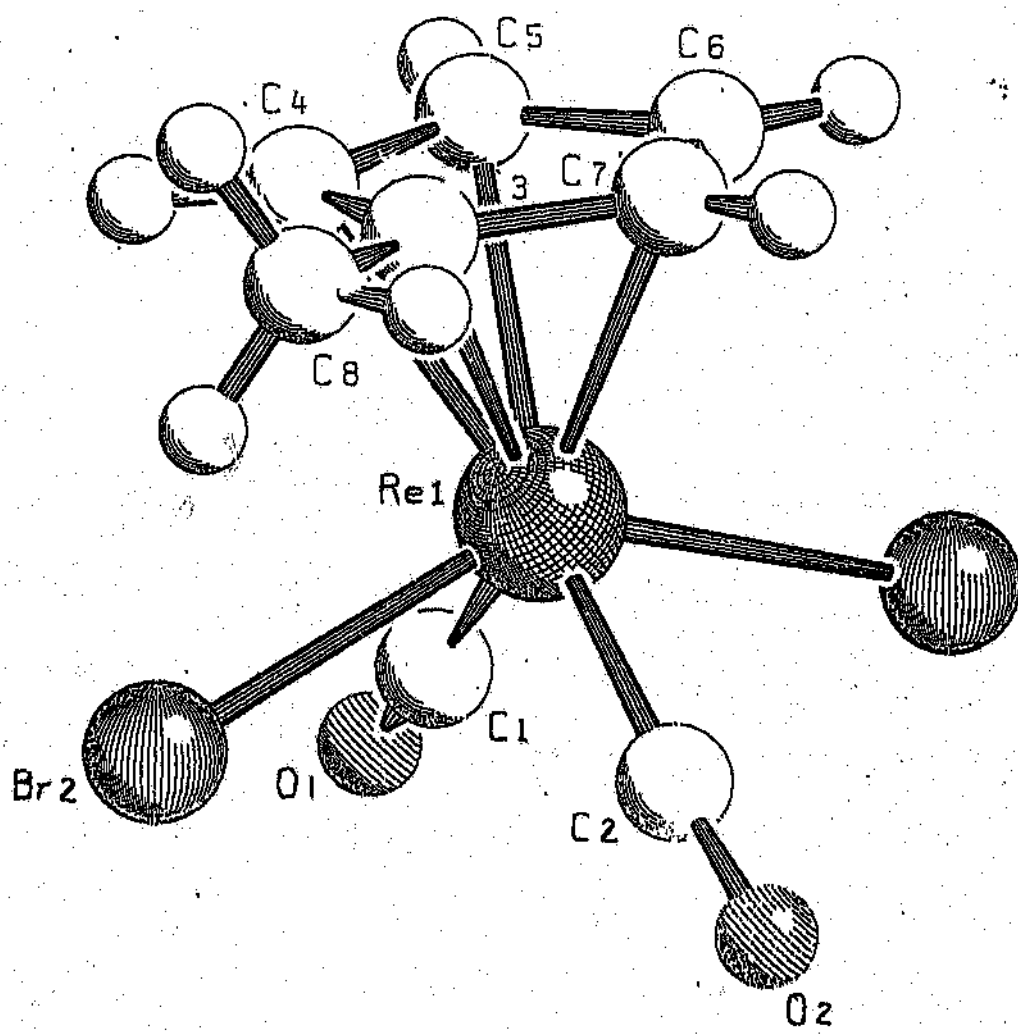

Figure 4.2. Perspective view (SCHAKAL plot) of *diag*-(η^5-C_5H_4Me)$Re(CO)_2Br_2$ showing the atom labeling.

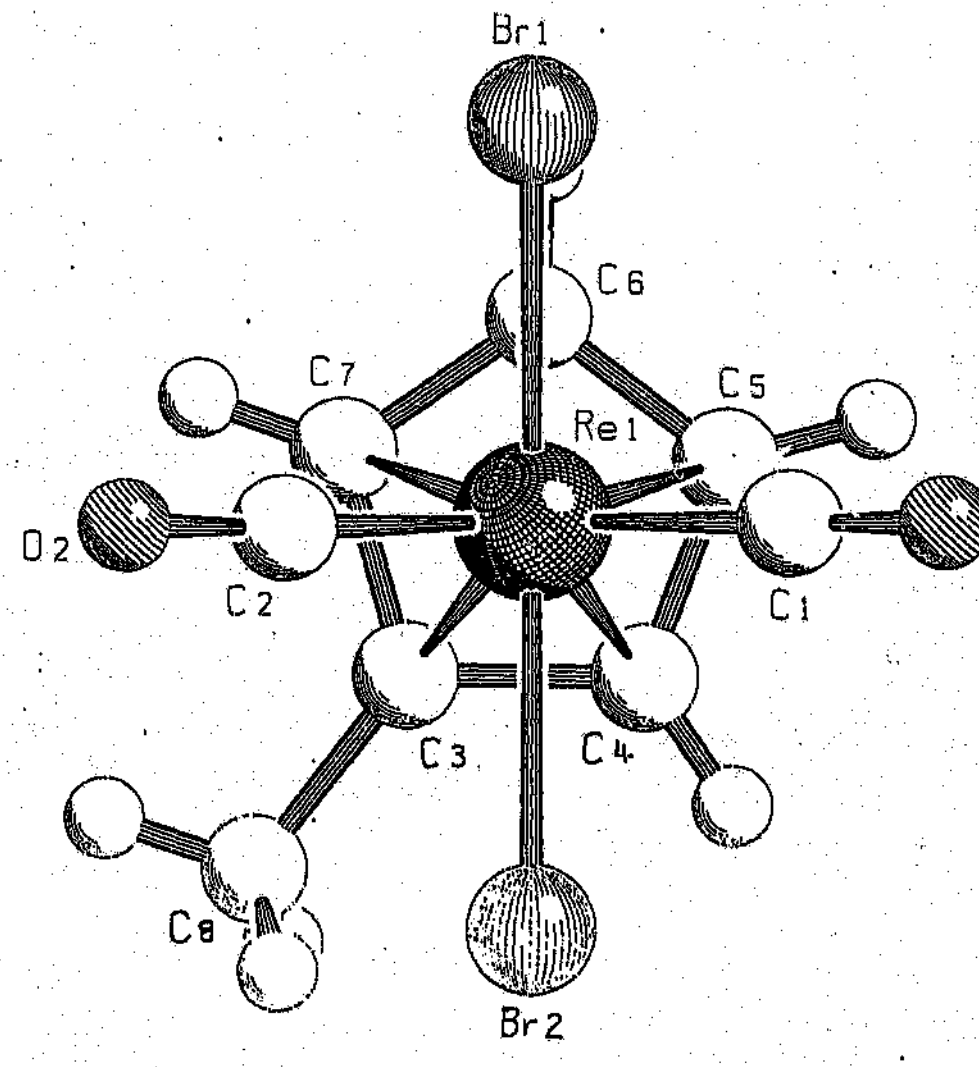

Figure 4.3. View of *diag*-(η^5-C_5H_4Me)$Re(CO)_2Br_2$ projected onto the plane of the Cp ring.

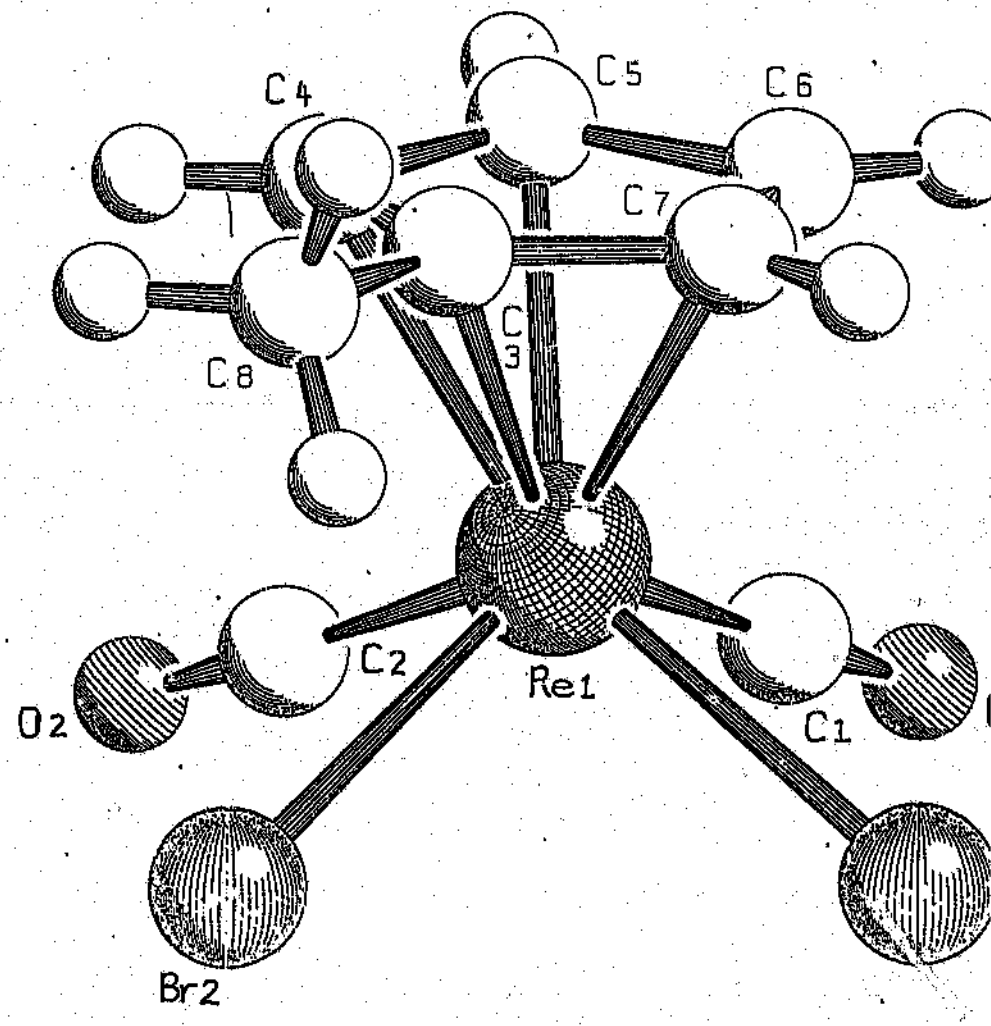

Figure 4.4. Perspective view (SCHAKAL plot) of *lat*-(η^5-C_5H_4Me)$Re(CO)_2Br_2$ showing the atom labeling.

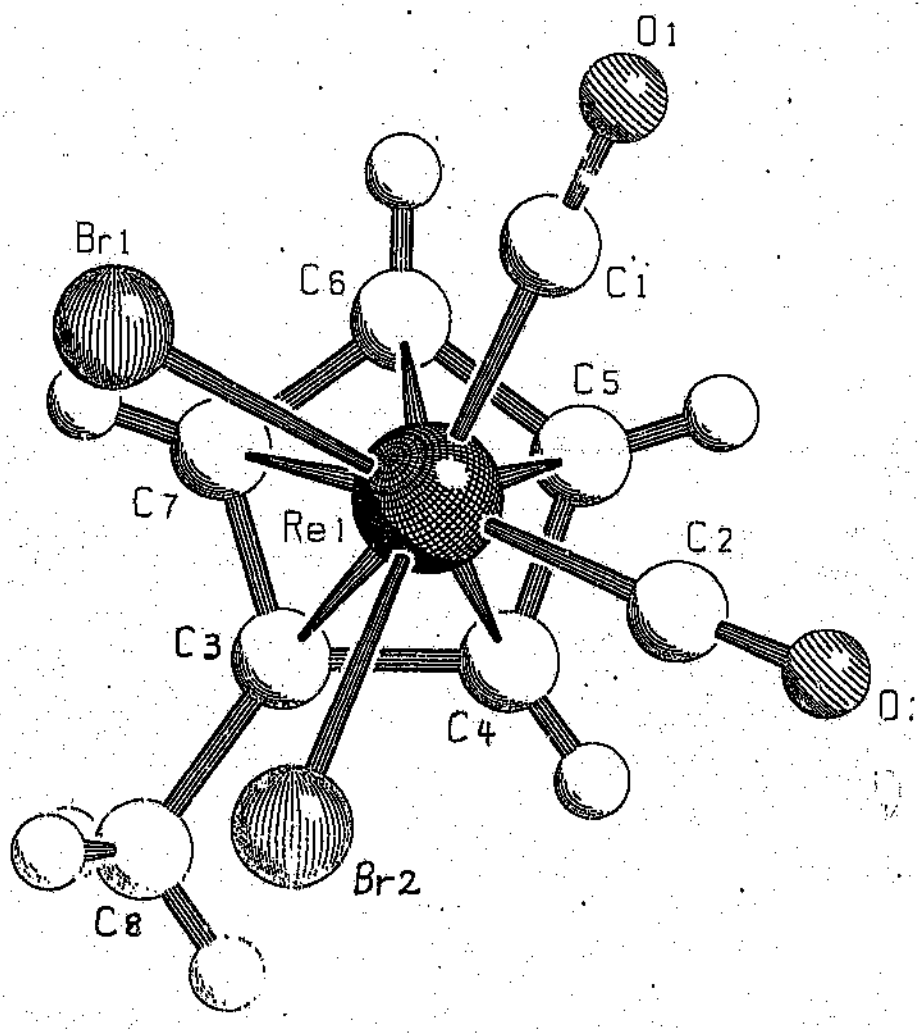

Figure 4.5. View of *lat*-(η^5-C_5H_4Me)$Re(CO)_2Br_2$ projected onto the plane of the Cp ring.

longest Re–C(ring) bonds are also the ones most nearly eclipsed by the Br ligand, the biggest atom among the four-leg ligands.

However, the role of intermolecular interactions can not be ruled out, although no dominant interaction yet identified.

4.3.2 Analysis of intermolecular interactions

There are two possible scenarios that can account for the observed solid-state reaction. The first is that the isomerization reaction occurs first. After the chemical reaction of one molecule is complete there is now stress in the crystal and the molecular structure of the others will now rearrange to relieve this stress. The second possibility is that on increasing the temperature the crystal undergoes a phase transition first, and that the chemical reaction follows this transition. It is known that any temperature-dependent phase transition is triggered by some interaction. On increasing the temperature an isomer may be rendered unstable and a reaction in which a rearrangement occurs to release the stress can take place. This reaction will proceed from a less symmetrical low temperature form to a more symmetrical arrangement at the higher temperature.[12]

For this set of complexes the isomerization reaction goes in opposite directions in solution and in the solid state. This suggests that on increasing the temperature an interaction occurs in the solid state which drives the isomerization reaction.

The diagonal isomer crystallizes in the triclinic space group P-1 while the lateral isomer crystallizes in a more symmetrical monoclinic space group, P $2_1/n$. Thus, it would be *expected* on symmetry grounds that the direction of the phase transition should be from the *diag* to the *lat* isomer in the solid state.[12]

Irrespective as to which is the correct proposal, the reaction involves going from a high energy form to a low energy form. What drives the reaction?

Intermolecular interactions in the solid state.

The difference in the intermolecular interactions between the isomers can be clearly seen from their packing diagrams (Figure 4.6 and 4.7).

In the diagonal isomer (Figure 4.6), the molecules align themselves along the direction of the two bromine atoms, with all the cyclopentadienyl rings arranged in the same layers. However they face in opposite directions in neighboring layers, with the methyl groups pointing to each other between two neighboring arrays. In the lateral isomer (Figure 4.7), the molecules line up in the direction of the cyclopentadienyl center and the methyl group. The two bulky bromine atoms are in the same plane as the neighboring ring but far away from the methyl group of that ring.

The melting point of the lateral isomer is significantly higher than that of the diagonal isomer (*diag*: 116-118 °C, *lat*: 158-160 °C). This could be a result of the

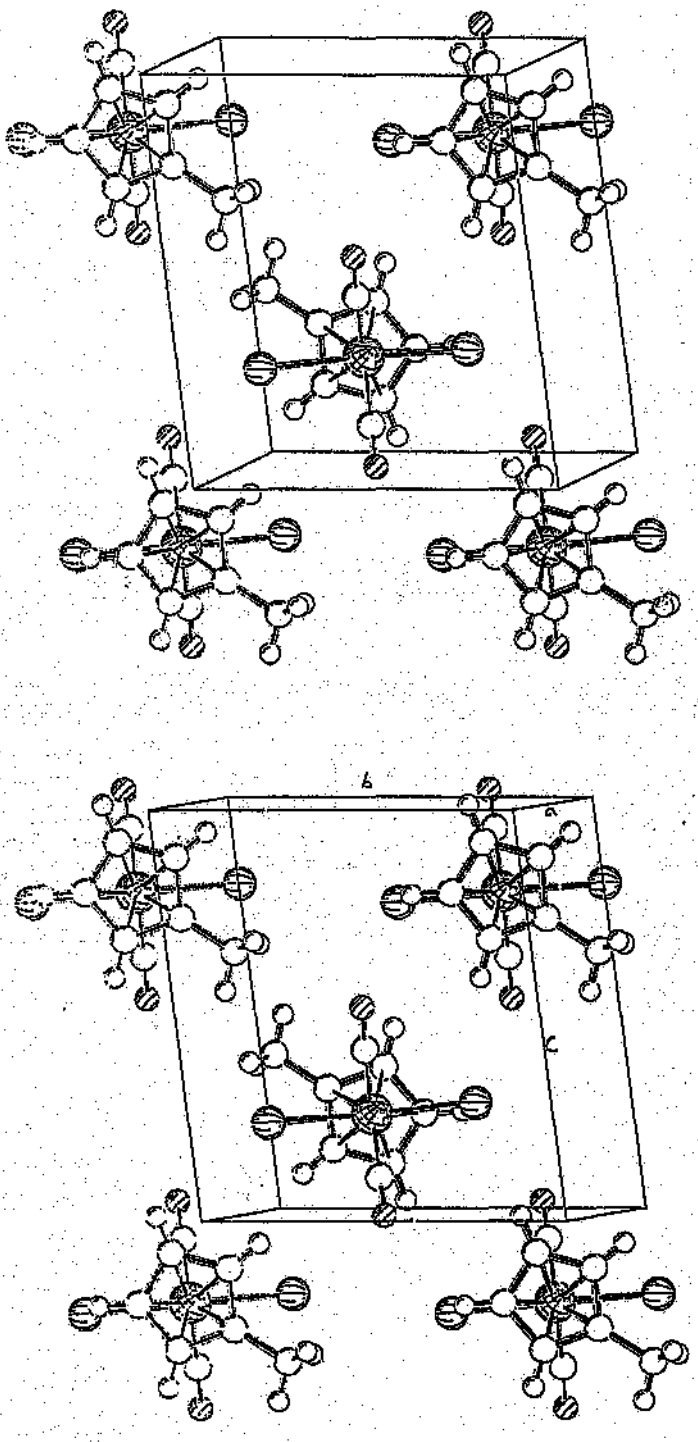

Figure 4.6. Packing diagram of *diag*-(η^5-C_5H_4Me)$Re(CO)_2Br_2$ projected on the [100] plane.

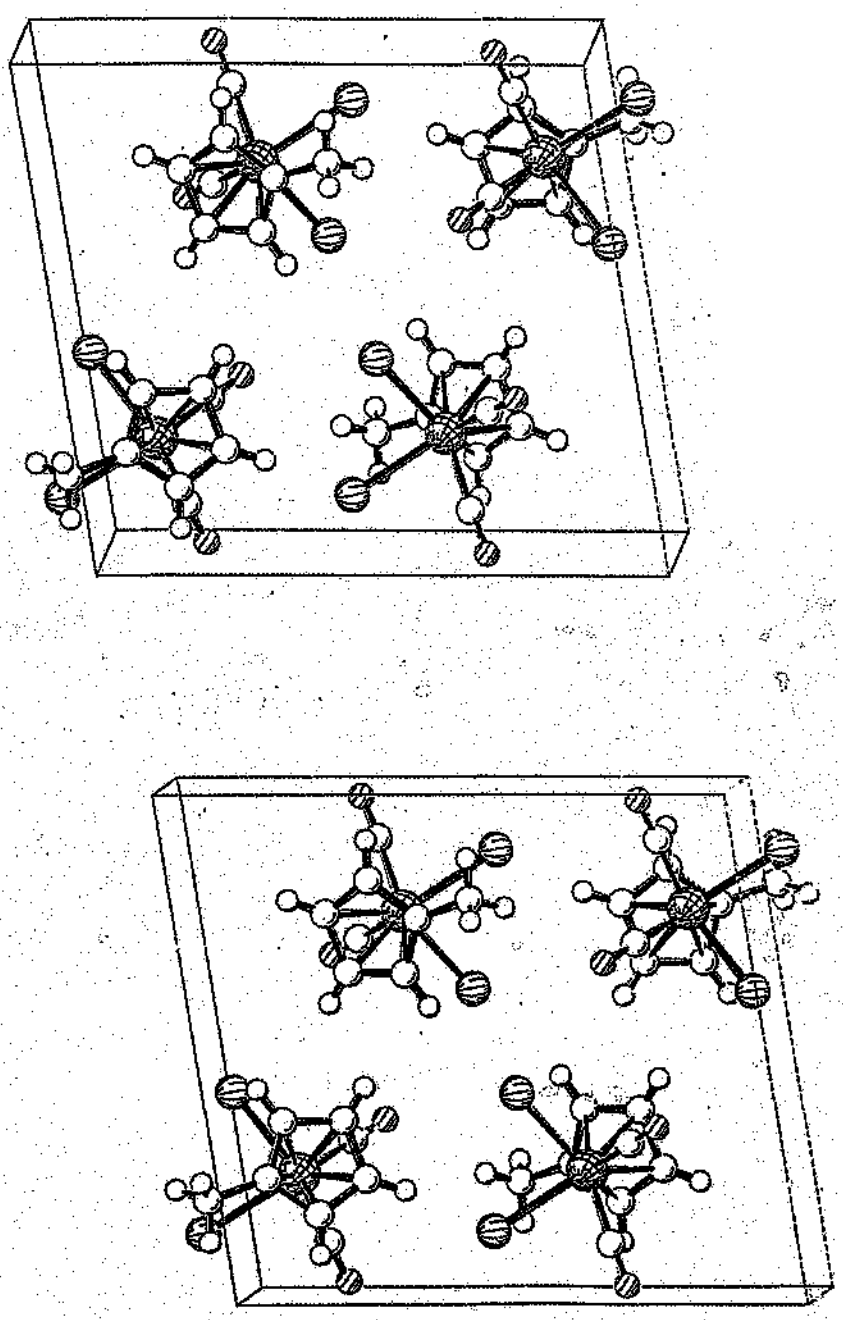

Figure 4.7. Packing diagram of *lat*-(η^5-C_5H_4Me)$Re(CO)_2Br_2$ projected on the [010] plane.

arrangement of lateral isomers in the $P2_1/c$ structure, which involves strong dipole-dipole intermolecular interactions. It is suggested that this obvious difference in intermolecular interaction is the driving force for the diagonal to lateral isomerization reaction in the crystal. Molecules will always tend t arrange themselves t minimize the lattice energy. The steric repulsion between two big bromine atoms from two neighboring molecules could also favor *diag*-to-*lat* isomerization.

Unfortunately the molecular mechanics calculations carried out on the two isomers did not reveal any non-bonded teractions of note. Further, the energies of the two isolated isomer molecules ob. from the calculations were approximately the same.[13]

The most important result obtained in this analysis has been the proposal that intermolecular interactions can invert the normal stability order of isomers found in solution. This has an important bearing on the notion that molecular structure is a function of the environment.

4.4 References

1. (a) Sheldrick, G. M. SHELXL-93, Universitat Gottingen, 1993. (b) Sheldrick, G. M. *Acta Crystallogr.*, **1990**, *A46*, 467.

2. Einstein, F. W. B.; Klahn-Oliva, A. H.; Sutto, D.; Tyers, K. G. *Organometallics*, **1986**, *5*, 53.

3. Ball, R. G.; Campen, A. K.; Graham, W. A. G.; Hamley, P. A.; Kazarian, S. G.; Ollino, M. A.; Poliakaff, M.; Rest, A. J.; Sturgeoff, L.; Whitewell, I. *Inorg. Chim. Acta*, **1997**, *259*, 137.

4. Klahn, A. H.; Manzur, C.; Toro, A.; Moore, M. *J. Organomet. Chem.*, **1996**, *516*, 51.

5. Filippou, A. C.; Lungwitz, B.; Kociok-Kohn, G.; Hinz, I. *J. Organomet. Chem.*, **1996**, *524*, 133.

6. Klahn, A. H.; Toro, A.; Arenas, M.; Manriquez, V.; Wittke, O. *J. Organomet. Chem.*, **1997**, *532*, 39.

7. Lee, S. W.; Yang, K.; Martin, J. A.; Bott, S. G.; Richmond, M. G *Inorg. Chim. Acta*, **1995**, *232*, 57.

8. Goldberg, K. I.; Berman, R. G. *J. Am. Chem. Soc.*, **1989**, *111*, 1285.

9. Alekandrov, G. G.; Struchkov, Yu. T.; Makarov, Yu. V. *Zhurnal Strukturnoi Khimii*, **1973**, *14*, 98.

10. Fischer, E. O.; Frank, A. *Chem. Ber.*, **1978**, *111*, 3740.

11. Kubacek, P.; Hoffman, R.; Havlas, Z. *Organometallics*, **1982**, *1*, 180.

12. Atkins, P. W.; *Physical Chemistry*, Oxford University Press, 3rd Ed. 1986, Chap 7 and 9.

13. A private communication with Dr D.C. Levendis, Department of Chemistry, University of the Witwatersrand.

CHAPTER 5

SOLID-STATE PHOTOCHEMICAL *DIAG-LAT* ISOMERIZATION OF $(\eta^5\text{-}C_5H_4R)Re(CO)(L)X_2$ ON THE SURFACE OF SILICA GEL

5.1. Introduction

Compared to the development of synthetic chemistry in the solution state, synthetic chemistry employing solid state reactivity has been less developed.[1] Indeed, a survey of the organometallic chemistry literature reveals that little exploration of the use of the solid phase in the synthesis of new molecules has been reported. From what has been reported the reactions can be divided into three types.[2]

Firstly, solid state reactions can occur within a solid. For example, a range of isomerization reactions have been carried out both thermally and photochemically in the solid state. Reactions include nitrito to nitro isomerization[3] and *cis* to *trans* isomerization of chromium,[4] ruthenium,[5] platinium[6] and rhenium[7] complexes.

Secondly, reactions can occur *between* solid particles. Here the intimacy and method of interaction (heating, shaking, grinding *etc.*) become critical and particle size typically plays a dominant role in determining the reaction rate. This

methodology has been exploited in organic chemistry[1] and materials science[8] but appears to be little developed in the synthesis of organometallic compounds.

Finally, the surfaces of solids can be used as reagents for carrying out reactions. Thus, reagents can be added to a surface and the surface-reagent interaction used to induce reactivity such that the reagent is converted into a product which can be extracted from the surface in a later step. In these reactions the product is formed in a solid state reaction and is to be differentiated from the use of the heterogeneous complexes to bring about reactions in the solution phase.[9,10] Studies of surface-organometallic complexes have been directed at the production of well controlled heterogeneous materials, e.g. $Mo(CO)_n$ on a range of surfaces,[11] for use in gas and liquid phase catalytic reactions.[12] The use of the surface as a reagent for the synthesis of new organometallic complexes has been less extensively exploited.[13]

In this chapter we wish to report on a novel example of the third type of solid state reaction. We (Chapter 3) and others[14] have reported that *lat*-(η^5-C_5R_4R')$Re(CO)_2X_2$ isomerizes to *diag*-(η^5-C_5R_4R') $Re(CO)_2X_2$ (R = H, Me; R' = H, alkyl group, X = halogen) in the solution phase. Herein we report that surface supported (η^5-C_5H_4R)Re(CO)(L)X_2 (L = CO, phosphite) undergoes a solid state photochemical isomerization reaction in the reverse direction to that observed in the solution phase, a reaction which indicates the influence of the surface as a ligand in the overall reaction. This reaction provides for a facile synthesis of *lat*-

$(\eta^5\text{-}C_5H_4R)Re(CO)(L)X_2$.

5.2. Experimental Section

The diagonal and lateral $(\eta^5\text{-}C_5H_4R)Re(CO)(L)Br_2$ (R = Me, Et, tBu, $Si(CH_3)_3$, L = CO; R = H, L = CO, $P(OMe)_3$, $P(OPh)_3$) complexes were prepared by the methods described in Chapter 3 and ref. 14(a). Silica gel, Kieselgel PF_{254} (Merck) for preparative thin layer chromatography was used as the support for most of the reactions. Dichlorodimethylsilane (98%) was obtained from Merck. Solvents were dried by conventional methods, distilled under nitrogen, and used immediately. Irradiation was carried out with two 200-W incandescent lamps. The B.E.T. surface area measurements of the inorganic solids were performed using the N_2 adsorption method with classical gas phase surface area equipment constructed in our dep: rtment.[15] Melting points were recorded on a Kofler hotstage melting point apparat is. Infrared spectra were measured on a Midac FTIR spectrometer, usually in KBr cells (solutions). NMR spectra were measured on a Bruker AC200 spectrometer operating at 200 MHz. Microanalyses were carried out at the CSIR, Pretoria, South Africa.

5.2.1. Irradiation Experiments

Experiments were performed as follows. Pyrex cylinders (22 mm × 90 mm) were used as reactors and were loaded with *diag*- or *lat*-$(\eta^5\text{-}C_5H_4R)Re(CO)(L)X_2$ (0.038 mmole) dissolved in CH_2Cl_2 (3 mL). Silica gel (300 mg) was added to the

reactor, the reagents well mixed, and the CH_2Cl_2 removed under vacuum. The cylinders were sealed under nitrogen (atmospheric pressure) and rotated with a motor (8 rpm) with cylinder axis in a horizontal position. Two 200-W incandescent lamps ($\lambda > 370$ nm) were located 30 cm from the cylinder and the whole experimental apparatus was set up in a ventilated fume hood; this ensured minimum local heating from the lamp at the sample.[16] A thermometer placed next to the sample cylinder indicated that the temperature of the reaction vessel never exceeded 25 °C. A control experiment was performed in the dark by completely wrapping a cylinder, containing the silica supported *diag*-(η^5-C_5H_4Me)$Re(CO)_2Br_2$, with an aluminum foil. After completion of the irradiation, the products were extracted from the surface of the silica gel with CH_2Cl_2, separated on a silica gel column (CH_2Cl_2/hexane), weighed, and identified by IR and NMR spectroscopy.

The photochemical isomerization reaction of the pure amorphous solid *diag*- or *lat*-(η^5-C_5H_4Me)$Re(CO)_2Br_2$ was carried out in the same manner as described above. The irradiation of *diag*-(η^5-C_5H_4Me)$Re(CO)_2Br_2$ on other inorganic solids was also performed in the same way as described above except that two or more Pyrex cylinders were sometimes used in order to irradiate the large quantities of material required in the study.

5.2.2. Syntheses of *Diag*- and *Lat*-(η^5-C_5H_4Me)Re(CO)[P(OPh)$_3$]Br$_2$.

A solution of *diag*-(η^5-C_5H_4Me)Re(CO)$_2$Br$_2$ (100 mg, 0.208 mmole) and P(OPh)$_3$ (212 mg, 0.683 mmole) in toluene (25 mL) was refluxed under N_2 for 20 h. IR spectra indicated that all the starting material had reacted. After solvent removal under reduced pressure, the red residue was dissolved in dichloromethane and chromatographed on a silica gel column prepared in hexane. Successive elution with dichloromethane/hexane (1:1) and dichloromethane gave *diag*-(η^5-C_5H_4Me)Re(CO)[P(OPh)$_3$]Br$_2$ (48 mg, 30% yield) from a red band, and *lat*-(η^5-C_5H_4Me)Re(CO)[P(OPh)$_3$]Br$_2$ (92 mg, 58% yield) from a brown band, respectively.

5.2.3. Syntheses of *Diag*- and *Lat*-(η^5-C_5H_4Me)Re(CO)$_2$I$_2$.

To a solution of (η^5-C_5H_4Me) Re(CO)$_3$ (730 mg, 2.09 mmole) in 50 mL of dimethyl sulfoxide, a solution of I_2 (530 mg, 2.09 mmole) in 20 mL of dimethyl sulfoxide was added dropwise. After the reaction mixture was stirred for an additional 1.0 h at room temperature, the reaction was quenched by adding 100 mL of water at 25 °C. The resulting brown precipitate, which contained unreacted (η^5-C_5H_4Me)Re(CO)$_3$ and both isomers of (η^5-C_5H_4Me)Re(CO)$_2$I$_2$, was filtered and dried at 25 °C (0.1 mmHg). This solid was dissolved in dichloromethane and chromatographed on a silica gel column prepared in hexane. Successive elution with hexane, hexane/dichloromethane (1:1) and dichloromethane gave unreacted

(η^5-C_5H_4Me)$Re(CO)_3$ (350 mg, 48% recovery), *diag*-(η^5-C_5H_4Me)$Re(CO)_2I_2$ (245 mg, 20% conversion, 39% yield) from a red band, and *lat*-(η^5-C_5H_4Me)$Re(CO)_2I_2$ (106 mg, 9% conversion, 17% yield) from a brown band, respectively.

5.2.4. Syntheses of *Diag*- and *Lat*-(η^5-$C_5H_4{}^iPr$)$Re(CO)_2Br_2$.

A solution of Br_2 (136 mg, 0.85 mmole) in 2 mL of trifluoroacetic acid was added dropwise at 25 °C to a solution of (η^5-$C_5H_4{}^iPr$)$Re(CO)_3$ (304 mg, 0.81 mmole) in 3 mL of trifluoroacetic acid. After the reaction mixture was stirred for an additional 1.0 h at room temperature, the reaction was quenched by pouring it into 100 mL of water at 25 °C. The resulting brown precipitate, which contained unreacted (η^5-$C_5H_4{}^iPr$)$Re(CO)_3$ and both isomers of (η^5-$C_5H_4{}^iPr$)$Re(CO)_2Br_2$, was filtered and dried at 25 °C (0.1 mmHg). This solid was dissolved in dichloromethane and chromatographed on a silica gel column prepared in hexane. Successive elution with hexane, hexane/dichloromethane (1:1), and dichloromethane gave unreacted (η^5-$C_5H_4{}^iPr$)$Re(CO)_3$ (171 mg, 56% recovery), *diag*-(η^5-$C_5H_4{}^iPr$)$Re(CO)_2Br_2$ (66 mg, 16% conversion, 37% yield) from a red band, and *lat*-(η^5-$C_5H_4{}^iPr$) $Re(CO)_2Br_2$ (60 mg, 12% conversion, 33% yield) from a brown band, respectively.

5.2.5. Syntheses of *Diag*- and *Lat*-(η^5-C_5H_4Me)$Re(CO)_2BrI$.

(i) A solution of *diag*-(η^5-C_5H_4Me) $Re(CO)_2Br_2$ (57 mg, 0.118 mmole) and *diag*-(η^5-C_5H_4Me)$Re(CO)_2I_2$ (68 mg, 0.118 mmole) in benzene (25 mL) was refluxed

under nitrogen for 20 h. After solvent removal with a rotatory evaporator, the red solid was dissolved in dichloromethane and chromatographed on a silica gel column (1.5 cm × 60 cm) prepared in hexane. Careful elution with hexane/dichloromethane (4:1) and hexane/dichloromethane (1:1) gave *diag*-(η^5-C_5H_4Me)$Re(CO)_2I_2$ (35.8 mg, 53% recovery), *diag*-(η^5-C_5H_4Me)$Re(CO)_2BrI$ (48.5 mg, 39% conversion, 67% yield), *diag*-(η^5-C_5H_4Me)$Re(CO)_2Br_2$ (18.0 mg, 32% recovery), *lat*-(η^5-C_5H_4Me)$Re(CO)_2I_2$ (2.4 mg, 1.8% conversion, 3.0% yield), *lat*-(η^5-C_5H_4Me)$Re(CO)_2BrI$ (7.1 mg, 5.7% conversion, 9.8% yield) and *lat*-(η^5-C_5H_4Me)$Re(CO)_2Br_2$ (8.9 mg, 7.8% conversion, 13% yield).

(ii) Silica gel (900 mg) was added into a solution of NaI (17.1 mg, 0.114 mmole) in water (2 mL). The slurry was well stirred and dried in an oven at 120 °C. This pre-treated silica gel was then added to a solution of *diag*-(η^5-C_5H_4Me)$Re(CO)_2Br_2$ (55 mg, 0.114 mmole) in dichloromethane (3 mL), the reagents were well mixed and the CH_2Cl_2 removed under vacuum. The reaction mixture was placed into three Pyrex cylinders (22 mm × 90 mm) and sealed. After irradiation with two 200-W incandescent lamps at room temperature for 48 h, the reaction products were extracted from silica gel with dichloromethane and chromatographed on a silica gel column prepared in hexane. Elution with hexane/dichloromethane (1:1) gave first a mixture of *diag*-(η^5-C_5H_4Me)$Re(CO)_2I_2$, *diag*-(η^5-C_5H_4Me)$Re(CO)_2BrI$ and *diag*-(η^5-C_5H_4Me)$Re(CO)_2Br_2$ (14.7 mg, 24% yield), then *lat*-(η^5-C_5H_4Me)$Re(CO)_2I_2$ (7.5 mg, 11% yield), *lat*-(η^5-

$C_5H_4Me)Re(CO)_2BrI$ (12.0 mg, 20% yield) and *lat*-(η^5-$C_5H_4Me)Re(CO)_2Br_2$ (12.0 mg, 22% yield), respectively.

All new complexes were characterized by elemental analysis and by IR and NMR spectroscopy (Table 5.1).

5.3. Results and Discussion

Diag-(η^5-$C_5H_4Me)Re(CO)_2Br_2$ was loaded onto silica as described in the experimental section and irradiated with two 200-W lamps. A series of experiments were performed in which the reaction was terminated after different reaction times (1-72 h, Fig. 5.1). The products were extracted from the silica (>85%), separated on a chromatographic column, weighed, and analyzed by IR and NMR spectroscopy. The data indicated that after 24 h a photostationary state of the isomers had formed with [*lat*]/[*diag*] ratio ~7. Thus an isomerization reaction takes place on irradiation of silica in the solid state which favors the lateral isomer. This ratio is different from that achieved in the thermal solid state isomerization reaction (Chapter 3). Further, Hill and co-workers have reported that photoisomerization of (η^5-$C_5Me_5)Re(CO)_2Br_2$ on Si(111) at 77K gave a reaction in which the diagonal isomer was formed from the lateral isomer.[7] We have further observed that irradiation of either pure amorphous solid *diag*- or *lat*-(η^5-$C_5H_4Me)Re(CO)_2Br_2$ in the absence of silica resulted in no photoisomerization activity.

Table 5.1. Spectroscopic and Analytical Data for $(\eta^5\text{-}C_5H_4R)Re(CO)(L)X_2$ Complexes

compound	mp (°C)	ν_{co}[a] (cm^{-1})	^1H NMR[b] (ppm) Cp ring	R	L	analysis (%) C	H
diag-$(\eta^5\text{-}C_5H_4Me)Re(CO)[P(OPh)_3]Br_2$	164 - 166	1988	4.53 (t, 2H), 4.65 (t, 2H)[c]	1.64 (s, 3H)[c]	6.88 - 7.56 (m, 15H)[c]	calcd 39.33	2.90
						found 39.39	2.68
diag-$(\eta^5\text{-}C_5H_4{}^iPr)Re(CO)_2Br_2$	112 - 114	1997, 2062	5.38 (t, 2H) 5.71 (t, 2H)	1.29 (d, 6H) 2.83 (m, 1H)		calcd 23.59	2.18
						found 23.35	1.88
diag-$(\eta^5\text{-}C_5H_4Me)Re(CO)_2I_2$	142 -144	1982, 2048	5.29 (t, 2H), 5.71 (t, 2H)	2.44 (s, 3H)		calcd 16.71	1.23
						found 16.54	1.04
diag-$(\eta^5\text{-}C_5H_4Me)Re(CO)_2BrI$	125-127	1989, 2054	5.52 (t, 2H), 5.70 (t, 2H)	2.36 (s, 3H)		calcd 18.19	1.34
						found 18.08	1.15
lat-$(\eta^5\text{-}C_5H_4Me)Re(CO)[P(OPh)_3]Br_2$	183 - 185	1959	4.62 (d, 1H), 4.72 (d, 1H), 4.77 (d, 1H), 5.07 (d, 1H)[c]	1.73 (s, 3H)[c]	6.75 - 7.55 (m, 15H)[c]	calcd 39.33	2.90
						found 39.38	2.69
lat-$(\eta^5\text{-}C_5H_4{}^iPr)Re(CO)_2Br_2$	127 - 129	1978, 2054	5.88 (d, 2H), 5.92 (d, 2H)	1.28 (d, 6H) 2.88 (m, 1H)		calcd 23.59	2.18
						found 23.36	1.92
lat-$(\eta^5\text{-}C_5H_4Me)Re(CO)_2I_2$	127-129	1972, 2040	5.78 (m, 4H)	2.58 (s, 3H)		calcd 16.71	1.23
						found 16.54	1.04
lat-$(\eta^5\text{-}C_5H_4Me)Re(CO)_2BrI$	135-137	1974, 2043	5.76 (m, 2H), 5.81 (m, 1H), 5.88 (m, 1H)	2.39 (s, 3H)		calcd 18.19	1.34
						found 17.95	1.14

[a] Recorded in CH_2Cl_2. [b] Recorded in $CDCl_3$, relative to TMS. s, singlet; d, doublet; t, triplet; m, multiplet. [c] Recorded in C_6D_6

A series of experiments were performed using a varying *diag*-(η^5-C_5H_4Me)$Re(CO)_2Br_2/SiO_2$ ratio achieved by changing the amount of SiO_2. BET surface areas for the loaded and unloaded SiO_2 samples were determined and a plot of the SiO_2 surface area against the percentage of lateral isomer formed (after 48 h reaction) is shown in Fig. 5.2. Clearly a photostationary state is established when the SiO_2 surface area is > 29 m^2 for 0.038 mmole of *diag*-(η^5-C_5H_4Me)$Re(CO)_2Br_2$. This corresponds to less than a monolayer coverage of the SiO_2[17] and suggests that only (η^5-C_5H_4Me)$Re(CO)_2Br_2$ in physical contact with the SiO_2 will undergo the photoisomerization reaction. A plot of SiO_2 surface area against the percentage of lateral isomer formed for *diag*-(η^5-C_5H_4R)$Re(CO)_2Br_2$ (R = Me, ^{i}Pr) gave similar results suggesting that the substituents on the cyclopentadienyl ring ligand had little effect on the solid state photochemical isomerization reaction. This result was further confirmed by the similar isomerization yields obtained for (η^5-C_5H_4R)$Re(CO)_2Br_2$ (R = H, Me, Et, ^{i}Pr, tBu, $Si(CH_3)_3$) at a fixed complex loading (Table 5.2). All above reactions were terminated after 48 h. By this time a photostationary state had been established as revealed by studying the isomerization reaction of both the lateral and diagonal isomers. The photostationary ratio of [*lat*]/[*diag*] increased (η^5-C_5H_4Me)$Re(CO)(L)Br_2$ > (η^5-C_5H_4Me)$Re(CO)_2Br_2$ > (η^5-C_5H_4Me)$Re(CO)_2I_2$ (Table 5.2). As can be seen from Table 5.2 most of the product was extractable from silica (generally 90-95%) and suggests that the method provides a facile procedure for isomerization of the rhenium complexes.

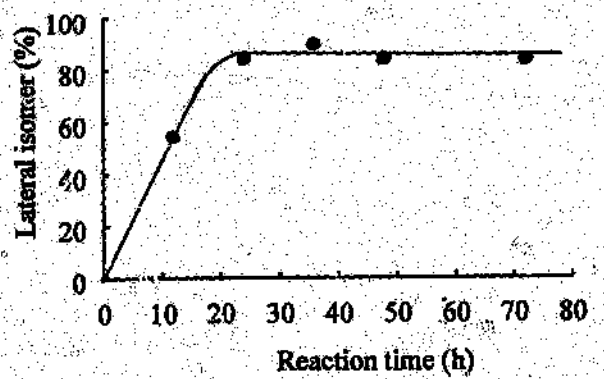

Figure 5.1. Solid-state photochemical isomerization reaction of *diag*-(η^5-C_5H_4Me)$Re(CO)_2Br_2$ after different time.

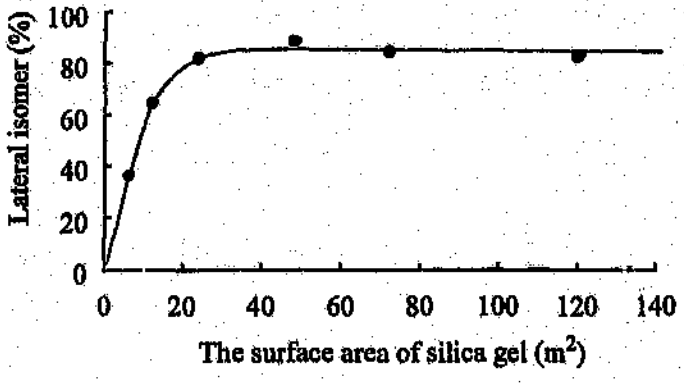

Figure 5.2. Solid-state photochemical isomerization reaction of *diag*-(η^5-C_5H_4Me)$Re(CO)_2Br_2$ as a function of silica gel area.

Table 5.2. Solid State Photochemical *Diag-Lat* Isomerization of (η^5-C_5H_4R)Re(CO)(L)X_2 on the Surface of Silica Gel[a]

No	complex	diag (%)[b]	Lat (%)[b]	Total recovery (%)[c]
1.	diag-(η^5-C_5H_5)Re(CO)$_2$Br$_2$	23.4	76.6	86.5
2.	diag-(η^5-C_5H_4Me)Re(CO)$_2$Br$_2$	15.7	84.3	94.0
3.	diag-(η^5-C_5H_4Et)Re(CO)$_2$Br$_2$	12.2	87.8	87.2
4.	diag-(η^5-C_5H_4^{i}Pr)Re(CO)$_2$Br$_2$	10.1	89.9	76.7[d]
5.	diag-(η^5-C_5H_4tBu)Re(CO)$_2$Br$_2$	10.3	89.7	87.9
6.	diag-[η^5-C_5H_4Si(CH$_3$)$_3$]Re(CO)$_2$Br$_2$	18.6	81.4	89.3
7.	diag-(η^5-C_5H_4Me)Re(CO)$_2$I$_2$	71.1	28.9	93.2
8.	diag-(η^5-C_5H_5)Re(CO)[P(OMe)$_3$]Br$_2$	0.0	100.0	79.4
9.	diag-(η^5-C_5H_5)Re(CO)[P(OPh)$_3$]Br$_2$	0.0	100.0	84.2
10.	diag-(η^5-C_5H_4Me)Re(CO)[P(OPh)$_3$]Br$_2$	0.0	100.0	82.4
11.	lat-(η^5-C_5H_5)Re(CO)$_2$Br$_2$	11.7	88.3	91.6
12.	lat-(η^5-C_5H_4Me)Re(CO)$_2$Br$_2$	11.0	89.0	89.1
13.	lat-(η^5-C_5H_4Et)Re(CO)$_2$Br$_2$	15.9	84.1	87.2
14.	lat-(η^5-C_5H_4^{i}Pr)Re(CO)$_2$Br$_2$	13.7	86.3	72.0
15.	lat-(η^5-C_5H_4tBu)Re(CO)$_2$Br$_2$	13.3	86.7	98.5
16.	lat-[η^5-C_5H_4Si(CH$_3$)$_3$]Re(CO)$_2$Br$_2$	11.5	88.5	89.3
17.	lat-(η^5-C_5H_4Me)Re(CO)[P(OPh)$_3$]Br$_2$	0.0	100.0	90.3

[a] (η^5-C_5H_4R)Re(CO)(L)X_2: 0.038 mmole; silica gel: 300 mg; reaction time: 48 h; room temperature. [b] Isolated yields. [c] Based on starting materials used. [d] Silica gel: 200 mg

By contrast, the solution isomerization reaction for $(\eta^5\text{-}C_5H_4R)Re(CO)_2Br_2$ (R = H, Me, Et, ^{i}Pr, tBu, $Si(CH_3)_3$) has been reported (Chapter 3) and indicated that the diagonal isomer was the dominant isomer formed in the equilibrium reaction. We have now also established that *diag*-$(\eta^5\text{-}C_5H_4Me)Re(CO)[P(OPh)_3]Br_2$ isomerizes completely into the lateral isomer in $CHCl_3$ after several days at room temperature. The isomerization reaction was much slower (> 2 weeks) when benzene was used as solvent. By contrast *lat*-$(\eta^5\text{-}C_5H_4R)Re(CO)_2I_2$ (R = H, Me) converted (> 90%) into the diagonal isomer after several hours at room temperature in $CHCl_3$; the *diag* to *lat* isomerization did not occur under these condition.

The *diag-lat* isomerization reaction of $(\eta^5\text{-}C_5H_4Me)Re(CO)_2Br_2$ was also performed in the dark (no reaction) and by irradiation with sunlight and UV light. The latter reactions also yielded photoisomerized products with conversions little different from that obtained with the 200-W lamp. This suggests that the solid state isomerization reactions on the surface of silica gel can be achieved by a range of wavelengths.

Other inorganic solids were also tested as potential supports for the photoisomerization reaction of $(\eta^5\text{-}C_5H_4Me)Re(CO)_2Br_2$ and the data are shown in Table 5.3. In general only the silica supports gave good conversions to the lateral isomer. ZnO, MgO, Al_2O_3 and $CaSO_4$ were found to be poor supports; they either caused complex decomposition or resulted in low conversions. Increasing the product by increasing the amount (surface area) of the supports which gave poor

Table 5.3. Solid State Photochemical *Diag-Lat* Isomerization of $(\eta^5\text{-}C_5H_4Me)Re(CO)_2Br_2$ on Various Inorganic Solids[a]

No	Inorganic solid	Surface area (m^2/g)	Amount (mg)	diag (%)	lat (%)	Total recovery (%)
1.	ZnO	29.7	300	99.4	0.6	90.2
2.	ZnO	29.7	2400	99.0	1.0	29.0
3.	$CaSO_4$	28.1	300	94.3	5.7	95.6
4.	$CaSO_4$	28.1	2400	92.0	8.0	68.3
5.	Al_2O_3 (neutral)	——	300	15.8	84.2	10.4
6.	MgO	62.5	300	83.6	16.4	33.3
7.	TiO_2	108	300	66.9	33.1	69.4
8.	TiO_2	108	750	10.0	90.0	6.0
9.	Zeolite[b]	271	300	56.3	43.7	95.1
10.	Nil	——	——	100.0	0.0	100.0
11.	Amorphous SiO_2	258	300	9.5	90.5	80.9
12.	Silica gel	240	300	15.7	84.3	94.0

[a] *diag*-$(\eta^5\text{-}C_5H_4Me)Re(CO)_2Br_2$: 0.038 mmole; reaction time: 48 h; room temperature. [b] HZSM-5.

result was also found to be unsuccessful. It should be pointed out that the quality of the surface coating which depends on the preparation method used could also perturb the efficiency of the photochemical isomerization reaction.

Reaction Mechanism

The solid state photochemical isomerization reactions of $(\eta^5\text{-}C_5H_4Me)Re(CO)_2Br_2$ were carried out on a series of silica gels containing different amounts of surface hydroxyl groups (obtained by pre-treatment of silica gel with different amounts of dichlorodimethylsilane). The results showed that the amount of isomerized product increased with the amount of surface hydroxyl groups (Table 5.3). Clearly, the surface hydroxyl groups play a crucial role in the solid state photochemical isomerization reaction.

The solid state photochemical isomerization reactions of an equimolar mixture of *diag*-$(\eta^5\text{-}C_5H_5)Re(CO)[P(OMe)_3]Br_2$ and *diag*-$(\eta^5\text{-}C_5H_4Me)Re(CO)[P(OPh)_3]Br_2$ were carried out and no intermolecular exchange between $P(OMe)_3$ and $P(OPh)_3$ ligands was found (Table 5.4). The intermolecular exchange between CO and $P(OPh)_3$ ligands was also not observed for the solid state isomerization reaction of *diag*-$(\eta^5\text{-}C_5H_4Me)Re(CO)_2Br_2$ in the presence of excess $P(OPh)_3$ ligand (Table 5.4). This suggests that the solid state photochemical *diag-lat* isomerization reactions of $(\eta^5\text{-}C_5H_4R)Re(CO)(L)X_2$ do not proceed via intermolecular exchange of CO, L, or cyclopentadienyl ligands.

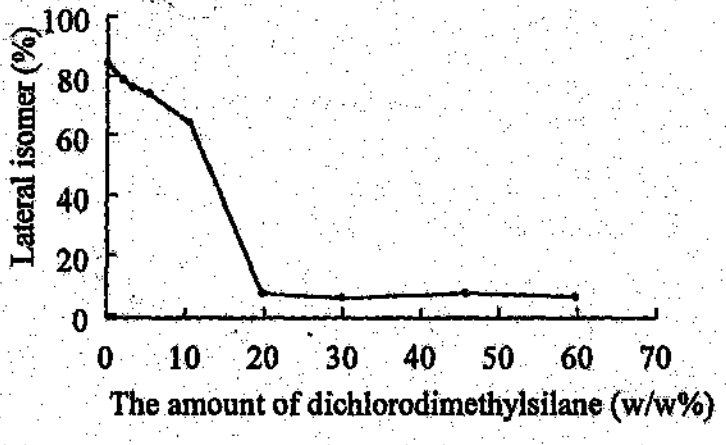

Figure 5.3. Solid-state photochemical isomerization reaction of *diag*-(η^5-C_5H_4Me)$Re(CO)_2Br_2$ on silica gel containing different amounts of surface hydroxyl group.

Table 5.4. Solid State Photochemical Isomerization of Mixed Rhenium Complexes[a]

No	reaction mixture	diag (%)	lat (%)	Total recovery (%)
1.	diag-(η^5-C_5H_4Me)$Re(CO)_2Br_2$ diag-(η^5-C_5H_4Me)$Re(CO)_2I_2$	38.6[b]	(A) 19.6[c] (B) 48.0[c] (C) 32.4[c]	82.2
2.[h]	diag-(η^5-C_5H_4Me)$Re(CO)_2Br_2$ diag-(η^5-C_5H_4Me)$Re(CO)_2I_2$	(H) 29.7[j] (I) 40.2[j] (J) 14.9[j]	(A) 2.0[c] (B) 5.9[c] (C) 7.4[c]	96.6
3.[i]	diag-(η^5-C_5H_4Me)$Re(CO)_2Br_2$ diag-(η^5-C_5H_4Me)$Re(CO)_2I_2$	(H) 34.1[j] (I) 0.0[j] (J) 57.3[j]	(A) 1.3[c] (B) 1.4[c] (C) 6.0[c]	72.6
4.	diag-(η^5-C_5H_4Me)$Re(CO)_2Br_2$ 20 fold NaI	(D) 64.3[d]	(E) 35.7[d]	99.0
5.	diag-(η^5-C_5H_4Me)$Re(CO)_2Br_2$ 20 fold NaCl	14.2[e]	85.8[e]	84.7
6.	diag-(η^5-C_5H_4Me)$Re(CO)_2I_2$ 20 fold NaCl	70.2[f]	29.8[f]	78.1
7.	diag-(η^5-C_5H_4Me)$Re(CO)_2Br_2$ 5 fold $P(OPh)_3$	15.0[e]	85.0[e]	90.5[e]
8.	diag-(η^5- C_5H_5)$Re(CO)[P(OMe)_3]Br_2$ diag-(η^5- C_5H_4Me)$Re(CO)[P(OPh)_3]Br_2$	0.0	(F) 45.3[g] (G) 54.7[g]	75.4

[a] Two equimolar complexes were mixed together and co-adsorbed on silica in impregnation method. Reaction conditions were the same as recorded in Table 2. [b] The mixture consisted of *diag*-(η^5-C_5H_4Me)$Re(CO)_2Br_2$, *diag*-(η^5-C_5H_4Me)$Re(CO)_2BrI$ and *diag*-(η^5-C_5H_4Me) $Re(CO)_2I_2$. [c] A: *lat*-(η^5-C_5H_4Me)$Re(CO)_2I_2$; B: *lat*-(η^5-C_5H_4Me)$Re(CO)_2BrI$; C: *lat*-(η^5-C_5H_4Me) $Re(CO)_2Br_2$. [d] D: *diag*-(η^5-C_5H_4Me)$Re(CO)_2I_2$; E: *lat*-(η^5-C_5H_4Me)$Re(CO)_2I_2$. [e] Only (η^5-C_5H_4Me)$Re(CO)_2Br_2$ was found in the product. [f] Only (η^5-C_5H_4Me)$Re(CO)_2I_2$ was found in the product. [g] F: *lat*-(η^5-C_5H_5)$Re(CO)[P(OMe)_3]Br_2$; G: *lat*-(η^5-C_5H_4Me)$Re(CO)[P(OPh)_3]Br_2$. [h] The

complexes were refluxed in the dark in benzene for 20 hours without silica gel. [i] Silica gel was treated with 30 % dichlorodimethylsilane. [j] H: *diag*-(η^5-C_5H_4Me)Re $(CO)_2I_2$; I: *diag*-(η^5-C_5H_4Me)Re $(CO)_2BrI$; J: *diag*-(η^5-C_5H_4Me) $Re(CO)_2Br_2$

The solid state photochemical isomerization reaction of an equimolar mixture of *diag*-(η^5-C_5H_4Me)$Re(CO)_2Br_2$ and *diag*-(η^5-C_5H_4Me)$Re(CO)_2I_2$ was carried out and a mixture of dibromide and diiodide complexes, as well as 48% (η^5-C_5H_4Me)$Re(CO)_2BrI$ (Table 5.1) were formed in the reaction (Table 5.4). Facile exchange of the Br and I (ions, free radicals) is possible on photolysis. This was also indicated by the formation of molecular iodine on irradiation of silica supported *diag*-(η^5-C_5H_4Me)$Re(CO)_2I_2$.[19] Irradiation of a mixture of *diag*-(η^5-C_5H_4Me)$Re(CO)_2Br_2$ and excess NaI on SiO_2 gave exclusively a photostationary mixture of *diag*- and *lat*-(η^5-C_5H_4Me)$Re(CO)_2I_2$ (Table 5.4). No halogen exchange between NaCl and *diag*-(η^5-C_5H_4Me)$Re(CO)_2X_2$ (X = Br, I) took place under the irradiation conditions. This may be related to the ease of formation of the halogen radical, X.[20]

Further experiments were performed to correlate solid state photochemical isomerization reactions with a halogen dissociation-association reaction. The solid state photochemical isomerization reaction of an equimolar mixture of *diag*-(η^5-C_5H_4Me)$Re(CO)_2Br_2$ and *diag*-(η^5-C_5H_4Me)$Re(CO)_2I_2$ was carried out on a completely dehydroxylated surface of silica gel. Neither isomerization activity, nor any Br and I exchange was detected (Table 5.4). The solid state photochemical isomerization reaction of an equimolar mixture of *diag*-(η^5-C_5H_4Me)$Re(CO)_2Br_2$ and NaI in the presence of the free radical scavenger, galvinoxyl, was also carried out and it was observed that the galvinoxyl greatly suppressed both Br and I ligand exchange and isomerization reaction (Table 5.5). Because the photochemical

reactions were carried out in solid state, not in solution, the role of galvinoxyl here is not completely clear. It is possible that competitive light absorption by galvinoxyl or surface occupation of galvinoxyl molecules reduced the efficiency of the photochemical reactions. However, the results clearly suggest that a close relationship exists between the halogen dissociation-association reaction and the solid state photochemical isomerization reaction.

The Br and I ligand exchange was also observed when an equimolar mixture of *diag*-(η^5-C_5H_4Me)$Re(CO)_2Br_2$ and *diag*-(η^5-C_5H_4Me)$Re(CO)_2I_2$ was refluxed in benzene in the dark (Table 5.4), which indicated that the halogen dissociation-association of (η^5-C_5H_4R)Re(CO)(L)X_2 can occur under both photochemical and thermal conditions and in both solid and solution phases.

Two mechanisms for the solid state photochemical isomerization reactions of (η^5-C_5H_4R)Re(CO)(L)X_2 on the surface of silica gel can be proposed (Scheme 5.1 and 5.2). Both the mechanisms include interaction of the halogen ligand X of (η^5-C_5H_4R)Re(CO)(L)X_2 with the surface of silica gel. These mechanisms are different to the original proposal made by Hill[7b] for similar compounds in which CO dissociation was shown to be the key step for photochemical isomerization at low temperature. However, a more recent report by Hill *etc.* has implicated metal-halogen bond cleavage in a *diag-lat* isomerization reaction of related rhenium complexes.[22]

Table 5.5. Solid State Photochemical Isomerization in the Presence of a Free Radical Scavenger[a]

No	Complex	diag (%)	lat (%)	Total recovery (%)
1.	diag-(η^5-C_5H_4Me)$Re(CO)_2Br_2$ + equimolar NaI	31.8[b]	(A) 23.8[c] (B) 38.1[c] (C) 38.1[c]	76.7
2.	diag-(η^5-C_5H_4Me)$Re(CO)_2Br_2$ + 3 fold galvinoxyl	78.3	21.7	83.1
3.	diag-(η^5-C_5H_4Me)$Re(CO)_2Br_2$ + equimolar NaI + 3 fold galvinoxyl	81.2[b]	(A) 1.1[c] (B) 6.1[c] (C) 11.6[c]	90.2

[a] Reaction conditions were same as recorded in Table 2. [b] The mixture of *diag*-(η^5-C_5H_4Me) $Re(CO)_2Br_2$, *diag*-(η^5-C_5H_4Me)$Re(CO)_2BrI$ and *diag*-(η^5-C_5H_4Me) $Re(CO)_2I_2$. [c] A: *lat*-(η^5-C_5H_4Me)Re $(CO)_2I_2$; B: *lat*-(η^5-C_5H_4Me)$Re(CO)_2BrI$; C: *lat*-(η^5-C_5H_4Me) $Re(CO)_2Br_2$.

These two mechanisms are shown in cartoon form in Scheme 5.1 and 5.2. In Scheme 5.1, upon irradiation, the ligand X dissociates to form a halogen ion and a diagonal three-legged cation intermediate which rearranges to the lateral configuration. The later recombines with X⁻ (or X'⁻) ion to form the lateral isomer. In Scheme 5.2, irradiation results in Re–X bond homolysis to form a halogen radical X· and a diagonal three-legged radical intermediate, which converts to a lateral radical intermediate and recombines with X· (or X'·) to form a lateral isomer. While the details of the two mechanisms proposed presently lack direct experimental support they provide a basis for further mechanistic studies on this unusual solid state photochemical isomerization reaction on silica gel.

5.4. Conclusions

The solid state diagonal to lateral isomerization of monosubstituted cyclopentadienyl four-legged piano stool rhenium complexes (η^5-C_5H_4R)Re(CO)(L)X_2 (R = H, alkyl; L = CO, $P(OR)_3$; X = Br, I) proceeds in good yield when the complexes are adsorbed on the surface of silica gel and irradiated with visible light. Unlike the thermal solid state or molten state isomerization reactions, the ring substituent has little effect on the photochemical solid state isomerization reactions of (η^5-C_5H_4R)Re(CO)(L)X_2. The photostationary ratio of *[lat]/[diag]* was mainly determined by the ligands L and X. The solution and matrix isomerization reactions of (η^5-C_5R_4R')Re(CO)$_2X_2$ (R = H, Me; R' =

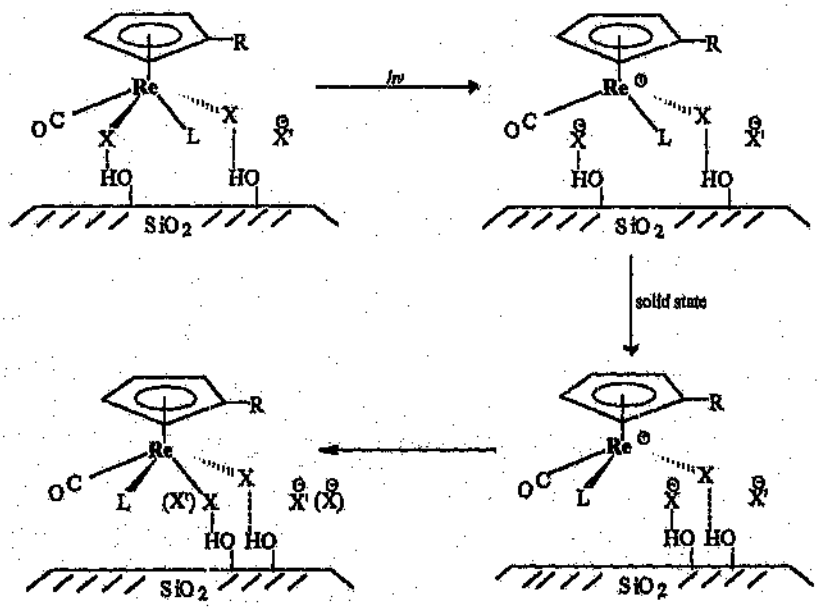

Scheme 5.1. Proposed mechanism 1 for the solid-state photochemical *diag-lat* isomerization of *diag*-(η^5-C_5H_4R)Re(CO)(L)X_2 on the surface of silica gel.

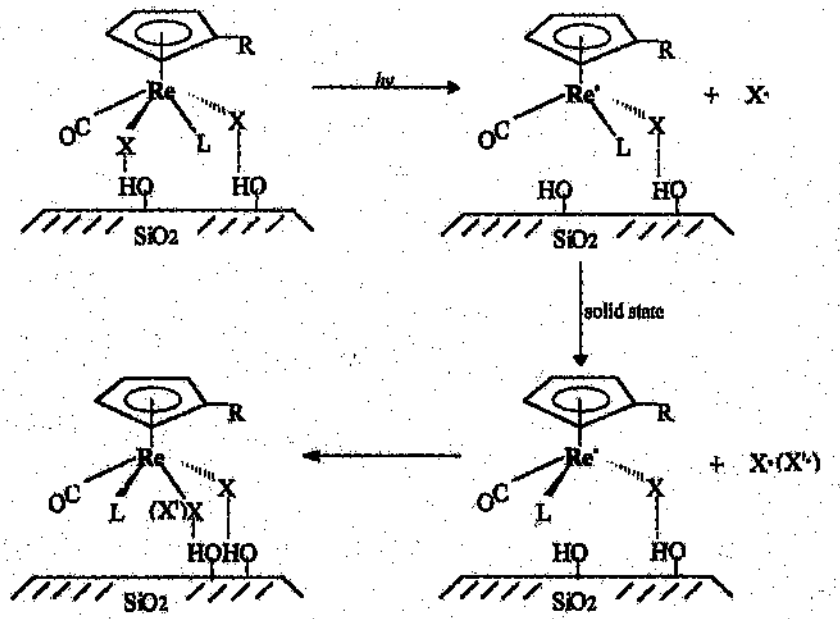

Scheme 5.2. Proposed mechanism 2 for the solid-state photochemical *diag-lat* isomerization of *diag*-(η^5-C_5H_4R)Re(CO)(L)X_2 on the surface of silica gel.

Me) gave results completely different from those observed for the solid state thermal and photochemical isomerization reactions discussed here. It was found that only monolayer adsorbed molecules on the silica surface underwent isomerization and studies showed that the hydroxyl group of silica gel plays a crucial role in the isomerization reactions. The isomerization reactions could be rationalized by a mechanism in which a halogen dissociative-associative process involving ions or radicals occurs under irradiation with visible light.

5.5. References

1. (a) Toda, F. *Acc. Chem. Res.* **1995**, *28*, 480. (b) West, A. *Solid State Chemistry and its Applications* Wiley, Chichester, 1994.
2. Reactions in matrices, e.g. matrix isomerization reactions, have been excluded from this discussion since the matrix molecules/atoms can be regarded as frozen 'solvent' molecules.
3. (a) Boldyreva, E. V. *Mol. Cryst. Liq. Cryst.* **1994**, *242*, 17. (b) Grenthe, I.; Nordin, E. *Inorg. Chem.* **1979**, *18*, 1869. (c) Dulepov, V. E.; Boldyreva, E. V. *React. Kinet. Catal. Lett.* **1994**, *53*, 289. (d) Masciocchi, N.; Kolyshev, A.; Dulepov, V.; Boldyreva, E.; Sironi, A. *Inorg. Chem.* **1994**, *33*, 2579.
4. Sedova, G. N.; Demchenko, L N. *Neorg. Khim.* **1981**, *26*, 435.
5. (a) Katsuki, K.; Ooyama, Y.; Okamoto, M.; Yamamoto, Y. *Inorg. Chim. Acta* **1994**, *217*, 181. (b) Krassowski, W. D.; Lemay, H. E., Jr.; Nelson, J. H. *Inorg. Chem.* **1988**, *27*, 4307.
6. (a) Macdonald, F. M.; Sadler, P. J. *Polyhedron* **1991**, *10*, 1443. (b) Louw, W. J. *Inorg. Chem.* **1977**, *16*, 2147. (c) Favez, R.; Roulet, R.; Pinkerton, A. A.; Schwarzenbach, D. *Inorg. Chem.* **1980**, *19*, 1356.
7. Palmer, B. J.; Becalska, A.; Hader, R.; Hill, R. H. *Polyhedron* **1991**, *10*, 877.
8. (a) Moore, J. J.; Feng, H. J. *Prog. in Mat. Sci.* **1995**, *39*, 243. (b) Thadhani, N. N. *Prog. in Mat. Sci.* **1993**, *37*, 117.
9. Gates, B. C. *J. Mol. Catal.* **1994**, *86*, 95.
10. (a) Mayo, P.; Nakamura, A.; Tsang, P. W. K.; Wong, K. S. *J. Am. Chem. Soc.* **1982**, *104*, 6824. (b) Mayo, P.; Ramnath, N. *Can. J. Chem.* **1986**, *64*,

1293.

11. (a) Reddy, K. P.; Brown, T. L. *J. Am. Chem. Soc.* **1995**, *117*, 2845. (b) Ang, H. G.; Chan, K. S.; Chuah, G. K.; Jaenicke, S.; Neo, S. K. *J. Chem. Soc. Dalton. Trans.* **1995**, 3753. (c) Nakamura, R.; Pioch, D.; Bowman, G.; Burwell, R. L. *J. Catal.* **1985**, *93*, 388, 399. (d) Brenner, A.; Hucul, D. A.; Hardwick, S. J. *Inorg. Chem.* **1979**, *18*, 1487. (e) Gonzales, P. N.; Villa Garcia, M. A.; Brenner, A. *J. Catal.* **1989**, *118*, 360.

12. *Chem. Rev.* **1995**, *95*. The edition (No. 3) contains numerous articles on solid state reactions.

13. (a) Roberto, D.; Cariati, E.; Ugo, R; Psaro, R. *Inorg. Chem.* **1996**, *35*, 2311. (b) Roberto, D.; Cariati, E.; Psaro, R.; Ugo, R. *J. Organomet. Chem.* **1995**, *488*, 109. (c) Theolier, A.; Smith, A. K.; Leconte, M.; Basset, J. M.; Zanderighi, G. M.; Psaro, R.; Ugo, R. *J. Organomet. Chem.* **1980**, *191*, 415.

14. (a) King, R. B.; Reimann, R. H. *Inorg. Chem.* **1976**, *12*, 183. (b) Einstein, F. W. B.; Klahn-Oliva, A. H.; Sutton, D.; Tyers, K. G. *Organometallics* **1986**, *5*, 53. (c) Hill, R. H.; Palmer, B. J. *Organometallics* **1989**, *8*, 1651.

15. Duvenhage, D. J. Ph.D Thesis, University of the Witwatersrand (1993), Johannesburg.

16. Abdel-Malik, M. M.; De Mayo, P. *Can. J. Chem.* **1984**, *62*, 1275.

17. The 'footprint'[18] of the *diag*-(η^5-C_5H_4Me)$Re(CO)_2Br_2$ was calculated from its X-ray structure as 22.5 $Å^2$ (Chapter 4). Thus 0.038 mmole of *diag*-(η^5-C_5H_4Me)$Re(CO)_2Br_2$ will cover an area of 5.2 m^2.

18. Matsuishi, T.; Shimada, T.; Morihara, K. *Bull. Chem. Soc. Jpn.* **1994**, *67*, 748.

19. The molecular iodine was separated from the isomerization products of *diag*-(η^5-C_5H_4Me)$Re(CO)_2I_2$ on a chromatography column and confirmed by reaction with starch in water (blue colour).

20. The bond energies of NaI, NaBr and NaCl are 72.7 kcal/mole, 86.7 kcal/mole and 97.5 kcal/mole, respectively.[21]

21. Huheey, J. E.; Keiter, E. A.; Keiter, R. L. *Inorganic Chemistry: Principles of Structures and Reactivity* 4th ed.; HarperCollins College Publishers, New York, 1993, A-25.

22. Xia, W.; Hill, R. H.; Klahn, A. H.; Leiva, C.; Buono-Core, G. E. *Polyhedron* **1996**, *10*, 3093.

CHAPTER 6

SYNTHESIS, CHARACTERIZATION AND ISOMERIZATION REACTIONS OF *DIAG*- AND *LAT*-(η^5-C_5H_4R)Re(CO)(L)X_2

6.1. Introduction

The chemistry of cyclopentadienyl half-sandwich rhenium complexes has been developed over the past three decades.[1] In this time many cyclopentadienyl *four-legged* piano stool rhenium complexes have been prepared, and the solution isomerization behavior and the chemical reactivity of these complexes have been studied.[3-7] However, it is only since 1976 that King and Reimann successfully separated the diagonal and lateral isomers of (η^5-C_5H_5)Re(CO)$_2$Br$_2$.[2]

The carbonyl substitution reactions of cyclopentadienyl dicarbonyldihalide rhenium complexes have been little exploited. Indeed as far as we aware, the King *et al* description of the reaction of *diag*-(η^5-C_5H_5)Re(CO)$_2$Br$_2$ with different phosphites, P(OR)$_3$, and isocyanides is the only example of the CO replacement on these complexes reported to date. The method used to prepare *lat*-(η^5-C_5H_5)Re(CO)(L)Br$_2$ by refluxing *diag*-(η^5-C_5H_5)Re(CO)$_2$Br$_2$ with 3.0 equiv. of phosphites in toluene was poor (yields were only 35-45%).[2] The reactions of the

pentamethylcyclopentadienyl rhenium complexes $Cp^*Re(CO)_2X_2$ (X = Cl, Br, I) with $P(OMe)_3$ in refluxing toluene were studied by Klahn *et al* and it was found that $Cp^*Re(CO)_2[P(OMe)_3]$, not the carbonyl substitution product, was the dominant product.[8] $Cp^*Re(CO)(PMe_3)X_2$ (X = Cl, Br, I) and *cis*-$Cp^*Re(CO)(L)I_2$ (L = $P(OMe)_3$, $P(OPh)_3$, PMe_3, PMe_2Ph) have rather been prepared indirectly by oxidative-addition of X_2 to the dinitrogen complexes $Cp^*Re(CO)(L)N_2$,[9] or by Me_3NO induced decarbonylation of cationic [*cis*- $Cp^*Re(CO)_2(L)I]^+$.[10]

In Chapter 3, we have reported the first thermal solid-state isomerization reaction of $(\eta^5\text{-}C_5H_4R)Re(CO)_2Br_2$ (R = Me), but work on related complexes (R = tBu, $SiMe_3$ etc.) indicated that the reaction may not be general. To further explore the generality of this unusual solid state reaction.[11] the substituted complexes $(\eta^5\text{-}C_5H_4R)Re(CO)(L)X_2$ have been considered for study. Trimethylamine N-oxide has been shown to be a valuable synthetic reagent in the preparation of substituted metal carbonyl complexes.[13] and its use for preparing new rhenium complexes seemed feasible. Thus, we decided to study the carbonyl substitution reactions of $(\eta^5\text{-}C_5H_4R)Re(CO)_2X_2$ using Me_3NO as a decarbonylating reagent. The results of this study are described below. The solid-state and solution *diag-lat* isomerization reactions of the new complexes are also reported.

6.2. Experimental

The diagonal and lateral (η^5-C_5H_4R)$Re(CO)_2Br_2$ (R = Me, tBu, $SiMe_3$) complexes were prepared by the methods described in Chapter 3. 2,6-dimethylphenylisocyanide, phosphites and phosphines were used as supplied by Fluka or Merck. Trimethylamine N-oxide dihydrate (Aldrich) was used as received. All reactions were carried out using standard Schlenk techniques under nitrogen. Solvents were dried by conventional methods, distilled under nitrogen, and used immediately. Melting points were recorded on a Kofler hot stage melting point apparatus. Infrared spectra were measured on a Midac FTIR spectrometer, usually in KBr cells (solutions). NMR spectra were measured on a Bruker AC 200 spectrometer operating at 200 MHz. Microanalysis were carried out at the CSIR, Pretoria, South Africa.

6.2.1 Preparation of diag-(η^5-C_5H_4R)$Re(CO)(L)X_2$

diag- or *lat-*(η^5-C_5H_4R)$Re(CO)_2X_2$ (100 mg, 0.174-0.208 mmole) (R = Me, tBu, $SiMe_3$; X = Br, I) and 1.1 equiv. of ligand L (L = $CNC_6H_3Me_2$, $P(OMe)_3$, $P(O^iPr)_3$, $P(OPh)_3$, PPh_3) were dissolved in 15 mL CH_2Cl_2 under nitrogen. $Me_3NO \cdot 2H_2O$ (2-5 equiv.) was added to the above magnetically stirred solution. The reactions were monitored by IR spectroscopy and were complete within 30 min. Solvent was removed by vacuum rotatory evaporation to leave a red residue, which was dissolved in CH_2Cl_2 and chromatographed on a silica gel column (2×50 cm) prepared in hexane. Successive elution with 1:1 CH_2Cl_2/hexane gave first *diag-*(η^5-

$C_5H_4R)Re(CO)(L)X_2$ from a red band, then a small amount (<5%) of *lat*-(η^5-$C_5H_4R)Re(CO)(L)X_2$ from a brown band. The yields, as well as the spectroscopic and analytical data for *diag*-(η^5-$C_5H_4R)Re(CO)(L)X_2$ are listed in Table 6.1 and 6.2.

Similar reactions with triethyl phosphine, triisopropyl phosphine, tributyl phosphine and pyridine resulted in decomposition of the starting materials.

6.2.2 Thermal solid-state isomerization of diag-(η^5-$C_5H_4R)Re(CO)(L)X_2$

Solid *diag*-(η^5-$C_5H_4R)Re(CO)(L)X_2$ (50 mg) in a 25 mL round-bottom flask was heated under nitrogen in an oil bath at temperatures at least 10-15 °C below their melting points for 0.5-6 h. No decomposition was observed. The solid residues were then dissolved in CH_2Cl_2 and chromatographed on a silica gel column. The composition of the new lateral isomers was confirmed by IR and NMR spectroscopy. The yields, as well as the spectroscopic and analytical data for the *lat*-(η^5-$C_5H_4R)Re(CO)(L)X_2$ complexes are listed in Tables 6.1, 6.2 and 6.3.

The *lat*-(η^5-$C_5H_4R)Re(CO)(PPh_3)_2$ complex decomposed on a silica gel column and purification of the complex was achieved by recrystalization from a mixture of dichloromethane and hexane at -15 °C .

6.2.3 Thermal solid-state halogen exchange reaction of diag-(η^5-C_5H_4Me)$Re(CO)_2Br_2$ with excess NaI

diag-(η^5-C_5H_4Me)$Re(CO)_2Br_2$ (200 mg, 0.416 mmole) and NaI (1.25 g, 8.31 mmole) were dissolved in acetone in a 25 mL round-bottom flask. The solvent was then removed by rotatory evaporation, and the residue was dried under vacuum (0.1 mm Hg) at 25 °C and heated under nitrogen in an oil bath at 100-105 °C for 18 h. After column separation (silica gel, 1:1 CH_2Cl_2/hexane), red microcrystaline *diag*-(η^5-C_5H_4Me)$Re(CO)_2I_2$ (239 mg, 100% yield) was obtained. IR (ν_{co}, CH_2Cl_2): 1982 cm^{-1}, 2043 cm^{-1}. ^1H NMR ($CDCl_3$): 2.44 ppm (s, 3H, CH_3); 5.59 ppm (t, 2H, Cp); 5.71 ppm (t, 2H, Cp).

6.2.4 Thermal solid-state reaction of diag-(η^5-C_5H_4Me)$Re(CO)[P(OPh)_3]Br_2$ with excess NaI

diag-(η^5-C_5H_4Me)$Re(CO)[P(OPh)_3]Br_2$ (80 mg, 0.105 mmole) and NaI (314 mg, 2.10 mmole) were dissolved in acetone in a 25 mL round-bottom flask. The solvent was then removed by rotatory evaporation, and the residue was dried under vacuum (0.1 mm Hg) at 25 °C and heated under nitrogen in an oil bath at 125-130 °C for 16 h. After column separation (silica gel, 1:1 CH_2Cl_2/hexane), *diag*-(η^5-C_5H_4Me)$Re(CO)_2I_2$ (30 mg, 0.052 mmole, 49.5% yield) was obtained as the only carbonyl product. IR (ν_{co}, CH_2Cl_2): 1982 cm^{-1}, 2043 cm^{-1}. ^1H NMR ($CDCl_3$): 2.44 ppm (s, 3H, CH_3); 5.59 ppm (t, 2H, Cp); 5.71 ppm (t, 2H, Cp).

Table 6.1. IR and NMR spectroscopic data for *diag*- and *lat*-(η^5-C_5H_4R)Re(CO)(L)X_2 complexes

complex	ν_{co}[a] (cm^{-1})	^{1}H NMR[b] (ppm) Cp ring		L
diag-(η^5-C_5H_4Me)Re(CO)($CNC_6H_3Me_2$)Br_2	1974	4.72 (t, 2H);4.90 (t, 2H)	1.82 (s, 3H)	2.35 (s, 6H);6.63 (m, 3H)
diag-(η^5-C_5H_4Me)Re(CO)[$P(OMe)_3$]Br_2	1969	4.71 (t, 2H); 4.9[illegible] (t, 2H)	1.80 (s, 3H)	3.48 (d, 9H)
diag-(η^5-C_5H_4Me)Re(CO)[$P(O^iPr)_3$]Br_2	1963	4.73 (t, 2H); 4.93 (t, 2H)	1.84 (s, 3H)	1.24 (s, 9H);1.27 (s, 9H);4.84 (m, 3H)
diag-(η^5-C_5H_4Me)Re(CO)[$P(OPh)_3$]Br_2[c]	1989	4.53 (t, 2H);4.65 (t, 2H)	1.64 (s, 3H)	6.88-7.56 (m, 15H)
diag-(η^5-C_5H_4Me)Re(CO)(PPh_3)Br_2	1963	4.75 (t, 2H); 5.00 (t, 2H)	1.82 (s, 3H)	6.95-7.69 (m, 15H)
diag-(η^5-C_5H_4Me)Re(CO)[$P(OPh)_3$]I_2	1976	4.63 (t, 2H); 4.73 (t, 2H)	1.82 (s, 3H)	6.75-7.59 (m, 15H)
diag-(η^5-C_5H_4Me)Re(CO)(PPh_3)I_2	1948	4.81 (t, 2H);5.09 (t, 2H)	2.00 (s, 3H)	6.64-7.64 (m, 15H)
diag-(η^5-C_5H_4tBu)Re(CO)($CNC_6H_3Me_2$)Br_2	1975	4.84 (t, 2H); 5.10 (t, 2H)	1.15 (s, 9H)	2.46 (s, 6H);6.68 (m, 3H)
diag-(η^5-C_5H_4tBu)Re(CO)[$P(OMe)_3$]Br_2	1971	4.56 (t, 2H); 5.28 (t, 2H)	1.18 (s, 9H)	3.53 (d, 9H)
diag-(η^5-C_5H_4tBu)Re(CO)[$P(O^iPr)_3$]Br_2	1960	4.62 (t, 2H);5.35 (t, 2H)	1.19 (s, 9H)	1.28 (d, 18H);4.89 (m, 3H)
diag-(η^5-C_5H_4tBu)Re(CO)[$P(OPh)_3$]Br_2	1992	4.44 (t, 2H); 4.92 (t, 2H)	1.06 (s, 9H)	6.76-7.58 (m, 15H)
diag-(η^5-C_5H_4tBu)Re(CO)(PPh_3)Br_2	1963	4.75 (t, 2H); 5.31 (t, 2H)	1.20 (s, 9H)	6.96-7.79 (m,

				15H)
diag-(η^5-$C_5H_4SiMe_3$)Re(CO)($CNC_6H_3Me_2$)Br_2	1976	4.83 (t, 2H);5.21 (t, 2H)	0.18 (s, 9H)	2.41 (s, 6H);6.63 (m, 3H)
diag-(η^5-$C_5H_4SiMe_3$)Re(CO)[$P(OMe)_3$]Br_2	1971	4.67 (t, 2H); 5.38 (t, 2H)	0.27 (s, 9H)	3.45 (d, 9H)
diag-(η^5-$C_5H_4SiMe_3$)Re(CO)[$P(O^iPr)_3$]Br_2	1963	4.70 (t, 2H); 5.47 (t, 2H)	0.28 (s, 9H)	1.26 (d, 18H);4.87 (m, 3H)
diag-(η^5-$C_5H_4SiMe_3$)Re(CO)[$P(OPh)_3$]Br_2	1993	4.51 (t, 2H);5.08 (t, 2H)	0.16 (s, 9H)	6.76-7.57 (m, 15H)
diag-(η^5-$C_5H_4SiMe_3$)Re(CO)(PPh_3)Br_2	1956	4.90 (t, 2H); 5.44 (t, 2H)	0.26 (s, 9H)	6.64-7.96 (m, 15H)
lat-(η^5-C_5H_4Me)Re(CO)($CNC_6H_3Me_2$)Br_2	1959	4.72 (m, 1H); 4.78 (m, 2H); 4.90 (m, 1H)	1.76 (s, 3H)	2.14 (s, 6H);6.63 (m, 3H)
lat-(η^5-C_5H_4Me)Re(CO)[$P(OMe)_3$]Br_2	1938	4.82 (m, 2H);4.94 (m, 1H); 4.95 (m, 1H)	1.76 (s, 3H)	3.47 (d, 9H)
lat-(η^5-C_5H_4Me)Re(CO)[$P(O^iPr)_3$]Br_2	1932	4.97 (m, 4H)	1.82 (s, 3H)	1.12 (s, 9H);1.15 (s, 9H);4.81 (br, 3H)
lat-(η^5-C_5H_4Me)Re(CO)[$P(OPh)_3$]Br_2[c]	1959	4.62 (d, 1H); 4.72 (d, 1H); 4.77 (d, 1H); 5.07 (d, 1H)	1.73 (s, 3H)	6.75-7.55 (m, 15H)
lat-(η^5-C_5H_4Me)Re(CO)(PPh_3)Br_2	1926	4.51 (m, 1H); 4.71 (m, 1H);4.92 (m, 1H); 4.99 (m, 1H)	1.90 (s, 3H)	6.75-7.55 (m, 15H)
lat-(η^5-C_5H_4Me)Re(CO)[$P(OPh)_3$]I_2	1950	4.43 (m, 2H); 4.69 (m, 1H);5.05 (m, 1H)	1.99 (s, 3H)	6.75-7.59 (m, 15H)
lat-(η^5-C_5H_4Me)Re(CO)(PPh_3)I_2	1922	4.35 (m, 1H); 4.68 (m, 1H);4.91 (m, 1H); 5.00 (m, 1H)	2.12 (s, 3H)	6.64-7.64 (m, 15H)
lat-(η^5-C_5H_4tBu)Re(CO)($CNC_6H_3Me_2$)Br_2	1957	4.98 (m, 2H); 5.11 (m, 1H);5.15	1.07 (s, 9H)	2.16 (s, 6H);6.62

		(m, 1H)		(m, 3H)
lat-(η^5-C_5H_4tBu)Re(CO)[P(OMe)$_3$]Br$_2$	1933	4.86 (m, 1H); 5.03 (m, 1H);5.23 (m, 1H); 5.35 (m, 1H)	1.17 (s, 9H)	3.46 (d, 9H)
lat-(η^5-C_5H_4tBu)Re(CO)[P(O^{i}Pr)$_3$]Br$_2$	1930	5.10 (m, 1H); 5.16 (m, 1H);5.25 (m, 1H); 5.49 (m, 1H)	1.22 (s, 9H)	1.12 (s, 9H);1.15 (s, 9H);4.79 (br, 3H)
lat-(η^5-C_5H_4tBu)Re(CO)[P(OPh)$_3$]Br$_2$	1953	4.94 (m, 1H); 5.03 (m, 1H);5.11 (m, 1H); 5.57 (m, 1H)	1.11 (s, 9H)	6.76-7.55 (m, 15H)
lat-(η^5-C_5H_4tBu)Re(CO)(PPh$_3$)Br$_2$	1924	4.89 (m, 1H); 4.97 (m, 1H);5.04 (m, 1H); 5.52 (m, 1H)	1.14 (s, 9H)	6.96-7.79 (m, 15H)
lat-(η^5-$C_5H_4SiMe_3$)Re(CO)(CNC$_6$H$_3$Me$_2$)Br$_2$	1958	5.07 (m, 2H); 5.21 (m, 1H);5.26 (m, 1H)	0.23 (s, 9H)	2.15 (s, 6H);6.62 (m, 3H)
lat-(η^5-$C_5H_4SiMe_3$)Re(CO)[P(OMe)$_3$]Br$_2$	1935	5.07 (m, 1H); 5.17 (m, 1H);5.32 (m, 1H); 5.39 (m, 1H)	0.28 (s, 9H)	3.45 (d, 9H)
lat-(η^5-$C_5H_4SiMe_3$)Re(CO)[P(O^{i}Pr)$_3$]Br$_2$	1931	5.25 (m, 1H); 5.31 (m, 1H);5.35 (m, 1H); 5.62 (m, 1H)	0.32 (s, 9H)	1.11 (s, 9H);1.14 (s, 9H);4.77 (br, 3H)
lat-(η^5-$C_5H_4SiMe_3$)Re(CO)[P(OPh)$_3$]Br$_2$	1952	4.98 (m, 1H); 5.13 (m, 1H);5.21 (m, 1H); 5.64 (m, 1H)	0.21 (s, 9H)	6.82-7.40 (m, 15H)
lat-(η^5-$C_5H_4SiMe_3$)Re(CO)(PPh$_3$)Br$_2$	1924	4.86 (m, 2H); 5.07 (m, 1H);5.67 (m, 1H)	0.28 (s, 9H)	7.35-7.80 (m, 15H)

[a] Recorded in CH_2Cl_2. [b] Recorded in C_6D_6, relative to TMS: s, singlet; d, doublet; t, triplet; m, multiplet; br, broad. [c] Ref. 12e.

lat-(η^5-C_5H_4tBu)Re(CO)($CNC_6H_3Me_2$)Br_2	——	194-196	calcd	36.43	3.54	2.24
			found	36.31	3.27	2.19
lat-(η^5-C_5H_4tBu)Re(CO)[$P(OMe)_3$]Br_2	——	154-156	calcd	25.21	3.58	
			found	25.01	3.58	
lat-(η^5-C_5H_4tBu)Re(CO)[$P(O^iPr)_3$]Br_2	——	170-172	calcd	32.44	4.87	
			found	32.50	4.50	
lat-(η^5-C_5H_4tBu)Re(CO)[$P(OPh)_3$]Br_2	——	158-160	calcd	41.75	3.50	
			found	41.82	3.46	
lat-(η^5-C_5H_4tBu)Re(CO)(PPh_3)Br_2	——	190-192	calcd	44.40	3.73	
			found	43.90	3.62	
lat-(η^5-$C_5H_4SiMe_3$)Re(CO)($CNC_6H_3Me_2$)Br_2	——	179-181	calcd	33.65	3.45	2.18
			found	33.41	3.27	2.15
lat-(η^5-$C_5H_4SiMe_3$)Re(CO)[$P(OMe)_3$]Br_2	——	143-145	calcd	22.68	3.49	
			found	22.46	3.43	
lat-(η^5-$C_5H_4SiMe_3$)Re(CO)[$P(O^iPr)_3$]Br_2	——	159-161	calcd	30.05	4.76	
			found	30.11	4.61	
lat-(η^5-$C_5H_4SiMe_3$)Re(CO)[$P(OPh)_3$]Br_2	——	137-139	calcd	39.47	3.44	
			found	39.16	3.43	
lat-(η^5-$C_5H_4SiMe_3$)Re(CO)(PPh_3)Br_2	——	187-189	calcd	41.92	3.65	
			found	41.89	3.45	

* Due to fast isomerization in solutions, the pure diagonal isomers of these complexes were not obtained.

Table 6.2. Analytical data for *diag*- and *lat*-(η^5-C_5H_4R)Re(CO)(L)X_2 complexes

complex	Yield (%)	m.p. (°C)		Analysis (%) C	H	N
diag-(η^5-C_5H_4Me)Re(CO)($CNC_6H_3Me_2$)Br_2	92	154-156	calcd	32.89	2.76	2.40
			found	32.82	2.64	2.32
diag-(η^5-C_5H_4Me)Re(CO)[$P(OMe)_3$]Br_2	75	114-116	calcd	20.81	2.79	
			found	20.69	2.68	
diag-(η^5-C_5H_4Me)Re(CO)[$P(O^iPr)_3$]Br_2	84	108-110	calcd	29.06	4.27	
			found	29.01	3.93	
diag-(η^5-C_5H_4Me)Re(CO)[$P(OPh)_3$]Br_2	89	164-166	calcd	39.33	2.90	
			found	39.39	2.68	
diag-(η^5-C_5H_4Me)Re(CO)(PPh_3)Br_2	70	186-188	calcd	41.97	3.10	
			found	42.06	2.88	
diag-(η^5-C_5H_4Me)Re(CO)[$P(OPh)_3$]I_2	60	----[a]	calcd	35.02	2.59	
			found	35.03	2.44	
diag-(η^5-C_5H_4Me)Re(CO)(PPh_3)I_2	84	176-169	calcd	37.10	2.74	
			found	36.96	2.61	
diag-(η^5-C_5H_4tBu)Re(CO)($CNC_6H_3Me_2$)Br_2	96	142-144	calcd	36.43	3.54	2.24
			found	36.35	3.31	2.19
diag-(η^5-C_5H_4tBu)Re(CO)[$P(OMe)_3$]Br_2	75	123-125	calcd	25.21	3.58	
			found	24.97	3.28	
diag-(η^5-C_5H_4tBu)Re(CO)[$P(O^iPr)_3$]Br_2	75	126-128	calcd	32.44	4.87	
			found	32.42	4.64	
diag-(η^5-C_5H_4tBu)Re(CO)[$P(OPh)_3$]Br_2	61	124-126	calcd	41.75	3.50	

			found	41.43	3.26	
diag-(η^5-C_5H_4tBu)Re(CO)(PPh_3)Br_2	76	172-174	calcd	44.40	3.73	
			found	44.41	3.69	
diag-(η^5-$C_5H_4SiMe_3$)Re(CO)($CNC_6H_3Me_2$)Br_2	75	144-146	calcd	33.65	3.45	2.18
			found	33.50	3.30	2.12
diag-(η^5-$C_5H_4SiMe_3$)Re(CO)[$P(OMe)_3$]Br_2	76	——[a]	calcd	22.68	3.49	
			found	22.70	3.57	
diag-(η^5-$C_5H_4SiMe_3$)Re(CO)[$P(O^iPr)_3$]Br_2	75	106-108	calcd	30.05	4.76	
			found	30.16	4.64	
diag-(η^5-$C_5H_4SiMe_3$)Re(CO)[$P(OPh)_3$]Br_2	84	124-126	calcd	39.47	3.44	
			found	39.20	3.40	
diag-(η^5-$C_5H_4SiMe_3$)Re(CO)(PPh_3)Br_2	63	155-157	calcd	41.92	3.65	
			found	42.17	3.69	
lat-(η^5-C_5H_4Me)Re(CO)($CNC_6H_3Me_2$)Br_2	——	192-194	calcd	32.89	2.76	2.40
			found	32.60	2.48	2.34
lat-(η^5-C_5H_4Me)Re(CO)[$P(OMe)_3$]Br_2	——	116-118	calcd	20.81	2.79	
			found	20.51	2.78	
lat-(η^5-C_5H_4Me)Re(CO)[$P(O^iPr)_3$]Br_2	——	178-180	calcd	29.06	4.27	
			found	29.02	4.06	
lat-(η^5-C_5H_4Me)Re(CO)[$P(OPh)_3$]Br_2	——	183-185	calcd	39.33	2.90	
			found	39.38	2.69	
lat-(η^5-C_5H_4Me)Re(CO)(PPh_3)Br_2	——	200-202	calcd	41.97	3.10	
			found	42.00	2.87	
lat-(η^5-C_5H_4Me)Re(CO)[$P(OPh)_3$]I_2	——	189-191	calcd	35.02	2.59	
			found	35.00	2.46	
lat-(η^5-C_5H_4Me)Re(CO)(PPh_3)I_2	——	227-229	calcd	37.10	2.74	
			found	37.01	2.63	

6.3. Results and discussion

6.3.1 Synthesis and characterization of diag- and lat-(η^5-C_5H_4R)Re(CO)(L)X_2

The initial approach to the preparation of monocarbonyl substitution products of (η^5-C_5H_4R)Re(CO)$_2X_2$ was attempted using the King method, i.e. refluxing (η^5-C_5H_4R)Re(CO)$_2X_2$ and ligands, L, in benzene or toluene [12e]. Indeed, the desired products (η^5-C_5H_4R)Re(CO)(L)X_2 were obtained. However, we found that the product selectivity, not unexpectedly, was poor. The product was obtained as a mixture of diagonal and lateral isomers (Fig 6.1), and the [*diag*]/[*lat*] ratio varied from reaction to reaction. Further, some unwanted side products, which were not characterized, were formed [9]. Catalytic carbonyl substitution using a PdO catalyst was attempted. This catalyst has previously been successfully used to catalyze reactions between Re(CO)$_5X$ and group 15 donor ligands [14]. Numerous reactions (varying temperature, time, etc.) indicated that PdO did not catalyze the carbonyl substitution reactions of (η^5-C_5H_4R)Re(CO)$_2X_2$.

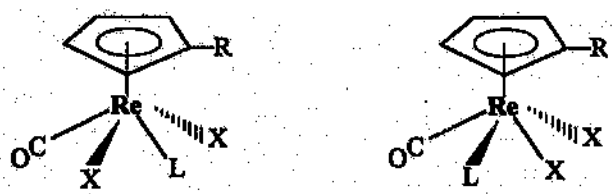

Fig. 6.1. The diagonal and lateral isomers of (η^5-C_5H_4R)Re(CO)(L)X_2.

Attempts to use Me_3NO as a decarbonylating agent were then undertaken. In the presence of excess Me_3NO, reactions of either *diag*- or *lat*-$(\eta^5\text{-}C_5H_4R)Re(CO)_2X_2$ (X = Br, I) with isocyanides, phosphites and triphenyl phosphine in CH_2Cl_2 at room temperature rapidly gave *diag*-$(\eta^5\text{-}C_5H_4R)Re(CO)(L)X_2$ in good yields. Usually, a few percent of *lat*-$(\eta^5\text{-}C_5H_4R)Re(CO)(L)X_2$ was also found in the product. Detailed studies indicated that these lateral isomers were formed by isomerization of the diagonal products (see below). No other products such as $(\eta^5\text{-}C_5H_4R)Re(CO)_2(I)$ or $(\eta^5\text{-}C_5H_4R)Re(L)_2X_2$ were found in the reaction mixture.

All the diagonal isomers of $(\eta^5\text{-}C_5H_4R)Re(CO)(L)X_2$ have a red color and the lateral isomers are brown in color. They all dissolve in organic solvents such as dichloromethane, chloroform, benzene and toluene, but the lateral isomers have lower solubility.

Reaction of $(\eta^5\text{-}C_5H_4R)Re(CO)_2X_2$ with L = PEt_3, P^iPr_3, P^tBu_3 or pyridine without Me_3NO resulted in extensive decomposition and no new monosubstituted neutral products were formed. (No attempt was made to analyze the reaction solution). This finding most certainly relates to the stronger basic properties of these ligands.[2]

The identification of the diagonal and lateral isomers of $(\eta^5\text{-}C_5H_4R)Re(CO)(L)X_2$ was based on IR and NMR spectroscopy and X-ray single crystal structures. The proton patterns of the cyclopentadienyl ring resonances of the diagonal isomers

occur as two 'pseudo' triplet peaks while those of the lateral isomers usually comprise of four multiplet peaks. The diagonal isomers were also observed to have higher carbonyl stretching frequencies than the lateral isomers. The structures of *diag*- and *lat*-(η^5-C_5H_4Me)Re(CO)[$P(OPh)_3$]Br_2, the first structures of cyclopentadienyl monocarbonyl substituted dihalogen rhenium complexes, were successfully determined by X-ray single crystal diffraction and unambiguously confirmed the assignments (Chapter 8).

6.3.2 Solid-state diag-lat isomerization of (η^5-C_5H_4R)Re(CO)(L)X_2

It was found that all the diagonal isomers of (η^5-C_5H_4R)Re(CO)(L)X_2 underwent thermal solid-state isomerization reactions to give the corresponding lateral isomers in good yields (> 70%) within a few hours (Table 6.3). It should be noted that the reaction temperatures reported here (Table 6.3) are not the minimum temperatures needed for solid-state isomerization reactions. The isomerization is unidirectional, i.e. from the diagonal to the lateral isomer; the lateral isomers remained unchanged under the same reaction conditions. Unlike the thermal isomerization reactions of (η^5-C_5H_4R)Re$(CO)_2Br_2$ in which the isomerization process is strongly influenced by the cyclopentadienyl ring substituent R and the solid-state isomerization is only observed for (η^5-C_5H_4R)Re$(CO)_2Br_2$ (R = Me, iPr; Chapter 3), all (η^5-C_5H_4R)Re(CO)(L)X_2 underwent thermal solid-state *diag*-to-*lat* isomerization. In these reactions the different cyclopentadienyl ring substituent R, ligand L and halogen X have no influence on the *direction* of the solid-state isomerization process. More importantly, our study indicates that thermal solid-

Table 6.3. Thermal solid-state *diag-lat* isomerization of *diag*-(η^5-C_5H_4R)Re(CO)(L)X_2

Complex	reaction temp. (°C)	reaction time (h)	yield (%)[a]
Diag-(η^5-C_5H_4Me)Re(CO)($CNC_6H_3Me_2$)Br_2	140-145	1.0	86
Diag-(η^5-C_5H_4Me)Re(CO)[P(OMe)$_3$]Br_2	100-105	2.0	96
Diag-(η^5-C_5H_4Me)Re(CO)[P(O^iPr)$_3$]Br_2	95-100	6.0	81
Diag-(η^5-C_5H_4Me)Re(CO)[P(OPh)$_3$]Br_2	145-150	5.0	80
Diag-(η^5-C_5H_4Me)Re(CO)(PPh_3)Br_2	145-150	2.0	72
Diag-(η^5-C_5H_4Me)Re(CO)(PPh_3)I_2	145-150	2.0	70
Diag-(η^5-C_5H_4tBu)Re(CO)($CNC_6H_3Me_2$)Br_2	130-135	1.0	94
Diag-(η^5-C_5H_4tBu)Re(CO)[P(OMe)$_3$]Br_2	105-110	2.0	82
Diag-(η^5-C_5H_4tBu)Re(CO)[P(O^iPr)$_3$]Br_2	105-110	2.0	70
Diag-(η^5-C_5H_4tBu)Re(CO)[P(OPh)$_3$]Br_2	108-110	2.0	85
Diag-(η^5-C_5H_4tBu)Re(CO)(PPh_3)Br_2	140-145	2.0	85
Diag-(η^5-$C_5H_4SiMe_3$)Re(CO)($CNC_6H_3Me_2$)Br_2	130-135	1.0	76
Diag-(η^5-$C_5H_4SiMe_3$)Re(CO)[P(O^iPr)$_3$]Br_2	90-95	2.0	70
Diag-(η^5-$C_5H_4SiMe_3$)Re(CO)[P(OPh)$_3$]Br_2	105-110	2.0	71
Diag-(η^5-$C_5H_4SiMe_3$)Re(CO)(PPh_3)Br_2	130-135	0.5	75

[a] Isolated yields.

state *diag-lat* isomerization is a common reaction for a wide range of cyclopentadienyl four-legged piano stool rhenium complexes. Reaction of *diag*-(η^5-C_5H_4Me)$Re(CO)_2Br_2$ and excess NaI in the solid state, under typical isomerization conditions, gave quantitative formation of *diag*-(η^5-C_5H_4Me)$Re(CO)_2I_2$. This methodology also offers a convenient method for the preparation of cyclopentadienyl dicarbonyldiiodide rhenium complexes. Reaction of a solid mixture of *diag*-(η^5-C_5H_4Me)$Re(CO)[P(OPh)_3]Br_2$ and excess NaI, surprisingly gave *diag*-(η^5-C_5H_4Me)$Re(CO)_2I_2$ (50% yield) instead of the expected *diag*-(η^5-C_5H_4Me)$Re(CO)[P(OPh)_3]I_2$. The above reactions indicate that both Re-Br and Re-$P(OPh)_3$ bonds can be broken during the solid-state halogen exchange processes.

These are remarkable results in that :

(i) The diagonal iodo isomer has formed in the solid state. Previously we had not been able to interconvert the iodo *diag-lat* isomers in the solid state [16] as a melt formed prior to isomerization. However the preference for the *diagonal* isomer is expected from a consideration of the melting points of the isomers.

(ii) The yield is near quantitative in the phosphite-iodide exchange reaction and implies no CO is lost when the ligand exchange occurs.

(iii) This is the first time we have observed the replacement of a neutral ligand by another neutral ligand (phosphite by CO) in the solid state.

previous paper[16] we proposed that isomerization was achieved by a flexing of the four ligands relative to the cyclopentadienyl ring followed by a turnstile process as shown in Fig 6.2. For this new set of compounds it appears that both the ring *and* the L ligand will provide the pivots for the 3-fold rotation of the Br and CO ligands. This is entirely consistent with the original proposal.

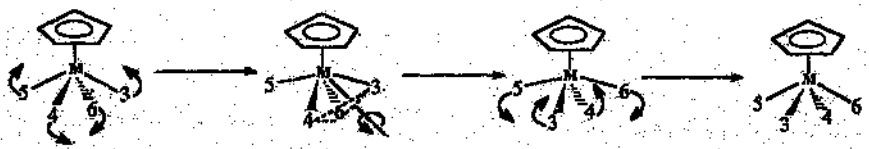

Fig. 6.2. Combined Berry-turnstile isomerization mechanism for $CpML_4$ complexes

Presumably during the flexing process all metal-ligand bonds are weakened (even the ring-Re bonds[16]) and in the presence of appropriate ligands e.g. iodide/ iodine atom, substitution can take place. This would lead to the unusual results obtained above. Clearly further studies will be needed to assess both the generality of the reaction and the mechanism of the ligand exchange.

6.3.3 Solution phase diag-lat isomerization of (η^5-C_5H_4R)Re(CO)(L)X

Both *diag*- and *lat*-(η^5-C_5H_4R)Re(CO)(L)X_2 are stable in solution in the dark, even in the presence of excess ligand, L. Only a few percent (<5%) of the lateral

isomer forms when the chloroform or benzene solutions of *diag*-(η^5-C_5H_4R)Re(CO)(L)X_2, covered with aluminum foil, were kept at room temperature for four weeks. No isomerization was observed for *lat*-(η^5-C_5H_4R)Re(CO)(L)X_2 under these conditions. However, the solution isomerization of (η^5-C_5H_4R)Re(CO)(L)X_2 proceeds readily on irradiation with visible light. The solution isomerization results for the study of three typical diagonal and lateral pairs, (η^5-C_5H_4Me)Re(CO)($CNC_6H_3Me_2$)Br_2, (η^5-C_5H_4tBu)Re(CO)[$P(OMe)_3$]Br_2 and (η^5-$C_5H_4SiMe_3$)Re(CO)(PPh_3)Br_2, in $CHCl_3$ and benzene under normal laboratory light are listed in Table 6.4. All diagonal isomers completely isomerized into the corresponding lateral isomers in $CHCl_3$ or benzene within 72 h, except the benzene solution of *diag*-(η^5-C_5H_4Me)Re(CO)($CNC_6H_3Me_2$)Br_2 (50% yield), this may be because that the weak repulsion between smaller $CNC_6H_3Me_2$ ligand and Br atom slowed down the isomerization process (see below), and it is known that free radicals are more difficult to survive in benzene than in $CHCl_3$. Our results (not shown) indicate that the isomerization reaction proceeded faster in $CHCl_3$ than in benzene and that the diiodide complexes are much easier to isomerize than the dibromide complexes. For example, *diag*-(η^5-C_5H_4Me)Re(CO)[$P(OPh)_3$]Br_2 was stable in the 1:1 mixture of CH_2Cl_2 and hexane under normal room . several hours, while more than 30% of lateral isomer was formed when *diag*-(η^5-C_5H_4Me)Re(CO)[$P(OPh)_3$]I_2 was irradiated in the same solvent mixture for 5 min.

Table 6.4. Solution *diag-lat* isomerization of *diag-* and *lat*-(η^5-C_5H_4R)Re(CO)(L)Br_2[a]

Complex	solvent	diag (%)[b]	lat (%)[b]
Diag-(η^5-C_5H_4Me)Re(CO)($CNC_6H_3Me_2$)Br_2	$CHCl_3$	0	100
Diag-(η^5-C_5H_4Me)Re(CO)($CNC_6H_3Me_2$)Br_2	benzene	50	50
Diag-(η^5-C_5H_4tBu)Re(CO)[$P(OMe)_3$]Br_2	$CHCl_3$	0	100
Diag-(η^5-C_5H_4tBu)Re(CO)[$P(OMe)_3$]Br_2	benzene	0	100
Diag-(η^5-$C_5H_4SiMe_3$)Re(CO)(PPh_3)Br_2	$CHCl_3$	0	100[c]
Diag-(η^5-$C_5H_4SiMe_3$)Re(CO)(PPh_3)Br_2	benzene	0	100[c]
Lat-(η^5-C_5H_4Me)Re(CO)($CNC_6H_3Me_2$)Br_2	$CHCl_3$	0	100
Lat-(η^5-C_5H_4Me)Re(CO)($CNC_6H_3Me_2$)Br_2	benzene	2	98
Lat-(η^5-C_5H_4tBu)Re(CO)[$P(OMe)_3$]Br_2	$CHCl_3$	0	100
Lat-(η^5-C_5H_4tBu)Re(CO)[$P(OMe)_3$]Br_2	benzene	0	100
Lat-(η^5-$C_5H_4SiMe_3$)Re(CO)(PPh_3)Br_2	$CHCl_3$	0	100[c]
Lat-(η^5-$C_5H_4SiMe_3$)Re(CO)(PPh_3)Br_2	benzene	0	100[c]

[a] The solutions were kept at room temperature under normal laboratory light for 72 h.

[b] Determined by TLC and ^1H NMR spectroscopy. [c] Some decomposition was observed.

As with the thermal solid-state isomerization reaction, only the *diag*-to-*lat* isomerization was observed for solutions of $(\eta^5\text{-}C_5H_4R)Re(CO)(L)X_2$. No isomerization was observed for *lat*-$(\eta^5\text{-}C_5H_4R)Re(CO)(L)X_2$ under the same irradiation conditions. This *diag*-to-*lat* isomerization direction, which is different from the solution isomerization direction of their parent complexes $(\eta^5\text{-}C_5H_4R)Re(CO)_2X_2$ (Chapter 3), may be accounted for by a ligand steric (and electronic) effect in which ligand L and X interactions are minimized. A mechanism for the solution photochemical *cis-trans* isomerism of $(\eta^5\text{-}C_5Me_5)Re(CO)_2X_2$ (X = Cl, Br, I) has been reported and a carbonyl dissociation-association process has been proposed.[17] A similar mechanism may apply here although a dissociative-associative process involving X groups seems more likely.

6.4. Conclusions

With the assistance of Me_3NO, reaction of *diag*- or *lat*-$(\eta^5\text{-}C_5H_4R)Re(CO)_2X_2$ (R = Me, tBu, $SiMe_3$; X = Br, I) with isocyanides, phosphites and triphenyl phosphine proceeded rapidly at room temperature to give *diag*-$(\eta^5\text{-}C_5H_4R)Re(CO)(L)X_2$ (L = $CNC_6H_3Me_2$, $P(OMe)_3$, $P(O^iPr)_3$, $P(OPh)_3$, PPh_3) in good yields. Solid-state *diag*-*lat* isomerization reactions were observed for all the monocarbonyl substituted rhenium complexes $(\eta^5\text{-}C_5H_4R)Re(CO)(L)X_2$, prepared in this study, indicating that the solid-state isomerization reaction is a common phenomenon for cyclopentadienyl four-legged piano stool rhenium complexes. The direction of the isomerization reaction was also found to be different from their parent complexes

$(\eta^5\text{-}C_5H_4R)Re(CO)_2X_2$ in which *lat*-to-*diag* solution isomerization occurred. *diag*-$(\eta^5\text{-}C_5H_4R)Re(CO)(L)X_2$ completely isomerized into the corresponding lateral isomers in chloroform or dichloromethane on irradiation with visible light at room temperature.

6.5. References

1. (a) Green, M. L. H.; Wilkinson, G. *J. Chem. Soc.* **1958**, 4314. (b) Casey, C. P.; Andrews, M. A.; McAlister, D. R.; Rinz, J. E.; *J. Am. Chem. Soc.* **1980**, *102*, 1927. (c) Goldberg, K. I.; Bergman, R. G. *J. Am. Chem. Soc.* **1989**, *111*, 1285. (d) Tam, W.; Lin, G. Y.; Wong, W. K.; Kiel, W. A.; Wong, V. K.; Gladysz, J. A. *J. Am. Chem. Soc.* **1982**, *104*, 141. (e) Klahn, A. H.; Sutton, D.; *Organometallics* **1989**, *4*, 198. (f) He, Y. X.; Batchelor, R. J.; Einstein, F. W. B.; Peterson, L. K.; Sutton, D. *J. Organomet. Chem.* **1997**, *531*, 27. (h) Cavanaugh, M. D.; Tetrick, S. M.; Masi, C. J.; Cutler, A. R. *J. Organomet. Chem.* **1997**, *538*, 41. (i) Bosch, W. H.; Englert, U.; Pfister, B.; Stauber, R.; Salzer, A. *J. Organomet. Chem.* **1996**, *506*, 273. (j) Nesmeyanov, A. N.; Kolobova, N. E.; Makarov, Yu. V.; Anisimov, K. N. *Izv. Akad. Nauk SSSR, Ser. Khim.* **1969**, 1826. (k) Nesmeyanov, A. N.; Kolobova, N. E.; Makarov, Yu. V.; Anisimov, K. N. *Zh. Obsch. Khim.* **1974**, *44*, 2222.
2. (a) King, R. B.; Reimann, R. H. *Inorg. Chem.* **1976**, *15*, 179. (b) King, R. B.; Reimann, R. H.; Darensbourg, D. J. *J. Organomet. Chem.* **1975**, *93*, C23.
3. Einstein, F. W. B.; Klahn-Oliva, A. H.; Sutton, D.; Tyers, K. G. *Organometallics* **1986**, *5*, 53.
4. Yang, G. K.; Bergman, R. G. *Organometallics* **1985**, *4*, 129.
5. Dong, D. F.; Hoyano, J. K.; Graham, W. A. G. *Can. J. Chem.* **1981**, *59*, 1455.
6. Nunn, C. M.; Cowley, A. H.; Lee, S. W.; Richmond, M. G. *Inorg. Chem.*

1990, *29*, 2105.

7. Klahn, A. H.; Manzur, C.; Toro, A.; Moore, M. *J. Organomet. Chem.* **1996**, *516*, 51.

8. Klahn, A. H.; Arenas, S. *Bol. Soc. Chil. Quim.* **1993**, *38*, 277.

9. Klahn, A. H.; Singer, R. D.; Aramini, J. M.; Sutton, D. *Inorg. Chem.* **1989**, *28*, 4217.

10. Arenas, M.; Silva, S.; Toro, A.; Klahn, A. H. *Bol. Soc. Chil. Quim.* **1994**, *39*, 285.

11. (a) Braga, D.; Grepioni, F. *J. Chem. Soc., Chem. Commun.* **1996**, 571. (b) Roberto, D.; Cariati, E.; Psaro, R.; Ugo, R. *J. Organomet. Chem.* **1995**, *488*, 109. (c) Roberto, D.; Cariati, E.; Ugo, R.; Psaro, R. *Inorg. Chem.* **1996**, *35*, 2311. (d) Boldyreva, E. V. *Mol. Cryst. Liq. Cryst.* **1994**, *242*, 17. (e) Chapter 5 of this thesis.

12. (a) Luh, T. Y. *Coord. Chem. Rev.* **1984**, *59*, 225. (b) Shen, J. K.; Gao, Y. C.; Shi, Q. Z.; Basolo, F. *J. Organomet. Chem.* **1991**, *401*, 295. (c) Blumer, D. J.; Barnett, K. W.; Brown, T. L. *J. Organomet. Chem.* **1979**, *173*, 71.

13. Leins, A. E.; Coville, N. J. *J. Organomet. Chem.* **1991**, *407*, 359.

14. Cheng, L.; Coville, N. J. unpublished results.

15. Smith, J M.; Coville, N. J. *Organometallics* **1996**, *15*, 3388.

16. Ball, R. G.; Campen, A. K.; Graham, W. A. G.; Hamley, P. A.; Kazarian, S. G.; Ollino, M. A.; Poliakoff, M.; Rest, A. J.; Sturgeoff, L.; Whitwell, I. *Inorg. Chim. Acta.* **1997**, *259*, 137.

17. (a) Hill, R. H.; Palmer, B. J. *Organometallics* **1989**, *8*, 1651. (b) Xia, W.; Hill, R. H.; Klahn, A. H.; Leiva, C.; Buono-Core, G. E. *Polyhedron* **1996**, *15*, 3093.

CHAPTER 7

THERMAL SOLID-STATE *DIAG-LAT* ISOMERIZATION STUDIES OF (η^5-C_5H_4R)Re(CO)(L)Br_2. DSC AND THERMOMICROSCOPY STUDIES

7.1. Introduction

Thermal solid-state reactions of coordination compounds have been under investigation since the original syntheses of these types of complexes over 100 years ago. A sub-class of these reactions are the solid-state isomerization reactions which include the metal coordinated NO_2 – ONO linkage isomerization reaction, a reaction still under investigation today.[1] Solid-state *cis-trans* isomerization reactions of classical coordination complexes have also been extensively studied since the early part of this century.[2]

By contrast, solid-state isomerization reactions involving organometallic complexes,[3,4] and even solid-state organometallic reactions in general,[5-9] have been little studied until recently.

In Chapter 3, we have reported that the complex (η^5-C_5H_4Me)Re(CO)$_2Br_2$

underwent *trans-cis (diag-lat)* isomerization in the solid state (Fig 7.1). The solid-state isomerization reaction appeared to be limited to this specific complex, as solid-state isomerization was not observed for the related complexes in which the methyl ring substituent was replaced by ethyl, t-butyl or trimethylsilyl groups, although they do isomerize in molten state. In Chapter 6, we have reported the synthesis of a range of CO substituted derivatives of the type $(\eta^5\text{-}C_5H_4R)Re(CO)(L)X_2$ (R = Me, tBu, $SiMe_3$; L = isocyanides, phosphites, PPh_3; X = Br, I). The new complexes have been prepared *via* solution reactions and in every instance the diagonal isomer of $(\eta^5\text{-}C_5H_4R)Re(CO)(L)X_2$ has been prepared in high yield. More importantly, the results showed that the new complexes all isomerized into the corresponding lateral isomers when heated in the solid-state. In this chapter, we wish to report our DSC and thermomicroscopy results on these new thermal solid-state organometallic isomerization reactions.

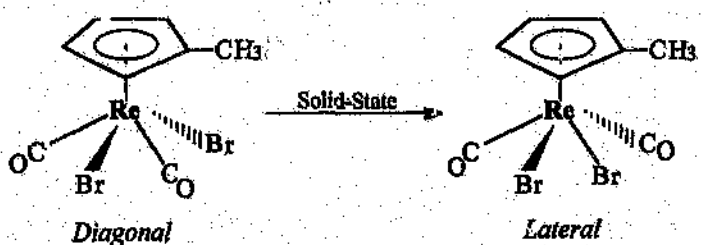

Fig. 7.1. Solid-state *diag*-to-*lat* isomerization of $(\eta^5\text{-}C_5H_4Me)Re(CO)_2Br_2$.

7.2. Experimental

The diagonal and lateral (η^5-C_5H_4R)Re(CO)(L)Br_2 (R = Me, tBu, $SiMe_3$; L = CO, $CNC_6H_3Me_2$, $P(OMe)_3$, $P(OPh)_3$) complexes were synthesized by the methods described in Chapter 3 and 6. Pertinent data for the new complexes are shown in Table 1. Differential scanning calorimetry was performed on 5-10 mg micro-crystal samples under flowing nitrogen on a Du Pont 910 DSC instrument. Data were recorded at a heating rate of 2.0 °C/min (unless otherwise stated). Micrographs were obtained on single crystal samples from a standard Zeiss microscope fitted with a MC 63 photomicrographic camera (64 x magnification) at room temperature. Samples were also isomerized by heating single crystal samples of *diag*-(η^5-C_5H_4R)Re(CO)(L)Br_2 in a flat-bottom flask in an oil bath under nitrogen for different periods of time. The crystals were monitored under the microscope (after cooling the samples to room temperature) during the course of the reaction and photographs were taken after appropriate time intervals until the isomerization processes was complete.

7.3. Results and Discussion

7.3.1. DSC

DSC measurements on *diag*-(η^5-C_5H_4Me)Re(CO)$_2Br_2$ were carried out at different heating rates (1.0, 2.0, 5.0, 10.0 and 20.0 °C/min) and the data are shown in Fig. 7.2. Two peaks were observed in the spectra at all the heating rates. The higher temperature peak, an endotherm (ca. 170 °C), corresponds to the melting point of

the lateral isomer product. It had variable shape and this was found to relate to the crystallinity of the material (see below).

The lower temperature peak corresponded to both the melting point of the diagonal isomer and the exothermic reaction associated with the *diag-lat* reaction. This peak at ca. 115 °C showed variable intensity and shape as the heating rate was varied. At the lowest heating rate shown (Fig 7.2a) only an exotherm is noted. This corresponds to the diagonal to lateral isomerization reaction of the complex (see below). As the heating rate was increased (Fig 7.2b – Fig 7.2e) this peak became larger and revealed exothermic behavior. Indeed, observation of the crystalline material under a microscope at high heating rates indicated melting to give a liquid phase followed by solidification. In this instance the isomerization reaction occurred in the molten state. It is thus apparent that when heat is supplied to crystals of $(\eta^5\text{-}C_5H_4Me)Re(CO)_2Br_2$, two competing processes can take place. Either the heat can go to breaking intermolecular bonds (melting results) or the heat supplied can be used to induce an intramolecular process (the isomerization reaction). The lower energy process is the isomerization reaction.

A DSC study was also carried out on different size crystals of $(\eta^5\text{-}C_5H_4Me)Re(CO)_2Br_2$ to assess the effect of this variable on the DSC spectrum (Fig 7.3). The three samples, large crystals (ca. 3 × 7 mm), small crystals (ca. 1 × 0.1 mm) and fine powder all gave similar spectra. However some significant differences were observed.

i) More complex features are observed for the lower temperature exotherm

for the large crystals. This suggests that the isomerization reaction is not occurring in a homogeneous manner but rather heterogeneously, e.g. at defects , and then spreads through the crystal framework.. This would not necessarily be detected in smaller crystals.

ii) The higher temperature (endothermic) peak also reveals a 'doublet' peak which is most clearly observed in Fig 7.3b. This relates to the crystallinity of the product and will be discussed further below.

The DSC curves of four typical complexes, *diag*-(η^5-C_5H_4Me)Re(CO)($CNC_6H_3Me_2$)Br_2, *diag*-(η^5-C_5H_4tBu)Re(CO)[$P(OMe)_3$]Br_2, *diag*-(η^5-C_5H_4tBu)Re(CO)($CNC_6H_3Me_2$)Br_2 and *diag*-(η^5-$C_5H_4SiMe_3$)Re(CO)($CNC_6H_3Me_2$)Br_2, as well as *diag*-(η^5-C_5H_4Me)Re$(CO)_2Br_2$, are shown. in Fig 7.4. All data were measured at a heating rate 2.0 °C/min. In all cases, an exotherm and an endotherm were observed.

It is apparent that the same phenomena are occurring for all the complexes. Thus, the low temperature exotherm/endotherm peak corresponds to the processes of melting and isomerization while the high temperature peak corresponds to the melting point of the lateral isomer. It is clear that the heating rate chosen determines the degree to which the two processes can be separated. Heating of the diagonal isomers at about 20° C below the melting point of the isomer has been found to be sufficient to induce the isomerization reaction to occur in the solid state without apparent liquid formation.

In all instances IR and NMR spectra were recorded on the materials both before and after the heating process. Spectra were also recorded on samples which had only been heated to a temperature beyond the first absorption in the DSC spectrum (i.e. prior to reaching the second thermal process). This data confirmed the composition of the materials. DSC spectra were also recorded on pure lateral isomers to confirm the position of the melting points assigned above.

The above data suggest that the thermodynamic product in the isomerization reaction is the isomer with the highest melting point. Clearly this 'thermodynamic product' is different to that found in the solution state (Chapter 3). As no gas phase data are available on the respective isomers it is not clear what the thermodynamic product will be in the absence of nearest neighbors (solvent, melt, crystal environment).

An attempt was made to determine the reversibility of the isomerization reaction in the solid-state by heating $(\eta^5\text{-}C_5H_4Me)Re(CO)_2Br_2$ slowly to 125 °C and then cooling the sample to 70 °C. No absorption peak was noted in the cooling process, or in the subsequent re-heating process through this temperature range. It is thus clear that that the isomerization reaction is irreversible in the solid state.

DSC spectra were also recorded on samples (e.g. $(\eta^5\text{-}C_5H_4tBu)Re(CO)_2Br_2$ and $(\eta^5\text{-}C_5H_4SiMe_3)Re(CO)_2Br_2$) which did not undergo isomerization in the solid-state. In these samples only endotherms corresponding to the respective melting

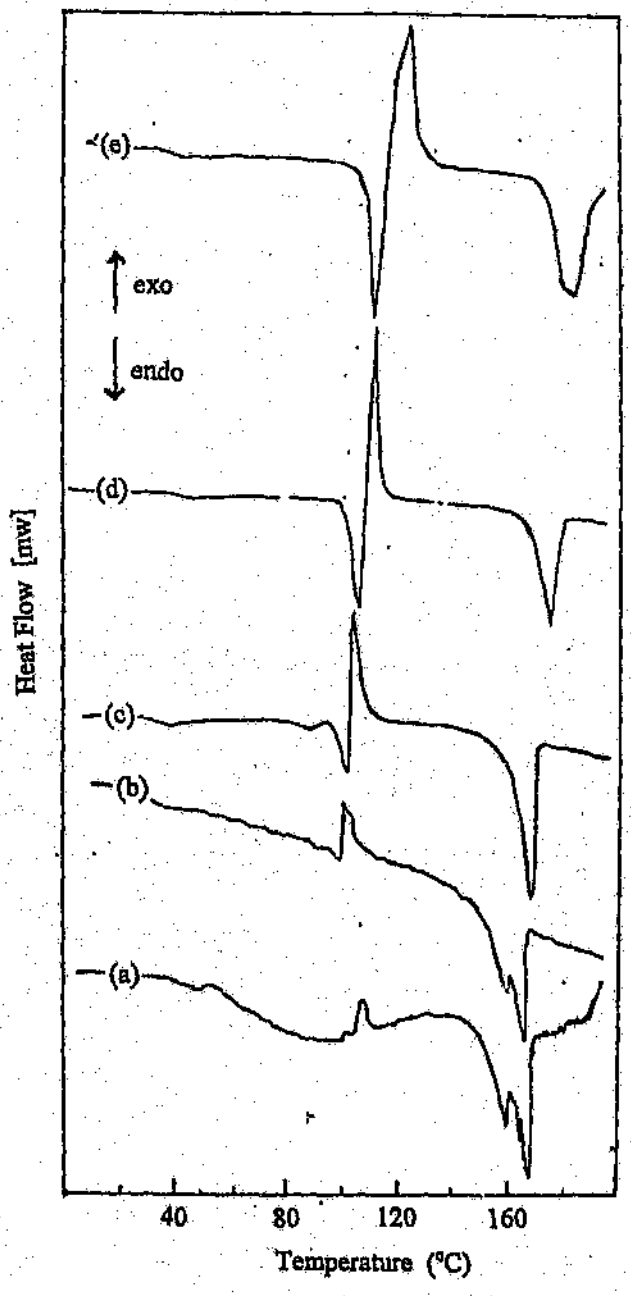

Figure 7.2. DSC curves for *diag*-(η^5-C_5H_4Me)$Re(CO)_2Br_2$ at different heating rates. (a) 1.0, ΔH_f = -10.9 J/mol, (b) 2.0, (c) 5.0, (d) 10.0 and (e) 20.0 °C/min.

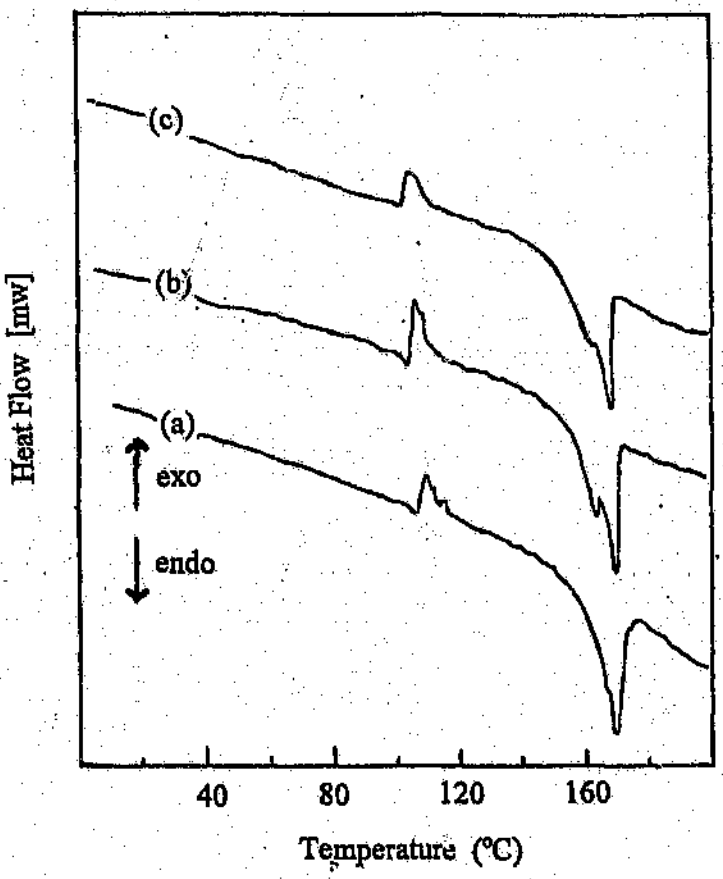

Figure 7.3. DSC curves for *diag*-(η^5-C_5H_4Me)$Re(CO)_2Br_2$, (a) large crystals, ΔH_i = -16.9 J/mol, (b) microcrystals, ΔH_i = -36.4 J/mol, (c) fine powder, ΔH_i = -13.5 J/mol.

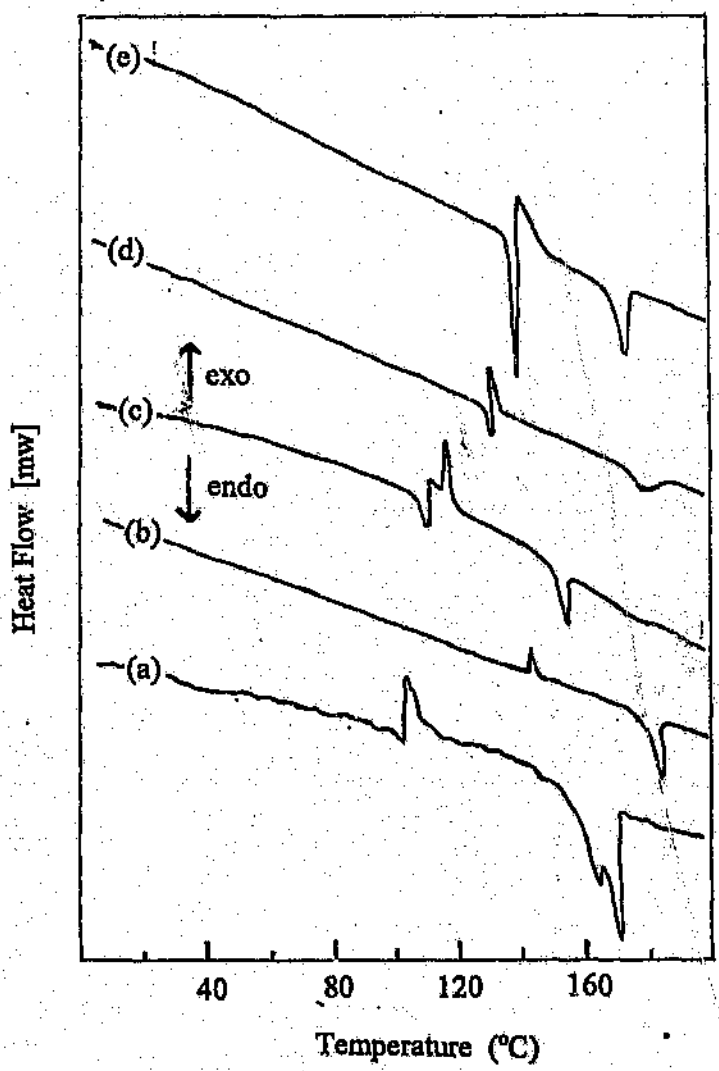

Figure 7.4. DSC curves of (a) *diag*-(η^5-C_5H_4Me)$Re(CO)_2Br_2$, (b) *diag*-(η^5-C_5H_4Me)$Re(CO)(CNC_6H_3Me_2)Br_2$, ΔH_f = -12.8 J/mol, (c) *diag*-(η^5-C_5H_4tBu)$Re(CO)[P(OMe)_3]Br_2$, (d) *diag*-(η^5-C_5H_4tBu)$Re(CO)(CNC_6H_3Me_2)Br_2$ and (e) *diag*-(η^5-$C_5H_4SiMe_3$)$Re(CO)(CNC_6H_3Me_2)Br_2$

points were detected for both the lateral and diagonal isomers .

The isomerization enthalpy change, ΔH_i, measured from the DSC spectra, (< 5 kJ/mole) was much lower than the values reported for *cis-trans* isomerization reactions of square planar complexes which are usually in the range of 5 to 50 kJ/mole.[3,4] Further, molecular mechanics calculations carried out on (1) (R = Me, L = CO) indicate a very small difference in the crystal energies between the diagonal and lateral isomers. It is hence noted that the *diag-lat* isomerization reactions of cyclopentadienyl four-legged piano stool transition metal complexes involves much less energy changes than those of coordinate compounds.

7.3.2. Thermomicroscopy studies

The thermal solid-state isomerization reactions of *diag*-(η^5-C_5H_4Me)$Re(CO)_2Br_2$, *diag*-(η^5-C_5H_4Me)$Re(CO)(CNC_6H_3Me_2)Br_2$ and *diag*-(η^5-C_5H_4Me)$Re(CO)[(P(OPh)_3]Br_2$ have been studied by thermomicroscopy. Pictures indicating the changes that occurred towards the end of the heating process are shown in Fig. 7.5-7.7

diag-(η^5-C_5H_4Me)$Re(CO)_2Br_2$ (Fig 7.5): It can be seen that the isomerization reaction started at the crystal edge and/or at surface imperfections in the single crystal and then moved isotropically through the entire crystal. This process is easy to monitor as the two different isomers have different colors (*diag* : red, *lat* : brown). The interface advance was accompanied by cracking. At the end of the

reaction small microcrystals could be observed at the edges of the dominant crystal. Indeed it is thought that this behavior is responsible for the complex pattern noted for the endotherm shown in Figs 7.2a and 7.2b. Because the material consists of crystals of two (dominant) different sizes a broadened 'doublet' melting point was observed.

diag-(η^5-C_5H_4Me)Re(CO)($CNC_6H_3Me_2$)Br_2 (Fig 7.7): Similar observations as observed for *diag*-(η^5-C_5H_4Me)Re(CO)$_2Br_2$ (Fig 7.5) were noted. The brown isomerization product was first formed at the edges and at surface defects of the red starting crystals. When the reaction was complete the whole crystal had changed into a dark brown cracked crystal.

diag-(η^5-C_5H_4Me)Re(CO)[$P(OPh)_3$]Br_2 (Fig 7.6): The crystal of this isomer did not disintegrate on heating but the crystal did change color during the heating process. The color change occurred at small nucleation points on the surface of the crystal and these nucleation sites became larger as the reaction progressed. This is a classical process well described in the literature.[10,11]

7.3.3. Mechanism

A consideration of the specific complexes investigated reveals the following:

i) The electronic or steric effects associated with the cyclopentadienyl ligand of individual molecules do not correlate with the isomerization reaction.

Thus, changing the methyl substituent for a t-butyl substituent in (1) yields complexes that undergo isomerization (L = $CNC_6H_3Me_2$) and do not undergo isomerization (L = CO) in the solid state.

ii) It appears that, to date, all complexes that contain a bulky ligand do undergo the isomerization reaction. It may be that these groups both provide more 'space'[7] in the crystal and possibly a pivot (see below) for the isomerization reaction to occur.

iii) The exothermic reaction always proceeds from the isomer of lowest melting point, suggesting that the reaction is controlled by thermodynamic factors.

As mentioned above, during the isomerization reaction, crystal disintegration generally was observed to occur. This implies that volume or phase changes (or both) are occurring in the process. If one assumes that the isomerization reaction occurs and is *then* followed by the phase change, two current, competing, theories are available to interpret the results of the above study: the topochemical principle[12,13] and the phase rebuilding principle.[14,15] The possibility that a phase change *drives* the isomerization reaction can however not be ruled out and the further studies on this issue will be presented in Chapter 8.

In a previous publication we suggested that the *diag-lat* isomerization reaction of $(\eta^5\text{-}C_5H_4Me)Re(CO)_2Br_2$ occurred *via* a Berry-Turnstile combined mechanism.

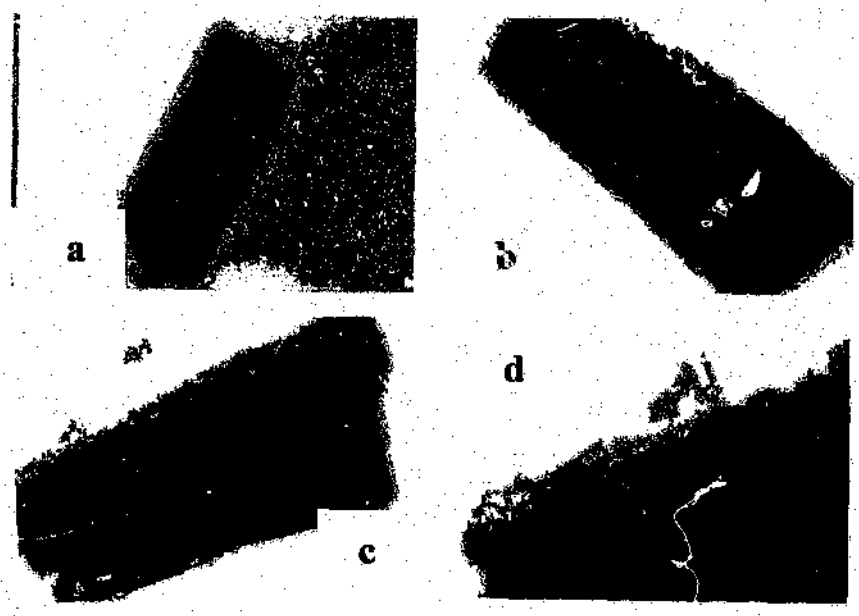

Figure 7.5. Micrographs of isomerization processes in a single crystal of *diag*-(η^3-C_5H_4Me)$Re(CO)_2Br_2$ at 100-102 °C, (a) 30 min, (b) 1.0 h, (c) 3.0 and (d) 3.0 h.

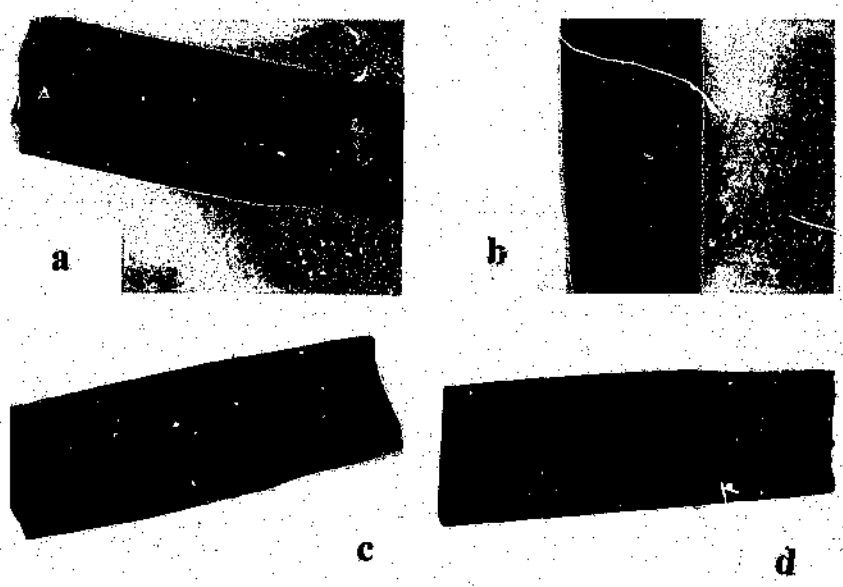

Figure 7.6. Micrographs of isomerization processes in a single crystal of *diag*-(η^5-C_5H_4Me)Re(CO)[P(OPh)$_3$]Br$_2$ at 145-147 °C, (a) 0 min, (b) 6.0 h, (c) 70 h and (d) 117 h.

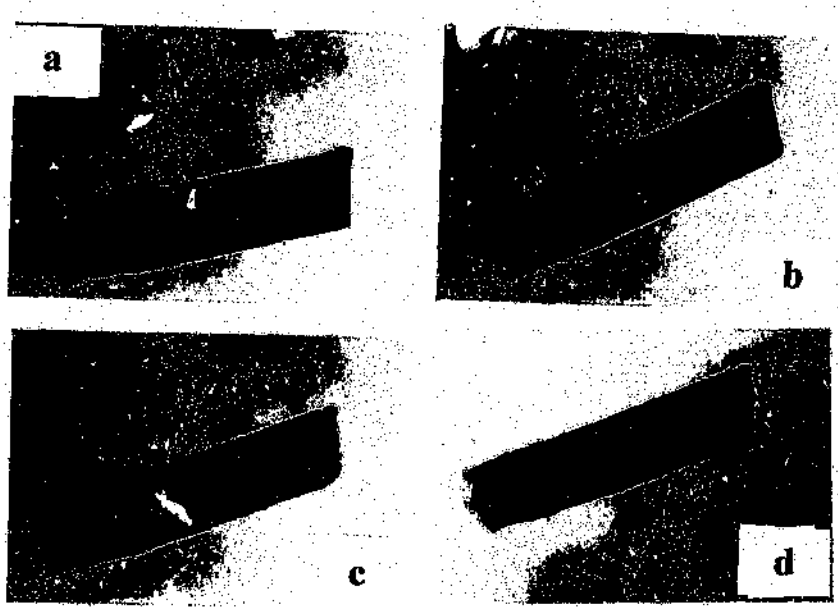

Figure 7.7. Micrographs of isomerization processes in a single crystal of *diag*-(η^5-C_5H_4Me)Re(CO)($CNC_6H_3Me_2$)Br_2 at 135-137 °C, (a) 0 min, (b) 2.0 h, (c) 6.0 h and (d) 17.0 h.

This proposal was based on a structure correlation analysis.[16] In this process two of the ligands act as pivots for the turnstile process. The studies described above are consistent with the proposal and would suggest that both the large cyclopentadienyl ligand and the L group are the pivots. However more information will be needed before further proposals can be made to determine more specifically the mechanism of the above reaction.

Notwithstanding the above, this study provides the first investigation of the thermal solid-state isomerization behavior of classical organometallic complexes. The synthetic strategies to produce complexes of the type described above are trivial and thus a convenient series of organometallic complexes are now available for further study.

7.4. Conclusions

The thermal solid-state *diag-lat* isomerization reactions of cyclopentadienyl four-legged piano stool rhenium complexes *diag*-(η^5-C_5H_4R)Re(CO)(L)Br_2 (R = Me, tBu, $SiMe_3$; L = CO, $CNC_6H_3Me_2$, $P(OMe)_3$, $P(OPh)_3$) have been studied by DSC and thermomicroscopy investigations. In all the reactions investigated the diagonal isomers convert to the lateral isomers *via* an exothermic reaction. The thermomicroscopy reactions suggest that the isomerization reaction occurs *via* a

Table 7.1. Properties of *diag*- and *lat*-(η^5-C_5H_4R)Re(CO)(L)Br_2.

Complex	Color	m.p. (°C)	Expt.[a]
(η^5-C_5H_4Me)Re(CO)$_2Br_2$	diag: maroon lat: brown	Diag: 116-118 lat: 158-160	D/T
(η^5-C_5H_4Me)Re(CO)(CNC$_6H_3Me_2$)Br_2	diag: yellow-red lat: brown	Diag: 154-156 lat: 192-194	D/T
(η^5-C_5H_4Me)Re(CO)[P(OPh)$_3$]Br_2	diag: red lat: brown	Diag: 164-167 lat: 183-185	D/T
(η^5-C_5H_4tBu)Re(CO)[P(OMe)$_3$]Br_2	diag: red lat: brown	Diag: 123-125 lat: 154-156	D
(η^5-C_5H_4tBu)Re(CO)(CNC$_6H_3Me_2$)Br_2	diag: yellow-red lat: brown	Diag: 142-144 lat: 194-196	T
(η^5-$C_5H_4SiMe_3$)Re(CO)(CNC$_6H_3Me_2$)Br_2	diag: yellow-red lat: brown	Diag: 144-146 lat: 179-181	D

[a] D: DSC measurements, T: thermomicroscopic studies.

nuclear formation and growth mechanism, similar to what has been observed for related compounds in other areas of chemistry.

7.5. References

1. Boldyreva, E.; Kivikoski, J.; Howard, J. A. K. *Acta Cryst.* **1997**, *B53*, 394.
2. (a) LeMay, H. E. Jr.; Bailar, J. C. Jr. *J. Am. Chem. Soc.* **1968**, *90*, 1729. (b) Ellis, R.; Wel, T. A.; Orchin, M. *J. Am. Chem. Soc.* **1970**, *92*, 1078. (c) Orrell, K. G. *Mech. Inorg. Organomet. React.* **1994**, *8*, 321-61, 469-74.
3. Krassowski, D. W.; Reimer, K.; LeMay, H. E. Jr.; Nelson, J. *Inorg. Chem.* **1988**, *27*, 4307.
4. Katsuki, K.; Ooyama, Y.; Okamoto, M.; Yamamoto, Y. *Inorg. Chim. Acta* **1994**, *217*, 181.
5. Bianchini, C.; Graziani, M.; Kaspar, J.; Meli, A.; Vizza, F. *Organometallics* **1994**, *13*, 1165
6. Siedle, A. R.; Newmark, R. A.; Lyon, P. A.; Hunt, S. L.; Day, V. W. *Inorg. Chim. Acta.* **1997**, *259*, 241.
7. Sekine, A.; Tatsuki, H.; Ohashi, Y. *J. Organometal. Chem.*. **1997**, *389*, 536.
8. Braga, D. *Chem. Rev.* **1992**, *92*, 633.
9. Miller, E. J.; Brill, T. B.; Rheingold, A. L.; Fultz, W. C. *J. Am. Chem. Soc.* **1983**, *105*, 7580.
10. Shakhtshneider, T. P.; Ivanov, E. Yu.; Boldyrev, V. V. *Thermochim. Acta* **1985**, *92*, 469.
11. Shakhtshneider, T.; Ivanov, E.; Boldyrev, V. *J. Therm. Anal.* **1988**, *33*, 525.
12. Cohen, M. D. *Angew. Chem. Int. Ed. Engl.* **1975**, *14*, 386
13. Schmidt, G. M. J. *Pure Appl. Chem.*, **1971**, *27*, 647.
14. Kaupp, G.; Schmeyers, J. *Angew. Chem. Int. Ed. Engl.* **1993**, *32*, 1587.

15. Kaupp, G. in *Comprehensive Supramolecular Chemistry* Vol. 8, Chapter 9, P382, Pergamon, New York, 1996.

16. Smith, J. M.; Coville, N. J. *Organometallics* **1996**, *15*, 3388.

CHAPTER 8

X-RAY SINGLE-CRYSTAL STRUCTURES OF *DIAG-* AND *LAT*-(η^5-C_5H_4Me)Re(CO)[P(OPh)$_3$]Br$_2$; AND *DIAG-* AND *LAT*-(η^5-C_5H_4tBu)Re(CO)$_2$Br$_2$: PAIRS OF COMPLEXES WITH UNIQUE SOLID-STATE BEHAVIOR PATTERNS

8.1. Introduction

It was shown in Chapter 3 that no solid-state isomerization reactions were observed for (η^5-C_5H_4R)Re(CO)$_2$Br$_2$ when R was an ethyl, *tert*-butyl or trimethylsilyl group. However, the thermal solid-state isomerization reactions proceed readily for the monocarbonyl substituted complexes (η^5-C_5H_4R)Re(CO)(L)Br$_2$ (L = $CNC_6H_3Me_2$, P(OR)$_3$, PPh_3) with *any* ring-substituent R (Chapter 6). It appears that the electronic and steric parameters associated with R have no obvious relationship with the isomerization process. Clearly, inter-molecular forces are overwhelming any obvious intra-molecular effects associated with the groups around the metal.

Thermomicroscopic studies revealed that the thermal solid-state isomerization

process of $(\eta^5\text{-}C_5H_4Me)Re(CO)[P(OPh)_3]Br_2$ was unusual in that no crystal cracking was observed in the process (Chapter 7). In addition, the structures of monocarbonyl substituted four-legged piano stool rhenium complexes have not previously been measured. Indeed the assignments of the diagonal and lateral isomers are based on NMR and IR parameters and the crystallographic data would confirm these assignments. [1]

Of further significance was the observation that the $(\eta^5\text{-}C_5H_4tBu)Re(CO)_2Br_2$ complex did not undergo thermal solid-state isomerization. These isomers thus provide a set of complexes to assess why the isomerization reaction did not occur. We have thus carried out the X-ray single-crystal structure determination of both *diag*- and *lat*-$(\eta^5\text{-}C_5H_4Me)Re(CO)[P(OPh)_3]Br_2$, and *diag*- and *lat*-$(\eta^5\text{-}C_5H_4tBu)Re(CO)_2Br_2$. The crystallographic analysis of *diag*- and *lat*-$(\eta^5\text{-}C_5H_4Me)Re(CO)_2Br_2$ (Chapter 4) revealed that the intermolecular interaction played an important role in the solid-state isomerization reaction. It was thus expected that the further structural analyses would lead to a better understanding of the isomerization reaction.

8.2. Experimental Section

The diagonal and lateral isomers of $(\eta^5\text{-}C_5H_4tBu)Re(CO)_2Br_2$ and $(\eta^5\text{-}C_5H_4Me)Re(CO)[P(OPh)_3]Br_2$ were synthesized by the methods described in Chapter 3 and 6. Single crystals of these complexes were crystallized from a

mixture of dichloromethane/hexane under nitrogen at -15 °C.

The crystallographic analysis was carried out by the same procedures as described in Chapter 4.

8.3. Results and Discussion

The stereoscopic views of the three-dimensional molecular structures of *diag*- and *lat*-(η^5-C_5[illegible]$)_3$]Br_2, and *diag*- and *lat*-(η^5-C_5H_4tBu)Re(CO)$_2Br_2$ (with atom [illegible] are given in Figures 8.1–8.8. Tables 8.1–8.2 summarize the crystal data and data collection conditions for these complexes. Crystallographic data, fractional atomic coordinates, bond lengths and bond angles, structure factors are given in Appendix A.

All four complexes have the expected molecular geometries, i.e. two bromine atoms lie on either end of a diagonal in the diagonal isomers and are *cis* to each other in the lateral isomers. The Re–C(CO), Re–C(ring), Re–Br bond lengths and the interbond angles Br_1–Re–Br_2 are similar to those reported for the corresponding isomers of (η^5-C_5H_4Me)Re(CO)$_2Br_2$ and *diag*-(η^5-C_5Me_5)Re(CO)$_2Br_2$.

The most interesting crystallographic features are obtained from the crystal packing diagrams of *diag*- and *lat*-(η^5-C_5H_4Me)Re(CO)[P(OPh)$_3$]Br_2 (Figure 8.9

and 8.10). Both isomers have exactly the same packing arrangements with the phenyl groups "interlocked" with those of the neighboring molecules. As a result, both isomers have the same monoclinic $P2_1/c$ space group and the same unit cell, i.e. they appear to be isostructural. Clearly, the *intermolecular* interactions in the bulk of the material are nearly the same in both isomers.

This structural feature, i.e. that both isomers have almost the same unit cell volum. 2481 $Å^3$ and 2467 $Å^3$), also explains the observation that no cracking of the crystal occurred in the reaction (Chapter 7). Also of notice that the molecular volume of $(\eta^5\text{-}C_5H_4Me)Re(CO)[P(OPh)_3]Br_2$ (602 $Å^3$) in the crystal is more than two times larger than that of $(\eta^5\text{-}C_5H_4Me)Re(CO)_2Br_2$ (269 $Å^3$). Thus the effect of a molecular rearrangement involving Br and CO could be much smaller in the crystal of the former and less likely cause crystal cracking.

As we expected, different molecular structures and packing diagrams from $(\eta^5\text{-}C_5H_4Me)Re(CO)_2Br_2$ were observed for $(\eta^5\text{-}C_5H_4tBu)Re(CO)_2Br_2$.

For *lat*-$(\eta^5\text{-}C_5H_4Me)Re(CO)_2Br_2$, one Br atom is eclipsed with methyl ring substituent (Figure 4.5), while the two Br atoms are staggered with respect to ring-substituent tBu for *lat*-$(\eta^5\text{-}C_5H_4tBu)Re(CO)_2Br_2$ (Figure 8.8).

We can see from the packing diagram of the diagonal isomer that all molecules align in the head-tail manner, but the direction of each two molecular layers is

Table 8.1. Crystal data and details of structure refinement for *diag*- and *lat*-(η^5-C_5H_4Me)*Re*(CO)[$P(OPh)_3$]Br_2

Complex	diag-(η^5-C_5H_4Me)Re(CO)[$P(OPh)_3$]Br_2	lat-(η^5-C_5H_4Me)Re(CO)[$P(OPh)_3$]Br_2
Identification code	OM 84	OM 85
Empirical formula	$C_{25}H_{22}Br_2O_4Pre$	$C_{25}H_{22}Br_2O_4PRe$
Formula weight	763.42	763.42
Temperature	296(2) K	296(2) K
Wavelength	0.71073 A	0.71073 A
Crystal system	Monoclinic	monoclinic
Space group	$P2_1/c$	$P2_1/c$
Unit cell dimensions	a = 15.8117(7)Å, α = 90.0° b = 11.1102(5)Å, β=93.6320(1)° c = 14.1533(6)Å, γ = 90.0°	a = 15.9490(7)Å, α = 90.0° b= 10.8893(5)Å, β= 94.5340(10)° c = 14.2549(7)Å, γ = 90.0°
Volume ($Å^3$)	2481.3(2)	2467.9(2)
Z	4	4
Density (calculated)	2.044 g/cm^3	2.055 g/cm^3
Absorption coefficient	8.212 nm^{-1}	8.256 nm^{-1}
F (000)	1456	1456
Crystal size	0.4 × 0.2 × 0.3 mm	0.2 × 0.1 × 0.2 mm
θ range for data collection	1.29 to 28.26 °	1.28 to 28.25 °
Index ranges	-17 ≤ h ≤ 20 , -14 ≤ k ≤ 13 , -17 ≤ l ≤ 18 ,	-21 ≤ h ≤ 16 , -13 ≤ k ≤ 14 , -18 ≤ l ≤ 18 ,
Reflections collected	14887	14894
Independent reflections	5630, [R(int) = 0.0296]	5633, [R(int) = 0.0282]
Refinement method	Full-matrix less-squares on F^2	Full-matrix less-squares on F^2
Data / restrains / parameters	5630 / 0 / 386	5633 / 0 / 382
Goodness-of-fit on F^2	0.904	0.944
Final R indices [I > 2σ (I)]	R1 = 0.0349, wR2 = 0.1054	R1 = 0.0336, wR2 = 0.1105
R indices (all data)	R1 = 0.0442, wR2 = 0.1155	R1 = 0.0428, wR2 = 0.1204
Largest diff. peak and hole / $e.Å^{-3}$	0.064 and -1.856	0.808 and -1.235

Table 8.2. Crystal data and details of structure refinement for *diag*- and *lat*-(η^5-C_5H_4tBu)$Re(CO)_2Br_2$

Complex	diag-(η^5-C_5H_4tBu)$Re(CO)_2Br_2$	lat-(η^5-C_5H_4tBu)$Re(CO)_2Br_2$
Identification code	OM 88	OM 87
Empirical formula	$C_{11}H_{13}Br_2O_2Re$	$C_{11}H_{13}Br_2O_2Re$
Formula weight	523.23	523.23
Temperature	296(2) K	296(2) K
Wavelength	0.71073 A	0.71073 A
Crystal system	Orthorhombic	monoclinic
Space group	Pbca	$P2_1/a$
Unit cell dimensions	a = 12.5359(6)Å, α = 90.0° b = 14.2599(7)Å, β = 90.0° c = 15.8258(8)Å, γ = 90.0°	a = 12.6873(8)Å, α = 90.0° b = 8.0422(5)Å, β = 95.4540(1)° c = 13.5376(8)Å, γ = 90.0°
Volume ($Å^3$)	2829.0(2)	1375.0(2)
Z	8	4
Density (calculated)	2.457 g/cm^3	2.527 g/cm^3
Absorption coefficient	14.224 nm^{-1}	14.632 nm^{-1}
F (000)	1920	960
Crystal size	1.1 × 0.3 × 0.1 mm	0.3 × 0.23 × 0.075 mm
θ range for data collection	2.52 to 28,29 °	1,51 to 28.14 °
Index ranges	$-16 \le h \le 11$, $-18 \le k \le 17$, $-19 \le l \le 20$,	$-16 \le h \le 15$, $-10 \le k \le 10$, $-12 \le l \le 17$,
Reflections collected	16047	8109
Independent reflections	3326, [R(int) = 0.1377]	3094, [R(int) = 0.1372]
Refinement method	Full-matrix less-squares on F^2	Full-matrix less-squares on F^2
Data / restrains / parameters	3326 / 0 / 148	3094 / 0 / 148
Goodness-of-fit on F^2	0.914	0.919
Final R indices [$I > 2\sigma(I)$]	R1 = 0.0680, wR2 = 0.1436	R1 = 0,0776, wR2 = 0.1743
R indices (all data)	R1 = 0.1017, wR2 = 0.1503	R1 = 0.1017, wR2 = 0.1785
Largest diff. peak and hole / e.$Å^{-3}$	3.180 and -5.745	3.584 and -4.681

opposite to that of the neighboring two layers (Figure 8.11). For the lateral isomer, the molecules are also layered. One polar and one non-polar interface alternately existed between two layers (Figure 8.12). It is difficult to compare the intermolecular interactions between diagonal and lateral isomers from these packing diagrams. But it is clear that the difference in intermolecular interaction between two isomers here is smaller than that between two isomers of the methyl analogues (Figure 4.6 and 4.7). This could be one reason why *lat*-(η^5-C_5H_4tBu)$Re(CO)_2Br_2$ did not isomerize in the solid-state, while the methyl analogue did. Further analysis on these structures such as molecular mechanism calculations is needed to get more information about this pair of complexes.

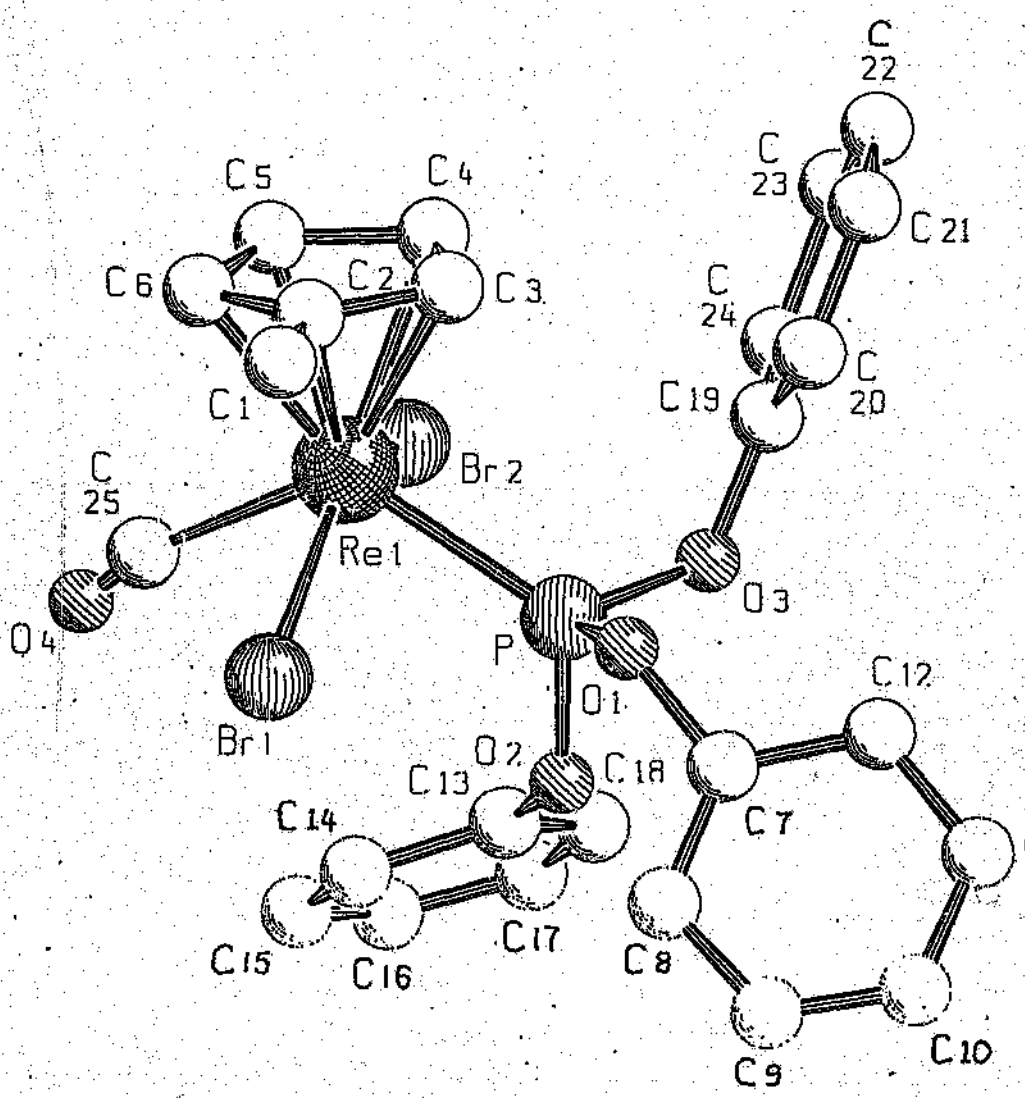

Figure 8.1. Perspective view (SCHAKAL plot) of *diag*-(η^5-C_5H_4Me)Re(CO)[$P(OPh)_3$]Br_2 showing the atom labeling (hydrogen atoms are omitted for clarity).

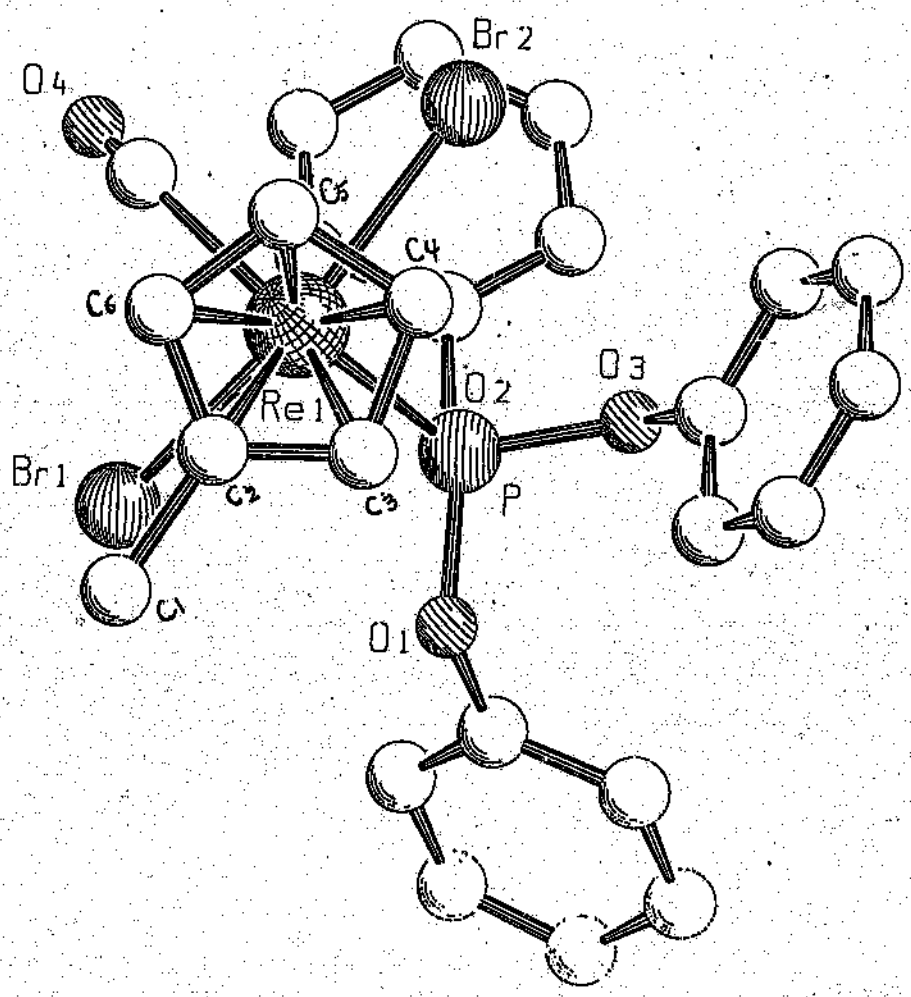

Figure 8.2. View of *diag*-(η^5-C_5H_4Me)Re(CO)[P(OPh)$_3$]Br$_2$ projected onto the plane of the Cp ring.

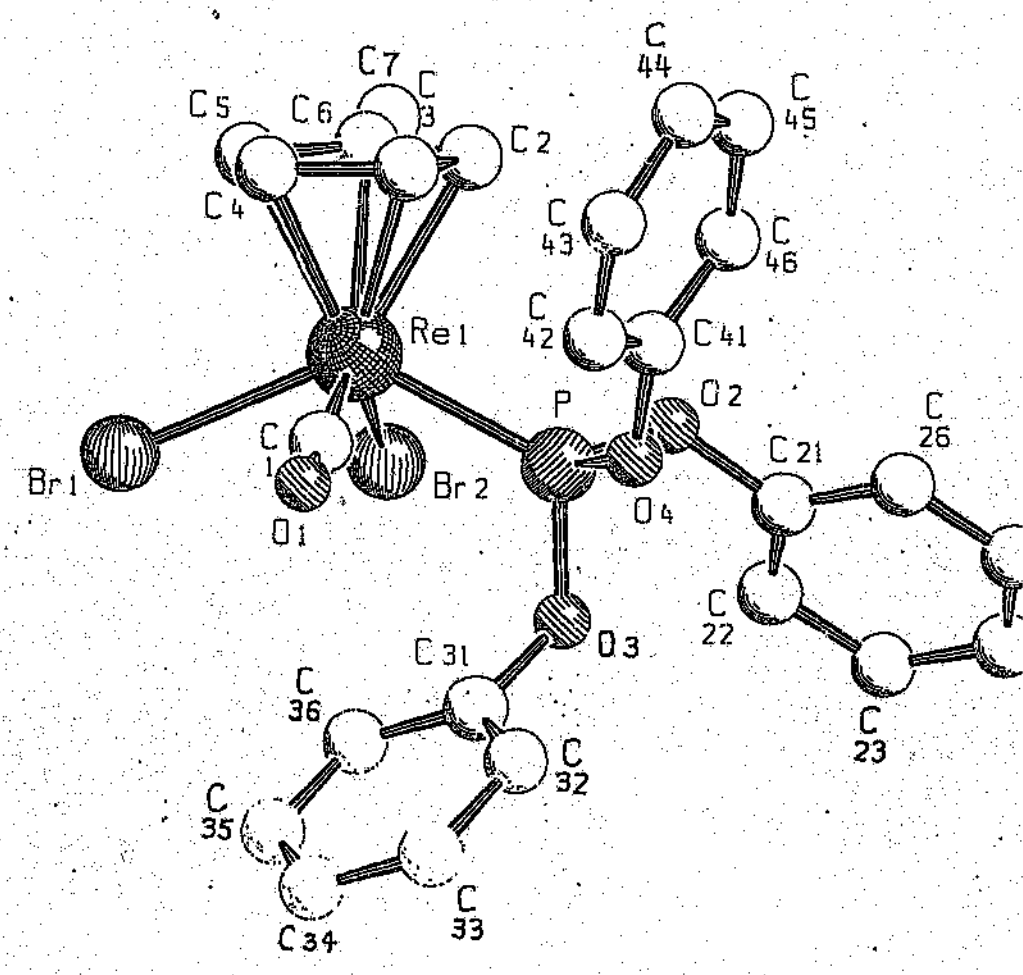

Figure 8.3. Perspective view (SCHAKAL plot) of *lat*-(η^5-C_5H_4Me)Re(CO)[P(OPh)$_3$]Br$_2$ showing the atom labeling (hydrogen atoms are omitted for clarity).

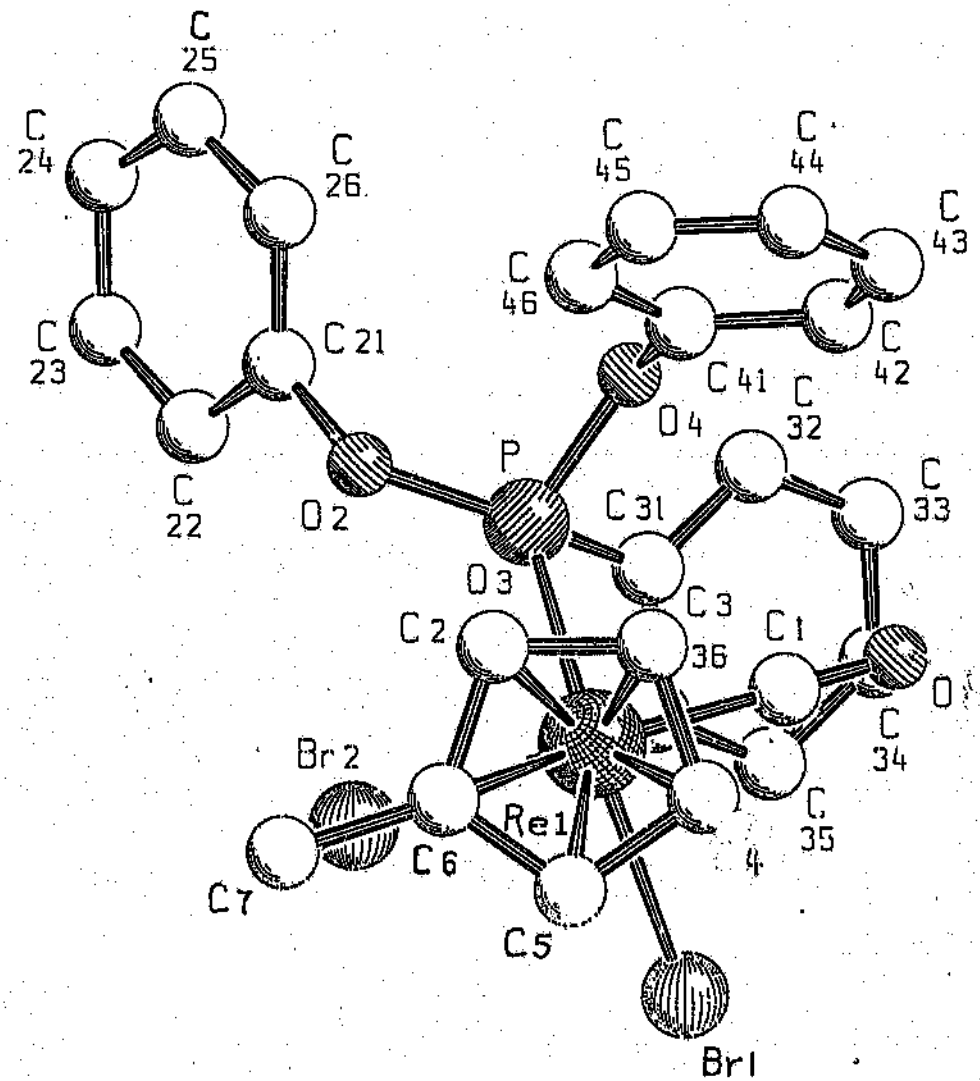

Figure 8.4. View of *lat*-(η^5-C_5H_4Me)Re(CO)[P(OPh)$_3$]Br$_2$ projected onto the plane of the Cp ring.

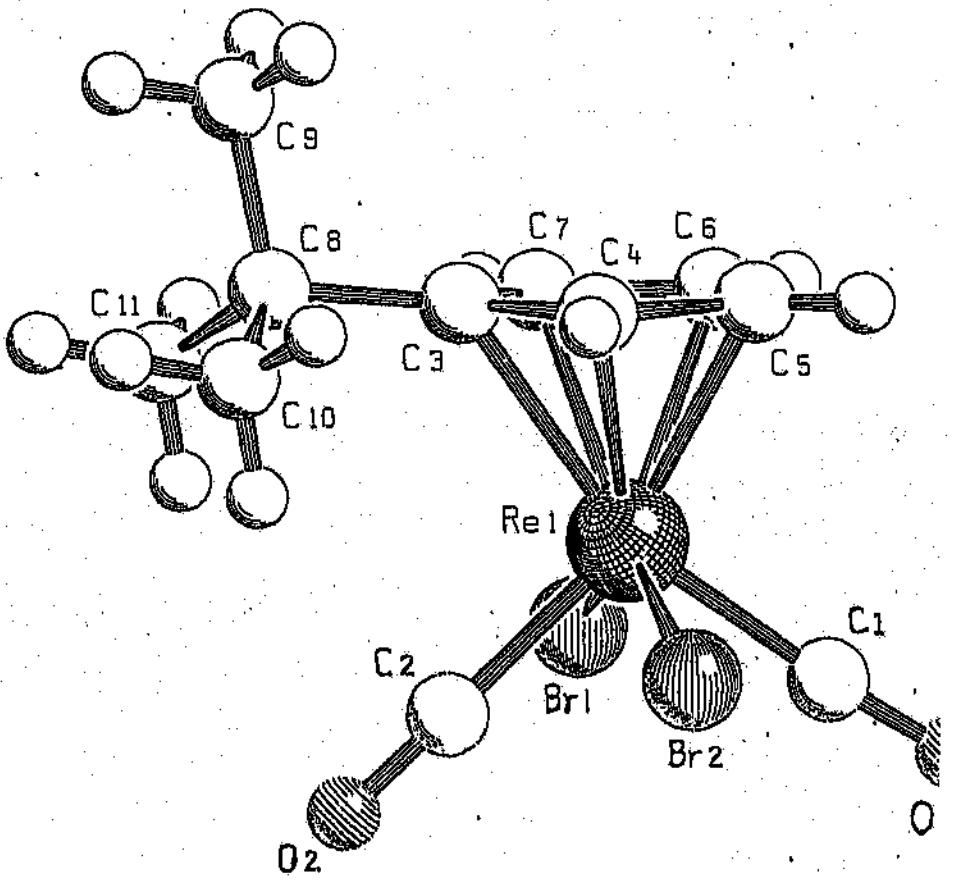

Figure 8.5. Perspective view (SCHAKAL plot) of *diag*-(η^5-C_5H_4tBu)$Re(CO)_2Br_2$ showing the atom labeling.

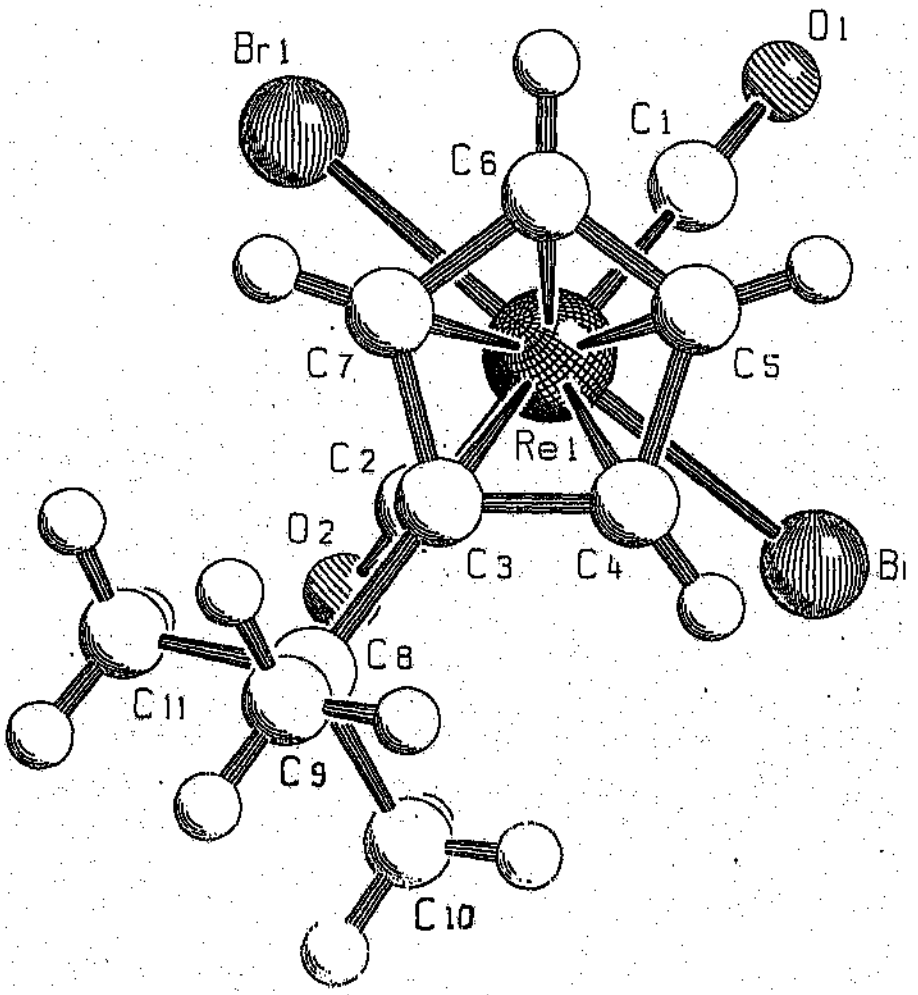

Figure 8.6. View of *diag*-(η^5-C_5H_4tBu)$Re(CO)_2Br_2$ projected onto the plane of the Cp ring.

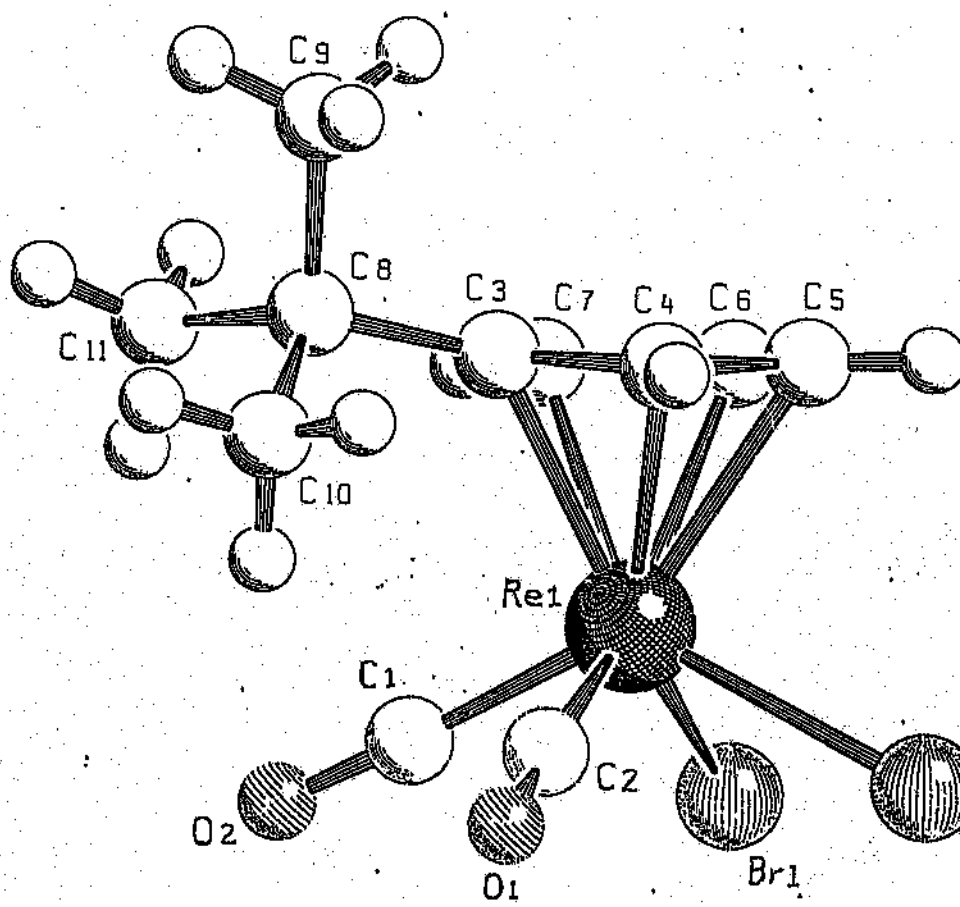

Figure 8.7. Perspective view (SCHAKAL plot) of *lat*-(η^5-C_5H_4tBu)Re(CO)$_2$Br$_2$ showing the atom labeling.

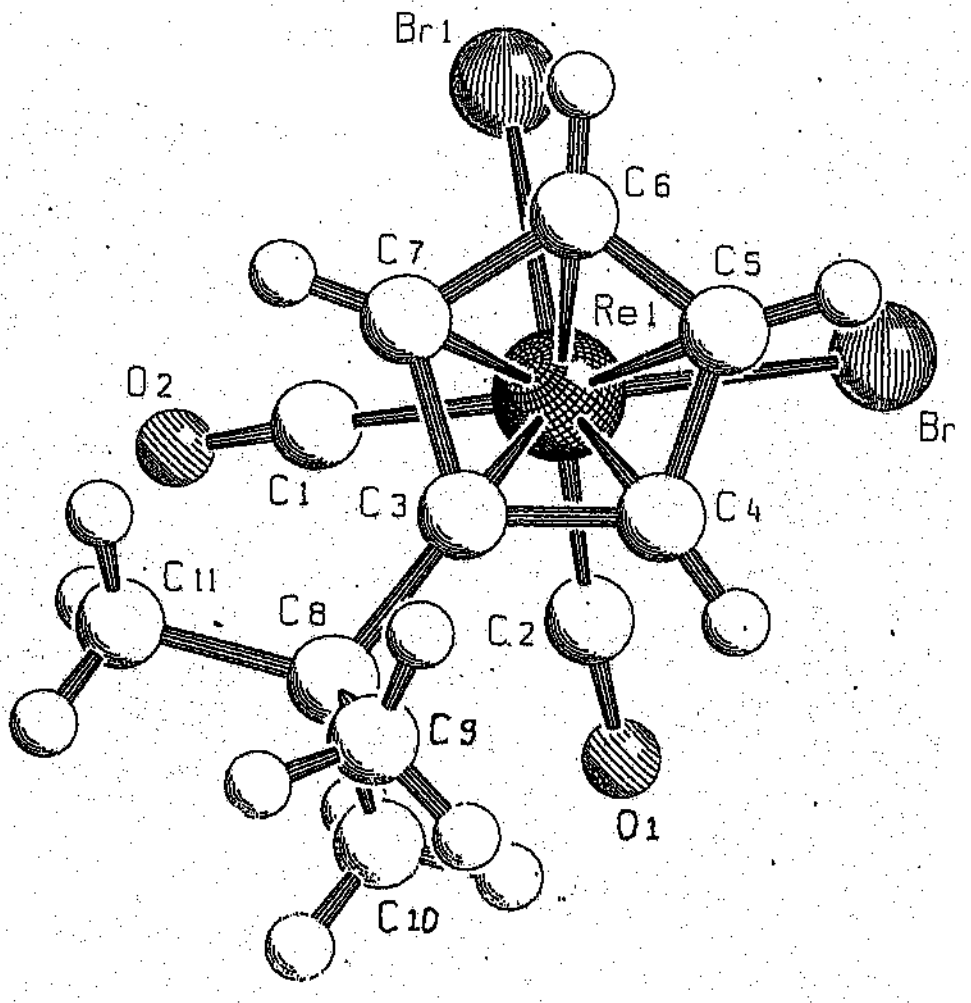

Figure 8.8. View of *lat*-(η^5-C_5H_4tBu)$Re(CO)_2Br_2$ projected onto the plane of the Cp ring.

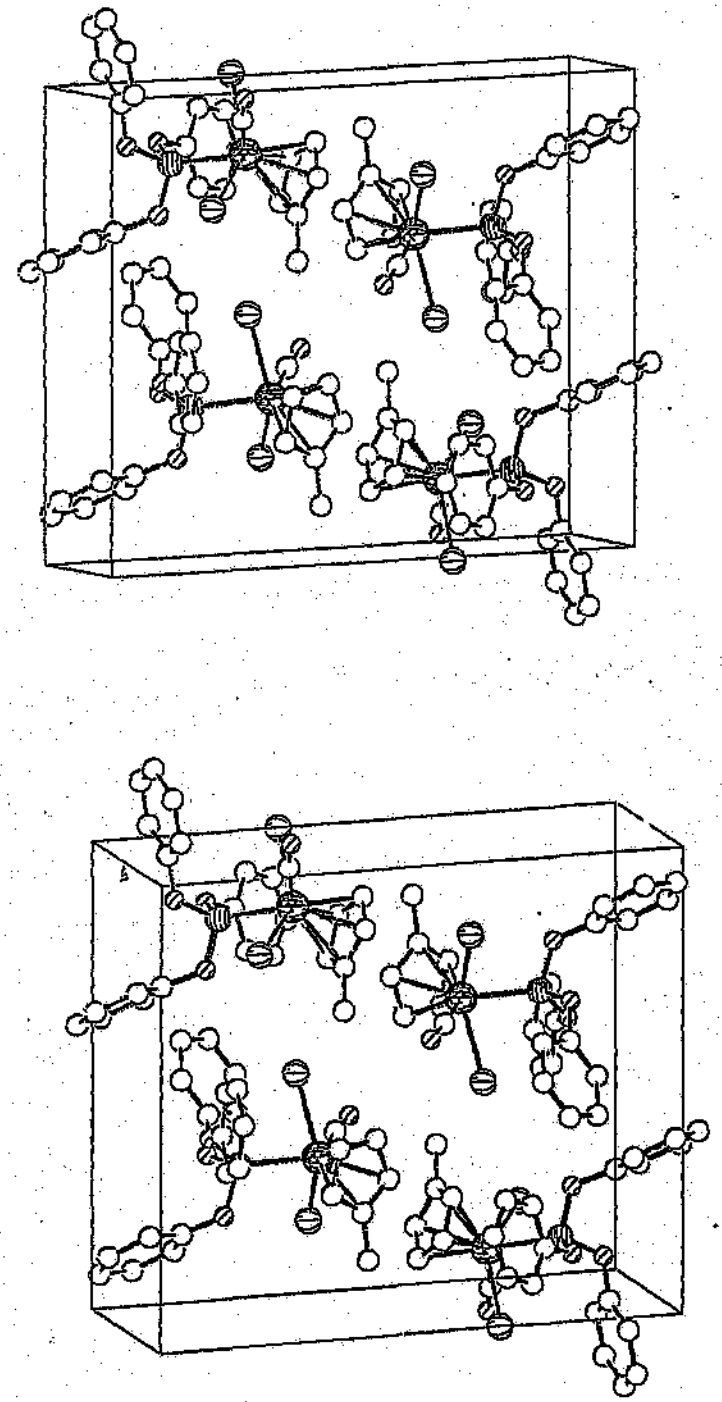

Figure 8.9. Packing diagram of *diag*-(η^5-C_5H_4Me)Re(CO)[P(OPh)$_3$]Br$_2$ projected on the [010] plane.

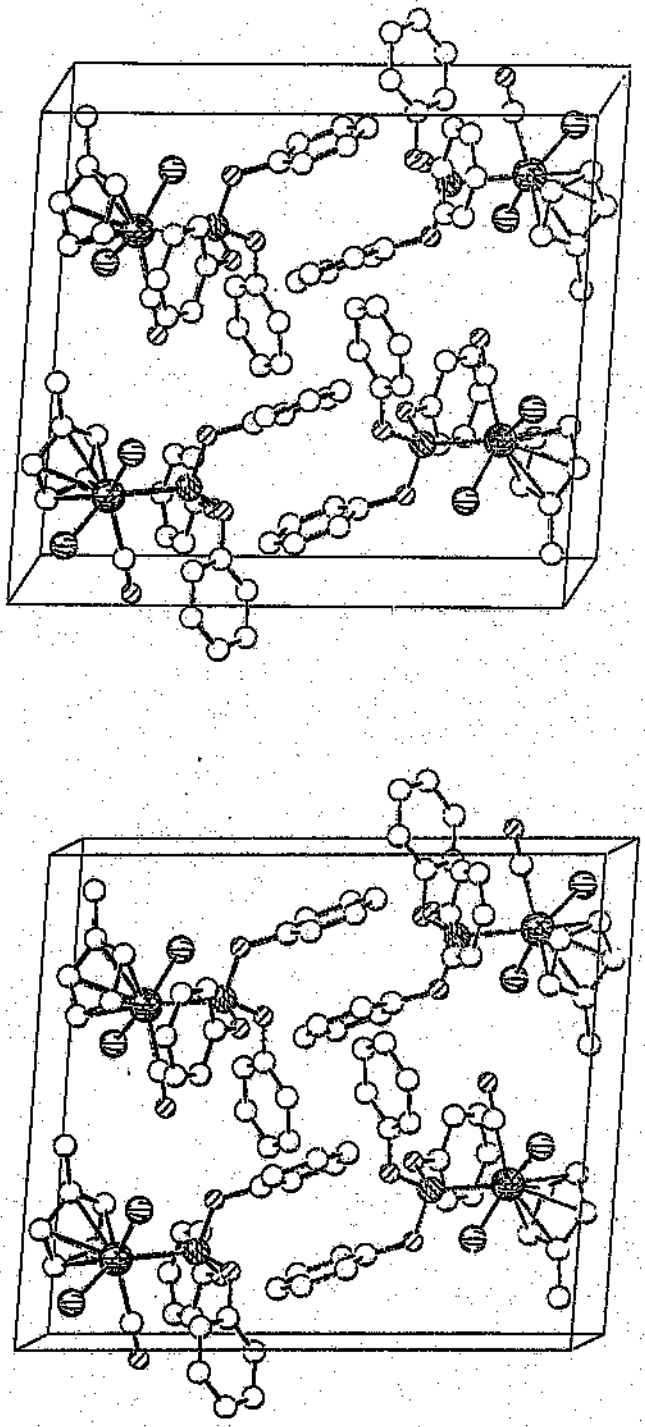

Figure 8.10. Packing diagram of *lat*-(η^5-C_5H_4Me)Re(CO)[P(OPh)$_3$]Br$_2$ projected on the [010] plane.

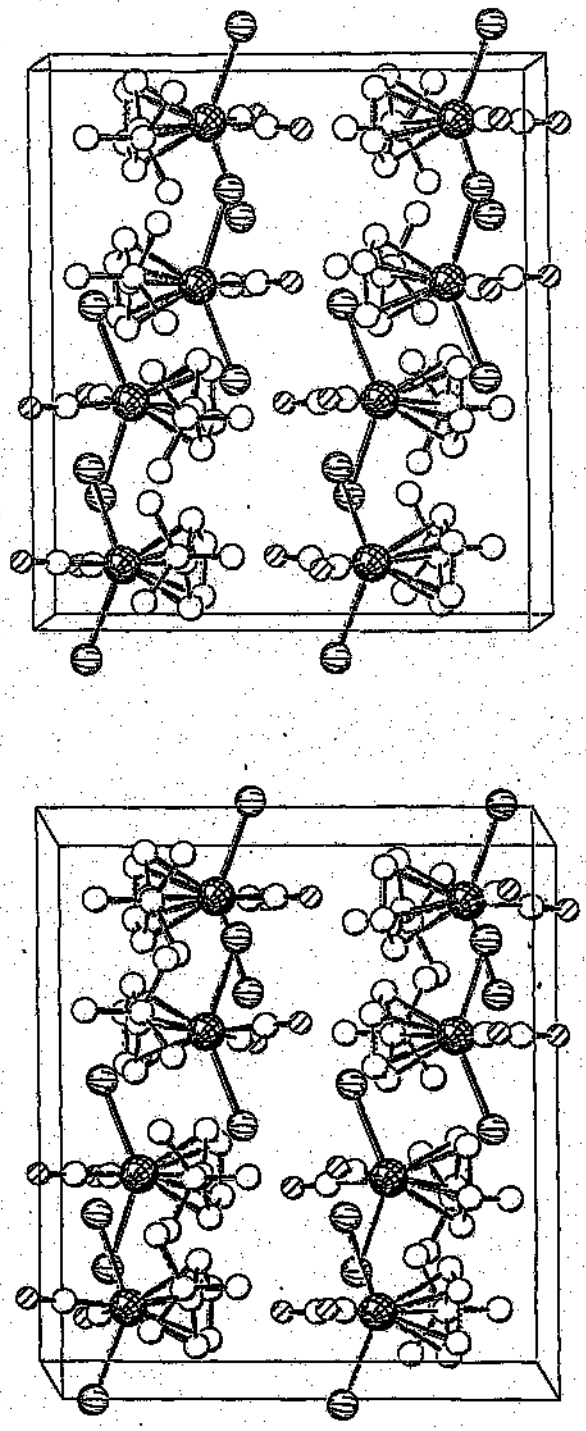

Figure 8.11. Packing diagram of *diag*-(η^5-C_5H_4tBu)$Re(CO)_2Br_2$ projected on the [001] plane.

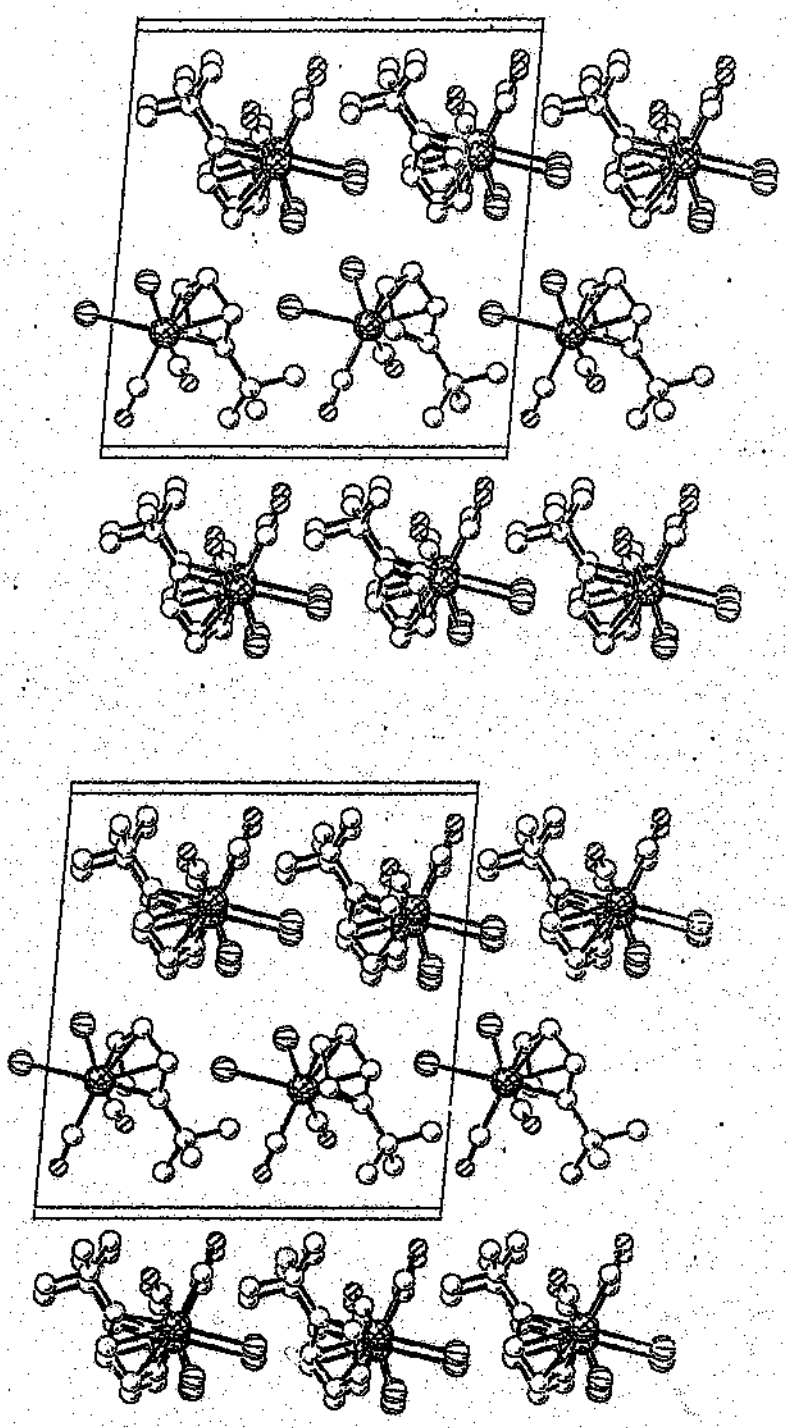

Figure 8.12. Packing diagram of *lat*-(η^5-C_5H_4tBu)$Re(CO)_2Br_2$ projected on the [010] plane.

8.4. References

1. King, R. B.; Reimann, R. H. *Inorg. Chem.*, **1976**, *15*, 179.

CHAPTER 9

STERIC EFFECT STUDIES ON (η^5-C_5H_4R)Re(CO)(L)Br_2 USING NMR PARAMETERS

9.1. Introduction

Nuclear magnetic resonance spectroscopy provides one measure of assessing the steric demands of ligands in organometallic chemistry.[1] Earlier studies on monosubstituted cyclpentadienyl three-legged half-sandwich complexes of the type (η^5-C_5H_4R)Fe(CO)(L)I (R = Me, tBu; L = phosphine, phosphite, isonitrile) have shown that $\Delta(H_2–H_5)$, the chemical shift separation of the cyclopentadienyl proton resonances on either side of the substituent R, not only varied proportionally with the size of the ligand L,[2,3] but was also influenced by the size of the substituent R on the ring. This relationship was studied in depth using a wide range of organometallic complexes in which L was kept constant and R was varied.[4] Studies on a series of complexes of the type (η^5-C_5H_4Me)Fe(CO)(PAr_3)I (Ar = Ph, p-C_6H_4Me, p-C_6H_4F) in which the ligands PAr_3 differed in the electronic effect, but not steric effect provided examples in which the variation in $\Delta(H_2–H_5)$ is relatively free of electronic influences.[5]

Investigation were extended to the four-legged piano stool molybdenum complexes *cis*-(η^5-C_5H_4R)$Mo(CO)_2(L)I$ (R = $SiMe_3$, tBu, Me, L = isonitrile, phosphine or phosphite). [6,7] A reasonable correlation was observed between $\Delta(H_2–H_5)$ and cone angles θ and solid angles Ω_s of the ligand L. It was also found that there is a better correlation between $\Delta(H_2–H_5)$ with Ω_s than θ.

Thus, it is of interest to extend these earlier studies to monosubstituted cyclopentadienyl rhenium complexes of the type (η^5-C_5H_4R)$Re(CO)(L)Br_2$ (R = Me, Et, ^{i}Pr, tBu, $SiMe_3$, L = CO, isonitrile, phosphite or phosphine).

9.2. Experimental Section

diag- and *lat*-(η^5-C_5H_4R)$Re(CO)(L)Br_2$ (R = H, Me, Et, ^{i}Pr, C_6H_{11}, tBu, $SiMe_3$; L = CO, isonitrile, $P(OR)_3$, PPh_3) were synthesized by the methods described in Chapter 3, 5 and 6. NMR spectra were recorded on a Bruker AC200 NMR spectrometer operating at 200 MHz. NOE spectra were recorded as described before.[8]

9.3. Results and Discussion

9.3.1. NOE Analysis

As expected, only two separated cyclopentadienyl proton absorption envelopes are seen in the NMR spectra of *diag*-(η^5-C_5H_4R)$Re(CO)(L)Br_2$, *diag*-(η^5-

$C_5H_4R)Re(CO)_2Br_2$ and *lat*-(η^5-$C_5H_4R)Re(CO)_2Br_2$. The complexes all have a mirror plane which passes through the molecule (Figure 9.1a – 9.1c). In the *lat*-(η^5-$C_5H_4R)Re(CO)(L)Br_2$ (Figure 9.1d), four distinct ring proton resonance sets are expected and were generally obtained.

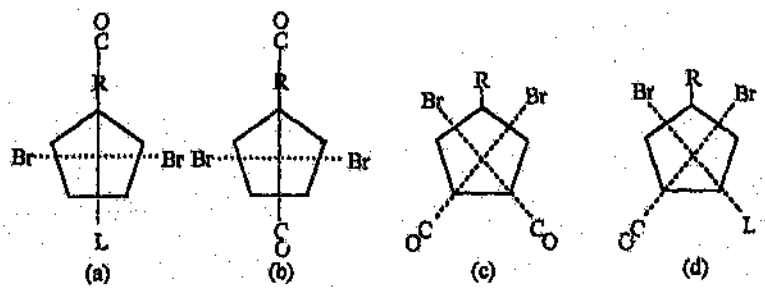

Figure 9.1. Newman projection of (a) *diag*-(η^5-$C_5H_4R)Re(CO)(L)Br_2$, (b) *diag*-(η^5-$C_5H_4R)Re(CO)_2Br_2$, (c) *lat*-(η^5-$C_5H_4R)Re(CO)_2Br_2$ and (d) *lat*-(η^5-$C_5H_4R)Re(CO)(L)Br_2$

To establish a correlation between the ring hydrogen atoms and the proton resonances, NOE experiments were carried out. Figure 9.2 shows the numbering scheme used in the analysis. Four typical complexes, *diag*-(η^5-$C_5H_4Me)Re(CO)[P(OMe)_3]Br_2$, *lat*-($\eta^5$-$C_5H_4Me)Re(CO)[P(OMe)_3]Br_2$, *lat*-($\eta^5$-$C_5H_4tBu)Re(CO)[P(OMe)_3]Br_2$ and *lat*-(η^5-$C_5H_4tBu)Re(CO)[P(OPh)_3]Br_2$ were chosen for the NOE analysis and the spectra are given in Figures 9.3–9.6.

For the *diag*-(η^5-$C_5H_4Me)Re(CO)[P(OMe)_3]Br_2$ complex, it is observed that

irradiation of the resonance at 1.80 ppm (ring methyl group) results in growth in the resonance at 4.71 ppm only (Figure 9.3d). Thus the resonance at 4.71 ppm can be assigned to the cyclopentadienyl ring proton 2 and 5. This is confirmed by irradiation of the resonance at 4.90 ppm which caused no growth of the resonance at 1.80 ppm. This allowed the assignment of the ring protons 3 and 4 to the resonance at 4.90 ppm.

For *lat*-(η^5-C_5H_4tBu)Re(CO)[P(OMe)$_3$]Br$_2$, irradiation of the resonance at 1.77 ppm (*tert*-butyl ring substituent) caused growth in resonances at 5.35 and 5.23 ppm, and hence permitted the assignment of the cyclopentadienyl ring protons 2 and 5 to these positions (Figure 9.5f). The assignment of position 2 was verified by irradiation of the resonance in position 4, which showed growth for position 5 and 3, but not 2 (Figure 9.5e). The relative positions of the cyclopentadienyl ring protons are 2, 5, 3, 4. It should be noted that the anticlockwise numbering in Figure 9.2 is arbitrary, so the relative positions could also be 5, 2, 4, 3. However, it does not affect the analysis on the chemical shift separation of proton 2 and 5.

The relative orders of the ring proton resonances for *lat*-(η^5-C_5H_4tBu)Re(CO)[P(OPh)$_3$]Br$_2$ and *lat*-(η^5-C_5H_4Me)Re(CO)[P(OMe)$_3$]Br$_2$ are 2, 5, 4, 3 and 2, 4, 5, 3, respectively, which were assigned by a similar NOE analysis (Figure 9.4 and 9.6).

9.3.2. Correlation of Cyclopentadienyl Ring Size with $\Delta(H_{2/5}-H_{3/4})$

of *diag*-(η^5-C_5H_4R)$Re(CO)_2Br_2$

^{1}H NMR data for *diag*- and *lat*-(η^5-C_5H_4R)$Re(CO)_2Br_2$ (R = H, Me, Et, iPr, tBu, $SiMe_3$) are given in Table 9.1. It was found that different solvents greatly influenced the chemical shift difference $\Delta(H_{2/5}–H_{3/4})$. For the *diag*-(η^5-C_5H_4R)$Re(CO)_2Br_2$ complexes, $\Delta(H_{2/5}–H_{3/4})$ was much smaller in C_6D_6 than in $CDCl_3$. Interestingly, only a small variation in the values for $\Delta(H_{2/5}–H_{3/4})$ were observed for the different ring-substituted lateral isomers (R = Me, tBu, $SiMe_3$) (Table 9.1), This indicates that the steric size of C_5H_4R was not a dominant factor to determining the proton NMR parameters under these conditions.

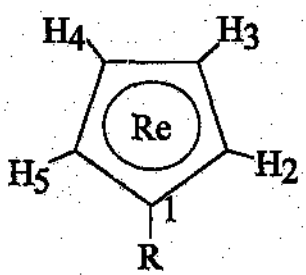

Figure 9.2. Labeling system used in NOE analysis.

A good correlation between $\Delta(H_{2/5}–H_{3/4})$ (not $\Delta(H_2–H_5)$) and the cone angles θ_2 (ring centroid as apex) of the substituted rings (Table 9.2) was observed for the *diag*-(η^5-C_5H_4R)$Re(CO)_2Br_2$ complexes in $CDCl_3$ (R^2 = 0.94, m.s.f. 0.0042, Figure 9.7). An attempt was also made to correlate the data with solid angles Ω_{av}

(Table 9.2). Here a poorer relationship between $\Delta(H_{2/5}–H_{3/4})$ and Ω_{av} (R^2 = 0.79, m.s.f. 0.015) was observed. The point corresponding to $C_5H_4SiMe_3$ is outside the regression line (Figure 9.8). Deleting this point gives a better correlation between $\Delta(H_{2/5}–H_{3/4})$ and Ω_{av} (R^2 = 0.94, m.s.f. 0.0026). The data suggest that $SiMe_3$ in $C_5H_4SiMe_3$ should have a bigger size than the tBu group in C_5H_4tBu.

9.3.3. Attempted Correlation between $\Delta(H_2–H_5)$ or $\Delta(H_2–H_3)$ and Steric Sizes of Ligand L of $(\eta^5\text{-}C_5H_4R)Re(CO)(L)Br_2$

Table 9.3 and 9.4 give the ^1H NMR data of the diagonal and lateral complexes of $(\eta^5\text{-}C_5H_4R)Re(CO)(L)Br_2$ (R = Me, tBu, $SiMe_3$; L = $CNC_6H_3Me_2$, $P(OMe)_3$, $P(O^iPr)_3$, $P(OPh)_3$, PPh_3), respectively. As for the dicarbonyl dibromide complexes, the chemical shift differences were greatly affected by the NMR solvent. C_6D_6 induced a bigger proton separation than $CDCl_3$ for the monocarbonyl substituted complexes. For example, only one ring proton adsorption envelope was generally observed for both *diag*- and *lat*-$(\eta^5\text{-}C_5H_4Me)Re(CO)[P(OPh)_3]Br_2$ complexes in $CDCl_3$.

Attempts were made to correlate the NMR parameters with the steric/electronic effects associated with L. All NMR parameters $\Delta(H_2–H_5)$ or $\Delta(H_2–H_3)$ correlated poorly with cone angles θ or solid angles Ω_s (Table 9.5) of the ligand L for both diagonal and lateral isomers of $(\eta^5\text{-}C_5H_4R)Re(CO)(L)Br_2$. This could be attributed

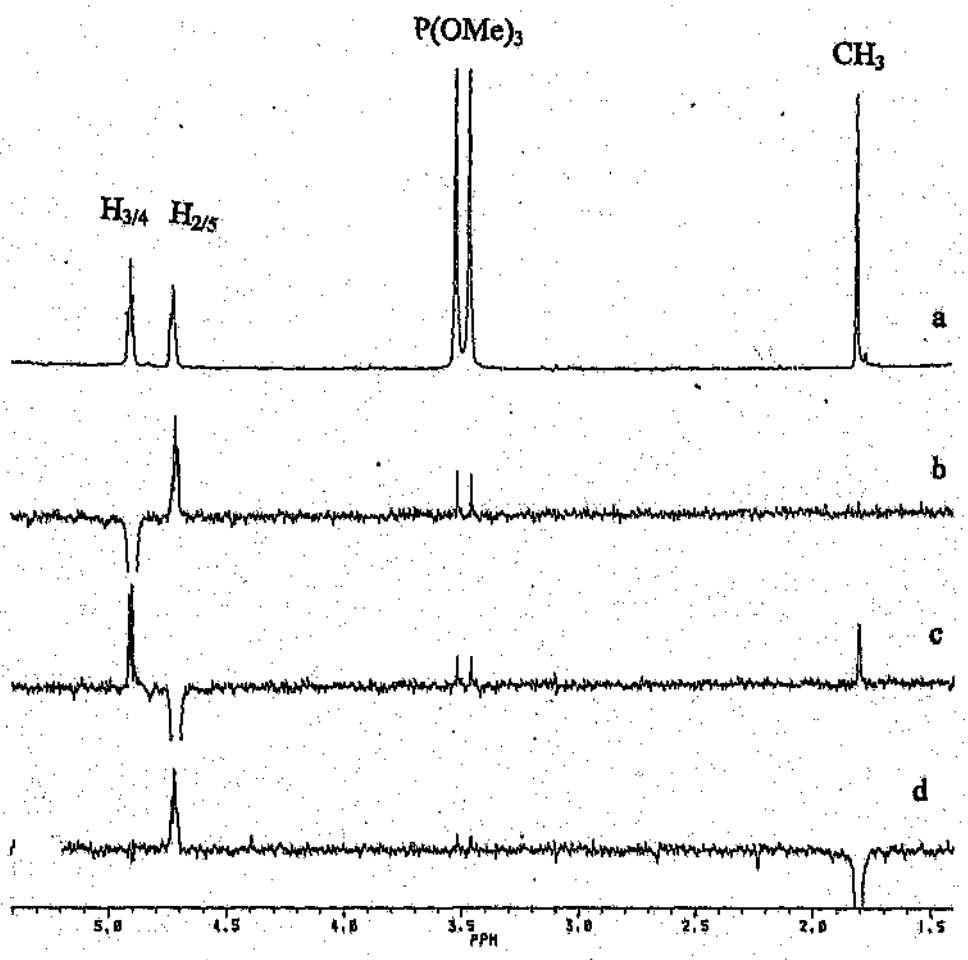

Figure 9.3. Selected NOE data for *diag*-(η^5-C_5H_4Me)Re(CO)[P(OMe)$_3$]Br$_2$. (a) No irradiation, (b) irradiation of $H_{3/4}$, (c) irradiation of $H_{2/5}$, (d) irradiation of CH_3 protons of the Cp ring.

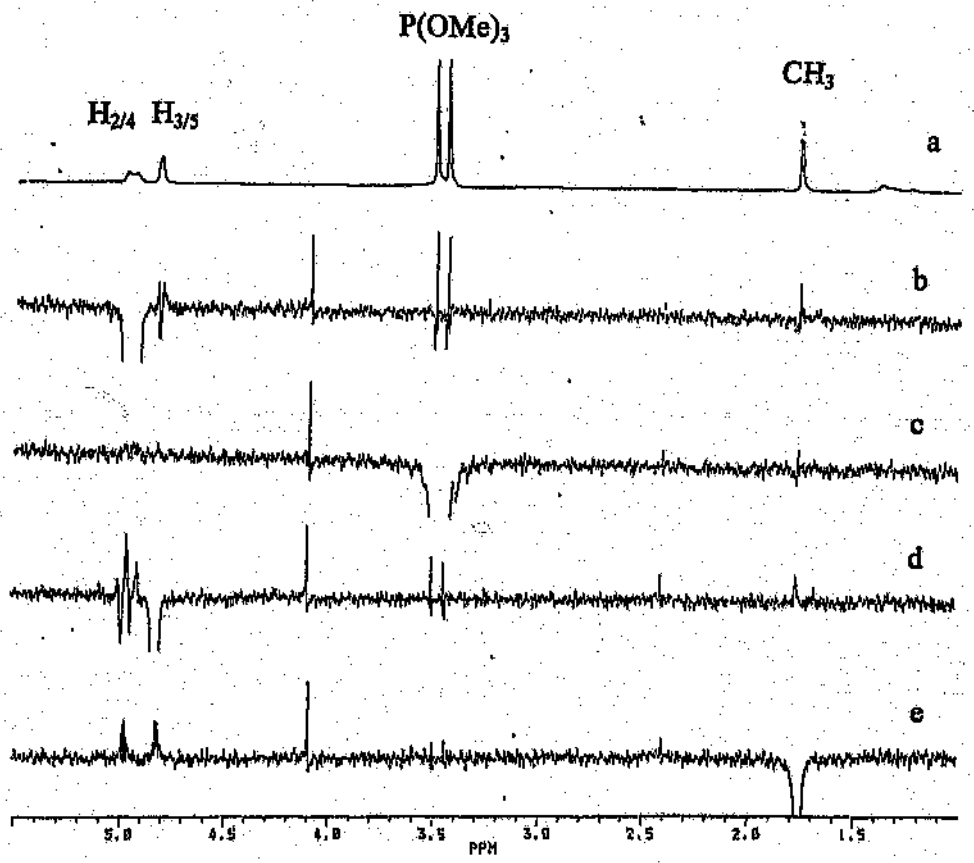

Figure 9.4. Selected NOE data for *lat*-(η^5-C_5H_4Me)Re(CO)[$P(OMe)_3$]Br_2. (a) No irradiation, (b) irradiation of $H_{2/4}$, (c) irradiation of methyl protons of $P(OMe)_3$, (d) irradiation of $H_{3/5}$, (e) irradiation of CH_3 protons of the Cp ring.

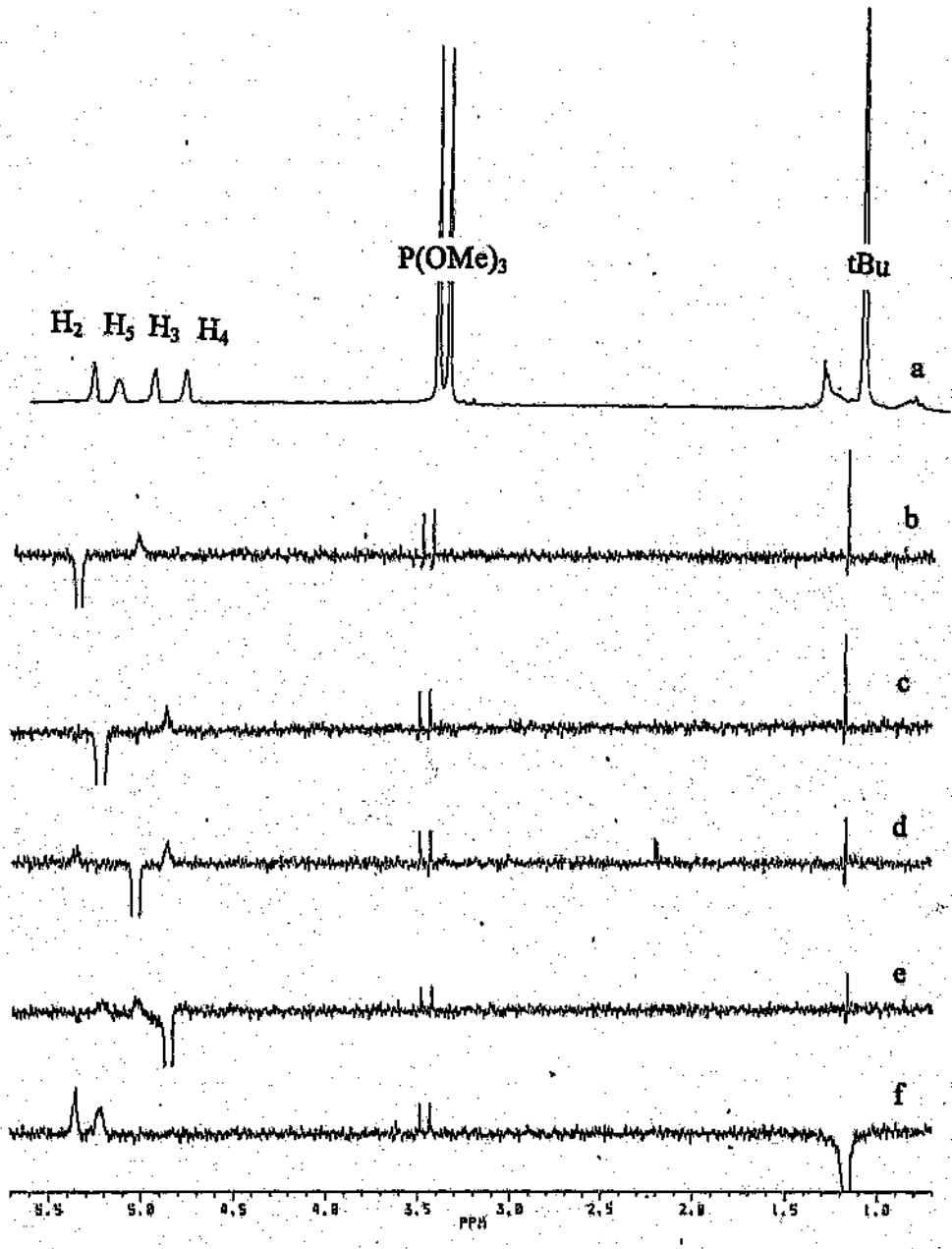

Figure 9.5. Selected NOE data for *lat*-(η^5-C_5H_4tBu)Re(CO)[P(OMe)$_3$]Br$_2$. (a) No irradiation, (b) irradiation of H_2, (c) irradiation of H_5, (d) irradiation of H_3, (e) irradiation of H_4, (f) irradiation of tBu protons.

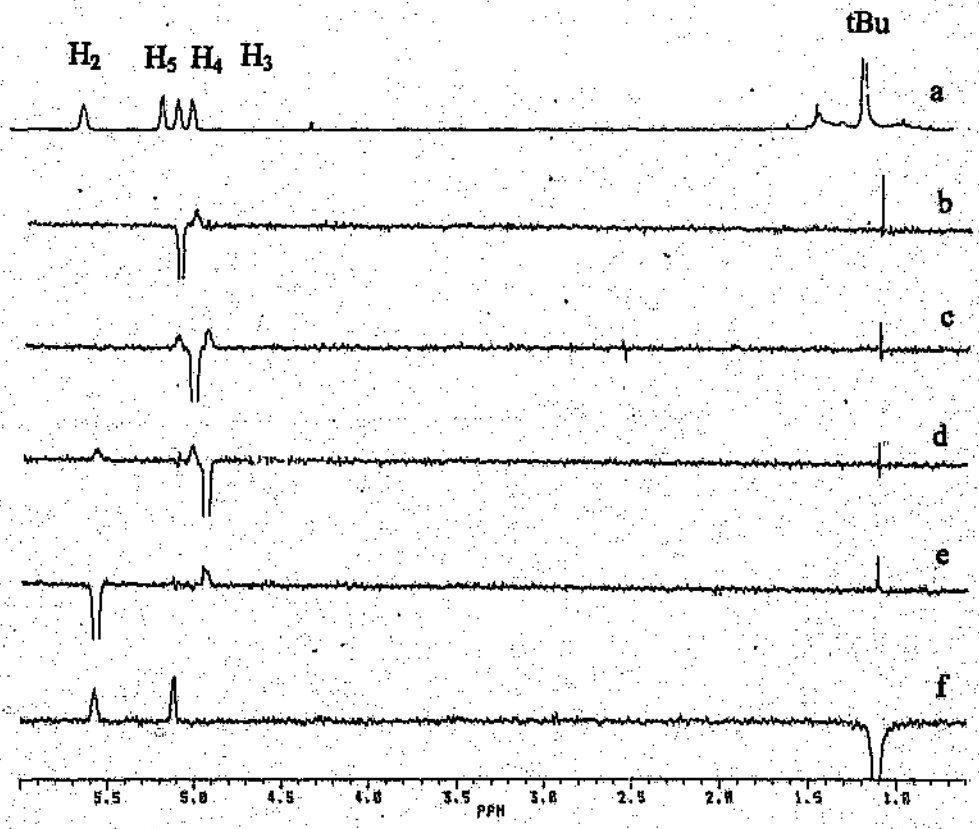

Figure 9.6. Selected NOE data for *lat*-(η^5-C_5H_4tBu)Re(CO)[$P(OPh)_3$]Br_2. (a) No irradiation, (b) irradiation of H_5, (c) irradiation of H_4, (d) irradiation of H_3, (e) irradiation of H_2, (f) irradiation of tBu protons.

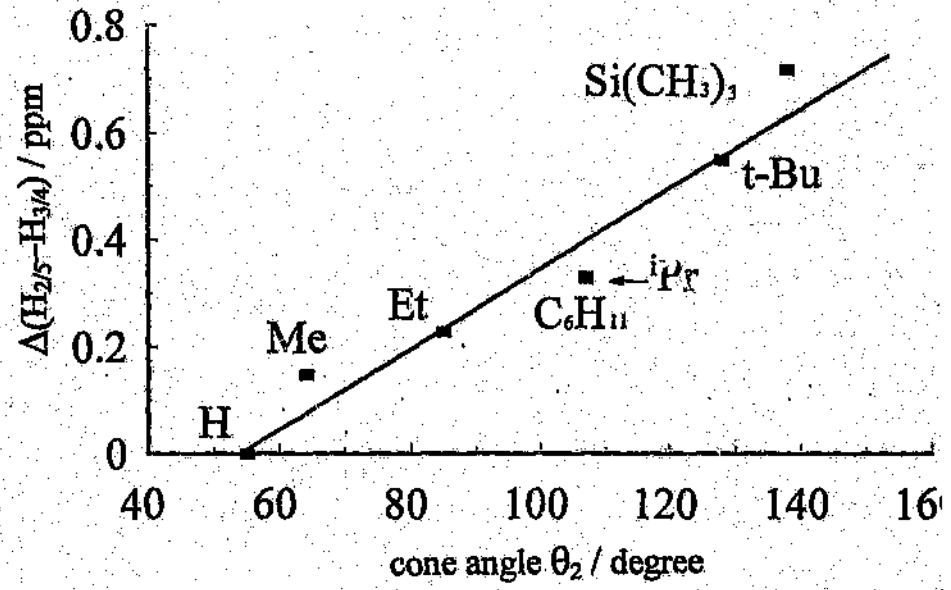

Figure 9.7. Plot of $\Delta(H_{2/5}–H_{3/4})$ versus θ_2 for *diag*-(η^5-C_5H_4R)$Re(CO)_2Br_2$ complexes.

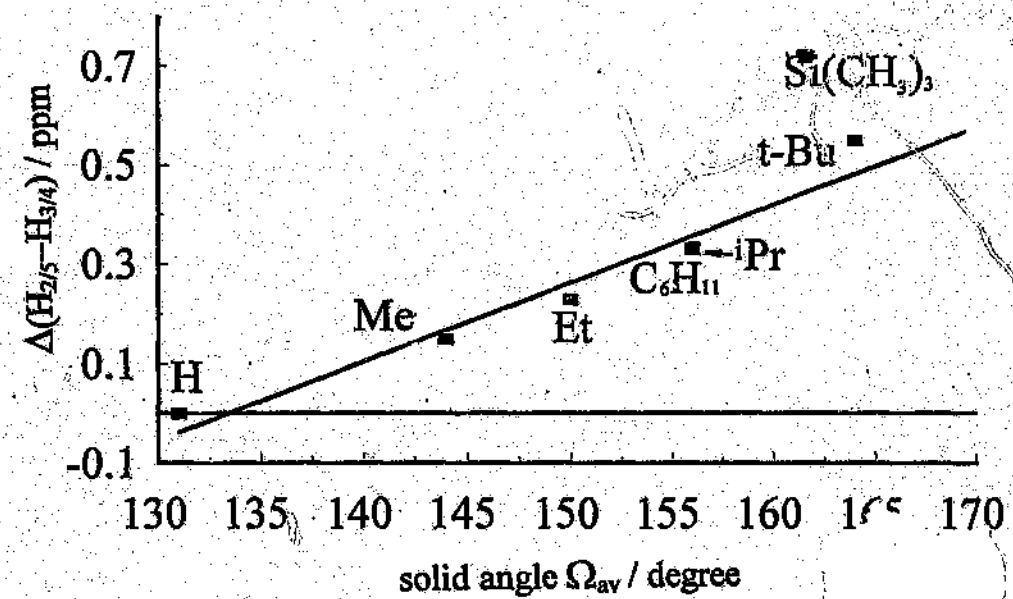

Figure 9.8. Plot of $\Delta(H_{2/5}–H_{3/4})$ against Ω_{av} for ... g-(η^5-C_5H_4R)$Re(CO)_2Br_2$ complexes.

Table 9.1. ^{1}H NMR Data for (η^5-C_5H_4R)Re(CO)$_2$Br$_2$[a]

isomer	R	$H_{2/5}$	$H_{3/4}$	$\Delta(H_{2/5}-H_{3/4})$
diag	H	5.76	5.76	0.00
diag	Me	5.50	5.65	0.15
		(4.40)	(4.54)	(0.14)[b]
diag	Et	5.46	5.68	0.22
diag	^{i}Pr	5.38	5.71	0.33
diag	C_6H_{11}	5.38	5.70	0.32
diag	tBu	5.21	5.76	0.55
		(4.53)	(4.70)	(0.17)[b]
diag	$SiMe_3$	5.23	5.94	0.71
		(4.60)	(4.90)	(0.30)[b]
lat	H	6.16	6.16	0.00
lat	Me	5.80	5.91	0.11
		(4.29)	(4.49)	(0.20)[b]
lat	Et	5.84	5.91	0.07
lat	^{i}Pr	5.88	5.92	0.04
lat	C_6H_{11}	5.87	5.89	0.02
lat	tBu	5.96	6.11	0.15
		(4.76)	(4.98)	(0.22)[b]
lat	$SiMe_3$	5.96	6.28	0.32
		(4.87)	(5.08)	(0.21)[b]

[a] ppm, recorded in $CDCl_3$, relative to TMS. [b] The data in parentheses were recorded in C_6D_6.

Table 9.2. Cone Angles θ_2 and Solid Angles Ω_{av} for C_5H_4R[a]

R	θ_2	Ω_{av}
H	55	131
Me	64	144
Et	85	150
^{i}Pr	107	156
C_6H_{11}	107	156
TBu	128	164
$SiMe_3$	138	161

[a]Ref. 9.

Table 9.3. ^{1}H NMR Data for *diag*-(η^5-C_5H_4R)Re(CO)(L)Br[a]

R	L	$H_{2/5}$	$H_{3/4}$	$\Delta(H_{2/5}-H_{3/4})$
Me	$CNC_6H_3Me_2$	4.72	4.90	0.18
		(5.66)	(5.76)	(0.10)[b]
Me	$P(OMe)_3$	4.71	4.90	0.19
Me	$P(O^iPr)_3$	4.73	4.93	0.20
Me	$P(OPh)_3$	4.53	4.65	0.12
		(4.99)	(5.02)	(0.02)[b]
Me	PPh_3	4.75	5.00	0.25
tBu	$CNC_6H_3Me_2$	4.84	5.10	0.26
tBu	$P(OMe)_3$	4.56	5.28	0.72
tBu	$P(O^iPr)_3$	4.62	5.35	0.73
tBu	$P(OPh)_3$	4.44	4.92	0.48
tBu	PPh_3	4.75	5.31	0.56
$SiMe_3$	$CNC_6H_3Me_2$	4.83	5.21	0.38
$SiMe_3$	$P(OMe)_3$	4.67	5.38	0.71
$SiMe_3$	$P(O^iPr)_3$	4.70	5.47	0.77
$SiMe_3$	$P(OPh)_3$	4.51	5.08	0.57
$SiMe_3$	PPh_3	4.90	5.44	0.54

[a] ppm, recorded in C_6D_6, relative to TMS. [b] The data in parentheses were recorded in $CDCl_3$.

Table 9.4. ^{1}H NMR Data for *lat*-(η^5-C_5H_4R)Re(CO)(L)Br_2[a]

R	L	H_2	H_3	H_4	H_5
Me	$CNC_6H_3Me_2$	4.86	4.72	4.78	4.78
		(5.66)	(5.75)	(5.75)	(5.66)
Me	$P(OMe)_3$	4.95	4.82	4.94	4.82
Me	$P(O^iPr)_3$	4.97	4.97	4.97	4.97
Me	$P(OPh)_3$	5.07	4.62	4.72	4.77
		(5.31)	(5.31)	(5.31)	(5.31)
Me	PPh_3	4.99	4.51	4.71	4.92
tBu	$CNC_6H_3Me_2$	5.15	4.98	5.11	4.98
tBu	$P(OMe)_3$	5.35	5.03	4.86	5.23
tBu	$P(O^iPr)_3$	5.49	5.10	5.16	5.25
tBu	$P(OPh)_3$	5.57	4.94	5.03	5.11
tBu	PPh_3	5.52	5.07	5.21	5.26
$SiMe_3$	$CNC_6H_3Me_2$	5.26	5.07	5.21	5.07
$SiMe_3$	$P(OMe)_3$	5.40	5.07	5.17	5.32
$SiMe_3$	$P(O^iPr)_3$	5.61	5.25	5.31	5.35
$SiMe_3$	$P(OPh)_3$	5.64	4.97	5.13	5.21
$SiMe_3$	PPh_3	5.67	4.86	4.86	5.07

[a] ppm, recorded in C_6D_6 relative to TMS. [b] The data in parentheses were recorded in $CDCl_3$.

Table 9.5. Cone Angles θ and Solid Angles Ω_s for Ligand L[a]

L	θ	Ω_s
CO	95	-----
$CNC_6H_3Me_2$	106	0.0892
$P(OMe)_3$	107	0.225
$P(O^iPr)_3$	130	0.319
$P(OPh)_3$	128	0.307
PPh_3	145	0.286

[a] Ref. 9.

to the dominance of electronic effects associated with ligand L on these parameters.

9.4. Conclusions

The cyclopentadienyl ring proton resonances of *diag*- and *lat*-(η^5-C_5H_4R)Re(CO)(L)Br_2 have been assigned by NOE analysis. A good correlation between the cone angles θ_2 or solid angles Ω_{av} of monosubstituted cyclopentadienyl ring and $\Delta(H_{2/5}-H_{3/4})$ (ortho and meta ring proton resonances) of the *diag*-(η^5-C_5H_4R)Re(CO)$_2Br_2$ complexes was observed ($CDCl_3$). However, no correlation was found for the corresponding lateral isomers under the same conditions. The $\Delta(H_2-H_5)$ or $\Delta(H_2-H_3)$ of *lat*-(η^5-C_5H_4R)Re(CO)(L)Br_2 (L ≠ CO) did not correlate with either cone angles θ or solid angles Ω_s of ligand L. No matter what size of the ligand L is, the resonance positions of H_2 and H_5 are coincident for all *diag*-(η^5-C_5H_4R)Re(CO)(L)Br_2 complexes. These results indicated that the electronic effects may be an important influence on the NMR parameters measured.

9.6. References

1. Coville, N. J.; du Plooy, K. E.; Pickl, W. *Coord. Chem. Rev.* **1992**, *116*, 1.
2. Johnston, P.; Loonat, M. S.; Ingham, W. L.; Carlton, L.; Coville, N. J. *Organometallics* **1987**, *6*, 2121.
3. du Plooy, K. E.; Marais, C. F.; Carlton, L.; Hunter, R.; Boeyens, J. C. A.; Coville, N. J. *Inorg. Chem.* **1989**, *28*, 3855.
4. Coville, N. J.; Loonat, M. S.; White, D.; Carlton, L. *Organometallics* **1992**, *11*, 1082.
5. White, D.; Johnston, P.; Levendis, I. A.; Michael, J. P.; Coville, N. J. *Inorg. Chem.* **1994**, *215*, 139.
6. Smith, J. M.; White, D. P.; Coville, N. J. *Bull. Chem. Soc. Ethiop.* **1996**, *10*, 1.
7. Coville, N. J.; Loonat, M. S.; Carlton, L. *S. Afr. J. Chem.* **1992**, *45*, 63.
8. White, D.; Carlton, L.; Coville, N. J. *J. Organomet. Chem.* **1992**, *440*, 15.
9. White, D.; Coville, N. J. *Adv. Organomet. Chem.* **1994**, *36*, 95.

CHAPTER 10

SOLID-STATE ISOMERIZATION REACTIONS OF $(\eta^5\text{-}C_5H_4R)M(CO)_2(L)I$ (M = W, Mo)

10.1. Introduction

Cyclopentadienyl tungsten and molybdenum carbonyl halide complexes, $CpM(CO)_2(L)X$, have been extensively investigated since their first preparation (L = CO) in the early 1950's.[1] Since then modification of complexes of this type has been achieved by replacing the ring protons with other substituents or modifying the ligand set (CO, L, X), and this has resulted in the synthesis of many hundreds of complexes of this type.[2,3] Extensive studies of these complexes have included thermal,[4-8] photochemical[9,10] and induced[11-13] substitution reactions (of CO, L, X), matrix isolation studies,[14] isomerization studies[10,15,16] etc. A significant breakthrough in this area of chemistry was the physical separation of the pure diagonal and lateral isomers of $(\eta^5\text{-}C_5H_5)M(CO)_2(PPh_3)I$ (M = Mo, W) in 1975.[17]

In Chapter 3, 5 and 6, We have reported the synthesis of a series of related rhenium piano stool complexes, $(\eta^5\text{-}C_5H_4R)Re(CO)(L)X_2$ (R = Me, Et, ^{i}Pr, tBu, $SiMe_3$; L = $CNC_6H_3Me_2$, $P(OR)_3$, PPh_3; X = Br, I). Of particular importance was the finding that these complexes underwent isomerization reactions *in the solid state*. Other than a short comment on the solid-state isomerization reaction of $(\eta^5\text{-}C_5H_5)Mo(CO)_2(PBu_3)I$,

no other solid-state isomerization reactions of these four-legged piano stool tungsten and molybdenum complexes have been reported in the literature.[15] Here we report results of the thermal solid state isomerization reactions of monosubstituted cyclopentadienyl tungsten and molybdenum complexes, $(\eta^5\text{-}C_5H_4R)M(CO)_2(L)I$, to further explore the generality of the reaction.

10.2. Experimental Section

$(\eta^5\text{-}C_5H_4Me)W(CO)_3I$,[18] $(\eta^5\text{-}C_5H_4Me)Mo(CO)_3I$[18] and $(\eta^5\text{-}C_5H_4tBu)W(CO)_3I$[19] were prepared by the standard procedures used to synthesize other ring-substituted analogues. Trimethylamine N-oxide dihydrate (Aldrich) was used as received. All reactions were carried out using standard Schlenk techniq[illegible]er nitrogen. Solvents were dried by conventional methods, distilled under nitrogen, and used immediately. Melting points were recorded on a Kofler hot stage melting point apparatus. Infrared spectra were measured on a Midac FTIR spectrometer, usually in KBr cells (solutions). NMR spectra were measured on a Bruker AC200 spectrometer operating at 200 MHz. Microanalysis were carried out at the CSIR, Pretoria, South Africa.

10.2.1. Preparation of *diag*- and *lat*-$(\eta^5\text{-}C_5H_4R)M(CO)_2(L)I$ (M = W, R = Me, tBu, L = $P(O^iPr)_3$, PPh_3; M = Mo, R = Me, L = PPh_3).

The complexes were prepared (55 % to 75 % total yield) by adopting the method developed by Blumer *et al*[11] for the synthesis of the related unsubstituted compounds. Isomer separation was achieved by dissolving the crude material in CH_2Cl_2 followed by

chromatography on a silica gel column (2 × 60 cm) with 1:1 CH_2Cl_2/hexane. The spectroscopic and analytical data of the complexes are given in Table 10.1.

10.2.2. Solid-State Isomerization of *diag*- and *lat*-(η^5-C_5H_4R)M(CO)$_2$(L)I.

5-10 mg of solid *diag*- or *lat*-(η^5-C_5H_4R)M(CO)$_2$(L)I (M = W, R = Me, tBu, L = P(O^{i}Pr)$_3$, PPh_3; M = Mo, R = Me, L = PPh_3) were sealed in a capillary tube under nitrogen and heated (totally immersed) in an oil bath for 1-15 h at a temperature at least 15 °C below the lower melting point of the two isomers. The color and shape of the starting materials showed no visible change, and no decomposition during the heating process. The identification of the diagonal and lateral products was achieved by means of TLC, IR and NMR spectroscopy. The melting points of both isomers, percentage of both isomers in the product, reaction conditions and isomerization direction are given in Table 10.2.

10.3. Results and Discussion

10.3.1. Preparation of *diag*- and *lat*-(η^5-C_5H_4R)M(CO)$_2$(L)I.

diag- and *lat*-(η^5-C_5H_4R)M(CO)$_2$(L)I (M = W, R = Me, tBu, L = P(O^{i}Pr)$_3$, PPh_3; M = Mo, R = Me, L = PPh_3) were prepared in good yield (60-70 %) by reaction of (η^5-C_5H_4R)M(CO)$_3$I with a 5-10 fold excess of ligand L and trimethylamine N-oxide in dichloromethane at room temperature. [11-13] The reaction proceeded slowly to completion if only a stoichiometric amount of ligand or trimethylamine N-oxide was

used. The separation of the diagonal and lateral isomers was achieved by silica gel column chromatography. It was found that the isomers of the triphenylphosphine complexes were more difficult to separate than the isomers of the triisopropyl phosphite compounds. All complexes were stable at room temperature in the solid state and had good solubility in organic solvents, including hexane.

The assignments of diagonal and lateral isomers of $(\eta^5\text{-}C_5H_4R)M(CO)_2(L)I$ were based on well-established infrared and proton NMR criteria.[15,16,20] The data are given in Table 10.1.

10.3.2. Solution State Isomerization of *diag*- and *lat*-$(\eta^5\text{-}C_5H_4R)M(CO)_2(L)I$

All *diag*- and *lat*-$(\eta^5\text{-}C_5H_4R)M(CO)_2(L)I$ studied are stable in solution (e.g. $CHCl_3$, benzene) at room temperature for a period of hours. However, when refluxed in benzene they quickly isomerized to a thermodynamic equilibrium. For example, when either *diag*- or *lat*-$(\eta^5\text{-}C_5H_4Me)Mo(CO)_2(PPh_3)I$ was refluxed in benzene for 4 h, the same [*diag*]/[*lat*] ratio, 30/70, was achieved. Equilibrium [*diag*]/[*lat*] ratios close to 50/50 were obtained for the other complexes. This result shows that the solution state isomerization of $(\eta^5\text{-}C_5H_4R)M(CO)_2(L)I$ is *not* unidirectional. Similar equilibrium studies on $(\eta^5\text{-}C_5H_5)Mo(CO)_2(L)X$ (L = PPh_3, PBu_3; X = Br, I)[15] and $(\eta^5\text{-}C_5H_4R)Mo(CO)_2(L)I$ (R = Me, tBu, $SiMe_3$; L = isonitrile, phosphine, phosphite)[12,21] in refluxing benzene have also been reported.

10.3.3. Solid-State Isomerization of *diag-* and *lat*-(η^5-C_5H_4R)M(CO)$_2$(L)I.

The four sets of isomers synthesized in this study were chosen to cover a range of M, L and R and to assess the effect of these variables on the isomerization reaction. It was found that all four pairs of (η^5-C_5H_4R)M(CO)$_2$(L)I (M = W, Mo) isomers underwent *diag-lat* isomerization reactions when they were heated in the solid state. The first attempt to study the isomerization reaction entailed reaction in a round-bottom flask, similar to reactions carried out in the previous studies (Chapter 3 and 6). However it was observed that the reactants/products sublimed out of the reaction flask. This made product analysis erratic. The reactant was then sealed in a capillary tube under nitrogen and the tube fully immersed in an oil bath. No sublimation was observed under these conditions and the product recovery was facile once the tubes had been opened. Because both isomers had similar red colors, the solid state isomerization reactions of the tungsten or molybdenum complexes could not be monitored visually and were only monitored after appropriate time periods by silica gel TLC, IR and NMR spectroscopy.

Both diagonal and lateral isomers of (η^5-C_5H_4R)M(CO)$_2$(L)I (M = W, Mo) were tested for the solid-state isomerization behavior (Table 10.2). It was found that the thermal solid-state isomerization reactions of monosubstituted cyclopentadienyl tungsten and molybdenum complexes (η^5-C_5H_4R)M(CO)$_2$(L)I are *unidirectional*. No isomerization in the reverse direction to that shown in Table 10.2 occurred, even after long reaction times (>24 h).

Three of the four sets of complexes underwent reaction from the *diag* to the *lat* isomer, a result in keeping with our studies on a wide range of Re complexes (Chapter 3 and 6). However a *lat* to *diag* isomerization occurred for $(\eta^5\text{-}C_5H_4Me)W(CO)_2[P(O^iPr)_3]I$. This suggests that the intermolecular interactions cannot simply relate to *diag/lat* intermolecular polar effects in the solid state.

In Chapter 6, we have reported on the solid state behavior of over 20 rhenium piano stool complexes. The choice of the metal M, the ring-substituent R and the ligand L do not seem to be the factors that determine the direction of the reaction, nor whether the reaction will proceed or not. This suggests that, in contrast to the solution phase studies, an understanding of the mechanism must entail an understanding of the *intramolecular forces* at play.

The only property that correlates with the *direction* of the solid-state isomerization reaction of $(\eta^5\text{-}C_5H_4R)M(CO)_2(L)I$ (M = W, Mo) is the melting point of the diagonal and lateral isomers (Chapter 3 and 6). The reaction *always* proceed from the low melting point isomer to the high melting point isomer, even if this difference is very small (see melting points listed), but even this difference is no guarantee that the reaction will proceed (Chapter 3). This suggests that the 'shape'[22] of the molecule and the way in which it sterically interacts with its nearest neighbors are important.

The intermolecular forces that override the intramolecular forces, which dominate in the solution phase, could thus be both steric (phase rebuilding[22], topotatic[23]) or

Table 10.1. Spectroscopic and Analytical Data for $(\eta^5\text{-}C_5H_4R)M(CO)_2(L)I$ (M = W, Mo) Complexes

compound	ν_{co}[a] (cm^{-1})	^1H NMR (ppm)[b]				analysis (%)	
		Cp	R	L		C	H
diag-$(\eta^5\text{-}C_5H_4Me)W(CO)_2[P(O^iPr)_3]I$	1956, 1870	5.12 (m, 2H), 5.20 (m, 2H)	2.32 (s, 3H)	1.32 (d, 18H), 4.57–4.63 (m, 3H)	calcd	31.22	4.31
					found	30.96	4.15
diag-$(\eta^5\text{-}C_5H_4Me)W(CO)_2(PPh_3)I$	1953, 1867	4.75 (m, 2H), 4.97 (m, 2H)	2.36 (s, 3H)	7.36–7.73 (m, 15H)	calcd	44.10	3.13
					found	43.80	2.84
diag-$(\eta^5\text{-}C_5H_4tBu)W(CO)_2[P(O^iPr)_3]I$	1956, 1871	5.10 (m, 2H), 5.19 (m, 2H)	1.29 (s, 9H)	1.32 (d, 18H), 4.58–4.64 (m, 3H)	calcd	34.50	4.92
					found	34.10	4.80
diag-$(\eta^5\text{-}C_5H_4Me)Mo(CO)_2(PPh_3)I$	1963, 1882	4.66 (m, 2H), 4.94 (m, 2H)	2.26 (s, 3H)	7.33–7.73 (m, 15H)	calcd	50.35	3.57
					found	50.12	3.68
lat-$(\eta^5\text{-}C_5H_4Me)W(CO)_2[P(O^iPr)_3]I$	1952, 1864	5.20 (m, 1H), 5.29 (m, 1H), 5.33 (m, 1H), 5.36 (m, 1H)	2.24 (s, 3H)	1.31 (m, 18H), 4.59–4.64 (m, 3H)	calcd	31.22	4.31
					found	31.00	4.21
lat-$(\eta^5\text{-}C_5H_4Me)W(CO)_2(PPh_3)I$	1950, 1862	5.04 (m, 1H), 5.16 (t, 2H), 5.64 (m, 1H)	2.31 (s, 3H)	7.28–7.73 (m, 15H)	calcd	44.10	3.13
					found	43.50	2.91
lat-$(\eta^5\text{-}C_5H_4tBu)W(CO)_2[P(O^iPr)_3]I$	1950, 1864	4.76 (m, 1H), 5.21 (m, 1H), 5.64 (m, 1H), 5.74 (m, 1H)	1.23 (s, 9H)	1.31 (m, 18H), 4.57–4.66 (m, 3H)	calcd	34.50	4.92
					found	34.56	4.96
lat-$(\eta^5\text{-}C_5H_4Me)Mo(CO)_2(PPh_3)I$	1961, 1875	4.91 (m, 1H), 5.02 (t, 2H), 5.49 (m, 1H)	2.22 (s, 3H)	7.35–7.48 (m, 15H)	calcd	50.35	3.57
					found	50.10	3.50

[a] Recorded in CH_2Cl_2. [b] Recorded in $CDCl_3$, relative to TMS: s, singlet; d, doublet; t, triplet; m, multiplet.

Table 10.2. Solid-State Isomerization Reactions of *diag*- and *lat*-(η^5-C_5H_4R)ML_4 Complexes (M = W, Mo, Re)

complex	m.p. (°C)	reaction temperature and time	diag (%)[a]	lat (%)[a]	isomerization direction
lat-(η^5-C_5H_4Me)W(CO)$_2$[P(O^{i}Pr)$_3$]I	128–130	113–115 °C, 1 h	80	20	lat → diag
diag-(η^5-C_5H_4Me)W(CO)$_2$[P(O^{i}Pr)$_3$]I	144–146	113–115 °C, 18 h	100	0	
diag-(η^5-C_5H_4Me)W(CO)$_2$(PPh$_3$)I	177–179	150–155 °C, 1 h	50	50	diag → lat
lat-(η^5-C_5H_4Me)W(CO)$_2$(PPh$_3$)I	179–181	150–155 °C, 20 h	0	100	
diag-(η^5-C_5H_4tBu)W(CO)$_2$[P(O^{i}Pr)$_3$]I	127–129	100–105 °C, 15 h	42	58	diag → lat
lat-(η^5-C_5H_4tBu)W(CO)$_2$[P(O^{i}Pr)$_3$]I	135–137	100–105 °C, 20 h	2	98	
diag-(η^5-C_5H_4Me)Mo(CO)$_2$(PPh$_3$)I	165[b]	145–150 °C, 30 min	18	82	diag → lat
lat-(η^5-C_5H_4Me)Mo(CO)$_2$(PPh$_3$)I	180–182	145–150 °C, 15 h	0	100	
diag-(η^5-C_5H_4Me)Re(CO)[P(OMe)$_3$]Br$_2$	114–116	100–105 °C, 2.0 h	14	86	diag → lat[c]
lat-(η^5-C_5H_4Me)Re(CO)[P(OMe)$_3$]Br$_2$	116–118	100–105 °C, 2.0 h	0	100	
diag-(η^5-C_5H_4Me)Re(CO)[P(O^{i}Pr)$_3$]Br$_2$	108–110	95–100 °C, 6.0 h	19	81	diag → lat[c]
lat-(η^5-C_5H_4Me)Re(CO)[P(O^{i}Pr)$_3$]Br$_2$	178–180	95–100 °C, 6.0 h	0	100	
diag-(η^5-C_5H_4tBu)Re(CO)[P(OMe)$_3$]Br$_2$	123–125	105–110 °C, 2.0 h	18	82	diag → lat[c]
lat-(η^5-C_5H_4tBu)Re(CO)[P(OMe)$_3$]Br$_2$	154–156	105–110 °C, 2.0 h	0	100	
diag-(η^5-C_5H_4tBu)Re(CO)[P(O^{i}Pr)$_3$]Br$_2$	126–128	105–110 °C, 2.0 h	30	70	diag → lat[c]
lat-(η^5-C_5H_4tBu)Re(CO)[P(O^{i}Pr)$_3$]Br$_2$	170–172	105–110 °C, 2.0 h	0	100	

[a] Determined by ^{1}H NMR spectroscopy. [b] Darkened. [c] Ref. 20.

electronic in nature. Thus an understanding of the reaction will only be possible from solid state packing information.[24] The crystal structure studies on three pairs of cyclopentadienyl rhenium complexes have been presented in Chapter 4 and 8.

The unexpected solid-state isomerization reaction of $(\eta^5\text{-}C_5H_4Me)W(CO)_2[P(O^iPr)_3]I$ which proceeds from the *lat* to the *diag* isomer was investigated by thermomicroscopy and DSC. Under a microscope the red *lat*-$(\eta^5\text{-}C_5H_4Me)W(CO)_2[P(O^iPr)_3]I$ crystals first melted at 128-130 °C, then quickly resolidified, and remelted at 141-142 °C, the latter temperature being close to that of the melting point of the diagonal isomer (m.p. 144-146 °C). Silica gel TLC and IR and NMR spectroscopy confirmed that the lateral isomer had converted to the diagonal product after the melting point process. This shows the isomerization reaction also proceeds in the melt. Indeed, when *lat*-$(\eta^5\text{-}C_5H_4Me)W(CO)_2[P(O^iPr)_3]I$ was heated at 132 °C (in molten state) for 15 min, 70% of the diagonal isomer was produced. In the DSC spectrum, the endothermic melting peak of *lat*-$(\eta^5\text{-}C_5H_4Me)W(CO)_2[P(O^iPr)_3]I$ (m.p. 128-130 °C) was not observed (heating rate: 1.0 °C/min). An endothermic peak at 143 °C corresponding to the melting point of the diagonal isomer was noted. Silica gel TLC and IR and NMR spectroscopy confirmed that the *lat*-$(\eta^5\text{-}C_5H_4Me)W(CO)_2[P(O^iPr)_3]I$ complex isomerized into the corresponding diagonal isomer after the DSC measurement.

10.4. Conclusions

The pure diagonal and lateral isomers of tungsten and molybdenum complexes (η^5-

$C_5H_4R)M(CO)_2(L)I$ (M = W, R = Me, tBu, L = $P(O^iPr)_3$, PPh_3; M = Mo, R = Me, L = PPh_3) have been synthesized and fully characterized by elemental analysis and IR and NMR spectroscopy. Like the rhenium complexes $(\eta^5\text{-}C_5H_4R)Re(CO)(L)X_2$, the tungsten and molybdenum complexes $(\eta^5\text{-}C_5H_4R)M(CO)_2(L)I$ undergo a unidirectional thermal solid-state isomerization reaction which is always from the low melting point isomer to the high melting point isomer. Thus, solid-state *diag-lat* isomerization reactions in which intermolecular forces outweigh intramolecular forces are a common phenomenon for cyclopentadienyl four-legged piano stool transition metal complexes.

10.5. References

1. Piper, T. S.; Cotton, F. A.; Wilkinson, G. *J. Inorg. Nucl. Chem.* **1956**, *3*, 104
2. Davis, R.; Kane-Maguire, L. A. P., in Wilkinson, G; Stone, F. G. A.; Abel, E. W., Eds., "Comprehensive Organometallic Chemistry", Pergamon Press, 1982, Vol. 3, p1185 and p 1335.
3. Morris, M. J., in Abel, E. W.; Stone, F. G. A.; Wilkinson, G., Eds., "Comprehensive Organometallic Chemistry", Pergamon Press, 1995, Vol. 5, p 407.
4. Treichel, P. M.; Barnett, K. W.; Shubkin, R. L. *J. Organomet. Chem.* **1967**, *7*, 449.
5. Manning, A. R. *J. Chem. Soc. (A)* **1967**, 1984.
6. George, T. A.; Turnipseed, C. D. *Inorg. Chem.* **1973**, *12*, 394.
7. Febvay, J.; Casabianca, F.; Riess, J. G. *Inorg. Chem.* **1985**, *24*, 3235.
8. Starker, K.; Curtis, M. D. *Inorg. Chem.* **1985**, *24*, 3006.
9. Alway, D. G.; Barnett, K. W. *Inorg. Chem.* **1980**, *19*, 1533.
10. Debad, J. D.; Hill, R. H. *Can. J. Chem.* **1990**, *68*, 2216.
11. Blumer, D. J.; Barnett, K. W.; Brown, T. L. *J. Organomet. Chem.* **1979**, *173*, 71.
12. Coville, N. J.; Loonat, M. S.; Carlton, L. *S. Afr. J. Chem.* **1992**, *45*, 63.
13. Albers, M. O.; Coville, N. J. *Coord. Chem. Rev.* **1984**, *53*, 227.
14. Xia, W.; Hill, R. H. *Polyhedron* **1992**, *11*, 1319.
15. Beach, D. L.; Dattilo, M.; Barnett, K. W. *J. Organomet. Chem.* **1977**, *140*, 47.
16. Faller, F. W.; Anderson, A. S. *J. Am. Chem. Soc.* **1970**, *92*, 5852.
17. Beach, D. L.; Barnett, K. W. *J. Organomet. Chem.* **1975**, *97*, C27.

18. King, R. B. "Organometallic Synthesis", Vol.1, Academic Press, New York, N.Y., 1955.

19. Cianfriglia, P.; Narducci, V.; Sterzo, C. L.; Viola, E. *Organometallics* **1996**, *15*, 5220.

20. King, R. B.; Reimann, R. H.; Dettensbourg, D. J. *J. Organomet. Chem.* **1975**, *93*, C23.

21. Smith, J. M.; White, D. P.; Coville, N. J. *Bull. Chem. Soc. Ethiop.* **1996**, *10*, 1.

22. Kaupp, G. in Atwood, J.L.; Davies, J.E.D.; MacNicol, D.D.; Votgle, F., Eds., "Comprehensive Supramolecular Chemistry", Pergamon, New York, Vol.8, Chap 9 , 1996.

23. Schmidt, G. M. J. *Pure Appl. Chem.* **1971**, 27, 647.

24. Braga, D. *Chem.. Rev.* **1992**, *92*, 633.

CHAPTER 11

THE SYNTHESIS AND SOLID-STATE STUDY OF THE DISUBSTITUTED CYCLOPENTADIENYL RHENIUM COMPLEXES $(\eta^5\text{-}C_5H_3R_1R_2)Re(CO)_2Br_2$ (R_1, R_2 = Me, $SiMe_3$, tBu).

11.1. Introduction

The organometallic chemistry of monosubstituted cyclopentadienyl transition metal complexes has been comprehensively investigated.[1] However, other than the pentasubstituted (e.g. C_5Me_5[2]) and the indenyl ligands,[3] multi-substituted cyclopentadienyl ring systems, attached to metal complexes, have been less extensively studied.[4-6] Not only will two (or more) ring substituents provide the possibility of inducing asymmetry into a metal-cyclopentadienyl complex but they can also provide more control over steric and electronic effects associated with the metal center.[7-9] These properties can in turn fine tune both the physical and catalytic properties associated with the transition metal complexes.

Disubstituted cyclopentadienyl rhenium complexes have little been studied. To our

knowledge $[\eta^5\text{-}C_5H_3(SiMe_3)_2]Re(CO)_3$,[10] $[\eta^5\text{-}1,2\text{-}C_5H_3(tBu)_2]Re(CO)_3$,[11] $[\eta^5\text{-}1,3\text{-}C_5H_3(Me)_2]Re(CO)_3$[12] and $[\eta^5\text{-}1,3\text{-}C_5H_3(Me)_2]Re(NO)(PPh_3)(Cl)$[13] are the only four compounds of this type that have been reported in the literature to *date*. Here we report a convenient preparation of some disubstituted cyclopentadienyl dicarbonyldibromide rhenium complexes $(\eta^5\text{-}C_5H_3R_1R_2)Re(CO)_2Br_2$ (R_1 = Me, tBu, $SiMe_3$; R_2 = $SiMe_3$). The solid-state and solution *diag-lat* isomerization reactions of these complexes have been studied and the results have been compared with their monosubstituted analogues.

11.2. Experimental

The $(\eta^5\text{-}C_5H_4R)Re(CO)_3$ (R = H, Me, tBu) complexes were prepared by the methods described in Chapter 3 and ref.14. All the reactions were carried out under nitrogen. Solvents were dried by conventional methods, distilled under nitrogen, and used immediately. Melting points were recorded on a Kofler hot stage melting point apparatus. Infrared spectra were recorded on a Midac FTIR spectrometer, usually in KBr cells (solutions). ^1H NMR spectra were measured on a Bruker AC200 spectrometer operating at 200 MHz. Microanalyses were carried out at the CSIR, Pretoria, South Africa.

11.2.1. Synthesis of $(\eta^5\text{-}C_5H_3R_1R_2)Re(CO)_3$ (R_1 = Me, tBu,; R_2 = $SiMe_3$).

To a stirred solution of $(\eta^5\text{-}C_5H_4R_1)Re(CO)_3$ (R_1 = Me, 738 mg; R_1 = tBu, 770

mg) in 30 mL of THF at -65 °C was added two equivalents of 1.6 M solution n-C_4H_9Li in hexane. After stirring at -40 °C to -50 °C for 2 h, ten equivalents of $(CH_3)_3SiCl$ was added to the solution. The reaction mixture was allowed to warm to 20 °C, and the solvent was removed under vacuum. The residue was chromatographed on a silica gel column (2 × 60 cm) with hexane. The product (η^5-$C_5H_3R_1R_2)Re(CO)_3$ was obtained as white needles. [η^5-1,3(2)-$C_5H_3(Me)(SiMe_3)]Re(CO)_3$: 638 mg, 72% yield, IR (cm^{-1}, CH_2Cl_2) ν_{co}: 1922, 2019. ^1H NMR (ppm, $CDCl_3$): 0.28 (s, 9H), 2.23(2.25) (s, 3H), 5.23–5.31 (m, 3H). [η^5-1,3-$C_5H_3(tBu)(SiMe_3)]Re(CO)_3$: 198 mg, 62% yield, IR (cm^{-1}, CH_2Cl_2) ν_{co}: 1922, 2018. ^1H NMR (ppm, $CDCl_3$): 0.22 (s, 9H), 1.23 (s, 9H), 5.21 (t, 1H), 5.33 (t, 1H), 5.43 (q, 1H).

11.2.2. Synthesis of [η^5-1,3-$C_5H_3(SiMe_3)_2]Re(CO)_3$.

To a stirred solution of (η^5-$C_5H_5)Re(CO)_3$ (2.0 g, 6.0 mmol) in 100 mL of THF at -65 °C was added 7.7 mL of 2.5 M solution of n-C_4H_9Li (19.2 mmol) in hexane. After stirring at -40 °C to -50 °C for 2 h, 8.3 mL of $(CH_3)_3SiCl$ (65.4 mmol) was added to the cold solution. The residue was placed on a silica gel column (2 × 60 cm), and careful elution with hexane resulted in the separation of [η^5-1,3-$C_5H_3(SiMe_3)_2]Re(CO)_3$ (400 mg, 14% yield) from (η^5-$C_5H_4SiMe_3)Re(CO)_3$ (1400 mg, 57% yield). Both materials were obtained as white solids. [η^5-1,3-$C_5H_3(SiMe_3)_2]Re(CO)_3$: IR ($cm^{-1}$, CH_2Cl_2) ν_{co}: 1922, 2018. ^1H NMR (ppm, $CDCl_3$): 0.24 (s, 18H), 5.36 (s, 1H), 5.43 (d, 2H).

11.2.3. Synthesis of *diag*- and *lat*-(η^5-$C_5H_3R_1R_2$)$Re(CO)_2Br_2$ (R_1 = Me, tBu, $SiMe_3$; R_2 = $SiMe_3$).

A solution of 1.1 equivalents of Br_2 in 5 mL of $CHCl_3$ was added dropwise to a solution of (η^5-$C_5H_3R_1R_2$)$Re(CO)_3$ (200–500 mg) in 15 mL of $CHCl_3$ at 0 °C. After the reaction mixture was stirred for an additional 60 min at 0 °C, the reaction was stopped and the solvent was removed under reduced pressure. The resulting dark red solid was dissolved in dichloromethane and chromatographed on a silica gel column prepared in hexane. Successive elution with hexane and hexane/dichloromethane (1:1) gave unreacted (η^5-$C_5H_3R_1R_2$)$Re(CO)_3$ (ca. 60% recovery), *diag*- and *lat*-(η^5-$C_5H_3R_1R_2$)$Re(CO)_2Br_2$ (R_1 = Me, tBu, $SiMe_3$; R_2 = $SiMe_3$; ca. overall 25 % yield) from a red and a brown band, respectively. The *diag*-[η^5-1,3-C_5H_3(Me)($SiMe_3$)]$Re(CO)_2Br_2$ and *diag*-[η^5-1,2-C_5H_3(Me)($SiMe_3$)] $Re(CO)_2Br_2$ complexes were successfully separated by careful column chromatography (2 × 60 cm, hexane). The separation of the 1,3 and 1,2 lateral isomers was also achieved by the same method (hexane/dichloromethane 2:1). Both the 1,3 diagonal and lateral isomers elute from the column before the 1,2 isomers. The ratio of 1,3 to 1,2 isomers was about 70/30. All new complexes were characterized by elemental analysis and by IR and NMR spectroscopy (Table 11.1).

11.2.4. Synthesis of *diag*-[η^5-1,3-$C_5H_3(SiMe_3)_2$]$Re(CO)_2$[$P(OPh)_3$] Br_2.

diag- or *lat*-[η^5-1,3-$C_5H_3(SiMe_3)_2$]$Re(CO)_2Br_2$ (60 mg, 0.098 mmol) and 1.1 equivalents of $P(OPh)_3$ were dissolved in 15 mL CH_2Cl_2 under nitrogen. $Me_3NO{\cdot}2H_2O$ (2–5 equiv.) was added to the above magnetically stirred solution. The reaction was monitored by IR spectroscopy and was found to be complete within 15 min. Solvent was removed by vacuum rotatory evaporation to leave a red residue, which was dissolved in CH_2Cl_2 and chromatographed on a silica gel column prepared in hexane. Elution with (1:1) CH_2Cl_2/hexane gave *diag*-[η^5-1,3-$C_5H_3(SiMe_3)_2$]$Re(CO)[P(OPh)_3]Br_2$ as a red solid (55 mg, 63% yield). The spectroscopic and analytic data of this complex are given in Table 11.1.

11.2.5. Solution Isomerization Studies on *lat*-[η^5-1,3-$C_5H_3(SiMe_3)_2$]$Re(CO)_2Br_2$.

A solution containing 20 mg of *lat*-[η^5-1,3-$C_5H_3(SiMe_3)_2$]$Re(CO)_2Br_2$ in 15 mL of benzene was refluxed under nitrogen for 6 h. Removal of solvent at 25 °C (0.1 mmHg) gave a red solid, shown by IR spectroscopy (ν_{co}) in dichloromethane to be (predominantly) the corresponding diagonal isomer. ^1H NMR spectroscopy showed that the product consisted of a 93/7 [*diag*]/[*lat*] mixture.

11.2.6. Solid-State Isomerization Studies on *diag*-(η^5-1,3-$C_5H_3R_1R_2$)$Re(CO)_2Br_2$ (R_1 = Me, $SiMe_3$; R_2 = $SiMe_3$).

Solid *diag*-(η^5-1,3-$C_5H_3R_1R_2$)$Re(CO)_2Br_2$ (R_1 = Me, R_2 = $SiMe_3$: m.p. 81-83 °C; R_1 = R_2 = $SiMe_3$: m.p. 105-107 °C) (10 – 20 mg) was heated in a 25-mL round-

bottom flask in an oil bath for 16 or more hours at a temperature at least 10 °C below the melting point of the material. The reaction was monitored by a combination of TLC and IR and NMR spectroscopy and the study indicated that no lateral isomer was formed in the reaction.

11.2.7. Solid-State Photochemical Isomerization of *diag*-[η^5-1,3-$C_5H_3(SiMe_3)_2$] $Re(CO)_2Br_2$.

diag-[η^5-1,3-$C_5H_3(SiMe_3)_2$]$Re(CO)_2Br_2$ (23.2 mg, 0.03 mmol), adsorbed on the surface of silica gel (300 mg), was irradiated with two 200W incandescent lamps at room temperature for 48 h. A detailed description of the experimental procedure is given in Chapter 5. Separation of the products on a silica gel column (CH_2Cl_2/hexane 1:1), gave *lat*-[η^5-1,3-$C_5H_3(SiMe_3)_2$]$Re(CO)_2Br_2$ (15.9 mg, 86% yield) and *diag*-[η^5-1,3-$C_5H_3(SiMe_3)_2$]$Re(CO)_2Br_2$ (4.7 mg, 20% recovery) .

11.3. Results and Discussion

11.3.1 Synthesis of (η^5-$C_5H_3R_1R_2$)$Re(CO)_3$ (R_1 = Me, tBu, $SiMe_3$; R_2 = $SiMe_3$)

Disubstituted cyclopentadienyl tricarbonyl rhenium complexes (η^5-$C_5H_3R_1R_2$)$Re(CO)_3$ (R_1 = Me, tBu; R_2 = $SiMe_3$) were easily obtained in good yield by deprotonation of (η^5-$C_5H_4R_1$)$Re(CO)_3$ in THF and subsequent treatment with trimethylchlorosilane. The reaction was selective to the disubstituted product; no tri- or multisubstituted product was detected. Further experiments indicated

Table 11.1. Spectroscopic and Analytical Data for (η^5-$C_5H_3R_1R_2$)Re(CO)(L)Br_2 Complexes

compound	m.p. (°C)	ν_{co}[a] (cm^{-1})	^{1}H NMR[b] (ppm)			analysis (%)		
			Cp	R	L		C	H
diag-[η^5-1,3-$C_5H_3(SiMe_3)_2$]Re(CO)$_2Br_2$	105–107	2058, 1995	4.95 (t, 1H), 5.44 (d, 2H)	0.38 (s, 18H)		calcd	25.53	3.36
						found	25.46	3.21
diag-[η^5-1,3-$C_5H_3(tBu)(SiMe_3)$]Re(CO)$_2Br_2$	75–77	2058, 1995	4.99 (t, 1H), 5.32 (t, 1H), 5.38 (t, 1H)	0.36 (s, 9H), 1.40 (s, 9H)		calcd	28.24	3.55
						found	28.30	3.50
diag-[η^5-1,3-$C_5H_3(Me)(SiMe_3)$]Re(CO)$_2Br_2$	81–83	2059, 1995	4.89 (t, 1H), 5.11 (t, 1H), 5.80 (t, 1H)	0.36 (s, 9H), 2.41 (s, 3H)		calcd	23.88	2.73
						found	24.01	2.60
diag-[η^5-1,2-$C_5H_3(Me)(SiMe_3)$]Re(CO)$_2Br_2$	80–82	2059, 1995	5.21 (t, 1H), 5.55 (t, 1H), 5.80 (t, 1H)	0.35 (s, 9H), 2.14 (s, 3H)		calcd	23.88	2.73
						found	23.60	2.70
diag-[η^5-1,3-$C_5H_3(SiMe_3)_2$]Re(CO)[P(OPh)$_3$]Br_2	145–147	1987	4.68 (t, 1H), 5.16 (d, 2H)	0.37 (s, 18H)	7.13–7.26 (m, 15H)	calcd	40.32	4.06
						found	40.37	4.04
lat-[η^5-1,3-$C_5H_3(SiMe_3)_2$]Re(CO)$_2Br_2$	134–136	2046, 1972	5.74 (t, 1H), 6.05 (d, 2H)	0.36 (s, 18H)		calcd	25.53	3.46
						found	25.73	3.26
lat-[η^5-1,3-$C_5H_3(tBu)(SiMe_3)$]Re(CO)$_2Br_2$	131–133	2045, 1972	5.71 (t, 1H), 5.90 (t, 1H), 6.05 (t, 1H)	0.35 (s, 9H), 1.34 (s, 9H)		calcd	28.24	3.55
						found	28.43	3.44
lat-[η^5-1,3-$C_5H_3(Me)(SiMe_3)$]Re(CO)$_2Br_2$	121–123	2045, 1972	5.55 (t, 1H), 5.74 (t, 1H), 5.93 (t, 1H)	0.30 (s, 9H), 2.31 (s, 3H)		calcd	23.88	2.73
						found	24.15	2.58
lat-[η^5-1,2-$C_5H_3(Me)(SiMe_3)$]Re(CO)$_2Br_2$	121–123	2045, 1972	5.59 (t, 1H), 5.91 (t, 1H), 5.96 (t, 1H)	0.32 (s, 9H), 2.29 (s, 3H)		calcd	23.88	2.73
						found	23.70	2.64

[a] Recorded in CH_2Cl_2. [b] Recorded in $CDCl_3$, relative to TMS: s, singlet; d, doublet; t, triplet; m, mutiplet.

that the amount of n-butyllithium used in the reaction determined the degree of ring substitution. For example, reaction of $(\eta^5\text{-}C_5H_5)Re(CO)_3$ with two equivalents of 1.6 M n-butyllithium/hexane solution followed by the addition of trimethylchlorosilane only gave the monosubstituted product $(\eta^5\text{-}C_5H_4SiMe_3)Re(CO)_3$, while the addition of three equivalents of 2.5 M n-butyllithium/hexane solution resulted in the formation of the disubstituted complex, $[\eta^5\text{-}1,3\text{-}C_5H_3(SiMe_3)_2]Re(CO)_3$. The dilithiocyclopentadienyl complex $[\eta^5\text{-}1,3\text{-}C_5H_3Li_2]Re(CO)_3$ is clearly formed under these deprotonation conditions.[13]

The position of addition of the second substituent was influenced by the size of ring substituent already attached to the ring. For the larger substituents e.g. *tert*-butyl and trimethysilyl, only the 1,3-disubstituted product was formed; for the smaller methyl group, both the 1,3- and 1,2-disubstituted complexes were produced, although even here the 1,3 isomer was the dominant product.

A small amount of $(\eta^5\text{-}C_5H_4SiMe_3)Re(CO)_3$ (ca. 20% yield) was also formed during the preparation of $[\eta^5\text{-}C_5H_3(Me)(SiMe_3)]Re(CO)_3$. The source of this material is not $(\eta^5\text{-}C_5H_5)Re(CO)_3$ as this material was not observed in the starting material. This unexpected reaction has not been pursued further.

11.3.2 Synthesis of *diag*- and *lat*-$(\eta^5\text{-}C_5H_3R_1R_2)Re(CO)_2Br_2$ (R_1 = Me, tBu, $SiMe_3$; R_2 = $SiMe_3$)

The bromination of $(\eta^5\text{-}C_5H_3R_1R_2)Re(CO)_3$ (R_1 = Me, tBu, $SiMe_3$; R_2 = $SiMe_3$) in $CHCl_3$ gave *diag*- and *lat*-$(\eta^5\text{-}C_5H_3R_1R_2)Re(CO)_2Br_2$ in 25 % yield (60 % based on recovered starting material). No attempt was made to optimize this yield. The diagonal isomers of $(\eta^5\text{-}C_5H_3R_1R_2)Re(CO)_2Br_2$ have a red color and the lateral isomers are brown. Both diagonal and lateral isomers are soluble in almost all organic solvents, including hexane. Similar to the unsubstituted or monosubstituted analogues, the diagonal isomers have better solubility properties than the lateral complexes.

It was found possible to separate the 1,2 and 1,3 isomers of *diag*- and *lat*-$[\eta^5\text{-}C_5H_3(Me)(SiMe_3)]Re(CO)_2Br_2$. This was achieved by careful column chromatography. The procedure thus provides for the facile synthesis of *mixed* 1,2 disubstituted cyclopentadienyl ligands. Generally disubstituted cyclopentadienyl transition metal complexes containing two *non-connected* substituents are prepared with the two substituents in the 1,3 positions. Other than ring systems containing two methyl substituents, indirect procedures are usually needed to synthesize the 1,2 substituted ring systems such as $[\eta^5\text{-}1,2\text{-}C_5H_3(tBu)_2]Re(CO)_3$ and $Zr[1,2\text{-}C_5H_3(tBu)_2]_2Cl$.[11,16-18] This arises from repulsive forces that exist between the 1 and 2 positions on the ring.

Identification of the 1,3 and 1,2 substituted complexes was based on their proton NMR spectra. Both spectra consist of three separated triplets corresponding to the three ring resonances (4.8 to 6.1 ppm).

Three differences are to be noted. Firstly, the central peak for the 1,3 diagonal isomer occurs at a higher field than the 1,2 isomer (5.55 versus 5.11 ppm). Secondly, the coupling constant $J_{H\text{-}H}$ of the most down field cyclopentadienyl proton resonance of *diag*-[η^5-1,2-$C_5H_3(Me)(SiMe_3)$]$Re(CO)_2Br_2$, is 2.61 Hz, which is characteristic of 1,2 isomers. Thirdly, the 1,3 complex has $J_{H\text{-}H}$ coupling constants of ca. 2 Hz for all three cyclopentadienyl resonances.

The carbonyl substitution reaction of a representative example of the new complexes, [η^5-1,3-$C_5H_3(SiMe_3)_2$]$Re(CO)_2Br_2$, was undertaken. Reaction of diagonal or lateral [η^5-1,3-$C_5H_3(SiMe_3)_2$]$Re(CO)_2Br_2$ with $P(OPh)_3$ in the presence of trimethylamine N-oxide gave only *diag*-[η^5-1,3-$C_5H_3(SiMe_3)_2$]$Re(CO)[P(OPh)_3]Br_2$ which was readily characterized by IR and NMR spectroscopy (see Table 1). The product (isomer) is thus the same as that found for monosubstituted ring systems (Chapter 6).

11.3.3 Solution and Solid-State Isomerization Reactions of [η^5-1,3-$C_5H_3(SiMe_3)_2$]$Re(CO)_2Br_2$

A representative disubstituted complex, [η^5-1,3-$C_5H_3(SiMe_3)_2$]$Re(CO)_2Br_2$, was chosen to assess the effect of the influence of two ring substituents on the solution, solid state and photolytic/solid state reactivity pattern of the new complexes. The following results were obtained:

(i) *solution studies: lat*-[η^5-1,3-$C_5H_3(SiMe_3)_2$]$Re(CO)_2Br_2$ isomerized to the corresponding diagonal isomer in 97% yield when refluxed in benzene for 6 h. This is a similar result to that found previously for (η^5-C_5H_4R)$Re(CO)_2Br_2$ (R = H, alkyl) (Chapter 3).

(ii) *solid state reactions:* No isomerization reaction was observed on heating either the diagonal or lateral isomers of (η^5-1,3-$C_5H_3R_1R_2$)$Re(CO)_2Br_2$ (R_1 = Me, $SiMe_3$; R_2 = $SiMe_3$) in the solid state for more than 16 h at a temperature 10 °C below the melting point of the *diag* isomer

(iii) *photolysis/SiO_2:* The photolyzed solid-state *diag*-to-*lat* isomerization of [η^5-1,3-$C_5H_3(SiMe_3)_2$]$Re(CO)_2Br_2$ on silica gel proceeded in good yield (86%) at room temperature under the irradiation of visible light.

The above results confirm our previous proposal that the ring-substituent has little effect on the direction of the solution *lat*-to-*diag* isomerization reaction and of the silica gel-mediated solid-state photochemical *diag*-to-*lat* isomerization reaction of cyclopentadienyl four-legged piano stool rhenium complexes (Chapter 3 and 5). Again, this would suggest that in these instances steric hindrance by nearest neighbor molecules does not take place and this leads to a predictable product outcome based on the electronic and steric properties of the individual molecules. (Note: the photolyzed silica gel mediated isomerization reaction only occurs in the first surface monolayer, see Chapter 5).

By contrast, an understanding of the *thermal* solid state isomerization reaction (or

lack thereof) cannot be obtained purely from a knowledge of the molecule independent of inter-molecular interactions. Indeed, even the one predictive rule discovered to date i.e. that the isomerization reaction proceeds from the complex with the low melting point to the high melting point, is a rule based on intermolecular forces (Chapter 4). It is thus clear that an understanding of solid state organometallic chemistry is still undeveloped and much work is still required to permit prediction of reactivity patterns.[19]

11.4. Conclusion

A convenient method to prepare disubstituted cyclopentadienyl rhenium complexes (η^5-$C_5H_3R_1R_2$)$Re(CO)_2Br$ (R_1 = $SiMe_3$; R_2 = $SiMe_3$) has been developed. The synthesis and separation of the first 1,2-disubstituted cyclopentadienyl transition metal complexes with different ring substituents *diag*- and *lat*-[η^5-1,2-$C_5H_3(Me)(SiMe_3)$]$Re(CO)_2Br_2$ have been reported. It was found that the solution isomerization and silica gel mediated solid-state photochemical isomerization reactions of (η^5-$C_5H_3R_1R_2$)$Re(CO)_2Br_2$ are similar to those of the unsubstitituted and monosubstituted analogues; i.e. the reaction proceeds from the *lat* to the *diag* isomer in solution and in the reverse direction in the solid-state (SiO_2). The finding that the disubstituted cyclopentadienyl complexes studied here did not undergo thermal solid-state isomerization reactions, is strongly suggestive of the importance of intermolecular forces being central to an interpretation of the data.

11.5. References

1. Coville, N. J.; du Plooy, K. E.; Pickl, W. *Coord. Chem. Rev.* **1992**, *116*, 1.

2. Maitlis, P. *Chem. Soc. Rev.* **1981**, *10*, 1.

3. Brintzinger, H. H.; Fischer, D.; Mulhaupt, R.; Rieger, B.; Waymouth, R. M. *Angew. Chem. Int. Ed. Engl.* **1995**, *34*, 1143.

4. Janiak, K.; Schumann, H. *Adv. Organomet. Chem.* **1991**, *33*, 291.

5. Okuda, J. *Top. Curr. Chem.* **1992**, *160*, 97.

6. Mohring ; Coville, N. J. *J. Organomet. Chem.* **1994**, *479*, 1.

7. Clark, T. L.; Killian, C. M.; Luthra, S.; Nile, T. A. *J. Organomet. Chem.* **1993**, *462*, 247.

8. White, D.; Carlton, L.; Coville, N. J. *J. Organomet. Chem.* **1992**, *440*, 15.

9. Smith, J. M.; White, D. P.; Coville, N. J. *Polyhedron* **1996**, *15*, 4541.

10. Abel, E. W.; Moorhouse, S. *J. Organomet. Chem.* **1971**, *29*, 227.

11. Hughes, P. R.; Lomprey, J. R. *Inorg. Chim. Acta* **1995**, *240*, 653.

12. Nesmeyanov, A. N.; Anisimov, K. N.; Kolobova, N. E.; Barichnikov, L. I. *Izv, Akad. Nauk. SSR, Ser. Khim.* **1963**, 19.

13. Crocco, G. L.; Gladysz, J. A. *Chem. Ber.* **1988**, *121*, 375.

14. Tam, W.; Lin, G. Y.; Wong, K. W.; Kiel, W. A.; Wong, V. K.; Gladysz, J. A. *J. Am. Chem. Soc.* **1982**, *104*, 141.

15. Bosch, W. H.; Englert, U.; Pfister, B.; Stauber, R.; Salzer, A. *J. Organomet. Chem.* **1996**, *506*, 273.

16. Hughes, R. P.; Kowalski, A. S.; Lomprey, J. R. *Organometallics* **1994**, *13*, 2691.

17. Hughes, R. P.; Lomprey, J. R.; Rheingold, A. L.; Yap, G. P. A. *J. Organomet. Chem.* **1996**, *517*, 63.

18. Hughes, R. P.; Lomprey, J. R.; Rheingold, A. L.; Haggerty, B. S.; Yap, G. P. A. *J. Organomet. Chem.* **1996**, *517*, 89.

19. Braga, D. *Chem. Rev.* **1992**, *92*, 633.

CHAPTER 12

CONCLUSION

In this thesis, the synthesis and solid-state chemistry of some Re, W and Mo organometallic compounds have been investigated. The solid-state studies have emphasized the thermal and photochemical solid-stat isomerization and halogen-exchange reactions of substituted cyclopentadienyl four-legged plano stool transition metal complexes.

The thermal solid-state and solution isomerization reactions of (η^5-C_5H_4R)$Re(CO)_2Br_2$ (R = Me, Et, ^{i}Pr, C_6H_{11}, tBu, $SiMe_3$) were first studied. All lateral complexes were converted to the corresponding diagonal isomers upon refluxing in toluene while *diag*-(η^5-C_5H_4R)$Re(CO)_2Br_2$ (R = Me, ^{i}Pr) isomerized to the corresponding lateral isomers in almost quantitative yield upon heating in the solid state. Thus, the first cyclopentadienyl rhenium complexes to isomerize in the solid state and the first examples of an organometallic compounds that undergo a phase-dependent reversible isomerization reaction under only thermal conditions have been found.

Not every organometallic complex readily undergoes solid-state reactions. In order to determine the range of complexes can isomerize in the solid state, a number of

monocarbonyl substituted rhenium complexes were synthesized and their thermal solid-state isomerization and halogen-exchange reactions were studied. It was found that all diagonal isomers of carbonyl substituted rhenium complexes (η^5-C_5H_4R)Re(CO)(L)X_2 (R = Me, tBu, $SiMe_3$; L = isonitrile, phosphite, phosphine; X = Br, I) isomerized into the corresponding lateral isomers in good yields upon heating in the solid state.

The mechanism of the thermal solid-state isomerization reaction of (η^5-C_5H_4R)Re(CO)(L)Br_2 (R = Me, tBu, $SiMe_3$; L = CO, $CNC_6H_3Me_2$, $P(OMe)_3$, $P(OPh)_3$) were investigated by DSC and thermomicroscopic methods. The results revealed that the solid-state isomerization reaction proceeded exothermically and it was proposed that the reaction occurred *via* a nuclear formation and growth mechanism.

The molecular structures and packing diagrams of the diagonal and lateral isomers of (η^5-C_5H_4Me)Re(CO)$_2Br_2$, (η^5-C_5H_4Me)Re(CO)[$P(OPh)_3$]Br_2 and (η^5-C_5H_4tBu)Re(CO)$_2Br_2$ were determined by X-ray single crystal and powder diffraction techniques. The study showed that both intermolecular and intramolecular interaction could be responsible for the solid-state rearrangement. The *diag*-to-*lat* thermal solid-state isomerization of (η^5-C_5H_4Me)Re(CO)$_2Br_2$ is a unique example in that the intermolecular interaction can induce a molecular rearrangement in the solid state. For the (η^5-C_5H_4Me)Re(CO)[$P(OPh)_3$]Br_2 complex, intramolecular interactions could provide the "driving force" of solid-

state isomerization. The mechanism of the solid-state isomerization of the cyclopentadienyl transition metal complexes $CpML_4$ (Cp = substituted or unsubstituted ring) may follow a combined Berry-turnstile rotation process.

Inorganic oxides can mediate or catalyze solid-state reactions of organometallic compounds. This has been shown by studies on the solid-state isomerization and halogen-exchange reactions of $(\eta^5\text{-}C_5H_4R)Re(CO)(L)X_2$. It was found that even complexes that did not isomerize under thermal conditions, would readily isomerize upon irradiation with visible light at room temperature after the complex had been adsorbed on the surface of silica gel. The silica gel hydroxyl groups were found to play a crucial role in mediating the process.

An attempt was made to correlate the steric sizes of cyclopentadienyl ring C_5H_4R and ligand L with the NMR parameters associated with a series of $(\eta^5\text{-}C_5H_4R)Re(CO)(L)Br_2$ complexes. The results indicate that electronic rather than the steric effects influence the NMR parameters.

A simple method was developed to synthesize disubstituted cyclopentadienyl rhenium complexes of the type $[\eta^5\text{-}1,3(2)\text{-}C_5H_3R_1R_2]Re(CO)_2Br_2$ (R_1 = Me, tBu, $SiMe_3$; R_2 = $SiMe_3$). The new materials showed similar solid-state and solution isomerization behavior as found for the similar monosubstituted analogues.

The thermal solid-state isomerization reactions of monosubstituted

cyclopentadienyl four-legged piano stool complexes of tungsten and molybdenum $(\eta^5\text{-}C_5H_4R)M(CO)_2(L)I$ (M = W, R = Me, tBu, L = $P(O^iPr)_3$, PPh_3; M = Mo, R = Me, L = PPh_3) were also studied. Like rhenium compounds, all tungsten and molybdenum complexes studied also undergo solid-state isomerization reactions, which indicated that the solid-state isomerization reaction is a common phenomenon for cyclopentadienyl four-legged piano stool transition metal complexes. It was further found that the solid-state isomerization reactions proceed always from the low melting point isomer to the high melting point isomer.

Appendix A. Crystallographic Data

See attached diskettes, which contains crystallographic data, non-hydrogen atomic coordinates and equivalent isotropic displacement parameters, bond lengths and angles, anisotropic displacement parameters, observed and calculated structure factors for the following complexes:

identification code	Complex
OM 68	lat-(η^5-C_5H_4Me)$Re(CO)_2Br_2$
OM 69	diag-(η^5-C_5H_4Me)$Re(CO)_2Br_2$
OM 84	diag-(η^5-C_5H_4Me)$Re(CO)[P(OPh)_3]Br_2$
OM 85	lat-(η^5-C_5H_4Me)$Re(CO)[P(OPh)_3]Br_2$
OM 87	lat-(η^5-C_5H_4tBu)$Re(CO)_2Br_2$
OM 88	diag-(η^5-C_5H_4tBu)$Re(CO)_2Br_2$

Appendix B. List of Publications

Part of the work in this thesis has been published as follows:

1. L. Cheng and N.J. Coville: **Phase-Dependent Diagonal and Lateral isomerism of the Rhenium Complexes (η^5-C_5H_4Me)$Re(CO)_2Br_2$,** *Organometallics* **15,** 867 (1996).

2. L. Cheng and N.J. Coville: **Solid-State Photochemical *diag-lat* Isomerization of (η^5-C_5H_4R)$Re(CO)(L)X_2$ on the Surface of Silica Gel,** *Organometallics* **16,** 591 (1997).

3. J.C.A. Boeyens, L. Cheng, N.J. Coville, D.C. Levendis and K. McIntosh: **The Importance of Inter-Molecular Forces in Crystal Structure Analysis: Solid-State Study of the *Diag*-to-*Lat* Isomerization of (η^5-C_5H_4Me)$Re(CO)_2Br_2$,** *J. Chem. Cryst.* in press (1998).

4. L. Cheng and N.J. Coville: **Synthesis and Solid-State Isomerization Reactions of *diag*- and *lat*-(η^5-C_5H_4R)$Re(CO)(L)X_2$,** *J. Organomet. Chem.* in press (1998).

5. L. Cheng and N.J. Coville: **DSC and Microscopic Studies on Thermal**

Solid-State *diag-lat* Isomerization of (η^5-C_5H_4R)Re(CO)(L)Br_2, *Thermochim. Acta* accepted (1998).

6. L. Cheng, L. Carlton and N.J. Coville: **The Synthesis and Solid-State Study of the Disubstituted Cyclopentadienyl Rhenium Complexes, (η^5-$C_5H_3R_1R_2$)Re(CO)$_2$$Br_2$ (R_1, R_2 = Me, tBu, $SiMe_3$),** *S. Afr. J. Chem.* in press (1998).

7. L. Cheng, J. Morar, B. Ngoma and N.J. Coville: **Solid-State Isomerization Reactions of (η^5-C_5H_4R)M(CO)$_2$(L)I (M = W, Mo),** *Organometallics* in preparation.

8. J.C.A. Boeyens, D.C. Levendis, L. Cheng and N.J. Coville: **X-ray Single-Crystal Structures of *diag*- and *lat*-(η^5-C_5H_4Me)Re(CO)[P(OPh)$_3$]Br_2; and *diag*- and *lat*-(η^5-C_5H_4tBu)Re(CO)$_2$$Br_2$: Pairs of Complexes with Unique Solid-State Behavior Patterns,** *J. Chem. Cryst.* in preparation.